Angiogenin promotes glioblastoma invasive growth through FOSL2-mediated upregulation of CD24 and MMP9

A dissertation

submitted by

Hailing Yang

In partial fulfillment of the requirements

for the degree of

Doctor of Philosophy

in

Cellular and Molecular Physiology

TUFTS UNIVERSITY

Sackler School of Graduate Biomedical Sciences

July 2015

ADVISOR: Guo-fu Hu, Ph.D.

Glioblastoma (GBM) is the most aggressive brain tumor and patients suffer from neurological debilitation and die from rapid disease progression due to the lack of effective therapeutics. The current treatment includes surgery, radiation, and chemotherapy. More recently, anti-angiogenic therapy with bevacizumab, a humanized anti-VEGF antibody, has been added and shown to improve neurological conditions. However, bevacizumab fails to extend overall patient survival, and results in a more invasive recurrent disease characterized by a robust perivascular invasion phenotype.

Angiogenin (ANG) is significantly upregulated in higher-grade gliomas, and is one of the two most upregulated genes in bevacizumab-resistant GBM. *ANG* expression is inversely correlated with GBM patient survival, particularly in the proneural subtype. However, the mechanism by which ANG contributes to GBM progression is unknown. I therefore established a PDGF-induced proneural GBM model under the ANG null background and investigated the function and mechanism of ANG in GBM tumorigenesis and progression. I showed that ANG deficiency is not sufficient to prevent PDGFB-induced mouse proneural GBM in the *Ink4a/Arf* null background. However, lack of ANG expression significantly extends animal survival as a result of decreased cancer cell proliferation, reduced extracellular matrix remodeling, and less perivascular tumor invasion. I found that ANG activates MMP-9 expression and consequently increases extracellular matrix remodeling and GBM invasion, which likely contributes to perivascular invasion *in vivo*. I also showed that ANG upregulates CD24 that mediates the interaction of GBM cells with endothelial cells thereby promoting perivascular invasion.

Mechanistically, I found that ANG induces MMP-9 and CD24 expression through upregulation of FOSL2, a member of the Fos family proteins and a transcription factor for both *CD24* and *MMP-9*. I found that ANG activates FOSL2 both transcriptionally through binding to its promoter region and post-translationally by stimulating its nuclear localization via the ERK pathway. Moreover, I found that expressions of *FOSL2*, *MMP-9*, and *CD24* are significantly correlated with ANG expression in GBM patients. Lastly, I showed that neomycin, an ANG inhibitor, significantly increased survival of GBM mice, accompanied with reduced expression of Mmp-9 and Fosl2, decreased extracellular matrix remodeling, and diminished perivascular invasion, resembling the phenotype observed in *ANG* knockout tumors.

In summary, I present two key findings: 1) ANG promotes perivascular invasion of GBM through the FOSL2-CD24/MMP-9 pathway; 2) ANG inhibition effectively reduces perivascular invasion and extends survival of mice in a proneural GBM model. This thesis has revealed an unexpected role of ANG, an angiogenic protein, in regulating perivascular invasion of GBM. More importantly, these findings suggest a novel strategy for GBM therapy based on ANG inhibition.

Key terms: Angiogenin, PLXNB2, FOSL2, CD24, MMP-9, glioblastoma, perivascular, invasion, mouse model, anchorage-independent growth.

Acknowledgements

Foremost, I would like to express my special appreciation and thanks to my advisor Dr. Guo-fu Hu for his immense knowledge, patience, and continuous support throughout my Ph.D. study. I am grateful to receive training and advice from Guo-fu, who has imparted not only a high standard of scholarship but also the philosophy of life. His teaching has ignited my passion for science and will continue to guide my future endeavors. Without his supervision and constant help, this dissertation would not have been possible. Besides my advisor, I would like to thank the rest of my thesis committee: Dr. Brent Cochran, Dr. Philip Hinds, Dr. Gary Sahagian, and Dr. Philip Tsichlis for their encouragement, insightful comments, and hard questions. I would also like to thank Dr. Paul J. Anderson from BWH for agreeing to serve as my outside examiner.

I am thankful to my colleagues, including Wenhao Yu, Hiroko Kishikawa, Jinhao Sheng, Hongbo Luo, Kevin Goncalves, Nil Vanli, Cunrui Li, Yulin Jia, and Shuping Li, who have made the Hu lab a pleasant and intellectually stimulating place to work. I thank Dr. Pavel Ivanov at BWH for his scientific coaching. I thank Dr. Miaofen Hu, whose great personality warms my heart every time we talk. Best wishes for your children, Jamie and Alex. I am also grateful to my friends at Tufts, Chi Luo, Zuyi Weng, Qiu Jin, and Qiming Wang, for their help and company. Especially, Mengqi Huang, thank you for helping me overcome my weaknesses and for being with me during the hardship.

Last but not least, I would like to thank my parents, Hua-qun Lin and Chun-ming Yang. I would not have made it through this journey without you, because you have provided me the ultimate support with your unconditional love and belief.

Table of Contents

List of Figures and Tables

List of abbreviations

3D: Three-dimensional

A2B5: c-series ganglioside–specific antigen

AA: Amino acid

ABE: Angiogenin binding element

AKT: Protein kinase B

Ala: Alanine

ALS: Amyotrophic lateral sclerosis

ANG: Angiogenin

AO/EtBr: Acridine orange/ethidium bromide

AP-1: Activator protein 1

APC: Astrocyte progenitor cell

Arf: Cyclin-dependent kinase inhibitor 2A

ASPM: Abnormal spindle-like microcephaly-associated

ATP: Adenosine Triphosphate

BAG-1: BCL2-associated athanogene

Bax: Bcl-2-like protein 4

BAX: BCL2-associated X protein

BBB: Blood brain barrier

Bcl-2: B-cell CLL/lymphoma 2

Bcl-X: BCL2-like 1

Bcl-XL: B-cell lymphoma-extra large

Bcl2l1: BCL2-like 1

bFGF: FGF2

bHLH-B2: Basic helix-loop-helix family, member e40

BIM: BCL2-like 11

c-Myb: v-myb avian myeloblastosis viral oncogene homolog

c-Myc: V-myc avian myelocytomatosis viral oncogene homolog

C.albicans: *Candida albicans*

cAb: Chimeric antibody

C/EBPβ: CCAAT-enhancer-binding proteins β

CD133: Prominin 1

CD15: Fucosyltransferase 4

CDK: Cyclin-dependent kinase

CDKN2A/B: cyclin-dependent kinase inhibitor 2A/B

cIAP-1: Cellular inhibitor of apoptosis protein-1

CMTMR: (5-(and-6)-(((4-chloromethyl)benzoyl)amino)tetramethylrhodamine)

ct-MEF: Colony-selected transformed mouse embryonic fibroblast

CT: Computed tomography

CXCR2: Chemokine (C-X-C motif) receptor 2

Cys: Cysteine

Cyto c: Cytochrome c

DNA: Deoxyribonucleic acid

DOX: Doxycycline

E-cad: Cadherin 1

E-selectin: CD62 antigen-like family member E

E12: Embryonic day 12

ECM: Extracellular matrix

EGF: Epidermal growth factor

eIF: Eukaryotic Initiation Factor 2

EMT: Epithelial-mesenchymal-transition

ER: Endoplasmic reticulum

ERK: Extracellular-signal-regulated kinases

ERRγ: Estrogen-related receptor gamma

F-12: Coagulation factor XII

FAK: Focal adhesion kinase

FGF1: Fibroblast growth factor 1

FGF2: Basic fibroblast growth factor

FHL3: Four and a half LIM domains protein 3

FOSL: FOS-like antigen

FoxO3a: Forkhead box O3

G-CIMP: Glioma-CpG island methylator phenotype

GAPDH: Glyceraldehyde-3-phosphate dehydrogenase

GBM: Glioblastoma

GNS: Glioma neural stem cells

GPCR: G protein coupled receptors

GPI: Glycosylphosphatidylinositol

GRP: Glial-restricted progenitor cell

H&E: Hematoxylin and eosin

H3K36me3: Histone 3 Lysine 36 trimethyl

HCLS1: Hematopoietic cell-specific Lyn substrate 1

Hiap2: Human inhibitors of apoptosis

HIF: Hypoxia-inducible factors

i.c.: Intracranial

IAP: Inhibitors of apoptosis proteins

IC_{50}: The half maximal inhibitory concentration

ICAM-1: Intercellular adhesion molecule 1

IDH1/2: Isocitrate dehydrogenase1/2

IF: Immunofluorescence

IGF1R: Insulin-like growth factor 1 receptor

IHC: immunohistochemistry

IL: Interleukin

ILK: Integrin-linked kinase

Importin: Karyopherin alpha 1 (importin alpha 5)

Ink4a: Cyclin-dependent kinase inhibitor 2A

IRES: Internal ribosome entry site

ITGA6: Integrin, alpha 6

K-Ras: Kirsten rat sarcoma viral oncogene homolog

Kd: Dissociation constant

L1CAM: L1 cell adhesion molecule

LamB1: Laminin, beta 1

LARGE: Like-glycosyltransferase

Lef1: Lymphoid enhancer-binding factor 1

LIF: Leukemia inhibitory factor

mAb: Monoclonal antibody

MAFB: v-maf avian musculoaponeurotic fibrosarcoma oncogene homolog B

MAL: T-cell differentiation protein

MAPK: Mitogen-activated protein kinase

MBP: Myelin basic protein

MDM2: Mouse double minute 2 homolog

MEF: Mouse embryonic fibroblast

MEK: Mitogen-activated protein kinase kinase

MET: Mesenchymal-epithelial-transition

Met: c-Met/hepatocyte growth factor receptor (HGFR)

mGBM: Mouse glioblastoma

MGMT: O^6-alkylguanine DNA alkyltransferase

MMP: Matrix metalloproteinase

MOI: Multiplicity of infection

MPTP: 1-methyl-4-phenyl-1,2,3,6-tetrahydropyridine

MRI: Magnetic resonance imaging

mRNA: Messenger RNA

mTOR: Mechanistic target of rapamycin

MYCN: V-myc avian myelocytomatosis viral oncogene neuroblastoma derived homolog

MYH9: Myosin, heavy chain 9

N-cad: Cadherin 2, type 1

Neo: Neomycin

NF-κB: Nuclear factor kappa-light-chain-enhancer of activated B cells

NF1: Neurofibromatosis type I

NR2E1: Nuclear receptor subfamily 2, group E, member 1

NRAGE: Melanoma antigen family D1

NRP-1: Neuropilin-1

o/n: Overnight

OB: Olfactory bulb

OPC: Oligodendrocyte progenitor cell

P-glycoprotein: Multidrug resistance protein 1

P-selectin: CD62P/Granule Membrane Protein 140

p21: CDKN1A/ cyclin-dependent kinase inhibitor 1A

p27: CDKN1B/Cyclin-dependent kinase inhibitor 1B

p53: Tumor protein p53

p73: Tumor protein p73

Paro: Paromomycin

Pb2: PLXNB2

PDGFR: Platelet-derived growth factor receptor

PDK: Pyruvate dehydrogenase kinase

PDZ-Rho-GEF: Rho guanine nucleotide exchange factor 11

PFA: Paraformaldehyde

pI: Isoelectric point

PI3K: Phosphoinositide 3-kinase

PLC: Phospholipase C

PLA2: Phospholipase A2

PLG: Plasminogen

PGI_2: Prostaglandin I2

PLXNB2: Plexin B2

Pol: Polymerase

PTEN: Phosphatase and tensin homolog

Ral GTPase: RALA/v-ral simian leukemia viral oncogene homolog A

Rb: Retinoblastoma 1

Rcas: Replication-competent avian retroviruses

RhoA: Ras homolog family member A

RhoGEF: Rho/Rac guanine nucleotide exchange factor

RNA: Ribonucleic acid

RNAi: RNA interference

Rnd3: Rho family GTPase 3

RNH1: Ribonuclease/angiogenin inhibitor 1

ROS: Reactive oxygen species

rRNA: Ribosome RNA

RT-PCR: Real-time PCR

RTK: Receptor tyrosine kinase

Runx1: Runt-related transcription factor 1

Runx1T1: Runt-related transcription factor 1; translocated to, 1

s.c.: Subcutaneous

S.pneumoniae: *Streptococcus pneumoniae*

S4C: Semaphorin 4C

S6K: Ribosomal protein S6 kinase

SA: Sodium arsenite

Sema4C: Semaphorin 4C

SGK: Serum/glucocorticoid regulated kinase

SHH: Sonic hedgehog

Slug: Snail family zinc finger 2

sPb2: Soluble PLXNB2

STAT3: Signal transducer and activator of transcription 3

Survivin: Baculoviral IAP repeat containing 5

SV40LT: SV40 large T antigen

SVZ: Subventricular zone

t-MEF: Transformed mouse embryonic fibroblast

tPA: Tissue-type plasminogen activator

FLAIR: Fluid Attenuated Inversion. Recovery

TAZ: Tafazzin

Tb-1: Trophoblast specific protein alpha

TBX2: T-box 2

TCGA: The cancer genome atlas

TGF-β: Transforming growth factor beta

Tie2: Tyrosine kinase with immunoglobulin-like and EGF-like domains 2

tiRNA: tRNA-derived, stress- induced small RNA

TNF-α: Tumor necrosis factor alpha

TrkB: Neurotrophic tyrosine kinase, receptor, type 2

tRNA: Transfer RNA

Tun: Tunicamycin

TvA: Tumor virus A

uPA: Urokinase-type plasminogen activator

uPAR: Urokinase receptor

VE-Cad: Vascular endothelial - cadherin, CD144

VEGF(A): Vascular endothelial growth factor (A)

VEGFR2: Vascular endothelial growth factor receptor 2

WB: Western blot

XIAP: X-linked inhibitor of apoptosis

YAP: Yes-associated protein 1

ZEB1/2: Zinc finger E-box binding homeobox ½

ZNF-238: Zinc finger and BTB domain containing 18

Chapter I: Introduction

1.1 The malady of glioblastoma

Glioblastoma multiforme (GBM) is the deadliest and the most common form of primary brain tumors (Dunn et al., 2012). Currently, there are approximately 50,000 people with this disease and about 10,000 new cases are diagnosed each year in the United States. Most European countries show a similar disease prevalence and incidence rate (Dolecek, Propp, Stroup, & Kruchko, 2012; Ohgaki & Kleihues, 2005). About 90% of GBM arise *de novo* without early symptoms, and the rest are secondary lesions that are progressed from lower grade gliomas (Ohgaki & Kleihues, 2013). No obvious cause leads to GBM, but several risk factors are associated with the disease including older age, male gender, high socioeconomic status, white race and non-Latino ethnicity, and non-ionizing electromagnetic fields (Chakrabarti, Cockburn, Cozen, Wang, & Preston-Martin, 2005; Hardell, Carlberg, & Hansson Mild, 2013). Despite tremendous progress in the brain tumor biology during the last two decades and approval of newly discovered targeted therapies, the median survival of the disease remains stagnant at 15 months (Grossman et al., 2010).

Patients usually show up in the clinics with symptoms like headache, nausea, and seizures. Patient's history record and brain imaging scan, either computerized tomography (CT) or magnetic resonance imaging (MRI), are used for preliminary diagnosis (Kesari, 2011). The diagnosis needs histological confirmation with biopsy during surgical removal of the tumor mass to guide the follow-up radio- and chemo-therapy. Pathological features of GBM include nuclear pleomorphism, dense cellularity,

pseudopalisading necrosis, vascular endothelial proliferation, and mitotic figures (Wen & Kesari, 2008).

The first-line therapy for GBM consists of surgery, radiation, and chemotherapy. Upon diagnosis of GBM, patients are prescribed glucocorticoids to reduce headache caused by swelling in the brain, and treated continuously after surgery until the tumor- or surgery-related edema is relieved. Sparing the normal brain tissues with vital functions, the surgery removes as much tumor tissues as possible since maximum resections are correlated with better prognosis (Pichlmeier, Bink, Schackert, Stummer, ALA Glioma Study Group, 2008). Radiation and chemotherapy, primarily DNA alkylating reagents such as temozolomide and carmustine, are used to induce apoptosis of the remaining tumor cells that have infiltrated into the surrounding tissues before surgery. Despite the aggressive combination of the above described clinical treatment regimes, residual GBM tumors develop resistance and reemerge (Dunn et al., 2012).

1.1.1 Glioblastoma cellular origin

Glioblastoma is classified as the grade IV astrocytoma according to the World Health Organization Classification System (Louis et al., 2007) which uses histology features and the presumed cellular origin as the basis of subtyping. Astrocytoma is one subtype of glioma that originates from glial cells, more specifically from astrocytes, as opposed to those from oligodendrocytes or neurons in the brain. Compared with the grade I-III astrocytomas, GBM is the fastest growing and most invasive tumor that is refractory to all current treatment regimes, thus having the poorest prognosis.

PI3K/mTOR, p53/MDM2, RAS/NF1, and EGFR signaling aberrations have been identified in early studies as the major drivers of GBM malignancy (Dunn et al., 2012). Human GBM can be recapitulated in mouse models from inhibiting NF1/p53 signaling in undifferentiated as well as mature glial and neuronal cells, (Alcantara Llaguno et al., 2009; Friedmann-Morvinski et al., 2012; T. Kondo & Raff, 2000; Koso et al., 2012; C. Liu et al., 2011), suggesting a complex and heterogeneous ontogenies involving multiple possible cell origins, even though GBM is a disease clinically classified merely by pathology features.

1.1.2 Glioblastoma signaling and molecular classification

More recent studies, including a large cohort analysis from The Cancer Genome Atlas (TCGA) using next-generation sequencing, have corroborated the early findings to show that *EGFR* mutations/amplification, *TP53* mutations, *CDKN2A/B* deletion, and *PTEN* mutations are the most frequent aberrations observed (>30%) in GBM (Cancer Genome Atlas Research Network, 2008). Furthermore, these large-scale studies have also identified new mutations such as those in *IDH1/2* and revealed gene expression clusters that can molecularly segment GBM into four major subtypes including proneural subtype with *PDGFR* amplification/mutation or *IDH1/2* mutation, mesenchymal subtype with *NF1* deletion/mutation, classical subtype with *EGFR* amplification/mutation, and neural subtype with *MBP*/*MAL* expression (Brennan et al., 2013; Cancer Genome Atlas Research Network, 2008; Verhaak et al., 2010).

The proneural subtype is the only subtype that does not respond to intensive concurrent radio-/chemo-therapy (Verhaak et al., 2010).Secondary GBMs developed from low-grade gliomas are enriched in this subtype and carry distinctive *IDH1* mutations. Studies using deep-sequencing revealed mutual exclusivity of 1p/19q and *TP53* mutations. *IDH1* mutation arises specifically in a distinct neural precursor population followed by TP53 mutation in low-grade gliomas and potentially progress to GBM (A. Lai et al., 2011). If IDH1 mutations are accompanied by 1p/19q deletion, it will give rise to oligodendroglioma (Ichimura et al., 2009). Another feature of proneural GBM is *PDGFR* mutation, encompassing amplification (Verhaak et al., 2010), intragenic deletion (exon 8-9) (Clarke & Dirks, 2003), and fusion with the extracellular domain of VEGFR2 (Ozawa

et al., 2010), all of which lead to constitutively active receptor signaling. GBM populations also can be segmented by DNA methylation patterns and patients ages. Proneural subtype GBM impacts the youngest GBM population and can be further stratified by patients with glioma-CpG island methylator phenotype (G-CIMP) status concurrent with *IDH1* mutations or patients with negative G-CIMP coexisting with *PDGFR* mutations (A. Lai et al., 2011; Noushmehr et al., 2010). The *IDH1* mutations and G-CIMP often coexist in the same patient as mutant *IDH1* was found to be the direct cause of the G-CIMP phenotype. GBM IDH1 variants convert alpha-ketoglutarate into (R)-2-hydroxyglutarate that can competitively inhibit alpha-ketoglutarate-dependent histone demethylases and methylcytosine hydroxylases, which in turn give rise to the G-CIMP phenotype (Dang et al., 2009; Turcan et al., 2012; W. Xu et al., 2011). G-CIMP/IDH1 GBM patients show high clinical response to radio-/chemo-therapy and have a better prognosis because of low expression of MGMT, which is due to the methylation of *MGMT* promoter and is 2-fold more frequently observed in G-CIMP positive tumors than in G-CIMP negative ones (Bady et al., 2012). Mechanistically, MGMT function as a DNA repair factor and its activation can avoid alkylating chemotherapy-induced apoptosis (Wick et al., 2012). *IDH* mutations, in addition to serve as a predictive clinical function, are also useful for differential diagnosis between diffusely infiltrating glioma and astrogliosis (Riemenschneider, Jeuken, Wesseling, & Reifenberger, 2010).

Mesenchymal GBM subtype features *NF1* mutations (Verhaak et al., 2010). NF1 is a negative regulator of Ras signaling and regulates adenylate cyclases in PKA signaling as well. Some evidence suggests that the mesenchymal subtype can be reprogrammed from

the proneural subtype. For example: additional *NF1* deletion leads proneural-to-mesenchymal transition in a mouse proneural GBM model (Ozawa et al., 2014). Mesenchymal glioma stem cells can be differentiated from proneural glioma stem cell via TNF-α/NF-κB activation (Bhat et al., 2013). TAZ is one of the major transcription factors responsible for mesenchymal gene signature while it is frequently hypermethylated in proneural GBM. Other major transcription factors for the mesenchymal subtype include STAT3, C/EBPβ, RUNX1, FOSL, bHLH-B2, ZNF-238, TAZ, YAP, MAFB, and HCSL1 (Bhat et al., 2011; Carro et al., 2010).

The classical GBM subtype is the most common subtype featuring *EGFR* mutation (Gan, Kaye, & Luwor, 2009). In addition to *EGFR* amplification, 50-60% patients also harbor the *EGFRvIII* deletion mutation that has not been seen in normal tissue and at much lower prevalence in other neoplasms (Gan, Cvrljevic, & Johns, 2013). Exons 2-7 of the *EGFR* gene containing the ligand-binding domain are deleted in *EGFRvIII*. This mutant exhibits impaired receptor internalization (Grandal et al., 2007) and confers a low level of constitutive active EGFR signaling that has an additive proliferative effect to *wtEGFR* signaling in U87MG cell line (Nagane et al., 1996). EGFR activation requires Neuropilin-1 (NRP-1)(Rizzolio et al., 2012), which is a co-receptor of VEGF that increase GBM aggressiveness via various mechanisms including VEGF-VEGFR2-NRP1 signaling in glioma stem cells (Hamerlik et al., 2012), potentiating c-Met signaling (B. Hu et al., 2007), and promoting GBM invasion through interaction with its cognate ligand Semaphorin 3A (Bagci, Wu, Pfannl, Ilag, & Jay, 2009). EGF-induced downstream signaling, including MEK/ERK, AKT, and S6K, is lower with the involvement of

EGFRvIII comparing to *wtEGFR* alone. But the baseline AKT activation is markedly higher and corresponds to a poorer prognosis in the *EGFRvIII* transgenic mouse GBM model (H. Zhu et al., 2009). This EGFRvIII-AKT correlation has been observed in human patients as well (Mizoguchi et al., 2006). EGFRvIII showed a more profound oncogenic effect than did the wild type EGFR, partially because it can trans-activate c-Met (L. Li et al., 2015), which is attributable to treatment resistance to EGFR inhibitor (Jun, Bronson, & Charest, 2014). It suggests that inhibition of both wtEGFR and EGFRvIII or c-Met signaling will be more effective in treating the classical subtype of GBM. Other oncogenic effects of EGFRvIII function involves activation of Bcl-X-mediated anti-apoptosis (Nagane, Levitzki, Gazit, Cavenee, & Huang, 1998), VEGF- and IL-8-mediated angiogenesis, and MMP-13-mediated invasion (Lal et al., 2002).

Neural GBM subtype affects the oldest population among the four subtypes and moderately responds to aggressive treatment (Verhaak et al., 2010). This subtype doesn't have prevalent mutations in any specific genes and shows a gene expression pattern similar to non-cancerous neurons in addition to possessing many of the abnormalities seen in other GBM subtypes.

Additionally, two distinct GBM young patient groups with Histone 3.3 G34 mutations and Histone 3.1/3.3 K27 mutations segregate from the four adult GBM subtypes described above (D. Sturm et al., 2012). Histone 3.3 G34 mutations impaire H3K36me3 modification leading to oncogenic *MYCN* upregulation (Bjerke et al., 2013). A gain-of-function mutation of K27M reprogram the epigenetic landscape and resulted in DNA

hypomethylation that subsequently give rise to genome instability (Eden, Gaudet, Waghmare, & Jaenisch, 2003; Lewis et al., 2013).

Ultimately, the designation of GBM molecular subtypes, however, is sometimes hard to define. As described above, the mesenchymal radiation resistant phenotype can be promoted through NF-κB (Bhat et al., 2013) or TAZ (Bhat et al., 2011) in the proneural GBM. Even within one GBM tumor, there could be satellites of more than one subtype of tumor, manifested with multiple active RTK signaling (EGFR, c-Met, PDGFRA), which subjects molecular classification to sampling bias (Snuderl et al., 2011).

Nevertheless, with the more precise molecular characterization, GBM has been broken down into subtypes that are more clinically predictable and manageable. In the future, molecular classification of GBM can also guide patient recruitments in designing clinical trials that will increase the success rate of bringing an effective investigational drug to the targeted patients.

1.1.3 Glioblastoma neural stem cells

GBM is one of the most notorious cancer types that don't respond well to radiation or chemotherapy. Using serum-free medium supplemented with F-12, EGF and FGF2, a small population of the primary GBM tumor can be propagated as neurospheres and this subpopulation, termed glioblastoma neural stem cells (GNS), displays multipotency, slow-cycling, expression of multidrug resistance gene, and long-term self-renewing capabilities, which has been regarded as the culprit for clinical difficulties (Galli et al., 2004; Singh et al., 2003) (Bao et al., 2006; Tso, 2011). Because of their multipotency, the GNS lines obtained from biopsy cultured *in vitro* can potentially become an important drug screen platform for personalized medicine (Pollard et al., 2009; Wakimoto et al., 2012). However, due to GBM heterogeneity, multiple subclones can be generated from the same biopsy, all exhibiting different sensitivities to therapeutic treatments (Soeda et al., 2015). Understanding which GNS subtype is most attributable to tumor recurrence will make a significant impact to GBM treatment.

The strong self-renewal capability of GNS lines allows for orthotopic xenograft tumor formation in mice from only 100 cells. This self-renewal potential or "stemness" of GNS cells is maintained by numerous factors, including TGF-β/LIF, SHH/c-Myc, Notch, Wnt/β-catenin, low-pH/HIF2α, and BMX/STAT3 (Hjelmeland et al., 2011; Hovinga et al., 2010; Z. Li et al., 2009; Peñuelas et al., 2009; Rheinbay et al., 2013; Sherry, Reeves, Wu, & Cochran, 2009; Jialiang Wang et al., 2008a). Upregulation of many of those factors is correlated with a poorer GBM prognosis.

These findings spiked large therapeutic enthusiasm in targeting GNS in the bulk tumor. However, unlike breast cancer stem cells, it is difficult to target this population *in vivo* since there is no consensus on which protein marker can clearly define all the suspected glioma stem cells. Early studies found that CD133-positive GBM cells showed neurosphere growth and can be induced to express all three-lineage markers. More importantly, CD133-positive cells show higher tumor-initiating potential than do the CD133-negative ones as the former only need 100 seeding cells for tumor establishment compared to the latter that require 1000-fold more (Singh et al., 2004). However, other lines of evidence suggest that CD133 is not a definitive marker because negative cells can also give rise to CD133 positive cells (Jian Wang et al., 2008b). Meanwhile, other surface markers of GBM subpopulation showing high stemness have been identified, which include CD15 (Son, Woolard, Nam, Lee, & Fine, 2009), Nestin (Zhang et al., 2008), CD44 (Pietras et al., 2014), L1CAM (Bao et al., 2008), A2B5 (Ogden et al., 2008), ITGA6 (Lathia et al., 2010), and NR2E1 (Z. Zhu et al., 2014). Based on the rationale that GNS possess multi-drug resistance, side population technique identifying ATP-binding cassette transporter, has also been used to evaluate and isolate GNS population (Bleau et al., 2009).

The rare GNS population, less than 1% of the tumor, preferentially resides in the perivascular niche (Calabrese et al., 2007). The brain endothelial cells in the niche microenvironment interact with GNS and are essential for regulating self-renewal of GNS and for tumor progression. IL-8 secreted by brain endothelial cells can guide GNS migration to the perivascular location. Knockdown of *CXCR2*, the IL-8 receptor, in GNS cells abolished the tumor-promoting effects of endothelial cells *in vivo* (Infanger et al.,

2013). Osteopontin, specifically expressed at the perivascular locations, activates HIF2α signaling through the CD44 receptor on GNS (Pietras et al., 2014). GNS has also been found to differentiate into endothelial or pericyte lineages to facilitate tumor angiogenesis (L. Cheng et al., 2013; Ricci-Vitiani et al., 2010; Rong Wang et al., 2010). Therefore, GNS confers functional plasticity to GBM progression and contributes to therapy resistance.

1.1.4 Glioblastoma invasion

GBM tumors, irrespective of cellular origin or molecular subtypes, all display exceedingly invasive phenotypes, which challenges surgical removal and inevitably gives rise to tumor recurrence that often occur in the neighboring area of the surgery (Cloughesy, Cavenee, & Mischel, 2014; Cuddapah, Robel, Watkins, & Sontheimer, 2014a). GBM tumors utilize the existing brain structures to facilitate invasion, where they form interactions with the neural microenvironment. This shared invasive phenotype may result from their primitive, undifferentiated cellular states that resemble the migration of neural progenitor cells during neurogenesis (Cuddapah, Robel, Watkins, & Sontheimer, 2014a). Both GBM and neural progenitor cells use glutamate-mediated Ca^{2+} (Ishiuchi et al., 2002; Lyons, Chung, Weaver, Ogunrinu, & Sontheimer, 2007) and K^+ channels (Cuddapah, Turner, Seifert, & Sontheimer, 2013) for migration. Despite their high invasive phenotype, there are very few cases of GBM metastasis outside of the brain, presumably because nonneural microenvironment could not provide the appropriate growth factors or nutrient supplements. Patients may also not survive long enough for metastasis to occur. For example, the median survival of general GBM is 15 months

while that of GBM cases with metastasis is 16-24 months (Slowik & Balogh, 1980).

Cell migration involves three steps: ECM attachment mediated by adhesion proteins (Wolfenson, Lavelin, & Geiger, 2013), contractile forces mediated by Rho GTPase and myosin (Beadle et al., 2008) (Kwiatkowska & Symons, 2013), and ECM detachment mediated by proteases including uPA, ADAMs, and matrix metalloproteinases (MMPs) (Kwiatkowska & Symons, 2013). The gelatinous brain parenchyma lacks fibrillar collagen and is filled with proteoglycans, axonal processes encased by myelin, and capillaries surrounded by collagens (type I and IV), fibronectin and vitronectin (Cuddapah, Robel, Watkins, & Sontheimer, 2014a; Gritsenko, Ilina, & Friedl, 2012). Proteoglycans are inhibitory to tumor migration (Tamaki, McDonald, Amberger, Moore, & Del Maestro, 1997). Activation of proteases contributes to ECM remodeling and is especially essential for cell migration in the brain given the narrow extracellular space, only 20-60 nm in width, in the parenchyma (Nicholson, Kamali-Zare, & Tao, 2011).

1.1.5 Glioblastoma and matrix metalloproteinase

Numerous MMP family members are upregulated in GBM, including MMP-1, MMP-2, MMP-9, MMP-11, MMP-14, and MMP-19 (Forsyth et al., 1999; Stojic et al., 2008) (Musumeci et al., 2015). In T98G GBM cells, EGF can induce *MMP-1* expression in an MAPK-dependent manner separate from PI3K/AKT signaling (Anand, Meter, & Fillmore, 2011). Activation of N-methyl-D-aspartate receptors of glutamate increases MMP-2 but not MMP-9 in U87 MG and U251MG cells (Ramaswamy, Aditi Devi, Hurmath Fathima, & Dalavaikodihalli Nanjaiah, 2014).

Elevated expression of both MMP-2 and MMP-9 are correlated with higher glioma grade (Rao et al., 1993; Maode Wang, Wang, Liu, Yoshida, & Teramoto, 2003). MMP-2 and MMP-9 are known to promote GBM invasion (Rahme & Israel, 2015; Zhao et al., 2010). MMP-2 and MMP-9 secreted by endothelial cells enhance perivascular migration of neural progenitors (L. Wang et al., 2006). However, in *MMP-2* knockout GBM, vessel density increased but showed dysfunctional phenotype characterized with low levels of VEGFR2 expression, reduced pericyte attachment, and lower perfusion. As a result, there is an increase in tumor cell apoptosis and in the number of tumor cells migrating along the blood vessels in *MMP-2* knockout GBM (R. Du et al., 2008), suggesting MMP-2 is not required for perivascular invasion of GBM. Moreover, only MMP-9 expression is localized at the perivascular niche in GBM (Forsyth et al., 1999). We therefore hypothesize that it is MMP-9 that promotes perivascular invasion of GBM. This is an important part of my thesis project.

GBM cells with robust stemness and high plasticity often reside at the perivascular niche as described above. Perivascular MMP-9 may function as a pro-invasive factor for GNS as it is co-localized with perivascular CD44, a GNS marker (Pietras et al., 2014), and cleaves its extracellular domain, leading to enhanced migration and invasion (Chetty et al., 2012). It was also reported in another study that the intracellular domain of CD44 elicited HIF2α-mediated signaling in GNS cells at the perivascular niche (Pietras et al., 2014), which is in agreement with our hypothesis that MMP-9 function is involved in GBM migration/invasion. *MMP-9* expression can be upregulated through RAF-MEK-ERK and also through AKT/mTOR pathways (Das, Shiras, Shanmuganandam, & Shastry, 2011). A negative regulator of MMP-9 expression is miRNA-211, whose expression is frequently silenced in GBM by aberrant promoter DNA methylation (Asuthkar, Velpula, Chetty, Gorantla, & Rao, 2012). Re-expression of miR-211 led to GNS apoptosis and increased chemosensitivity and radiosensitivity (Asuthkar et al., 2012). The role of MMP-9 in glioma migration appears to be associated with uPAR signaling since uPA can directly activate MMP-9 (Zhao et al., 2008). Knockdown of both uPAR and MMP-9 elicit a stronger inhibitory effect on glioma migration than the individual knockdown (Veeravalli & Rao, 2012) (Schuler et al., 2012). MMP-9 may also serve as a non-invasive marker for disease management as MMP-9 upregulation has been detected in the serum of high-grade glioma patients (Hormigo et al., 2006); MMP-9 expression has also been shown to be correlated with contrast-enhanced MRI and patient prognosis (Awasthi et al., 2012). MMP-9 inhibition by RNAi significantly reduced GBM invasion, growth and angiogenesis (Jadhav, Chigurupati, Lakka, & Mohanam, 2004;

Lakka et al., 2004). However, how MMP-9 is upregulated in the perivascular niche is still unknown.

1.1.6 Glioblastoma perivascular invasion: implication of FOSL2/CD24

GBM cells were found to utilize myelinated axons and collagen-rich vessels sheaths for migration nearly 80 years ago {Scherer:1938wo}. The majority of GBM tumor cells are associated with blood vessels and undergo perivascular invasion when orthotopically injected into mouse brain (Montana & Sontheimer, 2011). Perivascular invasion is advantageous to GBM infiltration because there is considerably less physical resistance in the perivascular space (Cuddapah, Robel, Watkins, & Sontheimer, 2014a). It was reported that GBM cells with perivascular invasion migrate 3-fold faster than those without perivascular invasion (Winkler et al., 2009).

Chemotactic factor bradykinin secreted by endothelial cells mediates tumor cell recruitment by regulating the volume of GBM cells during migration to the vessels via a G protein-coupled receptor-mediated ion channel (Montana & Sontheimer, 2011). Anti-angiogenesis therapy normalized tumor vasculature in the U87 orthotopic xenografts and promoted increased tumor invasion in the perivascular space (de Groot et al., 2010). Once being recruited to the vessels, adhesion molecules maintain a direct interaction between tumor cells and vessels facilitating perivascular migration. We hypothesize that CD24 is such a molecule that mediates the interaction of GBM cells to blood vessels.

CD24 is a heavily glycosylated cell surface protein linked to the cell membrane via a GPI anchor (Poncet et al., 1996) and is expressed in the hematopoietic system and neuronal tissues. It is also highly expressed in many carcinomas and is associated with invasive

growth and poor prognosis in breast, ovarian, colorectal, pancreatic, prostate, bladder cancer (Kristiansen, Sammar, & Altevogt, 2004). CD24 transduces signals through recruiting the Src family protein tyrosine kinase and activating the MAPK pathway for invasion (X. Fang, Zheng, Tang, & Liu, 2010). During neurogenesis, interaction between CD24 on neural progenitor cells and its adhesion receptor P-selectin on endothelial cells regulates proliferation and migration of neural precursor cells (Calaora, Chazal, Nielsen, Rougon, & Moreau, 1996; Goldman & Chen, 2011; Nieoullon, Belvindrah, Rougon, & Chazal, 2005).This CD24/P-selectin interaction has been implicated in the movement of breast cancer cells along the vessels during metastasis (Aigner et al., 1998). In GBM, *CD24* upregulation is correlated with a poor GBM prognosis (J. Deng et al., 2012). *CD24* overexpression increases GBM tumor invasiveness *in vivo* but not *in vitro* (Senner, Sturm, Baur, Schrell, Distel, & Paulus, 1999a), suggesting that CD24-mediated GBM invasion is dependent on microenvironmental factors, potentially through interaction with endothelial cells.

CD24 expression can be regulated by the Ral GTPase pathway in bladder cancer (S. C. Smith et al., 2006), by HIF-1α and androgen in prostate cancer (Overdevest et al., 2012; Thomas et al., 2012), and by FOSL2 in neuronal tissues (M. Smith et al., 2001). FOSL2 is a Fos family transcription protein that can heterodimerize with the Jun family protein to form the AP-1 complex modulating downstream gene expression (David, Rincon, Neff, Horne, & Baron, 2001; Nishina, Sato, Suzuki, Sato, & Iba, 1990). Phosphorylation of FOSL2 allows for efficient DNA binding (Gruda, Kovary, Metz, & Bravo, 1994) and triggers a positive feedback mechanism for *FOSL2* expression by binding to the AP-1 sites at its own promoter region (Murakami, Ui, & Iba, 1999). FOSL2 induces cell

adhesion factors including L1-CAM, integrin alpha 6, CD44, and ICAM-1 and also enhances E-selectin-mediated rolling of breast cancer cells (Schröder et al., 2010). L1-CAM functions as a receptor for 2,3-linked sialic acid on CD24 and can mediate neural outgrowth (Kleene, Yang, Kutsche, & Schachner, 2001). However, in tumor cells, CD24 primarily interacts with P-selectin (Aigner et al., 1997). Interaction between CD24 and P-selectin mediates breast cancer cell rolling on the surface of endothelial cells (Aigner et al., 1998). Perivascular infiltration of GBM cells is associated with a high proliferative status (Farin et al., 2006) and disruption of the blood-brain barrier. Therefore, targeting perivascular infiltration of GBM may be a complementary therapeutic option.

In GBM, FOSL2 is a master transcriptional factor regulating the gene signature in the mesenchymal GBM subtype (Carro et al., 2010). The functions of FOSL2 in other GBM subtypes are less well characterized. It also remains to be studied how *CD24* expression is regulated and how it promotes GBM invasion *in vivo*. Given that FOSL2 may respond to ANG-dependent ERK activation, we hypothesize ANG activates GBM perivascular invasion through FOSL2/CD24. This is another important part of my thesis project.

1.1.7 Unmet needs in current glioblastoma treatment scheme

1.1.7.1 Blood-brain-barrier for brain diseases

Drug delivery is an often-encountered issue in treating brain diseases because most of the drugs are not able to cross the blood-brain-barrier (BBB). BBB is a protection system consisting of brain endothelial cells, pericytes, and astrocytes that selectively transport blood elements into the brain extracellular fluid under normal conditions, a process governed by tight junctions and p-glycoprotein (Schinkel, 1999). The central nervous system is fragile and lacks an adaptive immune system. Brain damage is largely irreversible since neurons are poorly regenerative. Therefore, an intact BBB is important to filter bacteria and neurotoxins in the circulating blood. In the healthy condition, BBB is impermeable to 98% of all small-molecule drugs and nearly 100% of large molecules such as monoclonal antibodies (Pardridge, 2005). However, a partially compromised BBB is often observed in inflammation (de Vries, Kuiper, de Boer, Van Berkel, & Breimer, 1997) and in GBM (Liebner et al., 2000). The compromised BBB allows small chemotherapy agents or large monoclonal antibodies to access brain lesions, in either primary brain tumors or metastasis conditions. Nonetheless, partially compromised BBB still poses a large hurdle in drug delivery to the brain (Agarwal, Manchanda, Vogelbaum, Ohlfest, & Elmquist, 2013; Jain, 2007). New tools have been developed to achieve more effective drug delivery to the brain lesions. For example; noninvasive focused ultrasound can induce regional BBB disruption (Konofagou et al., 2012); reengineering drugs with Trojan horse delivery systems can allow access to the brain by receptor-mediated absorption (Pardridge, 2012); lipid modification can facilitate passive lipid-based uptake of the drug (J.-Q. Gao et al., 2013).

1.1.7.2 Anti-angiogenesis therapy

Vessel network supplying nutrients and oxygen to GBM is a prognostic factor in malignant astrocytoma (Birlik, Canda, & Ozer, 2006; Leon, Folkerth, & Black, 1996). In fact, one of the histological diagnostic features of GBM is vascular hyperplasia, suggesting that anti-angiogenesis could be a viable strategy for treating GBM. Bevacizumab is a monoclonal antibody inhibiting angiogenesis by the neutralizing tumor and stroma-related VEGF-A. It has been approved for treating GBM and other metastatic cancers including colon, renal, and cervix neoplasms. Clinical trials conducted for these diseases all showed robust objective response rates. For example, treatment of bevacizumab-alone for recurrent GBM patients doubled both objective response and 6-month-survival rates (Friedman et al., 2009). Bevacizumab also improved the quality of life by reducing the need for steroid in GBM patients, as the brain edema and high intracranial pressure-related neurological symptoms were effectively relieved by vessel normalization (Henriksson, Asklund, & Poulsen, 2011). However, patients didn't benefit from increased overall survival as tumors reappeared with a more invasive phenotype (Keunen et al., 2011; Norden et al., 2009; T. Xu, Chen, Lu, & Wolff, 2010). Similarly, in newly diagnosed GBM, bevacizumab also showed a higher progression-free-survival rate but failed to extend the overall survival (Chinot et al., 2014).

The paradox of strong response rate, monitored by MRI, and no impact on overall survival of GBM patients could be due to bevacizumab-related pseudo-response in T1-MRI assessment. Bevacizumab treatment reduces T1 contrast-enhanced signal due to its vasculature normalization effect. However, tumor progression is still occurring which can

be visualized by T2/FLAIR, suggest that GBM cells respond to anti-angiogenesis treatment by modulating progression. This pseudo-response illustrates the enhanced invasive phenotype of the recurrent GBM and may explain the discrepancy between the high response rate and no overall survival benefit observed in the clinic (Tanaka, Louis, Curry, Batchelor, & Dietrich, 2013).

Histological evaluation of the recurrent tumors revealed a tendency toward perivascular invasion in bevacizumab-treated GBM (A. J. Clark et al., 2012a). As mentioned above, the perivascular niche enriches GNS cells and provides permissive adhesion factors for GBM cell invasion. A recent study proposed a VEGF-independent autovascularization model for GBM invasion and growth (Baker et al., 2014). This model was based on the finding that brain tissues contained an extremely high density of microvessels so that the angiogenic switch may not be required for continuous tumor growth in the brain. Instead, GBM and other brain tumor cells migrate along the existing vessels to obtain oxygen, glucose, and other nutrients. ANG and bFGF are the two angiogenic factors that showed robust upregulation in U87 cells after bevacizumab treatment (Lucio-Eterovic, Piao, & de Groot, 2009). ANG is known to promote bladder cancer progression via MMP-2 upregulation (Miyake, Goodison, Lawton, Gomes-Giacoia, & Rosser, 2014) and bFGF is a major factor to sustain GNS stemness. Understanding how upregulated ANG/bFGF contribute to perivascular invasion of GBM will be important to overcome bevacizumab-resistant GBM recurrence.

1.1.8. Current lab tools for glioblastoma study

Patient-derived GBM cell lines have been used as a convenient system to conduct GBM research because most of the tumor biopsies can readily adapt to the plastic serum culture condition on the 2D plastic plates. Those cell lines can also be used to establish xenograft tumors in mice for *in vivo* studies. However, after long-term passages, the effects of serum-induced differentiation and prolonged 2D culture method decrease the heterogeneity in those serum lines, giving rise to new mutations, and resulting in different gene expression profiles from the parental tumors (J. Lee et al., 2006).

GNS cell culture is another *in vitro* system to conduct GBM research. Compared with the serum-adapted GBM cell lines, gene expressions and invasive growth pattern of those GNS xenografts more closely resemble to the parental tumors (J. Lee et al., 2006; Wakimoto et al., 2012). Like neural stem cell medium, the GNS culture medium uses defined growth factors (EGF/FGF) to sustain stemness. However, it usually takes longer and has a much lower efficiency to establish stable GNS lines from biopsies compared to serum-containing culture. Moreover, GNS intracranial xenografts can rarely recapitulate the necrotic features that are the hallmark of human GBM (Wakimoto et al., 2012). There are also other minor limitations, such as scale-up difficulties from slow-cycling neurospheres and the high cost of culture medium.

In order to maintain the heterogeneity of the parental tumors and also to increase the success rate of establishing cancer lines, tumor cells from GBM biopsy mixed with Matrigel can be subcutaneously injected into the flank of nude mice for *in vivo* passage

(Carlson, Pokorny, Schroeder, & Sarkaria, 2011). This method allows for almost 100% tumor success rate to establish primary cancer lines, maintains both GNS and differentiated tumor cells in the biopsy specimen, and displays the necrosis features in xenograft models. However, this method requires mixing tumor cells with Matrigel and it is unknown whether it would change gene expression in tumor cells or affect GNS. Moreover, this *in vivo* passaging method requires maintaining a large number of nude mice and thus is only suitable for labs with those resources.

Although use of human GBM xenograft in nude mice is well established, it lacks immunologic components involved in disease progression and not suitable for studying gliomagenesis. A transgenic mouse GBM model is an advantageous alternative. Proneural human GBM can be modeled by PDGF-β overexpression in *Nestin*$^{+}$ *Ink4a/Arf* null progenitor cells (Uhrbom & Holland, 2001); EGFR activation in *PTEN* null *Ink4a/Arf* null mouse brain can induce the classical subtype (H. Zhu et al., 2009); the mesenchymal GBM can be modeled by *NF1* and *TP53* mutations (Reilly, Loisel, Bronson, McLaughlin, & Jacks, 2000). Mouse GBM developed in these models resembles human GBM with vascular hyperplasia, pseudopalisading necrosis, and nuclear pleomorphism. However, these transgenic mouse models oversimplify the genomic alterations seen in human GBM. They are also limited to a small number of genetic backgrounds (Holliday, 1996; Rangarajan, Hong, Gifford, & Weinberg, 2004). Therefore, findings from these mouse models need to be cautiously validated in human GBM tissues.

1.2 The biology of Angiogenin

Angiogenin (ANG) was first identified from the conditioned medium of HT-29 colon adenocarcinoma cell line for its potent activity to induce extensive blood vessel growth (Fett et al., 1985; Strydom et al., 1985). Human *ANG* is located on chromosome 14, ranging from 20,684,176 to 20,694,185 base pair in the genomic locus 14q11.1-q11.2. Its amino acid sequence shares a 35% similarity with that of pancreatic ribonuclease A, and is highly conserved at residues responsible for RNA cleavage activity (Kurachi, Davie, Strydom, Riordan, & Vallee, 1985). Yet, ANG shows different substrate specificity compared to other pancreatic ribonucleases (Shapiro, Riordan, & Vallee, 1986). It is expressed in a wide spectrum of tissues but at a predominately high level in adult liver, where its expression escalates developmentally from fetus to adult stage (Strydom et al., 1985; H. L. Weiner, Weiner, & Swain, 1987).

Upon receptor-mediated endocytosis, ANG is translocated to the nucleus of the cells, likely mediated through early endosomes. There are debates on the dynamic of this process and what happens after ANG reaches the perinuclear region. In HUVE cells, ANG undergoes rapid nuclear translocation within 2 min without being released to the cytosol and saturates in the nucleus within 60 min (G. F. Hu et al., 2000). Whereas in aortic smooth muscle cells, ANG uptake peaks fast at 2 min but followed by constitutive uptake for 24 hr. Instead of directly entering the nucleus, perinuclear ANG gives rise to a disperse pattern of ANG in the cytoplasm in smooth muscle cells (Hatzi, Bassaglia, & Badet, 2000). There are also discrepancies in the half-life of ANG between the two cell lines. The exact reason for the discrepancies is not known, but differential uptake and

processing may contribute to distinct ANG function in endothelial cells and smooth muscle cells.

Its physiological roles involve reproduction, inflammation, innate immunity, repair of damaged tissues and hair growth. ANG regulates angiogenesis and morphological changes in the ovary during the reproductive cycle (H. S. Lee, Lee, Kang, Jeong, & Chang, 1999). In placenta development, ANG expression increases through pregnancy and spatially expands from the trophoblast layer to endothelial cells (Pavlov et al., 2003; Rajashekhar, Loganath, Roy, & Wong, 2002). Dysregulated ANG expression was observed in intrauterine growth retardation placenta (Rajashekhar, Loganath, Roy, & Wong, 2003). ANG is also an acute phase protein that responds to inflammation and trauma (Olson, Verselis, & Fett, 1998). Circulating ANG in the human body has been shown to be induced following inflammation and exhibits species-selective direct microbicidal activity against *C.albicans* and *S.pneumoniae* (Hooper, Stappenbeck, Hong, & Gordon, 2003; Koutroubakis et al., 2004). Upregulation of ANG induces expression of IL-1, IL-6, and TNF-α in blood leukocytes to promote inflammation, demonstrating its role in innate immune response (Shcheglovitova, Maksyanina, Ionova, Rustam'yan, & Komolova, 2003). During burn wound healing, ANG in the blister fluid can induce endothelial cell differentiation independent of VEGF (S.-C. Pan, Wu, Chen, Shieh, & Chiu, 2012a). ANG is also expressed in the hair follicle during the late growth phase and induces proliferation in dermal papilla cells and outer root sheath keratinocytes; local injection of ANG showed stimulatory effect on mouse hair growth (Zhou, Fan, & Li, 2009).

Our lab has generated germline knockout mice, B6.B6129S6-*Ang*^{tm1GH} (unpublished data), to understand the physiological functions of ANG. When *Ang* knockout mice inbreed, their litter sizes are 40-60% smaller than that of the wildtype, suggesting an important role of Ang in the uterus/prenatal development. Although the exact causes of those prenatal deaths are not concluded, they may be linked to impaired angiogenesis because reduced vascularization was observed in the dead E12.5 embryos. A small number of *Ang* knockout mice are able to live through early development and grow asymptomatically. Blood testing and gross necropsy of adult *Ang* knockout mice revealed an abnormality in red blood cells, platelet composition and the size of spleen, where B cell maturation and blood filtering primarily take place. In adult *Ang* knockout mice, graying hair and deregulated melanin deposition in the skin were found with high penetrance. Investigation of the physiological roles of ANG in those phenotypes is ongoing. This *Ang* knockout mouse line is an excellent tool to study the role of ANG in tumorigenesis and tumor progression.

1.2.1. Function as an angiogenic factor

Angiogenesis is a process by which new vessel networks are formed from existing vessels. The process starts with the exit of pericytes and vessel dilation that lead to destabilization of the pre-existing vessels, followed by vessel sprouting characterized by endothelial cells migration and proliferation, and lastly with recruitment of pericytes and vessel maturation (Bergers & Benjamin, 2003). Without angiogenesis, tumor mass stops growing after it reaches a size of 2 mm^3 (1x 10^6 cells) at which point extra oxygen and nutrients supply are required (Folkman, 1971; Folkman & Hochberg, 1973). Thus,

tumors are known to activate the angiogenesis program, a process also called the angiogenic switch. Angiogenesis is essential for all solid tumor progression and metastasis.

ANG is a potent angiogenic factor such that only 3.5 pmol of it is sufficient to induce extensive blood vessel growth in the rabbit cornea (Fett et al., 1985). It stimulates angiogenesis by inducing endothelial cells migration/invasion and proliferation. Exogenous ANG increased invasiveness of transformed bovine aortic endothelial cell line 5-fold, which was associated with 14-fold increase in the cell-associated proteolytic activity, presumably through neutralizing the inhibitory effect of actin on tissue-type plasminogen activator/plasmin (G. F. Hu & Riordan, 1993; G. Hu, Riordan, & Vallee, 1994). Active plasmin can further activate MMP-2 and MMP-9 to promote angiogenesis. (Monea, Lehti, Keski-Oja, & Mignatti, 2002; Ramos-DeSimone et al., 1999; Taraboletti et al., 2002). However, active plasminogen also exerts a negative feedback mechanism by promoting elastase-mediated ANG cleavage to temper angiogenesis (G. F. Hu, 1997). Phospholipase C activation and angiogenic activity of ANG appear to require the ribonucleolytic activity of ANG since modification of the responsible residues His-13/His-114 diminishes PLC activation and angiogenic activity (Bicknell & Vallee, 1988).

The ribosomes are the cytosolic machinery responsible for protein synthesis. In a eukaryote, they have two subunits of 60S and 40S in size. Ribosomal RNA (rRNA) is the major component in each subunit: 5S, 5.8S, and 28S in the 60S subunit and 18S in the 40S subunit. The rate-limiting step of ribosome biogenesis is rRNA transcription (Moss,

2004). The 18S, 28S and 5.8S rRNA are transcribed by RNA polymerase I as a 47S precursor that are immediately processed into 45S pre-rRNA before being further processed into mature rRNA. ANG contains a nuclear location signal sequence ^{30}MRRRG^{34} that mediated nuclear translocation of ANG in endothelial cells (Moroianu & Riordan, 1994). The mechanism underlying ANG nuclear translocation is still not fully understood, as the nuclear localization signal of ANG does not require the conventional importing machinery, independent of microtubules and lysosome (R. Li, Riordan, & Hu, 1997), importins and Ran, but needs cytosolic factors and ATP (Lixin, Efthymiadis, Henderson, & Jans, 2001). PLC activation but not PKC or RTK activation seems to be required for nuclear translocation of ANG (G. F. Hu, 1998). Nuclear ANG specifically binds to a string of CT repeats (CTCTCTCTCTCTCTCTCCCTC), termed Angiogenin-Binding-Element (ABE), in the intergenic spacer of the ribosomal RNA gene and activates its transcription (Z.-P. Xu, Tsuji, Riordan, & Hu, 2002; 2003). Later it was found that ANG also binds at the promoter region of rRNA gene. Histone methylation at the neighboring DNA are reduced upon ANG binding, resulting in RNA polymerase (Pol) I-mediated rRNA transcription activation (Sheng, Yu, Gao, Xu, & Hu, 2013; Z.-P. Xu et al., 2003). A strong interaction between Histone 3 and ANG was found, which suggests that ANG may recruit histone demethylase to mediate its effects on histone modification. However, a luciferase plasmid construct containing the ABE element also responds to ANG activation of Pol II-dependent transcription in the absence of histone modification (Z.-P. Xu, Tsuji, Riordan, & Hu, 2003), suggesting that DNA methylation or recruitment of other transcription factors may also play a major role and that ANG can actually regulate Pol II-mediated transcription. Nuclear localization of ANG and

activation of ribosomal biogenesis are essential for the angiogenic activity of ANG and is a common prerequisite for other angiogenic factors including VEGF, EGF and bFGF to induce endothelial cells proliferation and angiogenesis (Kishimoto, Liu, Tsuji, Olson, & Hu, 2005).

1.2.2 Function as a growth factor

1.2.2.1 Neoplastic transformation

Activation of ribosome biogenesis is linked to neoplastic transformation (Montanaro, Treré, & Derenzini, 2008). In many neoplasms, the frequently activated PI3K/AKT pathway enhances ribosomal protein production by inducing transcription of translation initiation factors and ribosomal proteins via the mTOR/S6 pathway (Jefferies et al., 1997). ANG-mediated rRNA transcription couples AKT/mTOR/S6-mediated synthesis of ribosomal protein in ribosome biogenesis and contributes to neoplastic transformation. In a mouse prostate intraepithelial neoplasia model where AKT activation is driving the oncogenic transformation, inhibition of ANG, the most significantly upregulated gene by AKT activation in this model, suppressed rRNA transcription and inhibited tumor growth (Ibaragi, Yoshioka, Li, et al., 2009b). In HeLa and various other types of cancer cell lines, nuclear ANG induces rRNA transcription and enhances tumor proliferation (Ibaragi, Yoshioka, Li, et al., 2009b; Kishimoto et al., 2014; Y. Liu et al., 2015; Tsuji et al., 2005). Nuclear translocation of ANG can be regulated by FHL3 (Xia et al., 2012), an ANG binding partner that also regulates Smad in the TGF-β pathway (L. Ding et al., 2009). It would be interesting to see if ANG/FHL3 binding will affect TGF-β signaling, which would further expand the implications of ANG in cancer. In addition to directly

affecting tumor cells, ANG also functions as a paracrine factor to modulate tumor microenvironment. For example, hepatoma cells secret ANG to promote pro-fibrotic transdifferentiation of hepatic stellate cells and that, in turn, feed tumor growth by modulating the ECM (Bárcena et al., 2015).

1.2.2.2 Anti-apoptosis mediated by cell cycle inhibitors and Bcl-2 family protein

ANG can also enhance growth by inhibiting cell cycle inhibitors and by reducing apoptosis. ANG inhibits p53 phosphorylation and contributes to MDM2-mediated p53 degradation. Reduced p53 leads to downregulation of cell cycle inhibitor p21 and pro-apoptotic Bax and upregulation of anti-apoptotic Bcl-2, which collectively gives rise to resistance to apoptosis and cell cycle progression (Sadagopan et al., 2012). p21 primarily functions as a cell cycle inhibitor by inhibiting CDK1/2-cyclin complexes in G1 and G2 phase leading to exit of cell cycle (Gartel & Tyner, 2002). This allows for either DNA repair and continued proliferation or initiation of the apoptosis cascade. Accumulation of p21 is linked to proteasome malfunction or DNA damage-induced cancer cell apoptosis (S. Kondo et al., 1996; Martinez et al., 2002). But in other scenarios p21 induction protects from apoptosis. Adriamycin induces apoptosis in *p21* null HCT116 colon carcinoma cells but growth arrest in p21 wildtype HCT116 cells (Bunz et al., 1999). Thus, p21 is capable of inducing growth arrest or senescence but its role in apoptosis depends on cellular contexts. ANG can also regulate p21 through ERRγ, which is the first Pol II transcribed gene reported to be governed by ANG (Ang, Sheng, Lai, Wei, & Gao, 2013). ANG binds to the first intron of ERRγ gene and suppresses its transcription activity. Down-regulation of ANG leads to increased ERRγ occupation in the promoter

regions of cell cycle inhibitor genes, p21 and p27. However, ANG binds to ERRγ intron through a sequence that is distinct from ABE sequence found in the rRNA gene. Whether ANG can interact with targeted genes at the promoter region remains to be investigated. Identification of other transcriptional targets of ANG and their characterization will help delineate the multi-functions of ANG in cancer progression and in anti-apoptosis.

Bcl-2 and Bax are the major sensors of death checkpoint in the intrinsic apoptosis pathway. Bcl-2 and other anti-apoptotic Bcl-2 family protein inhibit apoptosis by preventing Bax-dependent permeabilization of mitochondria, releasing of cytochrome c, and formation of apoptosome, which is the engine driving the apoptosis cascade. ANG can also upregulate Bcl-2 though NF-κB pathway and inhibit damages to mitochondrial membrane, protecting P19 neuronal carcinoma cells from serum withdrawal-induced apoptosis (S. Li, Yu, & Hu, 2012; S. Li, Yu, Kishikawa, & Hu, 2010). In addition to upregulation of Bcl-2 and downregulation of Bax by p53, in *TP53* mutant cancer cells there are additional regulation and post-translational mechanisms allowing Bcl-2 not to be inhibited by BH-3 only pro-apoptotic protein. For instance, Bim can sequester Bcl-2 and neutralize its anti-apoptotic effects. PI3K/AKT and MEK/ERK are frequently hyperactive in various types of cancer cells. Active PI3K/AKT downregulates Bim expression by directly phosphorylating its transcription activator FoxO3a and diminishing its stability and transcriptional activity (Gilley, 2003).Active MEK/ERK can post-translationally promote ubiquitin-mediated proteasome degradation of Bim via direct phosphorylation (Ley, Balmanno, Hadfield, Weston, & Cook, 2003). Through these regulatory pathways, the apoptosis pathway can be readily shut off in cancer cells.

1.2.2.3 Anti-apoptosis mediated by tRNA cleavage

In response to a stress condition, cells slow down or selectively suppress ATP-costly processes, e.g. protein translation, and decrease anabolic activities to conserve energy for repairing stress-induced damages (Yamasaki & Anderson, 2008). ANG is induced under inflammation and hypoxia conditions (Hartmann et al., 1999; Verselis, Olson, & Fett, 1999) as well as in stress conditions.

Under stress conditions, tumors activate stress-response mechanisms and secrete autocrine signaling molecules, such as ANG, to sustain tumor progression. The ribonucleolytic activity of ANG is responsible for cleaving tRNA at the TψC loop to generate the 30-50 bp 3' tiRNA (tRNA-derived, stress-induced small RNA) and 5' tiRNA (H. Fu et al., 2009; Yamasaki, Ivanov, Hu, & Anderson, 2009). A survival mechanism through tRNA cleavage has been observed in starvation-induced *Tetrahymena thermophile* (S. R. Lee & Collins, 2005) and implicated in all eukaryote cells in response to oxidative stress (Thompson, Lu, Green, & Parker, 2008). Stress leads to cytoplasmic translocation of nuclear ANG in a manner depending on RNH1 (Pizzo et al., 2013), through which ANG reprograms protein translation. The absence of ANG-mediated rRNA transcription in stress condition is compatible with reduced anabolic activity in the stress condition. Cytoplasmic ANG is found in the stress granules where dislocated translation initiation complex and untranslated mRNA accumulate (Emara et al., 2010). Stress granule formation is correlated with decreased translation initiation (Anderson & Kedersha, 2009). Both ANG and 5' tiRNA can potentiate stressed-induced stress granule formation (Shi et al., 2006), indicating that 5'tiRNA could be the major

mediator of the inhibitory effect of ANG on translation. Enzymatically inactive ANG mutants could not protect motoneuron from stress-induced apoptosis (Kieran et al., 2008; Skorupa et al., 2012), confirming the important role of tiRNA in anti-apoptosis actions of ANG.

Stress-induced phosphorylation of eIF2α sequesters eIF2β and reduces the amount of eIF2-GTP-$tRNA^{Met}$ that is required for translation initiation of most transcripts. Translation can also be halted in an eIF2α-independent pathway. For instance, 5'-$tiRNA^{Ala/Cys}$ forms a G-quadruplex structure (Ivanov et al., 2014) that protects the small RNA from further degradation, and cooperate with YB-1 to inhibit eIF4F-mediated capped mRNA translation and to attenuate eIF4G-mediated uncapped mRNA translation. The level of inhibition on uncapped mRNA is dependent on the strength of eIF4G binding to the internal ribosomal entry binding site (IRES) (Emara et al., 2010; Ivanov, Emara, Villen, Gygi, & Anderson, 2011). This translation control mechanism suggests ANG could selectively activate translations of anti-apoptotic genes including BAG-1 (Coldwell et al., 2001), Bcl-2 (Sherrill, Byrd, Van Eden, & Lloyd, 2004), cIAP1 (Graber, Baird, Kao, Mathews, & Holcik, 2010), Lef-1 (B. P. Tsai et al., 2014), Hiap2 (Warnakulasuriyarachchi, Cerquozzi, Cheung, & Holcik, 2004), and XIAP (Holcik, Lefebvre, Yeh, Chow, & Korneluk, 1999); angiogenic genes such as HIF1α (Lang, Kappel, & Goodall, 2002), VEGF (Stein et al., 1998), Tie2 (E.-H. Park, Lee, Blais, Bell, & Pelletier, 2005), FGF-1 (Martineau et al., 2004), FGF-2 (Bonnal et al., 2003), and IGF1R (Giraud, Greco, Brink, Diaz, & Delafontaine, 2001); and oncogenes and genes associated with epithelial-mesenchymal-transition (EMT) such as LamB1 (Petz, Them,

Huber, Beug, & Mikulits, 2012), vFLIP (Othman et al., 2014), c-Myc (Stoneley, Paulin, Le Quesne, Chappell, & Willis, 1998), c-Myb (Mitchell et al., 2005), Runx1 (Pozner et al., 2000) and RunX1T1 (Mitchell et al., 2005). As Bcl-2 translation is mediated through IRES mechanism, it explains how ANG induced a higher increase in Bcl-2 protein than its mRNA under starvation condition. In addition to inhibiting translation initiation, tiRNA can also directly elicit the anti-apoptosis effect by interacting with Cytochrome C to prevent apoptosome formation and to reduce downstream Caspase-9 cascade activation (Saikia et al., 2014).

The production of tiRNA is highly regulated by the availability of active ANG, the abundance of RNH1, the amount of tRNA substrate, and protein synthesis rate (Saikia et al., 2012). Some tRNA species can be methylated by Dnmt2 and become resistant to ANG-mediated cleavage (Schaefer et al., 2010). The mechanisms of tiRNA productions under different stress conditions also vary. ANG protein level doesn't change significantly under either oxidative or hypertonic stress, whereas RNH1 is sensitive to reactive oxygen species-mediated degradation under oxidative stress conditions (Saikia et al., 2012). Therefore, the inhibitory effect of RNH1 on ANG is abrogated by ROS attack.

1.2.2.4. Overcoming apoptosis during malignant transformation: anoikis and epithelial-mesenchymal transition

Anoikis is a distinct form of apoptosis that is caused by an inappropriate or insufficient contact of the cells with ECM (Frisch & Ruoslahti, 1997). Under normal conditions, integrins-mediated adhesion induces cell spreading and cytoskeletal organization and

suppresses anoikis (Howlett, Bailey, Damsky, Petersen, & Bissell, 1995; Muzio, Stockwell, Stennicke, Salvesen, & Dixit, 1998; Re et al., 1994). It is a natural protection mechanism against neoplasms and metastasis. The physiological tight junctions with neighboring normal cells and integrin-mediated ECM connection are frequently altered in the growing tumor mass thus posing a selection pressure for anoikis-resistant transformation.

Anoikis is primarily induced via a mitochondrial (intrinsic) pathway while cell surface death receptors (extrinsic) contribute to it as well. In non-transformed cells, loss of ECM adhesion reduces active Cyclin-CDK activity and thus is unable to pass the Rb-mediated G1 checkpoint (F. Fang, Orend, Watanabe, Hunter, & Ruoslahti, 1996). Bcl-2 family proteins are at the convergence point of the extrinsic and intrinsic apoptosis pathway and thus become an important modulator. Upon loss of ECM contact, PI3K/AKT and ERK signaling are decreased, which give rise to Bim accumulation in mitochondria to inhibit the pro-survival function of Bcl-XL (E. H. Cheng et al., 2001; Ley et al., 2003; Zha, Harada, Yang, Jockel, & Korsmeyer, 1996). Loss of ECM adhesion also reduces FAK activation and brings about downregulation of anti-apoptosis Bcl-2 protein (Frisch, Vuori, Kelaita, & Sicks, 1996a; Schlaepfer, Hanks, Hunter, & van der Geer, 1994).

Malignantly transformed cells become resistant to anoikis because the loss of ECM attachment is no longer sufficient to induce apoptosis. Benign carcinomas degrade the basement membrane and enter circulation upon acquiring an invasive phenotype during malignant transformation, a process termed epithelial-mesenchymal-transition (EMT). Anoikis resistance is a hallmark of EMT (Guadamillas, Cerezo, & Del Pozo, 2011). The

circulating tumor cells need to overcome even more anoikis stress to survive in the blood system in order to establish distant colonies. When cells become resistant to anoikis, they can be cultured in agarose and proliferate anchorage-independently. This anchorage-independent growth was found to reflect *in vivo* tumorigenicity (Shin, Freedman, Risser, & Pollack, 1975) and metastasis (Mori et al., 2009). Anoikis resistance transformation can be found not only in carcinomas, such as in breast cancer and colon cancer, but also is involved in non-carcinomas, such as melanoma, neuroblastoma and glioblastoma (Bonfoco, Chen, Paul, Cheresh, & Cooper, 2000; Russo et al., 2013; Z. Zhu et al., 2001), suggesting that this process is ubiquitous in cancer progression.

As anoikis resistance is a defining property of EMT, oncogenic aberrations that led to EMT essentially confer anoikis resistance and promote anchorage-independent growth (Frisch, Schaller, & Cieply, 2013). EMT initiation mechanisms are broadly classified by transcription factors, RNA modulation, TGF-β signaling, tyrosine kinase receptors signaling, and others including Wnt, Hedgehog, and Notch. In the classic fibroblast transformation model, immortalized mouse fibroblasts can be transformed with SV40LT and can be further made to metastasize (EMT phenotype) by expressing oncogenic Ras that leads to constitutive active RAS/RAF/MEK/ERK signaling. RAS/RAF signaling induces the EMT phenotype, increased cell motility and invasive behavior, by stimulating SNAIL1/2 and FOSL1 expression and activating Rho-GTPases activities (Frisch et al., 2013). Another FOS family protein, FOSL2, is required for constitutive active MEK- or virus-induced chicken embryo fibroblast transformation and anchorage-independent growth (Murakami et al., 1999; Suzuki et al., 1994). In addition to our hypothesis that

ANG-FOSL2 regulates perivascular invasion of GBM, this signaling pathway may also play a role in anchorage-independent growth or in EMT.

Deconstruction of epithelial junction resulting from loss of E-cadherin, claudins, and occludin are the early events in EMT (R. Y.-J. Huang, Guilford, & Thiery, 2012). E-cadherin is reduced in both EMT and anoikis-resistant cells. Loss of E-cadherin leads to inhibition of tumor suppressor *CDKN2A* (*Ink4a*/*Arf*) by suppressing its transcription factor TBX2 with active NRAGE, a protein sequestered in E-cadherin-ankyrin complex (Kumar et al., 2011). Down-regulation of E-cadherin is often accompanied by upregulation of N-cadherin, a phenotype termed E/N-cadherin switch, which can be promoted through TGF-β. (Araki et al., 2011)

TGF-β signaling is a dominant pathway that regulates EMT (J. Xu, Lamouille, & Derynck, 2009). In addition to regulating EMT transcription factors, TGF- β signaling is closely linked to ECM remodeling. MMP-2 and MMP-9 upregulated by TGF-β during EMT (E.-S. Kim, Kim, & Moon, 2004) further amplify TGF-β-induced EMT signaling through a positive feedback mechanism: the secreted latent form of TGF-β sequestered in ECM gets activated by MMP-2/9 (Nisticò, Bissell, & Radisky, 2012). Hippo pathway can mediate cooperation between TGF-β and Wnt signaling in inducing EMT and anoikis resistance (Gauger, Chenausky, Murray, & Schneider, 2011; Scheel & Weinberg, 2011; Varelas & Wrana, 2012). Transcription factors that are responsible for E-cadherin downregulation during EMT can also directly suppress apoptosis. For example, Twist inhibits *p14ARF* expression and suppresses Myc-ARF mediated apoptosis (Valsesia-

Wittmann et al., 2004). ZEB1 mediates E-cadherin to N-cadherin switch and MMPs upregulation in EMT. It also directly represses pro-apoptotic gene TP73 expression by binding to its first intron (Fontemaggi et al., 2001; Lamouille, Xu, & Derynck, 2014). NF-κB activates expression of *Twist1* as well as that of a series of anti-apoptotic genes including Bcl2, Bcl2l1, survivin, and IAP. Other coupling factors for EMT and anoikis resistance include FAK, ILK, and TrkB (Attwell, Roskelley, & Dedhar, 2000; Frisch, Vuori, Ruoslahti, & Chan-Hui, 1996b; Thiele, Li, & McKee, 2009).

EMT is required for tumor cells to metastasize to distant seeding regions (Yilmaz & Christofori, 2009). The reversal of EMT, a process termed Mesenchymal-Epithelial-Transition (MET), or shutdown of EMT is necessary for the distant colony to grow (Ocaña et al., 2012; J. H. Tsai, Donaher, Murphy, Chau, & Yang, 2012). Therefore, the plasticity state of EMT and MET is important for tumor progression. EMT has been implicated in cancer stem cell properties. Mesenchymal gene expression pattern has a $CD44^{hi}CD24^{low}$ breast cancer stem cell phenotype, which can be induced by expression of the master transcription factors SNAIL or TWIST (Mani et al., 2008).

Studies on the ANG natural inhibitor RNH1 have suggested a potential role of ANG in regulating EMT. Overexpression of *RNH1* led to restrained MMP-2 and MMP-9 expression as well as down-regulation of EMT factors including N-Cadherin, Snail, Slug, Vimentin and Twist both *in vitro* and *in vivo* in melanoma cell lines. The inhibited EMT phenotype corresponded to reduced *in vivo* tumor progression and less metastasis (X. Pan et al., 2012b). Similarly in bladder tumors, *RNH1* overexpression induces the EMT

phenotype by affecting integrin-linked kinase (Yao et al., 2013), a hub protein that is also required for TGF-β induced the EMT phenotype (Serrano, McDonald, Lock, & Dedhar, 2013). However, how the RNH1 function relates to MMP-2/9 expression, ILK signaling, and anchorage-independent growth is still unknown.

Loss-of-function mutations of *ANG* gene have been found in Amyotrophic Lateral Sclerosis (ALS) disease (Greenway et al., 2006) and Parkinson's disease (van Es et al., 2011). In ALS, ANG mutants led to neurite extension malfunction and increased stress-induced apoptosis in motor neurons (Kieran et al., 2008; Sebastià et al., 2009). Mutations of ANG affects neuronal survival and the ability to form stress granules (Thiyagarajan, Ferguson, Subramanian, & Acharya, 2012). Experiments have demonstrated a neuro-protective function of ANG against neurotoxins in dopaminergic neuronal cell lines (Steidinger, Standaert, & Yacoubian, 2011) and in an MPTP-induced mouse model for Parkinson's disease (Steidinger, Slone, Ding, Standaert, & Yacoubian, 2013).

1.2.3. ANG as a pro-invasive factor in cancer

As described above in endothelial cells, ANG promotes invasion through plasminogen activation induced by binding to actin during angiogenesis. Similar observations have been found in breast, bladder and prostate cancers where ANG promotes invasion through plasmin/MMPs. In breast cancer, ANG is co-localized with the plasminogen activation system and uPAR and that is required for the interaction of uPAR with uPA and generation of active plasmin (Dutta et al., 2014). ANG co-localizes with stress fiber components β-actin and MYH9, and regulates cytoskeleton dynamics as an essential

factor for FAK activation (Wei, Gao, Du, Su, & Xu, 2011). In prostate cancer, ANG expression correlates with the transition from benign prostate epithelial cell to invasive phenotype (Katona et al., 2005). In the prostate cancer microenvironment, tumor associated fibroblast invasion is increased in response to tumor secreted ANG (Jones, Ewing, Isaacsa, & Getzenberg, 2012). In bladder cancer, ANG can also transcriptionally activate MMP-2 through the ERK pathway independent of plasmin signaling (Miyake et al., 2014).

1.2.4. Targeting ANG in GBM

Nuclear translocation of ANG occurs only in fast-growing cells, like cancer cells and endothelial cell during angiogenesis. Under homeostasis, fibroblasts and epithelial cells do not need ANG to grow or to survive. This natural mechanism indicates that targeting ANG can specifically target cancers with minimal off-target effects. The ANG monoclonal antibody 26-2F, with IC_{50} of 1.6 nM, recognizes two surface loops juxtaposed in the 3D structure and can effectively inhibit ribonucleolytic and angiogenic activity of ANG (Fett, Olson, & Rybak, 1994). Treating xenograft bearing mice with 26-2F can effectively suppress tumor growth of various tumor types (Olson, Fett, French, Key, & Vallee, 1995; Olson, French, Vallee, & Fett, 1994). The clinical utility of targeting ANG has been demonstrated with an equally effective but less immunogenic mouse/human chimeric monoclonal antibody (cAb 26-2F) in a xenograft breast cancer model (Piccoli, Olson, Vallee, & Fett, 1998).

Neomycin is an aminoglycoside antibiotic and also a known PLC inhibitor that blocks nuclear translocation of ANG, and inhibits ANG-induced proliferation and angiogenesis in endothelial cells (G. F. Hu, 1998). However, it doesn't affect ANG-induced ERK activation in endothelial cells (S Liu, Yu, Xu, Riordan, & Hu, 2001). Neomycin has also been shown to inhibit the effects of ANG in xenograft growth of human prostate cancer in mice (Ibaragi, Yoshioka, Kishikawa, et al., 2009a; Yoshioka, Wang, Kishimoto, Tsuji, & Hu, 2006). However, neomycin has not been approved for treating any human cancers due to its severe side effects including permanent hearing loss, nerve damage, severe kidney damage, and muscle relaxation that can lead to paralysis or breathing problems (Ibaragi, Yoshioka, Li, et al., 2009b). Neamine, a derivative of neomycin with 20-fold lower toxicity (Williams, Bennett, Gleason, & Hottendorf, 1987), is equally effective in abolishing nuclear function of ANG and elicits a similar anti-tumor activity. (Hirukawa, Olson, Tsuji, & Hu, 2005). Similar inhibitory effects of neamine have been observed in breast cancer, oral cancer, and cervical cancer (Ibaragi, Yoshioka, Li, et al., 2009b; Kishimoto et al., 2014; Y. Liu et al., 2015). In those studies, neamine was given to mice via daily i.p. injection at 10 mg/kg and showed well-tolerated responses. For the more toxic neomycin, daily i.p. injection of 60 mg/kg has been used in a hepatocellular carcinoma mouse model and no severe adverse effects was reported (Bárcena et al., 2015). Temporal oral neomycin has been shown effective as a second-line therapy to treat irinotecan-induced diarrhea in colorectal patients, suggesting that an appropriate neomycin dosing can be possibly established for clinical usage (Alimonti et al., 2003; Kehrer et al., 2001). In sum, mAb 26-2F and neomycin are convenient, powerful ANG

inhibitors for research in early preclinical work. Neamine or other less-toxic derivatives are more suitable for further development.

1.2.5. The journey of identifying ANG receptor PLXNB2

Exogenous ANG enters cell nucleus in energy- and temperature-sensitive way, suggesting receptor-mediated endocytosis (Moroianu & Riordan, 1994). But ANG binds rapidly on the cell surface due to its high pI (>9.5) (Bicknell & Vallee, 1988), which is not a typical ligand-receptor interaction. This adds to the difficulty in identifying the *bona fide* ANG receptor. Later studies using calf pulmonary artery endothelial cells demonstrated two modes of interaction of ANG with the cell surface: 1) high specificity with dissociation constant of 5×10^{-9} M, and 2) low-specific/high-capacity with dissociation constant of 0.2×10^{-6} M (Badet et al., 1989). Interestingly the capacity of high specificity binding varies by cell density in the endothelial cells, indicating that the surface ANG receptor is controlled by cell density (Badet et al., 1989). A 42 kDa ANG binding protein (G. F. Hu, Chang, Riordan, & Vallee, 1991), with K_d of 5×10^{-10} M, was found in endothelial cells to interact with ANG at residues 60-68 and was later identified as α smooth muscle type actin (Hallahan, Shapiro, & Vallee, 1991; G. F. Hu, Strydom, Fett, Riordan, & Vallee, 1993). ANG inhibits surface actin polymerization and spatially interacts with plasminogen and plasminogen activator via actin (Dudani & Ganz, 1996; Pyatibratov et al., 2010). However, surface actin is not the receptor because its expression is not regulated by cell density, and it could not mediates internalization of ANG. In addition to α-actin, cell surface heparin can also interact with ANG and mediate its adhesive effect without significantly inhibiting its angiogenic and ribonucleolytic

activities (Soncin, Strydom, & Shapiro, 1997). However, high concentration of heparin (100 μg/ml) suppresses ANG nuclear translocation by 37% (G. F. Hu, Xu, & Riordan, 2000). One report suggested that syndecan-4, a 24 kDa heparin-containing proteoglycan, was the receptor for ANG in astroglia (Skorupa et al., 2012), as syndecan-4 is both required and sufficient to mediate ANG uptake. Syndecan-4 is in close proximity (<40 nm) with ANG and shows co-localization pattern in the cytosolic endosomes. It also revealed that cellular uptake of ANG is mediated by clathrin-dependent and not lipid raft-mediated endocytosis, and that interaction with heparin is essential for ANG uptake and concomitant tiRNA production. However, that study did not address the specificity of ANG/Syndeacan-4 interaction nor did it characterize essential interaction components in Syndecan-4. It is possible that ANG can interact with other proteoglycans as well. There is also no evidence showing that Syndecan-4 is downregulated in endothelial cells seeded at a high density where ANG can no longer enter the nucleus due to low cell surface receptor activity/expression. Therefore, it is highly likely that ANG is one of the angiogenic factors (e.g., FGF-2 and VEGF) (Fears & Woods, 2006; Tkachenko, Lutgens, Stan, & Simons, 2004) that Syndecan-4 binds as a co-receptor to mediated its endocytosis.

The difficulty of isolating the receptor mainly stems from the low expression in endothelial cells. Only when endothelial cells are cultured at low density (< 2 x 10^4 cells/cm^2) is ANG able to undergo nuclear translocation and induce endothelial cell proliferation (G. F. Hu, Riordan, & Vallee, 1997). In low-density endothelial cell culture, a 170 kDa protein was found to bind specifically to ANG (G. F. Hu et al., 1997). It is

interesting to note that when this putative protein is present, ANG no longer interacts with surface actin, suggesting that ANG/actin signaling may induce individual cell invasion, and that ANG interaction with the 170 kDa protein allows nuclear translocation and stimulates proliferation in the cells distant from the invading cells (G. F. Hu et al., 1997). However, the identity of this protein remained unknown for many years.

Important progress was made when the HeLa cancer cell line was examined for nuclear translocation of ANG. Different from endothelial cells, nuclear accumulation of ANG in HeLa cells is not cell density-dependent (Tsuji et al., 2005). This directly led to the discovery of the 170 kDa protein in another cancer cell line, where it is also constitutively present irrespective of cell density. This 170kDa protein is the extracellular cleavage product of PLXNB2 (unpublished data of our lab).

PLXNB2, one of the Plexin-B family protein, is a type-I transmembrane protein that is cleaved by proprotein convertases into α (170 kDa) and β (80 kDa) subunits at the cell surface (Artigiani et al., 2003; Tamagnone et al., 1999). The α subunit can either form a heterodimeric complex with the βsubunit at the cell surface or dissociate into the medium (Artigiani et al., 2003). Semaphorin-4C (Sema4C) is the cognate ligand for PLXNB2 and its binding to the extracellular Sema domain of PLXNB2 induces axonal growth cone collapse and shows pro-migratory effect on tumor cells (Tamagnone & Comoglio, 2000) (Giordano et al., 2002; Le et al., 2015). Physiological functions of PLXNB2 include those in neurogenesis (S. Deng et al., 2007; Hirschberg et al., 2010; Saha, Ypsilanti, Boutin, Cremer, & Chédotal, 2012), cardiovascular (Torres-Vázquez et al., 2004) and kidney

(Perälä et al., 2011) development, and immune system function (Roney et al., 2011). In the central nervous system, PLXNB2 regulates neural progenitor cell migration and proliferation along the rostral migratory stream from the subventricular zone (SVZ) to the olfactory bulb (OB) (S. Deng et al., 2007; Saha et al., 2012). Like the undifferentiated neural progenitor cells, GBM exhibits tropism towards SVZ and OB (Kroonen et al., 2011), and thus PLXNB2 may mediate GBM invasion into the OB. PLXNB2 activates RhoA by releasing inhibitory Rnd3 effects on RhoA and also by recruiting RhoGEF (PDZ-Rho-GEF and LARGE) via its C-terminal domain. It is responsible for its influences on cortical neuron migration and axonal guidance (Azzarelli et al., 2014; Perrot, 2002). The effect of PLXNB2 on cell migration/invasion depends on cellular contexts: in cancer cells, PLXNB2 promotes migration/invasion (Le et al., 2015), whereas in non-cancer cell type such as macrophage and neural progenitor cells PLXNB2 inhibits migration (Roney et al., 2011; Saha et al., 2012). One possible mechanism is that amplification of receptor tyrosine kinases in cancer cells may play a switch function for PLXNB2-mediated migration/invasion, which needs to be further examined. ANG binds to PLXNB2 at amino acid residues 423-441, a region that barely overlaps with the Sema4C binding domain (unpublished). An important question to address is then how the two ligands affect each other in binding to the receptor and induce differentially downstream signaling.

1.2.6. ANG/PLXNB2 and GBM

GBM tumors feature high secretion of angiogenic factors and vascular glomeruli formation not seen in lower gliomas. Consistently, increased ANG expression was found

to correlate with higher grade of gliomas. The astrocyte secretome can be significantly modulated *in vitro* by constitutive ANG uptake (Skorupa et al., 2013). Therefore, ANG signaling may have physiological functions other than angiogenesis in GBM. This hypothesis was even proposed before the identification of PLXNB2 as ANG's receptor (Eberle et al., 2000). PLXNB2 was originally identified for its high expression in malignant brain tumors cells (Shinoura et al., 1995). Thus, it is reasonable to hypothesize that deregulation of PLXNB2 and autocrine ANG signaling may contribute to brain tumor progression. Indeed, microarray data and large cohort data confirmed ANG and PLXNB2 are both highly expressed in GBM (Brennan et al., 2013; Freije et al., 2004; Sun et al., 2006). Recently, PLXNB2 was shown to mediate the pro-invasive effect of Sema4C in GBM by activating RhoA and Rac1 and Met phosphorylation (Le et al., 2015). Moreover, PLXNB2 knockdown significantly inhibited perivascular invasion in a GNS xenograft. This finding supports our hypothesis that PLXNB2 mediates autocrine ANG signaling (FOSL2/CD24) in promoting perivascular invasion.

Neomycin treatment in C6 rat glioma cells showed reduced proliferation, slower migration, and a differentiated phenotype (Cuevas, Diaz-González, & Dujovny, 2003; 2004a; 2004b), suggesting that ANG may contribute to GBM proliferation, migration/invasion and differentiation through PLXNB2. Given the safety concern of neomycin, we plan to evaluate in-house PLXNB2 mAb in treating mGBM.

Summary

There is an urgent need to understand the resistant mechanism of GBM in bevacizumab treatment and the role of tumor vasculature in GBM progression and disease management. As one of the most upregulated genes in bevacizumab-treated GBM (Lucio-Eterovic et al., 2009), ANG may mediate tumor escape via its known pro-angiogenic, anti-apoptosis, and pro-invasive functions. However, the *in vivo* function of ANG has never been studied in GBM. In my thesis study, I test the hypothesis that ANG promotes GBM perivascular invasion through regulating FOSL2-mediated expression and/or activation of CD24 and MMP-9. Meanwhile, I investigate the role of PLXNB2 in mediating ANG function in GBM. Because proneural GBM is the most non-responsive subtype in the clinic, we use a proneural mouse GBM model to conduct the *in vivo* studies. Understanding PLXNB2-mediated ANG function in GBM could help elucidate bevacizumab resistance and the treatment of the more invasive, recurrent GBM.

Chapter II

Materials and methods

Animal Studies

Ntv-a; *Ink4a/Arf*$^{-/-}$ mice and RCAS-HA-PDGFB plasmid were kind gifts from Dr. Eric Holland (Memorial Sloan Kettering Cancer Center, New York, NY). The mice were bred on C57BL6 background with *Ang*$^{-/-}$ mice from our lab. For brain tumor induction, five weeks old mice were anesthetized with intraperitoneal injections of ketamine (0.1 mg/g) and xylazine (0.02 mg/g). Chicken fibroblasts (DF-1 cells, ATCC) transfected with RCAS-HA-PDGFB were intracranially delivered via a Hamilton syringe on a stereotactic fixation device into the subventricle zone of recipient mice: bregma 1.7 mm, Lat −0.5 mm, and a depth 2.5 mm (Hambardzumyan, Amankulor, Helmy, Becher, & Holland, 2009). Mice were monitored and sacrificed at moribund either with significant weight loss (25%) or severe neurological symptoms. For drug treatment, neomycin or paromomycin was administered intraperitoneally at a daily dose of 10 mg/kg, starting two weeks after tumor induction. For *in vivo* ectopic growth of cancerous and transformed cells, U87 or tMEF cells, 1.25 x 10^6 per mouse, were injected s.c. into the left flank of male athymic or B6 mice, respectively. Mice were palpated daily for the first sign of tumor appearance, after which tumor size was estimated twice a week with a microcaliper and recorded in mm^3 (length X $width^2$). For Matrigel plug assay, 5 x 10^6 cells were mixed with Matrigel and s.c. injected into 8 week old female B6 mice. After 6 days, Matrigels were dissected from the mouse skins and examined for vessels formation and tumor growth. All mouse experiments were performed with the approval of Tufts University/Tufts Medical Center IACUC.

Antibodies, siRNA and chemical reagents

Rabbit polyclonal antibodies against mouse ANG (R165) were prepared in our lab. Antibodies against β-tubulin (Santa Cruz), CD24 (eBioscience, 14-0247), MMP-9 (Bioss, bs-0397R), p44/p42 ERK (Rabbit mAb Cell Signaling, #4695), CD31 (Abcam), FOSL2 (Santa Cruz), N-Cad (Santa Cruz), HA (Sigma) were used at 1:1000 in TBST + 5% BSA for Western and 1: 200 in immunofluorescence. FOSL2 siRNA (sc-35407) and scramble control (sc-37007) were from Santa Cruz Biotechnology. The MEK inhibitor PD98059 (Cayman chemical) and the MMP-9 inhibitor CTK8G1150 (Santa Cruz) were used at the recommended concentration unless otherwise indicated. CellTracker^{TM} Orange CMTMR (Life technologies, C2927) was used according to manufacture's protocol.

Bioinformatics data mining

cBioPortal (MSKCC, New York, NY) and Oncomine™ Platform (Life Technologies, Ann Arbor, MI) were used for gene analysis and visualization. Classification of GBM tumor cohort was characterized previously (Brennan et al., 2013). Pathway enrichment was conducted by the DAVID Functional Annotation Tool.

Brain slice invasion

Experiment was conducted as previously described (Montana & Sontheimer, 2011). Briefly, 17-22 day-old pups were decapitated. Brains were taken out and put in an ice-cold bath of artificial CSF (ACSF). Tissues were sliced using a Vibratome 3000 sectioning system. Slices (300 μm thick) were allowed to recover in ACSF for 1 h at room temperature, followed by recovery in ACSF at 37°C in 95%/5% CO2/O2 for 1 h.

Slices were then transferred into Transwell migration cell culture inserts (BD Biosciences) with 8 μm pores. Then, 50,000 U87-GFP or *ANG* knockdown cells were seeded on top of the slices and allowed to invade into the tissue for 4 h at 37 °C. During that period, 2% FBS was added to the bottom of migration chamber to create a concentration gradient. Following double washes with PBS, slices were fixed in 4% paraformaldehyde over night at 4 °C. In the following day, samples were washed three times with PBS and the slices were incubated with CD31 antibody and matched secondary antibody for vessel detection under confocal microscopy.

Cell Culture, Transfection, and Generation of Stable Cell lines

U87, U251, HEK293T, and HUVEC used in this study have been previously published (Bagci et al., 2009; Sheng et al., 2013; Tsuji et al., 2005). DF-1 cells were obtained from ATCC. GNS cell lines, including GNS-6-22, GNS-11-1, and GBM8, were kind gifts from Brent Cochran (Tufts University School of Medicine, Boston, MA). U87, U251, HEK293T, and DF-1 were cultured in DMEM supplemented with 10% FBS, 100 U/ml penicillin, and 100 μg/ml streptomycin. HUVEC were maintained in human endothelial basal growth medium plus 5 ng/ml bFGF. GIPZ non-silencing GPF control shRNA construct was obtained from Thermo Scientific Open Biosystems as previously published (Sheng et al., 2013). Lentiviral particles were harvested in HEK293T cells conditional medium 72 hours after co-transfection with pCMV-VSV-G, pCMVΔR8.2 and the GIPZ GFP plasmid. Stable cell lines were generated after 1 μg/ml puromycin selection of the lentiviral transduced cells. Transfections with RCAS-PDGFB-HA were performed using Lipofectamine LTX with Plus transfection kit (Thermo Fisher Scientific). Lentiviral

vector encoding K-RasV12 and SV40LT were kind gifts from Charlotte Kuperwasser (Tufts University School of Medicine, Boston, MA).

Cell proliferation, soft agarose assay and AO/EB staining

Cells were plated at the same density in multiple replicates and trypsinized and counted using a Coulter Counter at indicated time points. For anchorage-independent growth assays, cells were suspended in medium containing 0.4% agarose and plated onto a solidified layer of medium-containing 0.8% agarose in 6-well plates. Colonies were quantified in five fields in each well 3 weeks post seeding. AO/EB staining was conducted as previously described (S. Li et al., 2010). Briefly, cells were mixed with 1:1000 dilution of the AO/EB dye (100 μg/mL each of AO and EB in PBS solution) at room temperature for 5 min. Stained cells were placed on a clean microscope slide and covered with coverslips. Microscopic images were taken with a Nikon digital camera (Nikon Corporation, Japan). A total of 500 cells were counted from each group. For AO/EB staining of colonies, the apoptotic percentage of each colony was measured by dividing the number apoptotic cells by the proximate number of cells in each colony, assuming each cell is a sphere 10 μm in diameter. Total 15 colonies were measured for each condition.

Chromatin Immunoprecipitation

U87 cells were cross-linked with 1% formaldehyde for 10 min at 37℃. Cross-linking reaction was quenched with 0.125 M glycine. The cells were collected and re-suspended in 50 mM Tris buffer, pH 8.1, containing 1% SDS, 10 mM EDTA and protease inhibitor

cocktail as previously described (Sheng et al., 2013). The lysates were sonicated and diluted with ChIP dilution buffer containing 16.7 mM Tris, pH 8.1, 0.01% SDS, 1.1% Triton X-100, 1.2 mM EDTA, 16.7 mM NaCl, and protease inhibitor cocktail. The diluted lysates were mixed with salmon sperm DNA/protein G/A agarose at 4℃ for 1 h. For each IP reaction, the lysates were incubated with 10 µg of antibody overnight at 4℃ with rotation. The immuno-complexes were collected with protein G agarose, eluted and de-crosslinked at 65℃. After RNase A and proteinase digestion, immunoprecipitated DNA was extracted and used for PCR analysis. For PCR reactions, 10% of the immunoprecipitated materials were used as the DNA template in 35 cycles of amplification with the primers list in Table 1.

Endothelial and tumor cells co-culture

The 96-well plate was coated with 30 µl of growth factor-reduced Matrigel (Phenol red free and growth factor reduced, BD). HUVEC, 1.5 x 10^4 per well, stained with CMTMR, was seeded on the Matrigel and cultured in the endothelial medium for 4 h to form tube network. U87 stable GFP expressing cells were either co-seeded with HUVEC or added to the established tube network 4 hr after HUVEC seeding. Vessel association rates are measured by counting the number of tumor cells that are in contact with HUVEC as a percentage of 200-cells counts in each well. Data were recorded at the indicated time. Experiments were done in six replicates and were repeated at least three times.

For examining angiogenic activity of conditioned medium of U87 cells, media was collected from control and *ANG* knockdown cells cultured in basal serum free media

(0.1% BSA) for a period of 3 days. HUVEC cells were co-mixed with conditioned media and plated on the Matrigel-treated 96-well plate as described above. Cells were then observed over a period of 4-5 hours for tube formation with images taken during the maximal tube formation window (4-4.5 hours). bFGF and serum free media were used as positive and negative controls, respectively.

Immunofluorescence and Immunohistochemistry

Cells were cultured in their respective media on cover slips. Exogenous human ANG protein was added at a final concentration of 1 µg/ml and incubated with the cells for 1 h. Cells were fixed with 4 % formaldehyde at RT for 20 min, permeabilized with 0.1 % Triton X-100 for 15 min and followed with wash and 50 mM NH_4Cl incubation before blocking and antibody staining.

Animals used for histological analysis were euthanized, and tissues were removed and fixed in 10% neutral-buffered formalin for 72 hours. Fixed tissues were then embedded in paraffin, slide-mounted, serially sectioned, and followed by standard laboratory practice as previously described (Tsuji et al., 2005). During antigen retrieval, slides were immersed in sodium citrate buffer (10mM Sodium Citrate, 0.05% Tween 20, pH 6.0) and processed for 5 min with a pressure cooker (Cuisinart) (Dako). TUNEL staining was conducted with *In Situ* Cell Death Detection Kit, TMR red (Roche).

qRT-PCR, tiRNA, and Western blot analysis

Total RNA was extracted using the TRIZOL reagent (Invitrogen, Grand Island, NY) and reverse transcribed (0.5 mg) using the high capacity cDNA reverse transcription kit

(Applied Biosystems, Grand Island, NY). qPCR analysis was performed in 10 µl reactions using the ABI7900HT and SYBR green PCR master mix (Applied Biosystems). The relative mRNA level was determined using the $2^{-\Delta\Delta Ct}$ method with GAPDH as the internal control. tiRNA isolation was conducted with Trizol the same way as described above. Total RNA (2µg) was separated with 15% TBE-urea acrylamide gels and tiRNA were visualized with SYBR gold nucleic acid gel stain (Invitrogen). For Western blot analysis, cells were lysed with RIPA buffer and run through normal Western practices. Cellular fractionation was conducted as previously described (Kishimoto et al., 2005) (S. Li et al., 2013). Quantification was conducted with the Image J software (NIH).

Spheroid invasion and Trans-well migration/invasion assay

Tumor cells under growth condition were trypsinized and resuspended into single cell suspension (40,000 cell/µl) in complete culture medium and 30 µl was dispensed as previously described (Bagci et al., 2009). Spheroids were collected after two days and were mixed with pre-cold gel solution containing culture medium, collagen (1.5 mg/ml, BD), laminin (0.15 mg/ml, Sigma), and drugs or antibodies. While the collagen gel was still in liquid phase, 50 µl solution containing single spheroid was transferred into 96-well plate. After the gel was solidified, 100 µl complete medium containing drugs or antibodies was added. For quantification, 1.5 times radius of the spheroid was used as the threshold for calculating the number of actively invading cells. The total invasion area was measured with the ImageJ software by connecting the farthest invasive cells.

For transwell migration/invasion assays, 24-well 8.0 µm Transwell inserts were used.

$5X10^4$ cells were added to the top well suspended in serum-free medium, and the lower well was filled to medium containing 10% FBS. After 24h incubation, the remaining cells on the top of Tanswell membrane were removed with cotton swab and washed with PBS twice. Cells that migrated to the bottom surface of the filter were fixed and stained with 0.1% crystal violet, followed by dissolving in acetic acid and quantification.

Statistical analysis

The significance between experimental groups was determined by two-tailed Student's t-test. Data obtained from independent experiments were presented as the mean ± SEM; they were analyzed using Student's t test or one-way analysis of variance (ANOVA) with Kruskal–Wallis test, or two-way ANOVA for multiple comparisons using GraphPad Prism 4 (GraphPad Software, San Diego, CA). Kaplan-Meier survival curves were made using JMP (SAS Institute, Cary, NC) and analyzed using log-rank test.

Table 1. List of primers used in RT-PCR

mANG	F-5'-ctcatcgaagtggacaggca-3'	R-5'-agcgaatggaagcccttaca-3'
LoxP-mANG	F-5'-gaagttatccgcgggaagttc-3'	R-5'-agggtggaacttcaggattcaag-3'
Nestin-tva	F-5'-caggaccctcctggaggctga-3'	R-5'-gccctggggaaggtcctgccc-3'
LoxP-$Arf^{-/-}$	F-5'-ctatcaggacatagcgttgg-3'	R-5'-agtgagagtttggggacagag-3'
wt-$Arf^{+/+}$	F-5'- atgatgatgggcaacgttc-3'	R-5'-caaatatcccacgatgtc-3'
mGAPDH	F-5'-ctacccccaatgtgtccgtc-3'	R-5'-gttgctgttgaagtcgcaaa-3'
mTwist1	F-5'-ttcagaccctcaaactggcg-3'	R-5'-ccacgccctgattcttgtga-3'
mTgfb1	F-5'-agggctaccatgccaacttc-3'	R-5'-ccacgtagtagacgatgggc-3'

mZeb1	F-5’-acccctttcaagaaccgcttt-3’	R-5’-caattggccaccactgctaa-3’
mZeb2	F-5’-gagcttgaccaccgactc-3’	R-5’-ttgcaggactgccttgat-3’
mBmp7	F-5’-ggagtaatcgcaagcctcgt-3’	R-5’-acagtggcttctgcttggtt-3’
mSnail1	F-5’-gactccttccagccttggtc-3’	R-5’-cgggtacaaaggcactccat-3’
mSnail2	F-5’-catccttggggcgtgtaagt-3’	R-5’-atggcatgggggtctgaaag-3’
GAPDH	F-5’-gaaggtgaaggtcggagt -3’	R-5’-gaagatggtgatgggatttc -3’
ANG	F-5’-agaagcgggtgagaaacaa-3’	R-5’-cttccaacacaggctcctcg-3’
CD24	F-5’- tgctcctacccacgcaga-3’	R-5’-ggccaacccagagttggaa-3’
FOSL2-CD	F-5’-cgggtagatatgcctggctc-3’	R-5’-tctcaagggtctgacgaacg-3’
MMP9	F-5’-ttgacagcgacaagaagtgg-3’	R-5′-gccattcacgtcgtccttat-3’
FOSL2-ABE	F-5’-cgaacgagcggcgctcgg-3’	R-5’-cctgcccgggcggagcgg-3’
FOSL2-ABE-downstream	F-5’-ggcgaggcgggcccgtcc-3’	R-5’-gcgggcagggcgccgggg-3’
SV40LT	F-5’-gggtcttctacctttctcttcttt-3’	R-5’-gcagtggtggaatgccttt-3’
KRAS	F-5’-gagtttgtattaaaaggtactggtgga-3’	R-5’-tgtatcaaagaatggtcctgcac -3’

Chapter III

Angiogenin promotes glioblastoma invasion through FOSL2-mediated MMP-9 and CD24

ANG is a potent angiogenic protein widely expressed in high-grade glioma (GBM) tissues. In addition to its angiogenic activity ANG may also play a role in GBM tumorigenesis and invasiveness. To find the most relevant model to investigate *in vivo* roles of ANG, we analyzed GBM patients data from the TCGA study (Brennan et al., 2013) for a specific patient group where ANG may be most likely involved. We then used a relevant animal model to examine the role of ANG in GBM invasion.

Upregulation of ANG in gliomas and correlation with poor survival of proneural GBM

We analyzed public microarray data of glioma patients and found that *ANG* expression was upregulated more in high-grade glioma than in low-grade ones (Figure 3.1.A) (Sun et al., 2006). The Cancer Genome Atlas (TCGA) has conducted two major studies on low-grade and high-grade gliomas, which provides a rich resource for correlation analysis through online platforms such as cBioPortal and Oncomine (Table 2). Kaplan-Meier survival plot of low-grade glioma patients showed a significantly worse prognosis in glioma patient group with high *ANG* expression, with the median survival of 62 months compared to 87 months in *ANG* low group (Figure 3.1.B). It supports our hypothesis that ANG can contribute to diseases progression. In the highest-grade glioma, glioblastoma (GBM), *ANG* expression was 5-fold higher than that in control patients with no brain neoplasm (Figure 3.1.C). Increased *ANG* expression also corresponded to a poor survival. For example, the median overall survival shortened by 24% in *ANG* high group from the 415 days in *ANG* low patients (Figure 3.1.D). Within GBM subtypes, we found that *ANG* expression was consistently high in classical, mesenchymal, and neural subtypes and

relatively lower in the proneural subtype (Figure 3.1.E). However, the clinical significance (overall survival) of *ANG* expression was less obvious in the mesenchymal and neural group, where high and low *ANG* expressing GBM had similar prognosis (Figure 3.1.F). In the classical subtype, high *ANG* expression significantly shortened median survival to 327 days from 467 days in the *ANG* low patients and there was a more profound but not yet significant effect in the proneural subtype where median survival reduced from 404 days to 270 days. We believe that the effect of ANG might be actually more relevant in the proneural subtype because there were fewer patients observed in the classical subtype, and thus the result is sensitive to outliers. The greater difference in overall survival between *ANG* high and low groups and also a relative larger population persuaded us to investigate the function of ANG in the proneural GBM. Moreover, the proneural GBM is the only subtype that is progressed from the lower-grade glioma, which provides the best intervention window for treatment because high-grade GBM are extremely hard to detect early. Taken together, these data provides us a rationale to investigate how ANG contributes to proneural GBM progression.

A

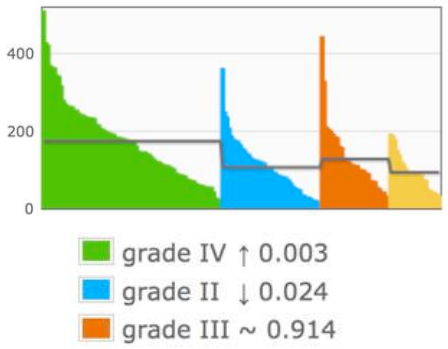
400
200
0
grade IV ↑ 0.003
grade II ↓ 0.024
grade III ~ 0.914

B

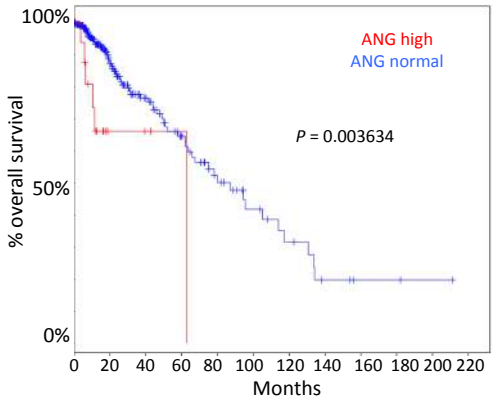
100%
50%
0%
% overall survival
ANG high
ANG normal
P = 0.003634
0 20 40 60 80 100 120 140 160 180 200 220
Months

C

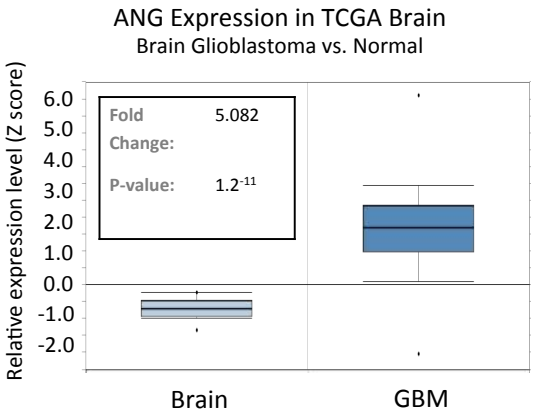
ANG Expression in TCGA Brain
Brain Glioblastoma vs. Normal
Relative expression level (Z score)
6.0
5.0
4.0
3.0
2.0
1.0
0.0
-1.0
-2.0
Fold Change: 5.082
P-value: 1.2-11
Brain
GBM

D

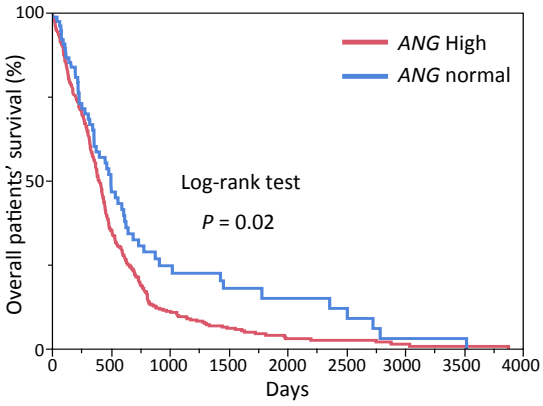
100
50
0
Overall patients' survival (%)
ANG High
ANG normal
Log-rank test
P = 0.02
0 500 1000 1500 2000 2500 3000 3500 4000
Days

E

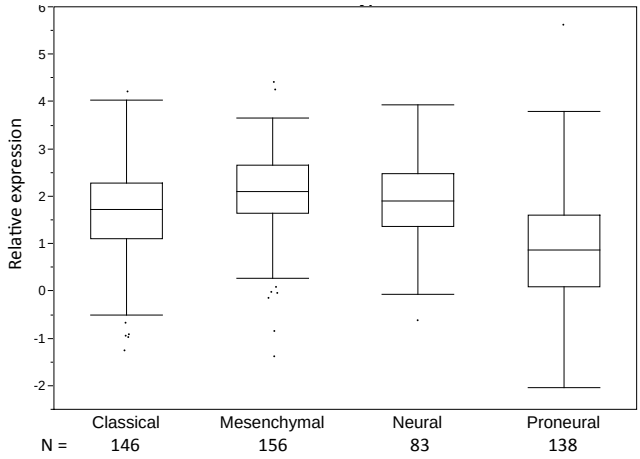
Relative expression
Classical
Mesenchymal
Neural
Proneural
N = 146 156 83 138

F

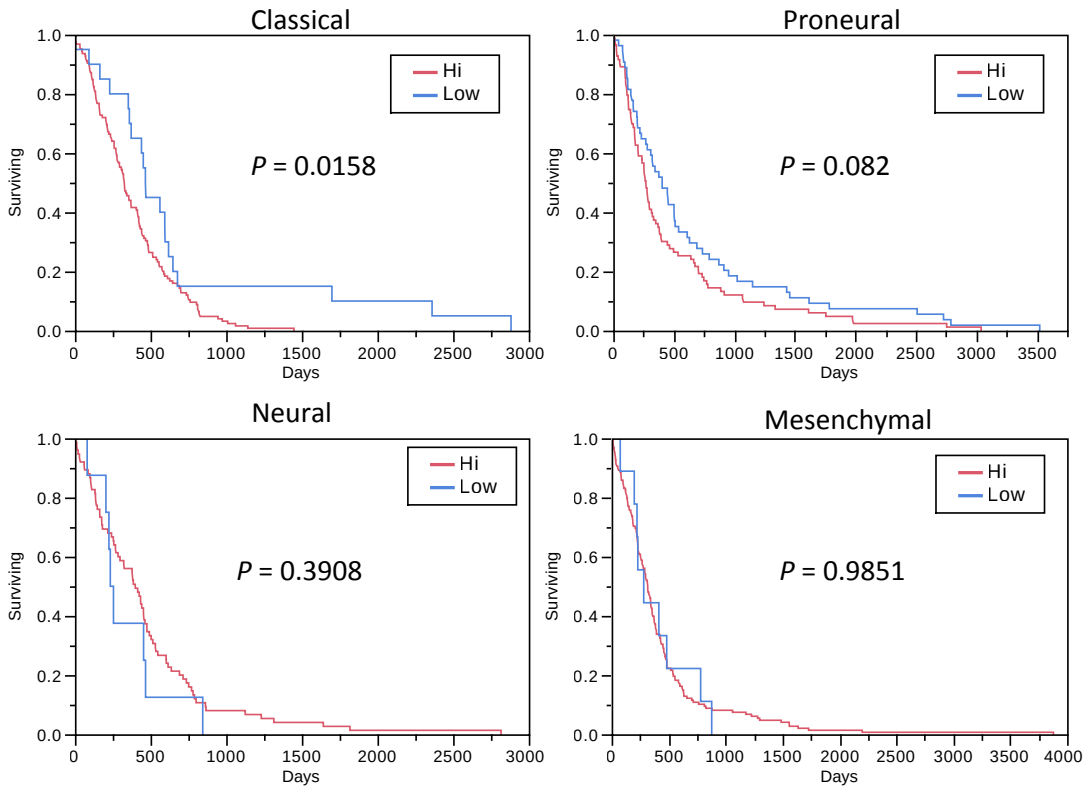

Figure 3.1. *ANG* is upregulated in gliomas, and increased expression is correlated with poor survival in classical and proneural GBM.

(A) *ANG* expression escalates in the higher grade of gliomas (Sun et al., 2006).

(B) Survival plot of low-grade glioma patients showing poorer prognosis in *ANG* high group (TCGA; ANG high, N = 32; ANG normal, N =322).

(C) *ANG* expression in GBM patients' biopsy is 5 fold greater than that in the control patients. (Control group, N = 10; TCGA GBM Cell, N = 557). The Oncomine™ Platform (Life Technologies, Ann Arbor, MI) was used for analysis and visualization. Data shown are mean ± SEM.

(D) *ANG* expression correlates with GBM patients' overall survival. Kaplan-Meier survival plots of GBM patients with high level of ANG expression (*ANG* High, N = 91) compared to the rest of the cohort (*ANG* normal, N = 433) (TCGA GBM Cell cohort).

(E) Relative *ANG* expression in four subtypes of GBM (TCGA GBM Cell cohort).

(F) Survival plots comparing patients with high or low *ANG* expression stratified by GBM subtypes (TCGA GBM Cell cohort).

Table 2. Basic characterization of available GBM databases

	All tumor	Tumor CNA	Sequenced	All comoplete	RPPA	mRNA	MicroRNA	Methylation	Molecular subtypes
Brain Lower Grade Glioma (TCGA, Provisional)	530	513	289	286	260	A27/R527	N	Y	N
GBM (TCGA, Provisional)	611	577	290	136	214	A401/R166/U528	N	Y	N
GBM (TCGA, Nature 2008)	206	206	91	91	0	206	Y	Y	Y
GBM (TCGA, Cell 2013)	574	563	291	291	214	R154	N	N	Y

Generation of *Ang*$^{-/-}$ proneural mouse GBM model.

The functional significance of ANG in proneural GBM can be studied with a transgenic proneural mouse GBM model. Proneural subtype of human GBM has been reported to be modeled by overexpression of platelet-derived growth factor B (PDGFB) in neuronal precursor cells (*Nestin* positive) in *Ntv-a Ink4a*/*Arf*$^{-/-}$ mice via avian retrovirus delivery through chicken fibroblasts (Holland, Hively, DePinho, & Varmus, 1998; Pietras et al., 2014). When DF-1 chicken fibroblasts carrying Rcas-HA-PDGFB vectors were injected into the brain, the Rcas-packaged avian retroviruses can infect *Nestin* positive neuronal progenitor cells and insert the PDGFB gene into the genome of recipient cells, which ultimately will give rise to aggressive mouse glioblastoma (mGBM), mimicking human proneural GBM (Figure 3.2.A). We obtained *Nestin-TvA Ink4a*/*Arf*$^{-/-}$ mice from Dr. Eric Holland of Memorial Sloan Kettering Cancer Center. These mice were crossed with *Ang* knockout mice to produce *Ang*$^{-/-}$ glioblastoma mice after two generations (Figure 3.2.B-C).

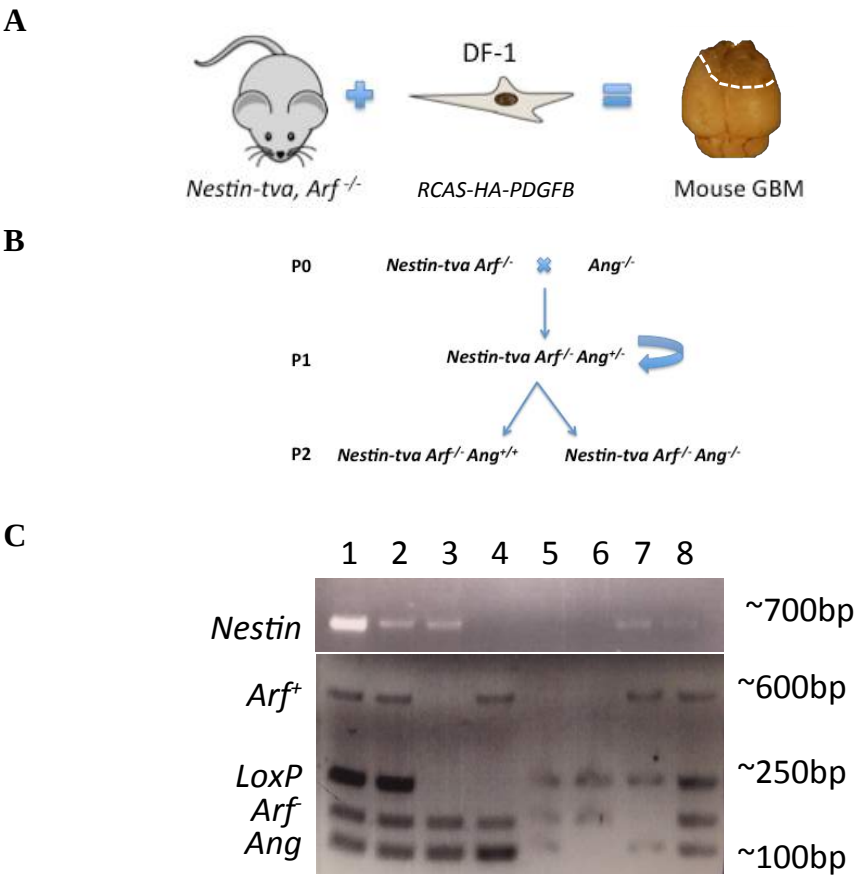

Figure 3.2. Generation of *Ang*$^{-/-}$ mouse proneural GBM model.

(A) The mouse GBM is induced by i.c. injecting DF-1/Rcas-HA-PDGFB cells into the mouse brain SVZ region.

(B) Breeding diagram of generating *Nestin-TvA Arf*$^{-/-}$ *Ang*$^{+/+}$ (*Ang*$^{-/-}$) mice.

(C) Genotyping of P2 mice. #1, *Nestin*$^{+}$; *Arf*$^{+/-}$; *Ang*$^{+/-}$; #2, *Nestin*$^{+}$; *Arf*$^{+/-}$; *Ang*$^{+/-}$; #3, *Nestin*$^{+}$; *Arf*$^{-/-}$; Ang$^{+/+}$; #4, *Arf*$^{+/+}$; *Ang*$^{+/+}$; #5, *Arf*$^{+/-}$; *Ang*$^{+/-}$; #6, *Arf*$^{-/-}$; *Ang*$^{-/-}$; #7, *Nestin*$^{+}$; *Arf*$^{+/+}$; *Ang*$^{+/-}$; #8, *Nestin*$^{+}$; *Arf*$^{+/-}$; *Ang*$^{+/-}$.

Ang deficiency reduces tumor lesions and prolongs survivals in the proneural GBM mouse model

By generating *Ang*$^{-/-}$ mice in *Ntv-a Ink4a/Arf*$^{-/-}$ background, we obtained the first mouse tumor model that would reveal the *in vivo* roles of *Ang* in tumorigenesis and invasion. Tumor induction was conducted in a blinded fashion by delaying genotyping to the time of autopsy. A control group consisting of *Ang*$^{+/+}$ *Ntv-a Ink4a/Arf*$^{-/-}$ (*Ang*$^{+/+}$) mice undergoing sham surgery was included for histology comparison. Compared to the control, PDGFB overexpression effectively induced lesions, significantly enlarged the brain size with presumably high intracranial pressure and traces of bruises on the surface of the brain that was in close proximity to the skull (observations during autopsy) (Figure 3.3.A). Lesions in the fixed tissues extended from the subventricular zone to the olfactory bulb, which mimic the track along which neuronal progenitor cells migrate through the rostral migratory stream during brain development (Cuddapah, Robel, Watkins, & Sontheimer, 2014a). This is in line with other findings that GBM re-activates invasive signaling pathways implicated in neuronal development (Rieger, Wick, & Weller, 2003). In addition, there were also signs of severe vascularization in the lesion areas (observation during histological processing) (Figure 3.3.A). The distinctive features of human GBM such as necrosis, pseudopalisades and vascular proliferation, were observed in all tumor sections examined from both *Ang*$^{+/+}$ and *Ang*$^{-/-}$ groups (Fig. 3.4), indicating the high-grade nature of the resulting mouse gliomas in both genotypes.These data suggest that loss of *Ang* activity is not sufficient to impede PDGFB-induced transformation in neuronal progenitor cells, as the tumor induction rates were 100% in all three groups.

The size of tumor lesions and degree of vascularization were reduced in *Ang*$^{-/-}$ mice compared to *Ang*$^{+/+}$ mice as shown in both coronal and sagittal sections (Fig. 3.3.B-C). The *Ang* deficient tumors displayed lower tumor cellularity and notably less infiltrative cells in the other hemisphere, in the cortex, and in the olfactory bulb (Fig. 3.3.B-C). These observations suggested a role of ANG in GBM invasive. Overall, there was a significant difference (P = 0.0001) in survival between *Ang*$^{+/+}$ (N = 15) and *Ang*$^{-/-}$ (N = 19) groups but not between *Ang*$^{+/+}$ and *Ang*$^{+/-}$ (N = 22) (P = 0.07), which suggests that only complete loss of *Ang* activity leads to a longer survival in this proneural mouse GBM model (Fig. 3.3.D).

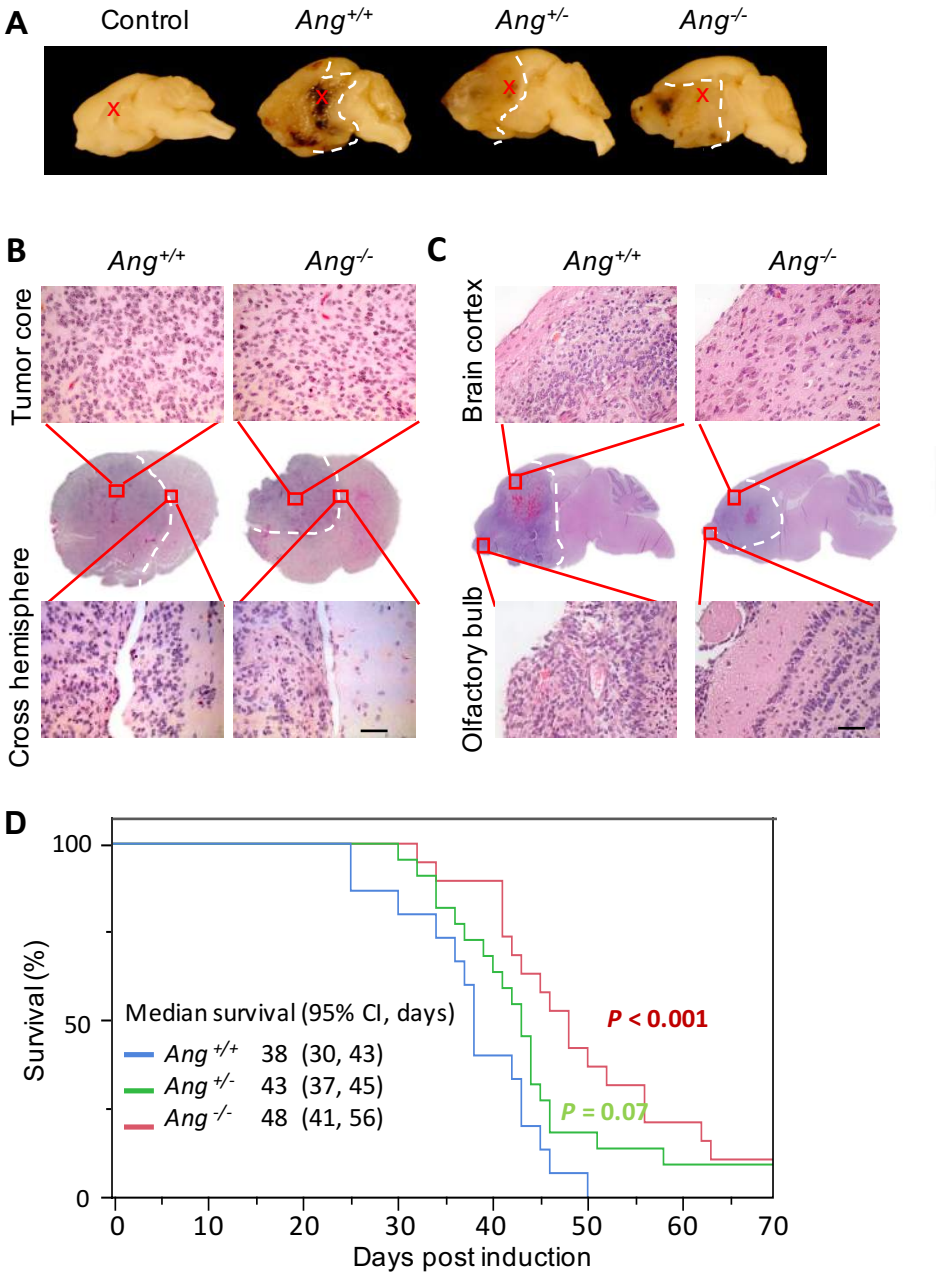
A
Control
Ang+/+
Ang+/-
Ang-/-
B
Ang+/+
Ang-/-
Tumor core
Cross hemisphere
C
Ang+/+
Ang-/-
Brain cortex
Olfactory bulb
D
Survival (%)
100
50
0
Median survival (95% CI, days)
Ang +/+ 38 (30, 43)
Ang +/- 43 (37, 45)
Ang -/- 48 (41, 56)
P < 0.001
P = 0.07
0
10
20
30
40
50
60
70
Days post induction

Figure 3.3 *Ang* knockout reduces tumor lesions and prolongs survivals in the proneural GBM mouse model

(A) Representative gross histology of fixed sagittal brain tissues of the experimental groups. Control: mouse received DF-1 i.c. injection but no tumor was induced. Dotted lines mark approximate tumor boundary. Red cross: SVZ injection site.

(B) The coronal H&E sections of $Ang^{+/+}$ and $Ang^{-/-}$ mGBM with high magnification of tumor core and brain midline.

(C) High magnification sagittal sections of cortex and olfactory bulb. Bar = 50 μm. Dotted lines mark approximate tumor boundary. Images shown are from representative tumor sections.

(D) Overall survival of *Nestin-TvA*, $Arf^{-/-}$ $Ang^{-/-}$ mice (N = 19) is significantly improved, as compared with mice in $Ang^{+/+}$ background (N = 15), $P < 0.001$. Difference between $Ang^{+/-}$ (N = 22) and $Ang^{+/+}$ or $Ang^{-/-}$ group was not statistically significant, $P = 0.07$ and $P = 0.15$, respectively.

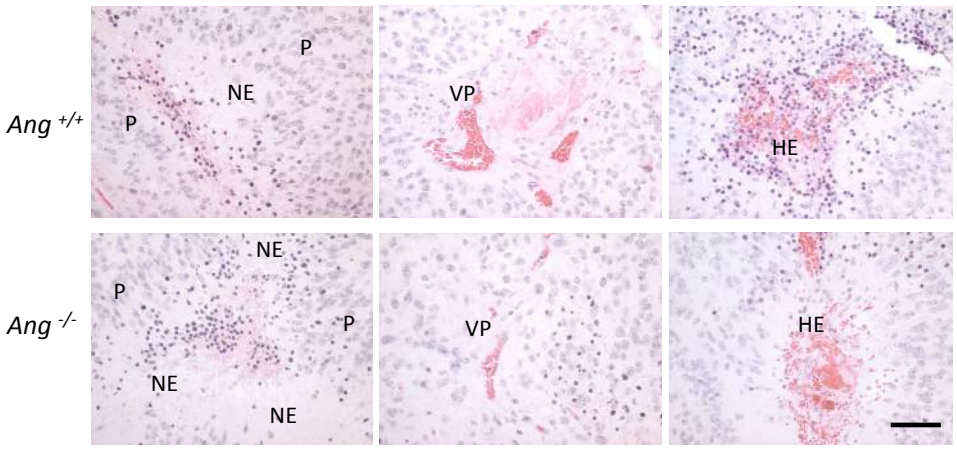

Figure 3.4. Histopathology features of *Ang*$^{+/+}$ and *Ang*$^{-/-}$ mouse GBM.

High magnification shows distinct human GBM features in both *Ang*$^{+/+}$ and *Ang*$^{-/-}$ mouse tumor sections. NE, necrosis; P, pseudopalisades; VP, vascular proliferation; HE, hemorrhage. Bar = 50 µm.

ANG activates MMP-9 and promotes GBM invasion

At the tumor edge of induced mouse GBM, there were marked differences in extracellular matrix (ECM) homogeneity (Figure 3.5.A). *Ang*$^{-/-}$ tumors showed a reduced extracellular space, a denser ECM, and a more consistent matrix density (Figure 3.5.B). Eosin-stained ECM consists of collagen, fibronectin, and laminin and is subjected to MMP-mediated remodeling during tumor invasion (Brennan et al., 2013; Cancer Genome Atlas Research Network, 2008; Cancer Genome Atlas Research Network et al., 2013; Cuddapah, Robel, Watkins, & Sontheimer, 2014a; P. Lu, Takai, Weaver, & Werb, 2011; Sun et al., 2006; Verhaak et al., 2010). A more homogenous ECM in *Ang*$^{-/-}$ tumor implies a reduced remodeling process. It is then very interesting to note that both *MMP-9* and *ANG* were the most up-regulated genes in GBM cells after VEGF antibody treatment (Holland et al., 1998; Lucio-Eterovic et al., 2009; Pietras et al., 2014). We therefore explored the role of ANG in regulating *MMP-9* expression in GBM. Exogenous ANG protein increased *MMP-9* mRNA by 2.9- and 1.8-fold in U87 and U251 human GBM cell lines, respectively (Figure 3.5.C). This increased *MMP-9* expression corresponded to a 2-fold increase in protease activity as shown in an *in vitro* gelatin zymography assay (Figure 3.5.D). Like the upregulation effect of *MMP-2* by ANG in bladder cancer (Cuddapah, Robel, Watkins, & Sontheimer, 2014a; Miyake et al., 2014), we also found that ANG-induced *MMP9* upregulation was mediated through the MEK/ERK pathway in GBM cells, because MEK inhibitor (PD98059) completely abolished ANG-induced MMP-9 upregulation at the protein level (Figure 3.5.E). To verify that MMP-9 is upregulated by ANG *in vivo*, we performed immunohistochemistry on U87 orthotopic xenograft tissue sections. In the serial sections, U87 tumor cells at the invasive edge

expressed particularly high levels of both ANG and MMP-9 (10.1 ± 0.5%), as compared to cells that expressed only ANG (1.4 ± 0.2%) or MMP-9 (4.9 ± 0.3%) (Figure 3.5.F). It indicates an *in vivo* spatial correlation between ANG and MMP-9 expressions. We also noted that MMP-9-positive cells were more abundant than ANG-positive cells. One possible reason for that could be that tumor-secreted ANG can have both autocrine and paracrine effects on inducing MMP-9 expression in GBM. However, we cannot exclude the possibility that MMP-9 expression can also be induced in an ANG-independent manner in GBM.

Next, to examine the role of ANG-induced MMP-9 in GBM invasion, we used a 3D invasion model to mimic the *in vivo* brain environment. This model was adapted from the early work from Ronaldo F. Del Maestro's lab (Del Duca, Werbowetski, & Del Maestro, 2004; Rieger et al., 2003). We used stable GFP-expressing U87 and U251 lines to facilitate visualization and quantification in a 3D collagen/laminin matrix. In this 3D model, GBM spheroids secrete collagen-modifying proteases, such as MMP-9, thereby facilitating tumor cells infiltration into the matrix. The dispersal area, defined by the total peripheral area of the infiltrative tumor cells, and the numbers of active invasive tumor cells are the primary readouts. Through a 2-day culture, we observed that the U87 tumor cells invaded into an area that is ~10 times of the size of the spheroid at day 0 (Figure 3.6.A). The pro-invasive effect of ANG is relevant in this model, as exogenous ANG increased the invasive area by 54.1%, whereas the ANG neutralizing mAb decreased the invasion area by 2.2-fold (Figure 3.7.A). Consistently, similar effects were observed in U251 (Figure 3.7.B). To test the role of MMP-9 in ANG-induced GBM invasion, we

incubated U87 spheroids with CTK8G1150 (IC_{50} = 5 nM), a specific MMP-9 inhibitor, for 48 hr and found that CTK8G1150 inhibited ANG-induced invasive area as well as the number of invading cells (Figure 3.6.A). Significantly, in the presence of this MMP9 inhibitor, ANG antibody 26-2F showed no additional inhibitory effect on U87 invasion (Figure 3.6.B). In conclusion, MMP-9 responds to ANG *in vivo* and mediates the invasive effect of ANG at the invasive edge of GBM tumor.

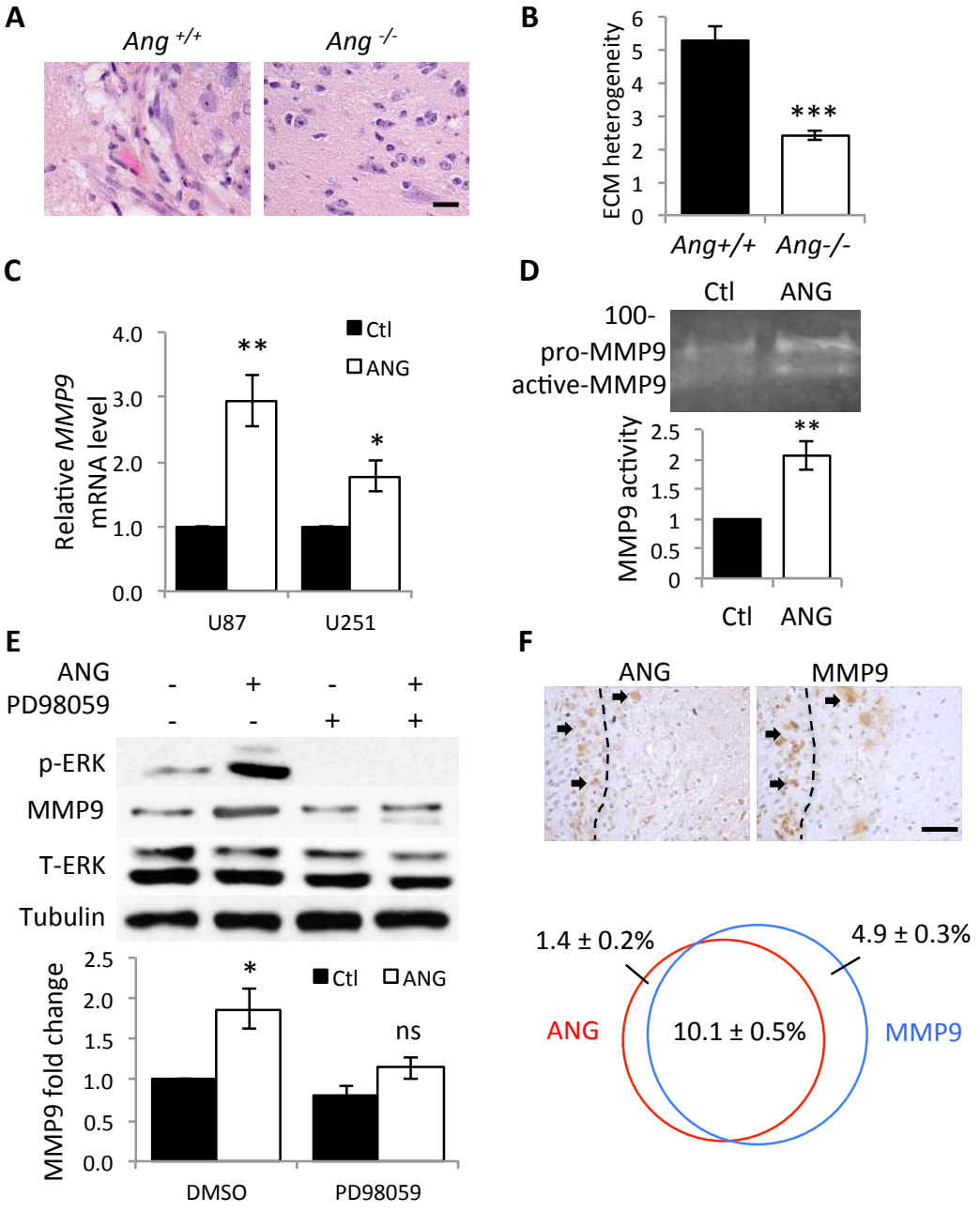
A
Ang +/+
Ang -/-
B
ECM heterogeneity
***
Ang+/+
Ang-/-
C
Relative MMP9 mRNA level
Ctl
ANG
**
*
U87
U251
D
Ctl
ANG
100-
pro-MMP9
active-MMP9
MMP9 activity
**
Ctl
ANG
E
ANG
PD98059
p-ERK
MMP9
T-ERK
Tubulin
MMP9 fold change
Ctl
ANG
*
ns
DMSO
PD98059
F
ANG
MMP9
1.4 ± 0.2%
4.9 ± 0.3%
ANG
10.1 ± 0.5%
MMP9

Figure 3.5. ANG increases MMP-9 expression through MEK/ERK pathway.

(A) H&E staining of the extracellular matrix of *Ang*$^{+/+}$ and *Ang*$^{-/-}$ mGBM tissues in the high power field. Bar = 25 μm.

(B) The different variance of matrix homogeneity between *Ang*$^{+/+}$ and *Ang*$^{-/-}$ tumors. Data collected from 15 line plots in 3 random fields.

(C) Real-time PCR of *MMP9* mRNA levels, normalized to GAPDH in U87 and U251 cells, which were treated with exogenous ANG (1 μg/ml), compared to PBS control treatment. Data shown are means ± SEM of 3 independent experiments.

(D) The conditioned medium of U87 cells treated with ANG or PBS control was subjected to zymography assay. Image is for a representative experiments. Bar graphs are means ± SEM of two independent experiments.

(E) U87 cells were pre-incubated with MEK inhibitor (PD98059, 50 nM) and then treated with PBS or ANG. Densitometry of MMP-9 bands was quantified and normalized to Tubulin.

(F) Immunohistochemistry staining of ANG and MMP-9 at the invasive tumor edge on serial tumor sections of U87 orthotopic xenograft. Arrows indicate tumor cells co-expressing ANG and MMP-9 at the invasive edge. Percentages of tumor cells expressing ANG or MMP-9 are shown. Dotted line: approximate tumor edge. Bar = 50 μm. Data shown are mean ± SEM from 3 randomly selected fields.. * $P < 0.05$; ** $P < 0.01$; ***, $P < 0.001$; n.s., no statistical difference by Student's *t* test.

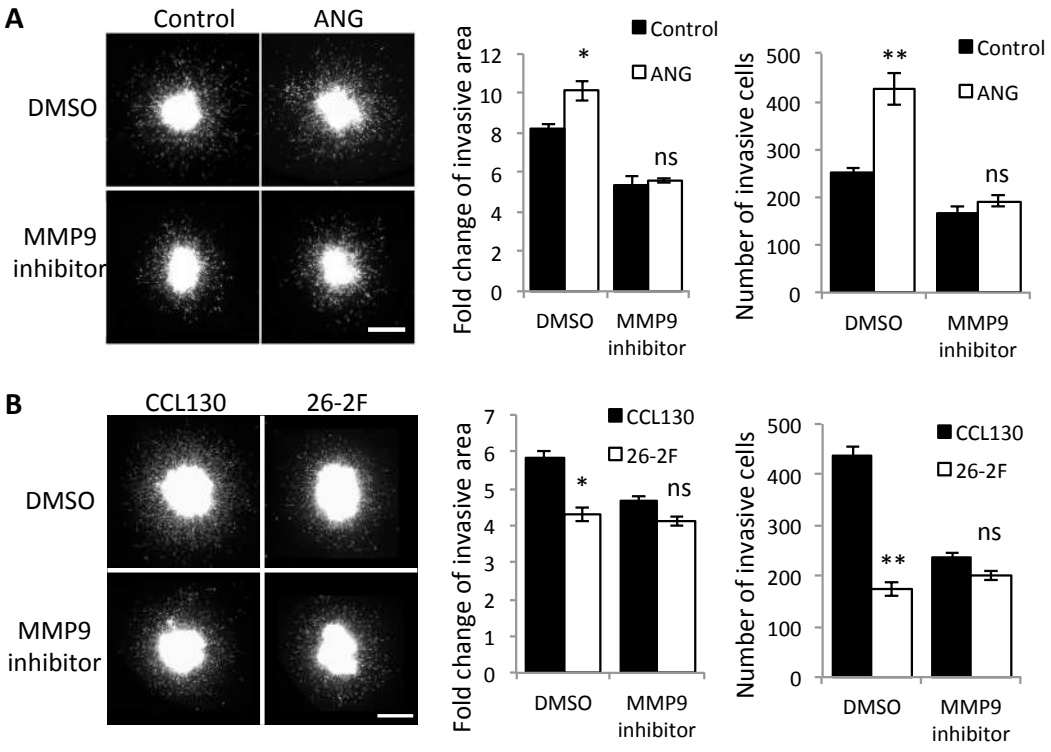

Figure 3.6. MMP9 inhibitor reduces ANG-induced GBM spheroid invasion in collagen/laminin matrix.

(A) U87 spheroids were treated with ANG (1 μg/ml) alone or in combination with MMP-9 specific inhibitor, CTK8G1150 (50 nM) for 48 h.

(B) U87 spheroids were treated with 26-2F (50 μg/ml) alone or in combination with MMP-9 specific inhibitor, CTK8G1150 (50 nM) for 48 h. Bar = 200 μm.

The invasive area was normalized to that of day 0 and the numbers of invasive cells were counted as those migrated over half radius of the spheroid. Images shown are representative pictures from 2 independent experiments of 6 replicates each. Data shown are mean ± SEM. * $P < 0.05$; ** $P < 0.01$; ***, $P < 0.001$; n.s., no statistical difference by Student's *t* test.

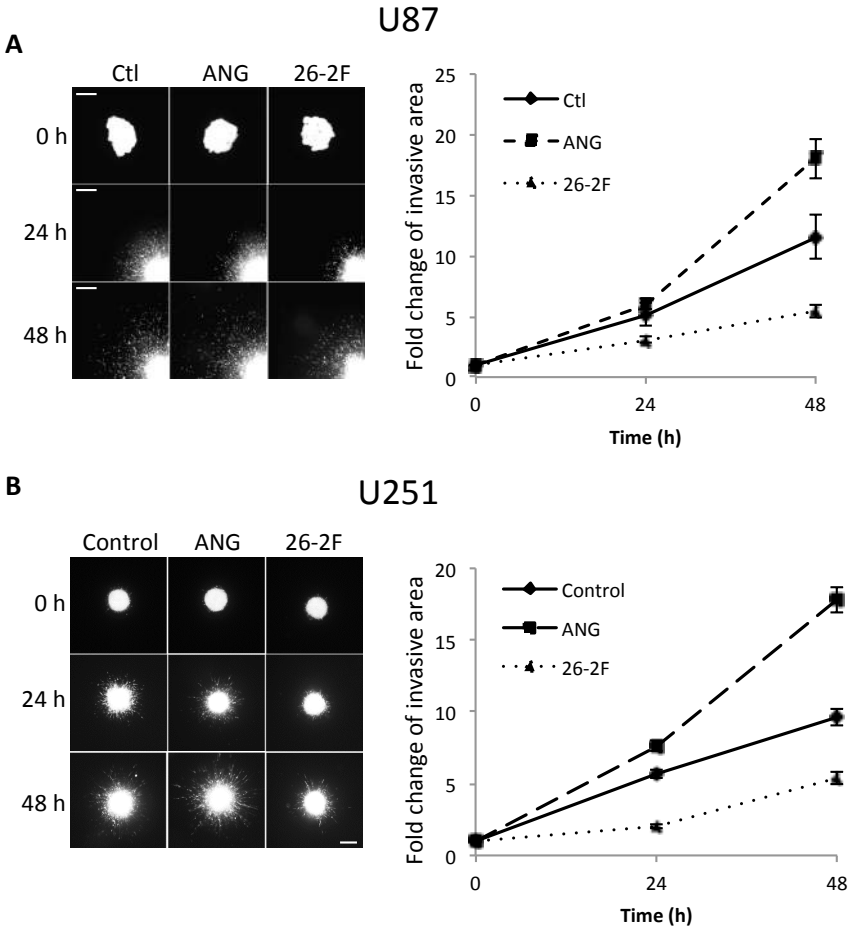

Figure 3.7. ANG regulates *in vitro* invasion of GBM.

U87 (A) and U251 (B) cells were cultured in hanging-drop format for spheroid formation and was seeded into 3D collagen/laminin matrix in DMEM + 10% FBS in the presence of ANG (1 μg/ml) or neutralizing ANG mAb 26-2F (50 μg/ml). Tumor cells infiltrated into the matrix were observed for 2 consecutive days. Bar = 500 μm. Exogenous ANG significantly enhances U87 and U251 invasion, and inhibition of endogenous ANG by 26-2F antibody more strongly reduced U87 and U251 invasion. The invasive area was measured as the maximum tumor dispersal area. Data were normalized to 0 hr.

ANGinduced up-regulation of MMP-9 is mediated by FOSL2

The AP-1 transcription complex is essential for *MMP-9* transcription (H. Sato, Kita, & Seiki, 1993). FOSL2 is a Fos family protein that can heterodimerize with the Jun family protein to form the AP-1 complex (David et al., 2001). We found that the *FOSL2* gene contains an ANG-binding-element (ABE) (Z.-P. Xu et al., 2003) in its promoter region: 28,392,938–CTCTCTCTCTCTCTCTCTCTC–28.392,967 (Figure 3.8.A). ABE is a DNA sequence containing 5'–CTCTCTCTCTCTCTCTCCCTC– 3' that has a high affinity to ANG. ANG binds to the ABE in the rRNA genomic region and stimulates rRNA transcription by modulating epigenetics and by recruitment of transcription factors (Sheng et al., 2013; Tsuji et al., 2005). We therefore examined whether ANG regulates MMP-9 through FOSL2. We used a pool of siRNA to knockdown *FOSL2* expression (Figure 3.8.B) and examined the resultant changes in MMP-9 expression in response to ANG stimulation (Figure 3.8.C). siRNA treatment showed a high efficiency of knockdown at the protein level and effectively abolished ANG-induced upregulation of MMP-9. CD24, another gene that can be transcriptionally activated by FOSL2/AP-1 (M. Smith et al., 2001), also lost response to ANG in *FOSL2* knockdown.

To verify that ANG can specifically bind to the ABE of *FOSL2*, we synthesized three sets of primers targeting the ABE, downstream region of ABE, and the coding region of *FOSL2* gene, respectively, to conduct ChIP on the U87 genomic DNA. Only *FOSL2*-ABE showed positive signal in the ANG antibody pulled-down products, suggesting that ANG specifically binds to the ABE of *FOSL2* but not to the ABE-adjacent region or to the coding region of the gene (Figure 3.8.D). In addition, we showed that the levels of

both the mRNA and the protein of FOSL2 were increased upon addition of exogenous ANG in both U87 and U251 cell lines (Figure 3.8.E-F).

Active FOSL2 interacts with the c-Jun family proteins to form an AP-1 complex that is localized to the nucleus and modulates downstream gene expression (Nishina et al., 1990). We, therefore, examined nuclear localization of FOSL2 upon ANG stimulation by immunofluorescence. We found that exogenous ANG increased nuclear localization of FOSL2 (Figure 3.8.G). As nuclear localization of FOSL2 is modulated by its stability via direct ERK phosphorylation, which is one of the pathways that ANG activates in many cell types (S Liu et al., 2001; Murakami et al., 1999), we examined if ANG-induced nuclear translocation of FOSL2 occurs in an MEK/ERK-dependent manner. Immunoblotting confirmed nuclear accumulation of phosphorylated FOSL2 upon ANG stimulus in DMSO control group, but not in MEK inhibitor (PD98059)-treated group, indicating that nuclear localization of FOSL2 no longer took place upon ANG stimulation when ERK was inhibited (Figure 3.8.H).

In a cohort of 557 GBM patients, *FOSL2* and *MMP9* expression were highly correlated with *ANG* expression (Figure 3.9).The patients group with either elevated *FOSL2* or *MMP-9* expression had a poorer prognosis compared to the rest of the cohort (Figure 3.10). In conclusion, we have identified FOSL2 as a mediator of ANG in up-regulating *MMP-9* expression.

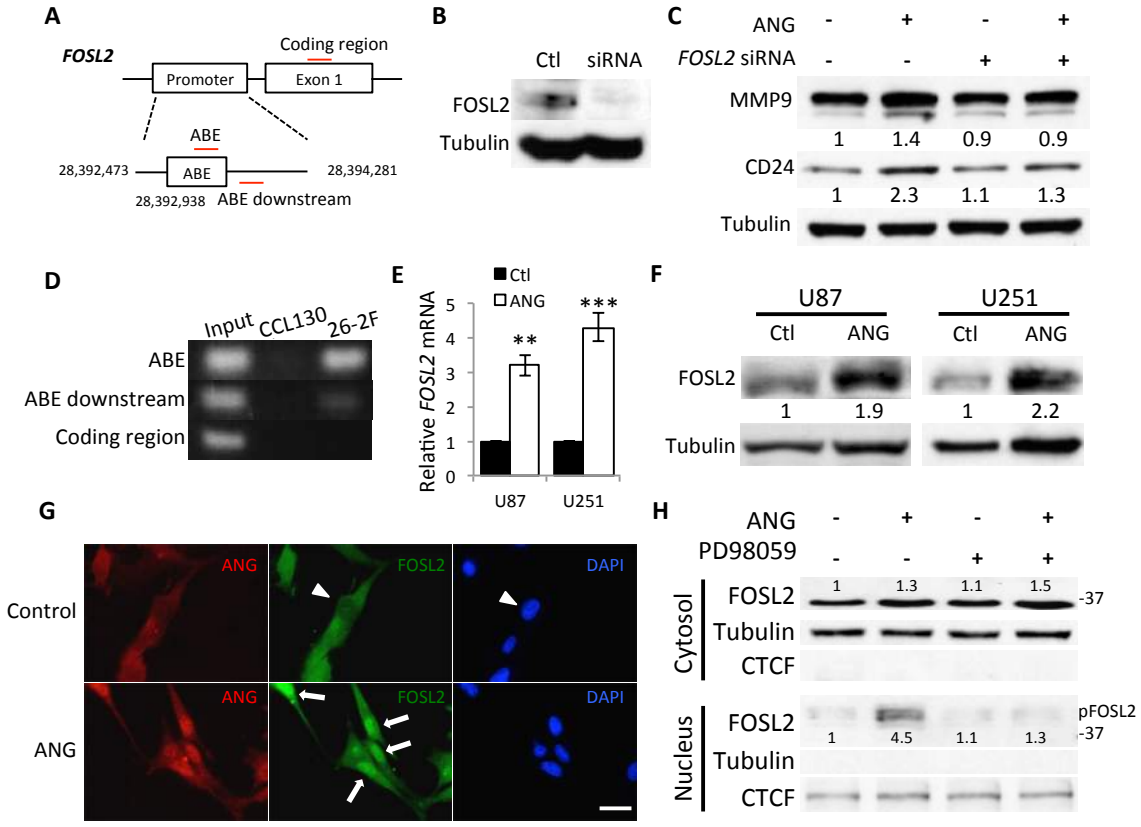
A
FOSL2
Coding region
Promoter
Exon 1
ABE
28,392,473
ABE
28,394,281
28,392,938
ABE downstream
B
Ctl
siRNA
FOSL2
Tubulin
C
ANG
FOSL2 siRNA
MMP9
1
1.4
0.9
0.9
CD24
1
2.3
1.1
1.3
Tubulin
D
Input
CCL130
26-2F
ABE
ABE downstream
Coding region
E
Ctl
ANG
Relative FOSL2 mRNA
**
***
U87
U251
F
U87
U251
Ctl
ANG
FOSL2
1
1.9
1
2.2
Tubulin
G
Control
ANG
ANG
FOSL2
DAPI
H
ANG
PD98059
Cytosol
FOSL2
1
1.3
1.1
1.5
-37
Tubulin
CTCF
Nucleus
FOSL2
1
4.5
1.1
1.3
pFOSL2
-37
Tubulin
CTCF

Figure 3.8. ANG-stimulated up-regulation of MMP-9 is mediated through FOSL2, whose expression and localization can be directly modulated by ANG.

(A) The diagram of human *FOSL2* promoter and the first exon. Three sets of primers (Red) were designed to target ANG-binding element (ABE) region, ABE downstream region, and the coding region.

(B) FOSL2 was knockdown by a pool of siRNA in U87 cells.

(C) U87 transfected with FOSL2 siRNA or control was treated with ANG/PBS and cell lysates were subjected to western blotting. Band intensity was quantified with ImageJ and normalized to that of β-tubulin.

(D) ChIP U87 genomic DNA was precipitated by ANG antibody and PCR amplified with the three sets of primers. Non-immune IgG (CCL130) was used as the negative control.

(E, F) FOSL2 transcription and protein levels were shown upon exogenous ANG (1 μg/ml) treatment in U87 and U251 cells. Western quantification was performed with ImageJ normalized to control and Tubulin.

(G) Immunofluorescence of FOSL2 nuclear localization after ANG treatment for 30 min in U87 cells. Arrowheads indicate cells without distinct nuclear FOSL2 signal. Arrows show nuclear accumulation of FOSL2 upon ANG treatment. Bar = 20 μm.

(H) Exogenous ANG with or without MEK inhibitor was added to U87. The cytosol and nuclear fractions were examined for FOSL2 by Western. Data shown are mean ± SEM. * $P < 0.05$; ** $P < 0.01$; ***, $P < 0.001$; n.s., no statistical difference by Student *t* test.

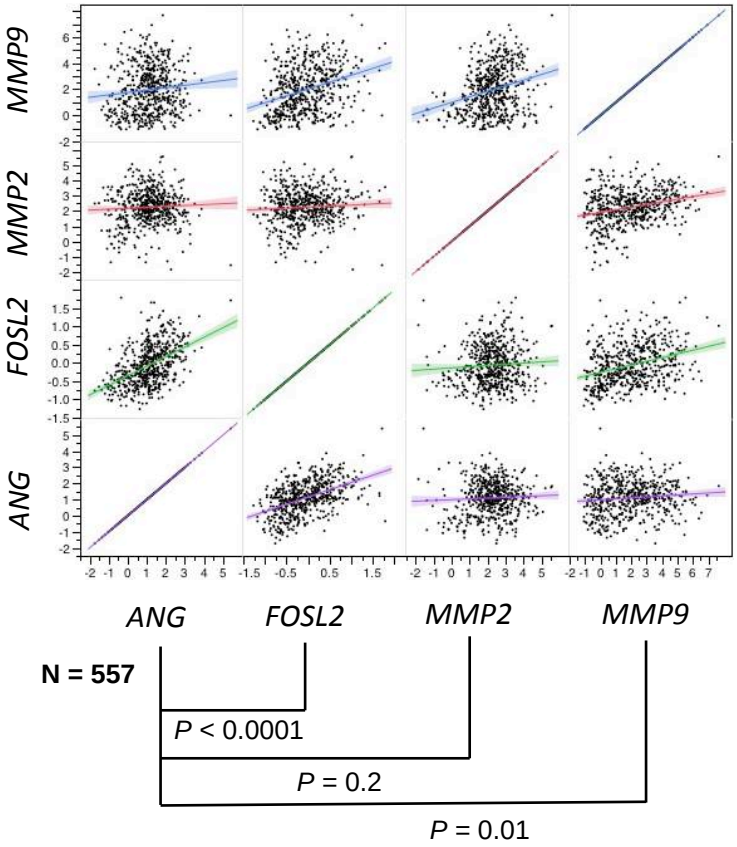

Figure 3.9. mRNA correlation of ANG with *FOSL2*, *MMP-2* and *MMP-9* in human GBM. mRNA correlation of *ANG* with *FOSL2* ($P < 0.0001$), *MMP-2* ($P = 0.2$) and *MMP-9* ($P = 0.01$) from a cohort of TCGA GBM tumor samples (N = 557).

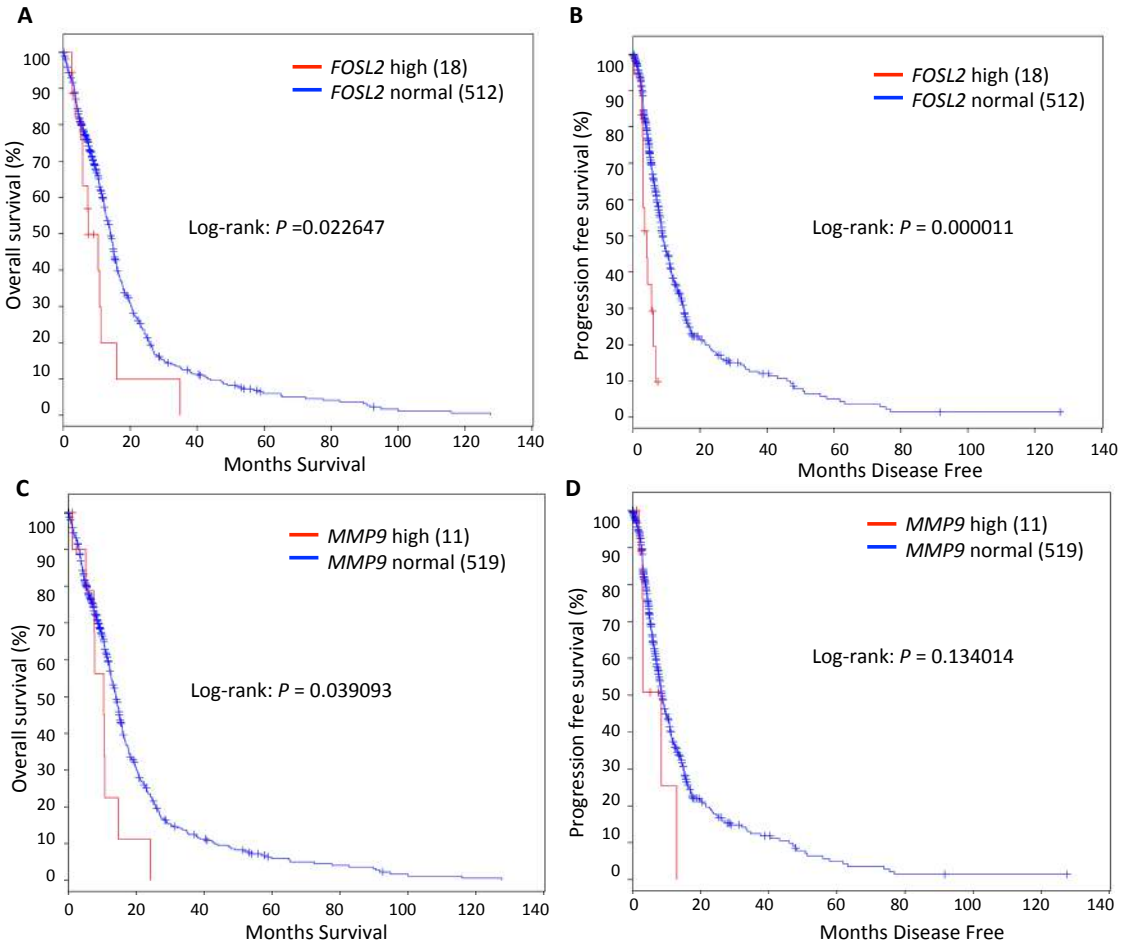

Figure 3.10. Correlation of *FOSL2* and *MMP-9* expression with GBM patient survival.

(A, B) Kaplan-Meier plots of overall survival (A) and progression-free survival (B) in GBM patients with high level of *FOSL2* expression (*FOSL2* high, N = 18) compared to the rest of the cohort (*FOSL2* normal, N = 512, expression z-score < ± 1.4).

(C, D) Kaplan-Meier plots of overall survival (C) and progression-free survival (D) in GBM patients with high level of *MMP-9* expression (*MMP-9* high, N = 11) compared to the rest of the cohort (*MMP9* normal, N = 519, expression z-score < ± 1.4). Cohort source and raw mRNA data were from TCGA and cBio portal.

CD24 mediates the association of GBM with endothelial cells

CD24 is known to be highly expressed in gliomas and promotes invasion *in vivo* but not *in vitro* (Senner, Sturm, Baur, Schrell, Distel, & Paulus, 1999b). Yet, the mechanism by which CD24 increases glioma invasion *in vivo* is elusive but the difference between its *in vitro* and *in vivo* behaviors suggests the involvement of microenvironmental factors. The interaction between CD24 and its ligand P-selectin, a molecule expressed in endothelial cells, is responsible for breast cancer cells rolling on the blood vessels during metastasis (Aigner et al., 1998; Schröder et al., 2010). In GBM, although metastasis is rarely seen and is not related to disease fatality, perivascular infiltration of tumor cells that follow the blood vessel sheath has long been documented and was believed to be a major reason underlying diffusive invasion and also one of the mechanisms through which tumor cells develop resistance against VEGF inhibitors (Baker et al., 2014; Cuddapah, Robel, Watkins, & Sontheimer, 2014b). Thus, such perivascular invasion represents a distinct target for treating GBM. We proposed a perivascular GBM invasion model where interaction between invasive GBM cells and endothelial cells is mediated by CD24/P-selectin signaling which can be regulated by ANG.

First, by using a co-culture assay, we studied how *CD24* overexpression modulates U87 cells (labeled with GFP) interacting with endothelial cells (labeled with a fluorescence dye). CD24 overexpression increased vessel co-option, a distinct form of brain tumor invasive behavior that promotes aggressive tumor progression independent of angiogenesis (Baker et al., 2014; Holash, 1999), by 41% (Figure 3.12.A). The EC-associated, CD24-overexpressed cells displayed more elongated morphology and a 54%

reduction in circularity, indicating that CD24 expression enhanced association of GBM cells to endothelial cells, which was accompanied by an increase in surface area (Figure 3.12.B).

Next, we examined if exogenous ANG could increase the association of U87-ctl or U87-CD24 with the established tubule network. Pre-incubation of ANG increased the association by 35%, similar to the effect of CD24 overexpression. However, ANG did not enhance U87 association with the tubule network any further in when *CD24* was overexpressed, indicating that ANG and CD24 function in the same pathway mediating tumor interaction with endothelial cells (Figure 3.11.A). When the seeding density of tumor cells was increased by 5-fold and observation time postponed from 2 hr to 8 hr, almost all the U87 cells were found to interact or were in close proximity to the tubule network. Even though, there was a significant difference between the ways that U87-CD24 and U87-ctl interacted with HUVE cells (Figure 3.12.C).

Because our hypothesis was that CD24 functions downstream of ANG, we examined the rescue effect of CD24 overexpression to the defect of *ANG* knockdown U87 (U87-shANG) cells in their interactions with endothelial cells. In U87-shANG, the association rate dropped to less than 40%, but was reversed by *CD24* expression, confirming our hypothesis that CD24 functions downstream of ANG in regulating association of GBM cells with EC network (Figure 3.11.B). *CD24* expression in the scramble control showed a similar enhanced association of 32%.

To examine the effect of ANG on perivascular invasion of GBM in a more natural setting, we investigated the invasive capacity and vessel interaction of U87-NC and U87-shANG in an *ex vivo* invasion assay with brain slices. *ANG* knockdown cells showed a reduced infiltration into the brain tissues with most of the cells staying on the seeding surface of the tissues, as shown in the Z section of the brain slice, whereas U87-NC group displayed a more dynamic and active infiltration pattern (Figure 3.12.D). At the places we could discern tumor cells near the mouse vessels (CD31 staining, high magnification), we found a reduced interaction surface area and less perivascular invasion in the U87-shANG group, in agreement with the *in vitro* data, suggesting that *ANG* knockdown reduced perivascular invasion and contributed to a less aggressive infiltrative growth (Figure 3.12.D). In the mouse GBM tissues, $Ang^{-/-}$ tumors showed a 10-fold less vessel-associated, CD24 positive tumor cells than did $Ang^{+/+}$ tumors (Figure 3.11.C). In non-tumor tissues areas, we could not detect any interactions in both $Ang^{+/+}$ and $Ang^{-/-}$ brain tissues (Figure 3.12.E). These data validated our hypothesis that ANG regulates perivascular invasion of GBM, at least for the $CD24^{+}$ invading GBM cells.

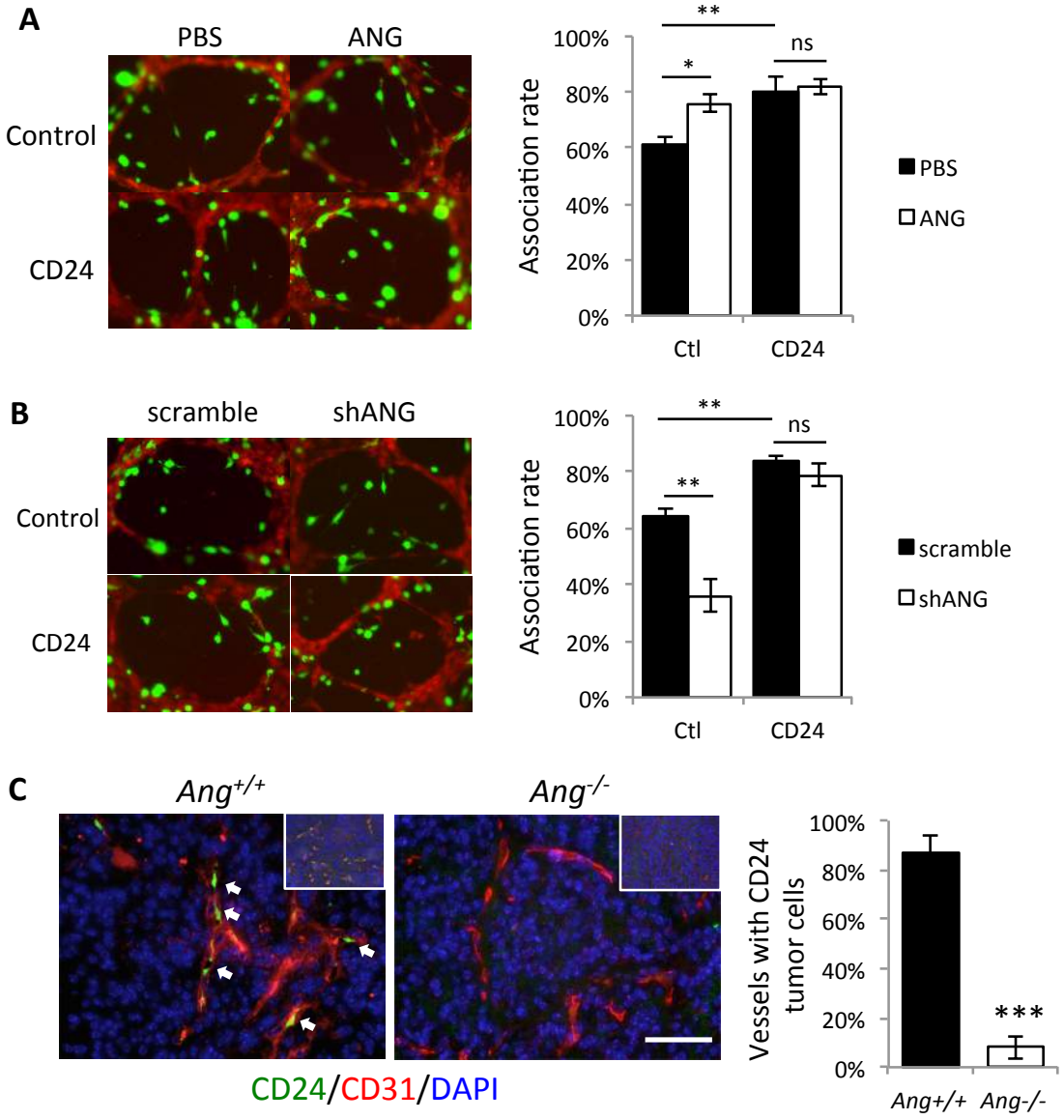
A
PBS
ANG
Control
CD24
Association rate
100%
80%
60%
40%
20%
0%
**
*
ns
Ctl
CD24
PBS
ANG
B
scramble
shANG
Control
CD24
Association rate
100%
80%
60%
40%
20%
0%
**
**
ns
Ctl
CD24
scramble
shANG
C
Ang+/+
Ang-/-
CD24/CD31/DAPI
Vessels with CD24 tumor cells
100%
80%
60%
40%
20%
0%
***
Ang+/+
Ang-/-

Figure 3.11. CD24 mediates GBM association with endothelial cells and is implicated in reduced perivascular invasion in *Ang*$^{-/-}$ mouse GBM.

(A) U87-GFP-ctl and U87-GFP-CD24 were pre-treated with ANG were seeded on an established vessel network formed by HUVECs, stained with CMTMR cell tracker dye (Life Technology). ANG (1μg/ml) was present in the tube formation medium (basal medium + 5% FBS + bFGF (2.5 ng/ml) in the corresponding ANG-pretreated group. Percentages of tumor cells associated with HUVEC network were quantified. Pictured were taken 2 hr after seeding of tumor cell.

(B) *ANG* knockdown U87 cells showed a reduced association with tubule network, which can be rescued by CD24 overexpression. Percentages of tumor cells associated with HUVEC network were quantified. Pictured were taken 2 hr after seeding of tumor cells.

(C) Co-immunofluorescence of CD24 and CD31 for perivascular CD24^{hi} *Ang*$^{+/+}$ and *Ang*$^{-/-}$ mouse glioblastoma cells. The insets are low magnification images. The percentage of brain vessel that are associated with CD24 positive cells were quantified. Five random fields for each of the two animals in the two groups were measured. Bar = 50 μm. Data shown are mean ± SEM. * $P < 0.05$; ** $P < 0.01$; ***, $P < 0.001$; n.s., no statistical difference by Student *t* test.

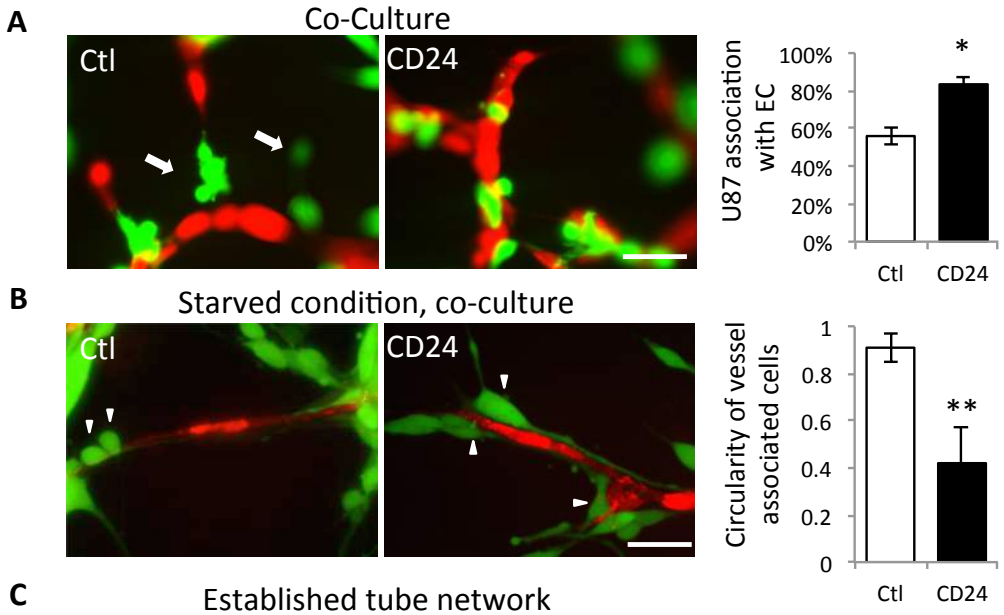

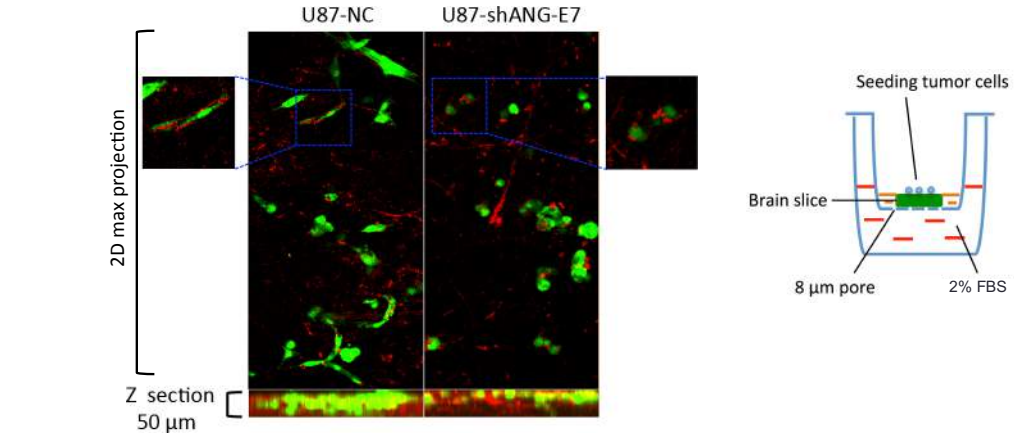

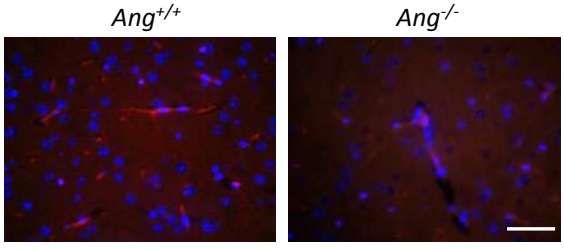

CD24 + CD31 + Nucleus

Figure 3.12. CD24 and ANG contribute to the U87 association with endothelial cells.

(A) U87-GFP-ctl and U87-GFP-CD24 were co-seeded with HUVEC in the tube formation medium. Pictures were taken 3 hours after seeding. The arrows indicate tumor cells not associated with the vessel network. Bar = 20 μm. The percentage of tumor cells associated with HUVEC network was quantified.

(B) U87-GFP-ctl and U87-GFP-CD24 were seeded with HUVEC in the basal medium without angiogenic factors. Pictures were taken 24hr after seeding. Arrowheads indicate EC-associated tumor cells. The dotted line marked the outline of HUVECs. Bar = 20 μm.

(C) Morphologies of control and CD24 overexpressing U87 in association with HUVEC after 8 hr incubation with the established tube network in full medium.

(D) *Ex vivo* invasion assay with brain slices showing ANG is required for perivascular infiltration of U87 cells. Z section is showing more U87-NC cells in the tissue slice compared to *ANG* knockdown. High magnification displays interaction between infiltrative U87 cells and mouse brain vessels. Illustration of the *ex vivo* experiment setup.

(E) Brain vessels are not associated with CD24 positive cells in the non-lesion areas of the brain. IF of CD24 and CD31 staining in the non-tumor area of mouse brain tissues. Data shown are mean ± SEM. * $P < 0.05$; ** $P < 0.01$; ***, $P < 0.001$; n.s., no statistical difference by Student *t* test.

Ang regulates two invasive pathways in mouse GBM

Given that both MMP-9 and CD24 expression can be regulated by ANG in a FOSL2-dependent manner, and that the FOSL2 transcriptional activity depends on its stabilization in the nucleus, which is modulated by ANG/ERK, we proposed a model that ANG induces ECM degradation (MMP-9) and perivascular invasion (CD24) via ABE-mediated transcriptional regulation and ERK-mediated post-transcriptional regulation of FOSL2 (Figure 3.13.A). By Western and immunohistochemistry, we confirmed lack of Ang expression and reduced expressions of Fosl2, Mmp9, and CD24 in *Ang*$^{-/-}$ mouse GBM (Figure 3.13.B-C). N-Cad that is not directly regulated by ANG in GBM was used as a negative control. Its expression did not change in *Ang* knockout mGBM. HA is co-expressed with PDGFB, and the similar expression levels in *Ang*$^{+/+}$ and *Ang*$^{-/-}$ tumors indicates that the difference seen was not because of differential PDGF levels between *Ang*$^{+/+}$ and *Ang*$^{-/-}$ groups. In #46 mouse lysate, we observed a relatively high level of Fosl2 and a strong reduction of Mmp9 expression. Since only nuclear Fosl2 is capable to function as a transcription factor, the level of nuclear Fosl2 in #46 tissue might be less than that in #33 and #97, which requires further investigation.

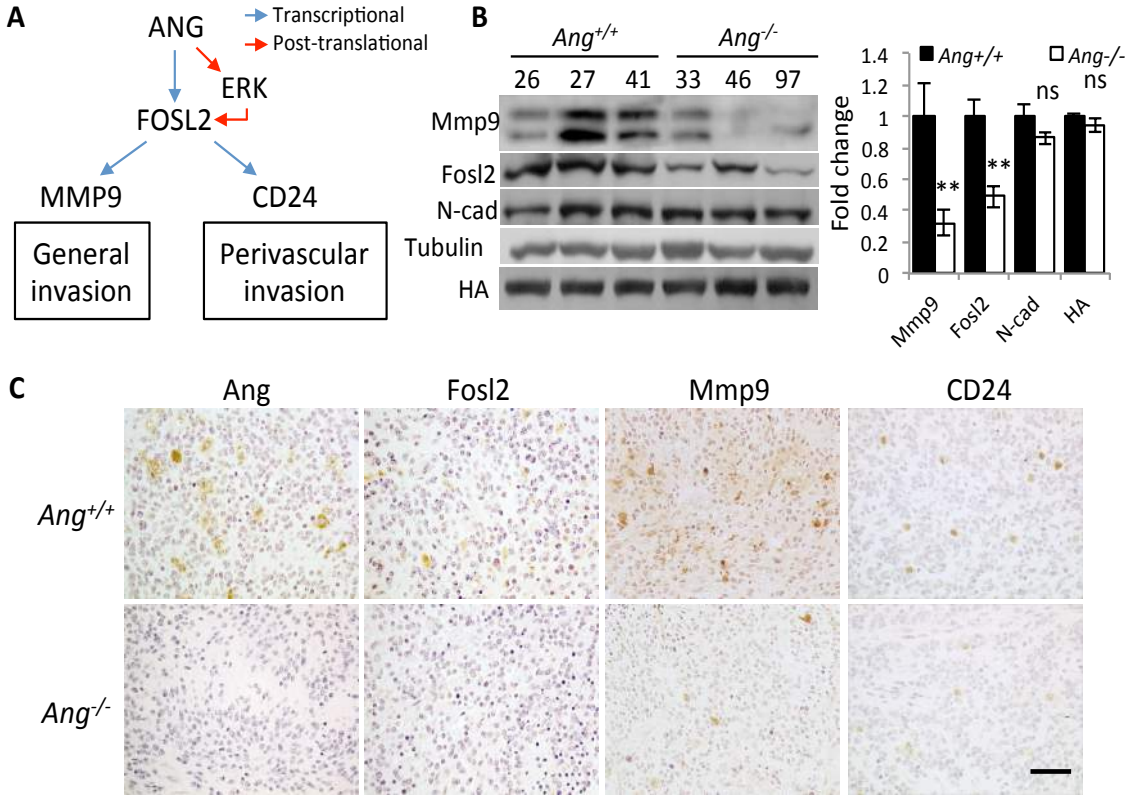

Figure 3.13. Fosl2, Mmp9, and CD24 were reduced in *Ang*$^{-/-}$ mouse GBM.

(A) A proposed model: ANG activates MMP-9 and CD24 through FOSL2 and contributes to two types of glioblastoma invasions.

(B) Mmp9, Fosl2 and CD24 protein are reduced in *Ang*$^{-/-}$ mouse glioblastoma. *Ang*$^{+/+}$ (226, 227 and 241) and *Ang*$^{-/-}$ (233, 246 and 297) tumor lysates were subjected to Western blot for Mmp9, Fosl2, N-Cad, and β-tubulin.

(C) Immunohistochemistry of *Ang*$^{+/+}$ and *Ang*$^{-/-}$ mGBM sections for Ang, Mmp9, Fosl2, and CD24. Bar = 50 μm.

Data shown are mean ± SEM. * $P < 0.05$; ** $P < 0.01$; ***, $P < 0.001$; n.s., no statistical difference by Student's *t* test.

Neomycin, an ANG inhibitor, reduces perivascular invasion in the mouse GBM model and increases animal survival

To examine the potential therapeutic value of targeting ANG in human GBM, we examined the effect of neomycin, an aminoglycoside that specifically blocks nuclear translocation of ANG, on survive and invasion in the mouse GBM model. Paromomycin, a structurally very similar aminoglycoside that differs from neomycin only in the C6 position with a –OH instead of an $–NH_2$ but does not block nuclear translocation of ANG (G. F. Hu, 1998), was used as a control. Daily injection of neomycin significantly increased survival of GBM mice as compared to paromomycin treatment ($P < 0.001$) (Figure 3.14.A). One mouse in the neomycin group appeared to be protected from tumor induction and survived more than 90 days without any neurologic or other symptoms, except a 20.4% reduction in weight compared to an aged-matched non-experimental mouse. Similar to the histologic phenotype observed in $Ang^{-/-}$ mouse GBM, neomycin treatment led to a denser extracellular matrix, an indication of less ECM remodeling (Figure 3.15). We also observed the cellular localization of Ang shifted to more cytosolic and an overall low Ang level in the neomycin-treated group. Furthermore, Mmp-9 and Fosl2 were decreased in the neomycin-treated group (Figure 3.14.B). Tumor cells with high Fosl2 expression were seen surrounding the arteries in the Paromomycin group but were absent in the neomycin-treated group. Vessel-associated, CD24 positive tumor cells were reduced by 61% in neomycin-treated group (Figure 3.14.C). Overall, we found that neomycin prolongs survival of GBM mice by inhibiting the activity of ANG in promoting ECM remodeling and perivascular invasion.

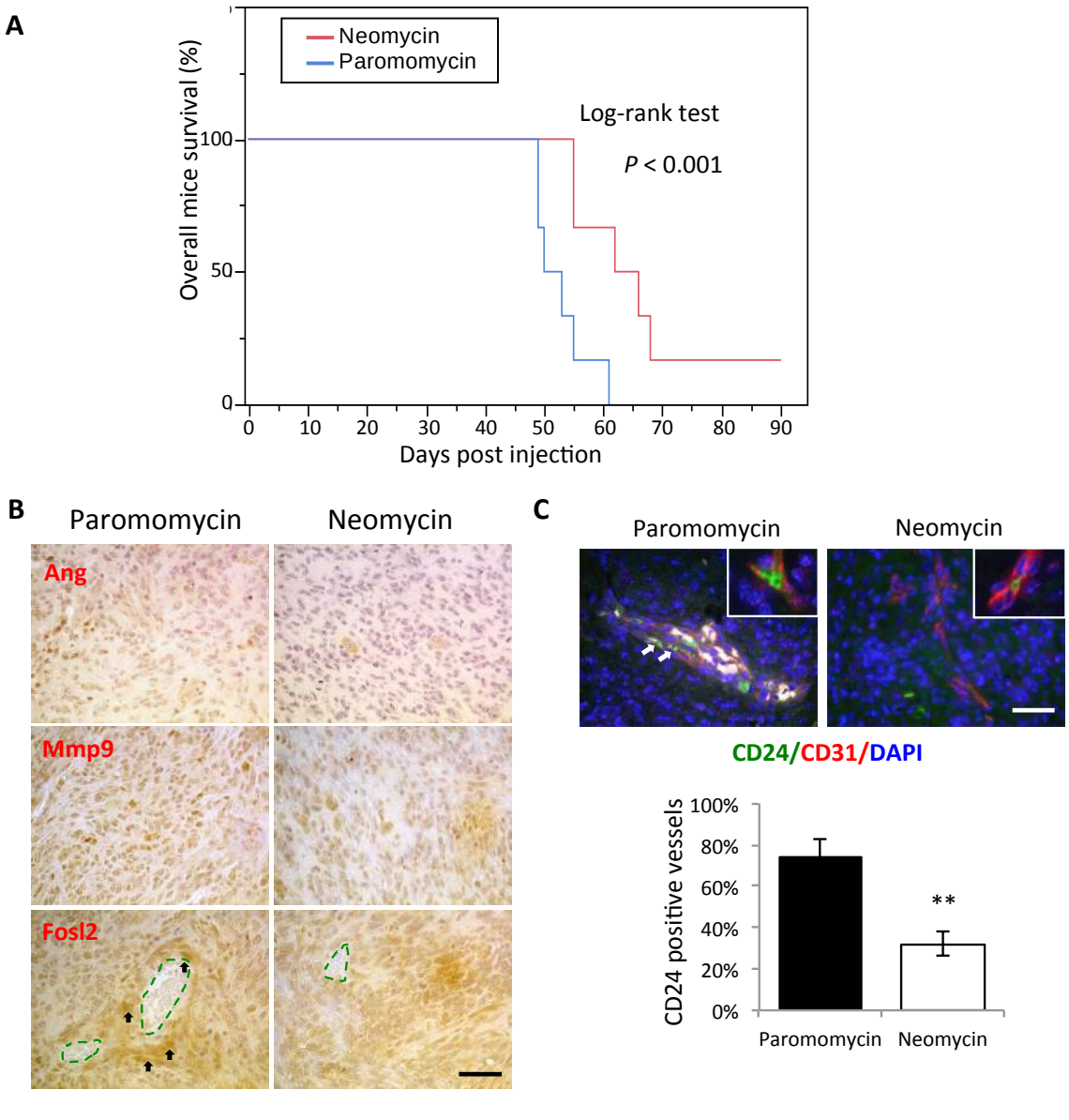
A
Neomycin
Paromomycin
Log-rank test
P < 0.001
Overall mice survival (%)
100
50
0
0
10
20
30
40
50
60
70
80
90
Days post injection
B
Paromomycin
Neomycin
Ang
Mmp9
Fosl2
C
Paromomycin
Neomycin
CD24/CD31/DAPI
CD24 positive vessels
100%
80%
60%
40%
20%
0%
**
Paromomycin
Neomycin

Figure 3.14 Therapeutic effect of ANG inhibitor toward mouse GBM.

(A) ANG inhibitor neomycin extends survival in mouse GBM model. Kaplan-Meier Survival plots of mice bearing GBM received daily i.p. injection of neomycin or paromomycin (10 mg/kg), initiated 14 days after tumor induction. (N = 6, in each group). 95% confidence interval for $Ang^{+/+}$ (55, 90) and $Ang^{-/-}$ (49, 61).

(B) Immunohistochemistry of Ang, Mmp9 and Fosl2 in paromomycin- and neomycin-treated tumor sections. Green dotted lines mark arteries.

(C) Brain tumor vessels were examined for association with CD24 positive tumor cell in the drug-treated tumors. Five pictures under high power field were taken from 2 animals in each group. Bar = 50 μm. Data shown are mean ± SEM. * $P < 0.05$; ** $P < 0.01$; ***, $P < 0.001$; n.s., no statistical difference by Student's *t* test.

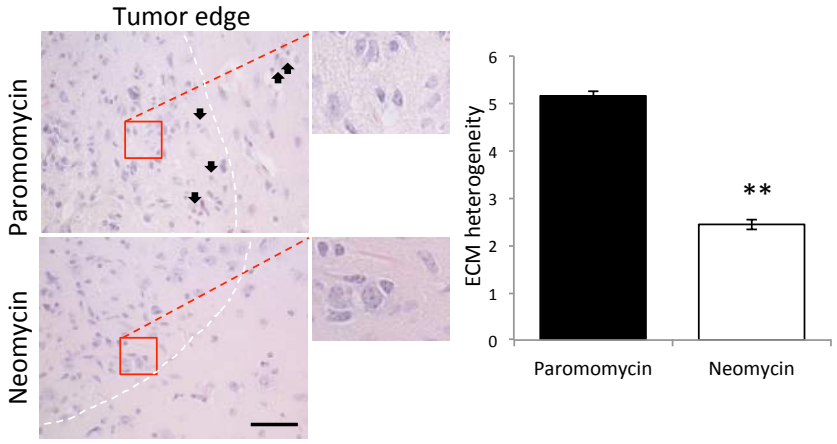

Figure 3.15 Histopathology of drug-treated mGBM

Profiles of eosin-stained matrix of the drug-treated mGBM tissues. Standard deviations of ECM were measured (20 lines were measured in each group). Bar = 50 μm. Data shown are mean ± SEM.

Discussion

ANG and GBM pseudopalisading necrosis

The vasculature network is involved in the formation of pseudopalisading necrosis, a hallmark of GBM. A better understanding of this phenotype is important because it has never been observed in other tumor types, and the pseudopalisading tumor cells around the necrosis site are highly motile, migrating away from the central hypoxic, necrotic area. Therefore, they may contribute to aggressive tumor invasion.

The exact cause for this necrosis phenotype is still in debate. Currently, there are two models: 1) the distant cells away from the blood vessel undergo necrosis due to hypoxia; 2) high proliferating tumor cells induce thrombosis and degeneration of the associated microvessel and thus result in hypoxia (Figure 6.3). It is known that GBM contains severe hypoxic (pO2s ≈ 0.1%) region and that this stress environment selects highly invasive tumor cells that may add to the aggressiveness of the tumor (Evans et al., 2004).

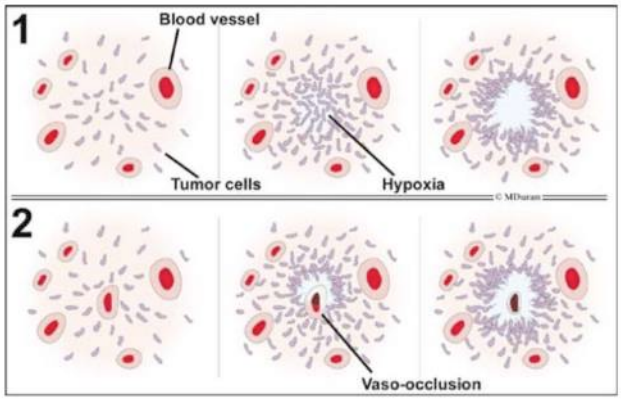

Figure 3.16. Two possible mechanisms for pseudopalisading necrosis formation in GBM. Adapted from Brat and Van Meir, 2004.

However, *Ang* knockout mGBM, which showed better prognosis than the wildtype mGBM, had a 2-fold increase in necrosis (24% in *Ang* knockout *vs.* 11% in WT) (Figure 3.5). In addition to a larger necrosis area, there was intense eosin staining, with an unidentified cause, and more necrotic cells in *Ang*

knockout tumors. According to the grading system at St. Anne-Mayo, GBM without necrosis showed a median survival of 12.5 months, modestly better than the 10.5 months median survival with necrosis (Barker, Davis, Chang, & Prados, 1996). It is interesting that $Ang^{-/-}$ mGBM are more necrotic but had a better survival.

A unique feature of the necrosis in *Ang* knockout mGBM is the multiple layers of pseudopalisading cells and more apoptotic/necrotic cells in the necrosis sites that result in robust apoptosis. Enhanced apoptosis might overset necrosis and played a more predominant role than necrosis therefore leading to a better prognosis in the *Ang* knockout mGBM.

ECM remodeling in GBM

In the *Ang* knockout mGBM, the extracellular matrix is more intact and less permissive for GBM invasion. Considering that MMP-9 expression is mainly restricted to the perivascular space in human GBM, other ECM remodeling factors, especially MMP-2, whose expression is not limited to the perivascular regions and was reduced by *PLXNB2* knockdown in U87, is likely to mediate this ECM remodeling. However, we could not detect any MMP-2 activity by the zymogen assay in U87 conditioned medium with or without ANG stimulus. It is possible that MMP-2 is more abundant in other human GBM cells lines or in GBM tissues. In U87 cells, ANG stimulation induces a 1.8-fold increase in MMP-9 protein level and an additional 20% increase in enzymatic activity as shown by the zymogen assay. This additional increase may result from actin/ANG mediated

plasminogen activation. In general, increased MMP-9 activity in response to ANG is primarily due to its transcription activation.

We used an *in vitro* GBM spheroid system to model the brain tumor invasion and ANG-mediated ECM remodeling. The spheroid center is hypoxic and thus promotes tumor cells dispersal into a 3D collagen matrix, which mimics the *in vivo* circumstance where pseudopalisading GBM cells migrat away from the hypoxic, necrotic area. MMP-9 inhibitor abolished the pro-invasive effect of ANG. Inhibition of ANG in addition to the MMP-9 inhibitor showed no further impedement of spheroid invasion. GBM proliferation is affected by ANG or other treatment, but this is not a confounding factor in the invasion experiment. In this spheroid model, the majority of proliferative cells reside on the surface or in the close proximity to the spheroid; the active invading cells at the front edge are less likely to undergo proliferation (Tamaki et al., 1997). The two quantification methods only considered the location of invading cells at the front and the number of invading cells that were far away from the spheroid and thus was insensitive to proliferation effects. Furthermore, we limited observation to two days that also reduced confounding effects from cell proliferation.

This invasion model is more relevant to the perivascular invasion than vessel-independent parenchyma invasion, because collagen type I is primarily in the vessel sheath not in the parenchyma, although tumor-secreted collagen I may be involved in the process. In conclusion, we demonstrated that MMP-9 is responsible for ANG-induced *in vitro* invasion, which likely contributes to perivascular invasion *in vivo*.

Regulation of FOSL2 by ANG

We demonstrated a specific binding of ANG to the ABE in the promoter region of *FOSL2*. A previous study showed that ANG inhibited ERRγ transcription by binding to the first intron of the gene (Ang et al., 2013). The intron binding sequence appeared to differ from the classic ABE sequence. Therefore, the manner by which ANG regulates expression of the targeted genes could be affected by the location of the binding site and also by the DNA sequence to which it binds. Further studies are needed to identify the co-factors that are recruited to promote transcription.

In addition to transcriptional activation of FOSL2 by ANG, its activity can also be modulated by phosphorylation via ANG-dependent MEK/ERK activation. We showed that in the presence a MEK inhibitor, ANG no longer stimulated p-FOSL2 accumulation in the nucleus. This is in agreement with an early finding that FOSL2 can be regulated by ERK phosphorylation but not by JNK1/2 (Murakami et al., 1997). Fos family protein was reported to enter nucleus via dimerization with Jun family protein (Chida, Nagamori, & Kuroki, 1999). While phosphorylation of c-Fos by JNK was discovered, how the phosphorylation modulates its dimerization with Jun during the nuclear translocation is not known (Tanos et al., 2005). Here, we demonstrated that p-FOSL2, once phosphorylated by ERK, is exclusively in the nucleus. The distinct localization of p-FOSL2 and non-p-FOSL2 prompts us to hypothesize that the phosphorylation at C-terminus plays a dominant role in mediating FOSL2 localization. It may share some regulatory mechanism that governs ERK5 localization: the N-terminal region of ERK5 interacts with its C-terminal region and this interaction promotes its nuclear export, while

phosphorylation of ERK5 prevents this interaction and leads to nuclear accumulation in an importin-dependent manner (Kondoh, Terasawa, Morimoto, & Nishida, 2006).

Figure 3.17 Correlation of *ANG* and *CD24* in a cohort of GBM patients.
Correlation stratified by High or Low *ANG* expression (A) or by GBM subtypes.
Statistical analysis Whole cohort P =0.03; *ANG* Low (P =*0.0006*), *ANG* Hi P = 0.3;
Proneural P =0.0005; Neural P =0.31; Mesenchymal P =0.28; Classical P =0.06.

We showed that ANG upregulated MMP-9 and CD24 through FOSL2 in U87 cells. This regulation is highly relevant in human GBM, because *ANG* expression is significantly correlated with *FOSL2* and *MMP-9* in a cohort of GBM patients (TCGA, Cell 2013). However, we did not detect a positive correlation between *ANG* and *CD24* in the same cohort (Figure 6.4.A). By stratification analysis, it turned out that the correlation significantly differs between proneural GBM and non-proneural GBM (Figure 6.4.B). Higher *ANG* is correlated with greater *CD24* only in the proneural GBM, which supports our *in vivo* finding in the proneural mGBM that *Ang* knockout abolished CD24-mediated perivascular invasion.

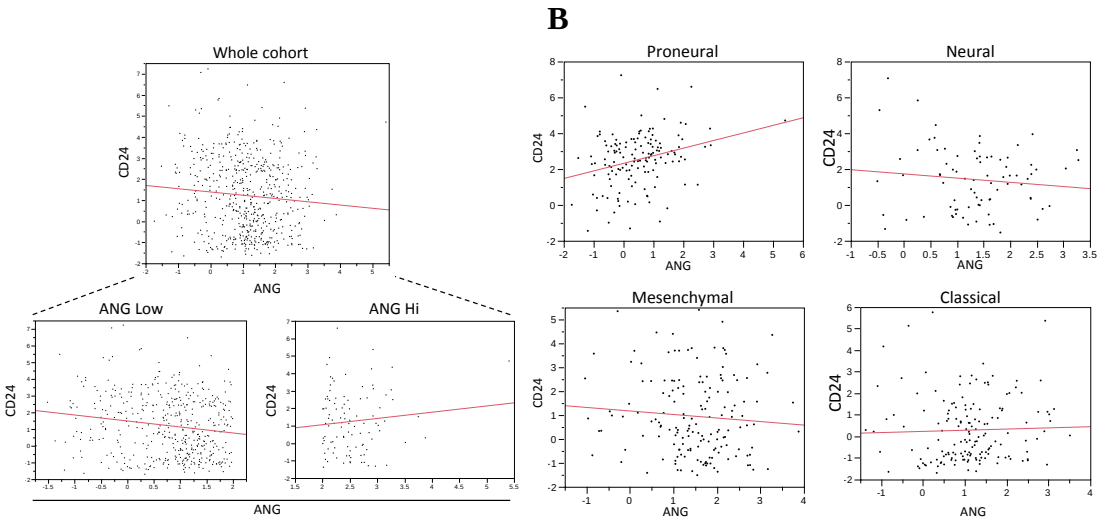

Upon entering the nucleus, p-FOSL2 can amplify the activation signal by binding to the promoter of its own genes. We hypothesize that inhibition of this ANG/FOSL2 activation

could be mediated through a phosphatase that deactivates the positive feedback mechanism of FOSL2 and promotes its nuclear export. Identifying this phosphatase could be pursued in future study.

Perivascular invasion as a preferred mode of action in brain tumors

Brain tissue is soft because it lacks rigid collagen protein and is enriched with slimy proteoglycan that slows down cell migration. Additionally, the carbohydrate component of proteoglycan is resistant to protease degradation. Therefore, brain ECM poses a barrier to tumor invasion even after extensive remodeling by MMPs. Primary brain tumors and brain metastases all show widespread perivascular invasion as a unique way to infiltrate into brain tissues (Baker et al., 2014). There are a few factors that contribute to this unique phenotype. 1) brain requires extensive perfusion of oxygen to sustain high metabolism and thus microvessel density is extremely high, consequently it is relatively easy for tumor cells to find a neighboring vessel and nearly impossible for individual cell to avoid contacting microvessel during invasion and proliferation; 2) microvessels provides readily oxygen perfusion, adhesion factors, and amenable collagen ECM to activate intracellular signaling including FAK, PI3K, and ERK pathway for perivascular invasion; 3) because GNS cells often reside in the perivascular niche, it is possible that the early tumor-initiating cells are also in the perivascular niche. As they migrate along the vessels, the progeny and differentiated brain tumor cells spread and infiltrate into the tissues. In all possible scenarios, microvessels and vasculature network is an integral component of GBM invasion.

The perivascular invasion of GBM cells involves three distinct steps. 1) recruitment of tumor cells to the vessels; 2) maintenance of a close interaction with endothelial cells to obtain oxygen and nutrients; 3) activation of invasion signaling to facilitate ECM degradation and disruption of pericyte binding (Cuddapah, Robel, Watkins, & Sontheimer, 2014b). Bradykinin released by endothelial cells functions as a chemoattractant for GBM cells by activating $K_{Ca}3.1$ channel-mediated migration (Cuddapah et al., 2013; Montana & Sontheimer, 2011). However, inhibition of Bradykinin receptor on GBM cells doesn't completely abolish chemotaxis, suggesting that there are other unidentified factors involved as well (Montana & Sontheimer, 2011). We found that ANG promotes perivascular invasion by both increasing the interaction between tumor and endothelial cells and also by inducing ECM remodeling through MMP-9 activation. In addition to GBM cells, endothelial cells also secrete ANG. We hypothesize that endothelial cell-secreted ANG may also function as a chemoattractant for GBM cells, because ANG is known to induce tumor invasion, and endothelial cells do not re-uptake ANG during the non-proliferation condition. If this hypothesis is true, ANG activates GBM perivascular invasion at all three key steps.

Chapter IV

Angiogenin is essential for glioblastoma proliferation and angiogenesis

The inhibitory effect of ANG on p53 (Sadagopan et al., 2012) suggests that ANG may play a role in tumorigenesis and in cancer transformation. In the mouse GBM model described in Chapter III, *Ang* appeared to be not involved in tumor initiation. Here, we use *in vitro* assays to interrogate the effects of ANG deficiency on oncogene-induced transformation and on GBM progression, especially in proliferation and apoptosis. Lastly, we carry out *in vitro* and *in vivo* assays to confirm the angiogenic activity of ANG in GBM.

ANG is essential for anchorage-independent growth and K-Ras-V12/SV40LT cellular transformation

The proliferative effect of ANG has been well studied in endothelial cells and neoplasia, such as in prostate and bladder cancers (Ibaragi, Yoshioka, Kishikawa, et al., 2009a; Kishimoto et al., 2005; Miyake et al., 2014). ANG level escalates in the higher grade of glioma, and this observation has led to the conjecture that the function of ANG, besides angiogenesis, may result in malignant transformation in glioma (Eberle et al., 2000). First, we assessed the role of ANG in mouse embryonic fibroblast (MEF) transformation. We used lentivirus to introduce oncogenic K-Ras-V12/GFP and SV40LT/puromycin in freshly isolated MEFs from wildtype and *Ang* knockout mice. The infection rate was ~60% corresponding to an MOI level of 1. The stably transformed MEF (t-$Ang^{+/+}$ and t-$Ang^{-/-}$) lines were obtained after GFP sorting and puromycin selection. After virus transduction, $Ang^{+/+}$ MEF showed significant morphology changes, becoming more elongated and spindle-like while this change was not obvious in $Ang^{-/-}$ MEF (Figure 4.1.A). K-Ras-V12 and SV40LT were expressed at similar levels in the two t-MEFs as

shown by semi-quantitative PCR (Figure 4.1.B). In a 7-day proliferation assay, *Ang*$^{+/+}$ multiplied modestly faster than *Ang*$^{-/-}$, but the difference became insignificant in the transformed MEFs, indicating that the slowdown in proliferation due to lack of Ang activity in *Ang*$^{-/-}$ MEF was overcome by SV40LT/K-Ras-V12. Importantly, it also suggested that Ang was not required in SV40LT/K-Ras-V12-driven proliferation under 2D growth condition (Figure 4.1.C). Next, t-MEFs were examined for anchorage-independent growth, which measured cellular resistance to anoikis and tumorigenic potential (Guadamillas et al., 2011; Shin et al., 1975). Although both t-MEFs showed a similar proliferative rate in 2D culture, there was a significant growth difference in agarose where t-*Ang*$^{-/-}$ generated less and smaller colonies, suggesting that Ang activity is required for SV40LT/KRasV12-mediated tumor formation (Figure 4.1.D). These data suggested that signaling pathway that governs anchorage-independent growth is independent of proliferation in the 2D culture in response to ANG.

In benign tumors, local proliferation is unchecked but tumor cells need to undergo epithelial-mesenchymal-transition (EMT) or malignant transformation in order to acquire the invasive phenotype and metastasize to other organs. Anoikis is a type of specified apoptosis due to loss of ECM contact. It is a hallmark of cells that have not fully differentiated into mesenchymal status. We examined apoptosis in tMEFs and found t-*Ang*$^{-/-}$ colony had a 3-fold higher apoptosis rate than that in t-*Ang*$^{+/+}$, as shown by EB staining (Figure 4.1.E-F). We hypothesized that the absence of Ang activity leads to a progressive loss of mesenchymal status in *Ang*$^{-/-}$ tMEF. Fibroblasts are of mesenchymal origin and thus the lack of *Ang* activity in *Ang*$^{-/-}$ fibroblasts might fail to maintained

mesenchymal gene program during transformation or initiate mesenchymal-to-epithelial transition (MET). E-Cad, a marker for epithelial lineage was upregulated, whereas mesenchymal marker, N-Cad, was downregulated, as shown by immunoblotting (Figure 4.2.A). Interestingly, Fosl2, an immediate mediator of Ang as we identified earlier (Chapter III), which has been shown to be associated with mesenchymal gene expression in GBM (L. A. D. Cooper et al., 2012), was also reduced in *Ang* knockout tMEF. Furthermore, the majority of EMT regulators including *Zeb1/2, Twist1* and *Tgf-ß1* were downregulated as well in t-*Ang*$^{-/-}$ while Snail1/2 and an EMT blocker, *Bmp7*, were not significantly changed (Figure 4.2.B). During MET, cells frequently show reduced motility and become less invasive (Kalluri & Weinberg, 2009). In transwell migration/invasion experiments, we showed that t-*Ang*$^{-/-}$ displayed reduced migration and invasion, by 73% and 60%, respectively (Figure 4.2.C-D). MMPs contribute to invasion and EMT (Kalluri & Weinberg, 2009). qRT-PCR showed a reduced *Mmp2, Mmp3,* and *Mmp9* expression in t-*Ang*$^{-/-}$ (Figure 4.2.E), which further supported the contention that *Ang* knockout induces MEF into an epithelial phenotype during SV40LT/KRas-V12-induced transformation.

The first round t-MEFs colonies were selected for a serial agarose-passaging assay (Figure 4.1.G), which revealed an even greater defect in colonies-forming potential in *Ang* knockout t-MEF (colonies-forming transformed MEF, ct-MEF). Lastly, we examined tumor growth potential of t-MEF in nude mice. We found that *Ang* knockout tMEF failed to establish s.c. tumor during the 50 days observation period (N = 2) (Figure 4.1.H). However, t-*Ang*$^{+/+}$ established robust tumors. Moreover, the ct-*Ang*$^{+/+}$ showed an

increased *in vivo* tumor growth rate over t-*Ang*$^{+/+}$. It was difficulty in scaling up the ct-*Ang*$^{-/-}$ and thus precluded its analysis in this experiment. These *in vivo* growth data supported the findings from *in vitro* agarose experiments and further demonstrated a less essential role of Ang in oncogene driven cell cycling under growth condition but a pivot role in protecting cells from anoikis and promoting malignant transformation of fibroblasts.

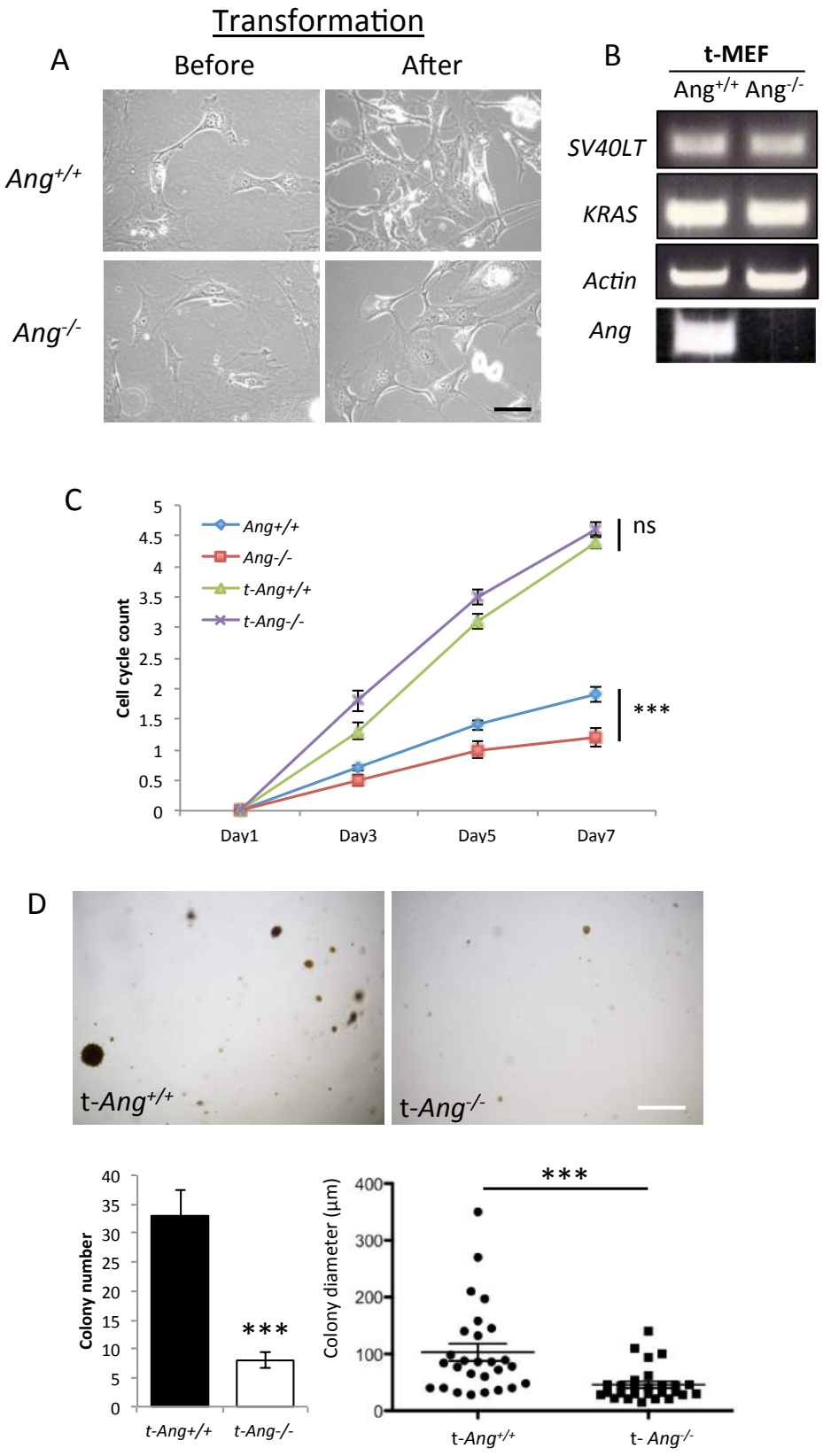
Transformation
A
Before
After
Ang+/+
Ang-/-
B
t-MEF
Ang+/+ Ang-/-
SV40LT
KRAS
Actin
Ang
C
Cell cycle count
Ang+/+
Ang-/-
t-Ang+/+
t-Ang-/-
ns
***
Day1
Day3
Day5
Day7
D
t-Ang+/+
t-Ang-/-
Colony number
***
t-Ang+/+
t-Ang-/-
Colony diameter (µm)
***
t-Ang+/+
t- Ang-/-

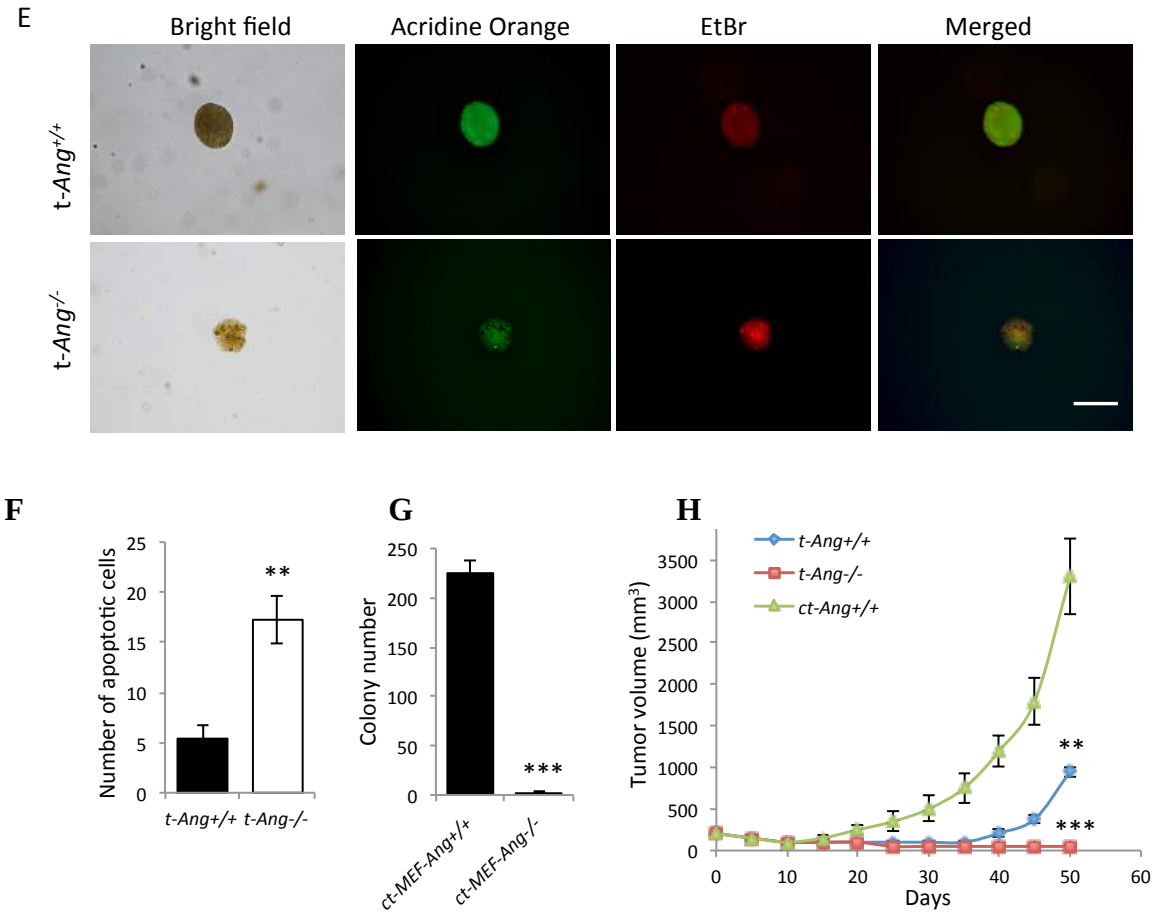
E
Bright field
Acridine Orange
EtBr
Merged
t-Ang+/+
t-Ang-/-
F
Number of apoptotic cells
25
20
15
10
5
0
**
t-Ang+/+
t-Ang-/-
G
Colony number
250
200
150
100
50
0
***
ct-MEF-Ang+/+
ct-MEF-Ang-/-
H
Tumor volume (mm3)
3500
3000
2500
2000
1500
1000
500
0
t-Ang+/+
t-Ang-/-
ct-Ang+/+
**
***
0
10
20
30
40
50
60
Days

Figure 4.1. *Ang* knockout inhibits SV40-LT/K-Ras-V12 mediated MEF transformation.

(A) Morphology of MEFs before and after K-Ras-V12/SV40LT transduction. Bar = 50 μm.

(B) mRNA level of transfected of SV40LT, K-Ras and ANG by PCR in t-*Ang*$^{+/+}$ and t-*Ang*$^{-/-}$.

(C) Cell cycle counts of t-MEFs and parental untransformed MEFs.

(D) MEF colonies in agarose after 14 days. Total number of colonies and the diameter of each colony were quantified. Bar = 500 μm.

(E) High magnification (x 100) images of colonies stained with AO/EtBr. Number of dead cells per colony was counted. Bar = 200 μm.

(F) Quantification of apoptotic cells number per colony as shown in panel B.

(G) Colonies were harvested from t-MEF and were tested in serial colony formation assay.

(H) T-MEFs (*Ang*$^{+/+}$ and *Ang*$^{-/-}$) and ct-*Ang*$^{+/+}$ MEF were examined for tumor establishment in nude mice (N = 2).

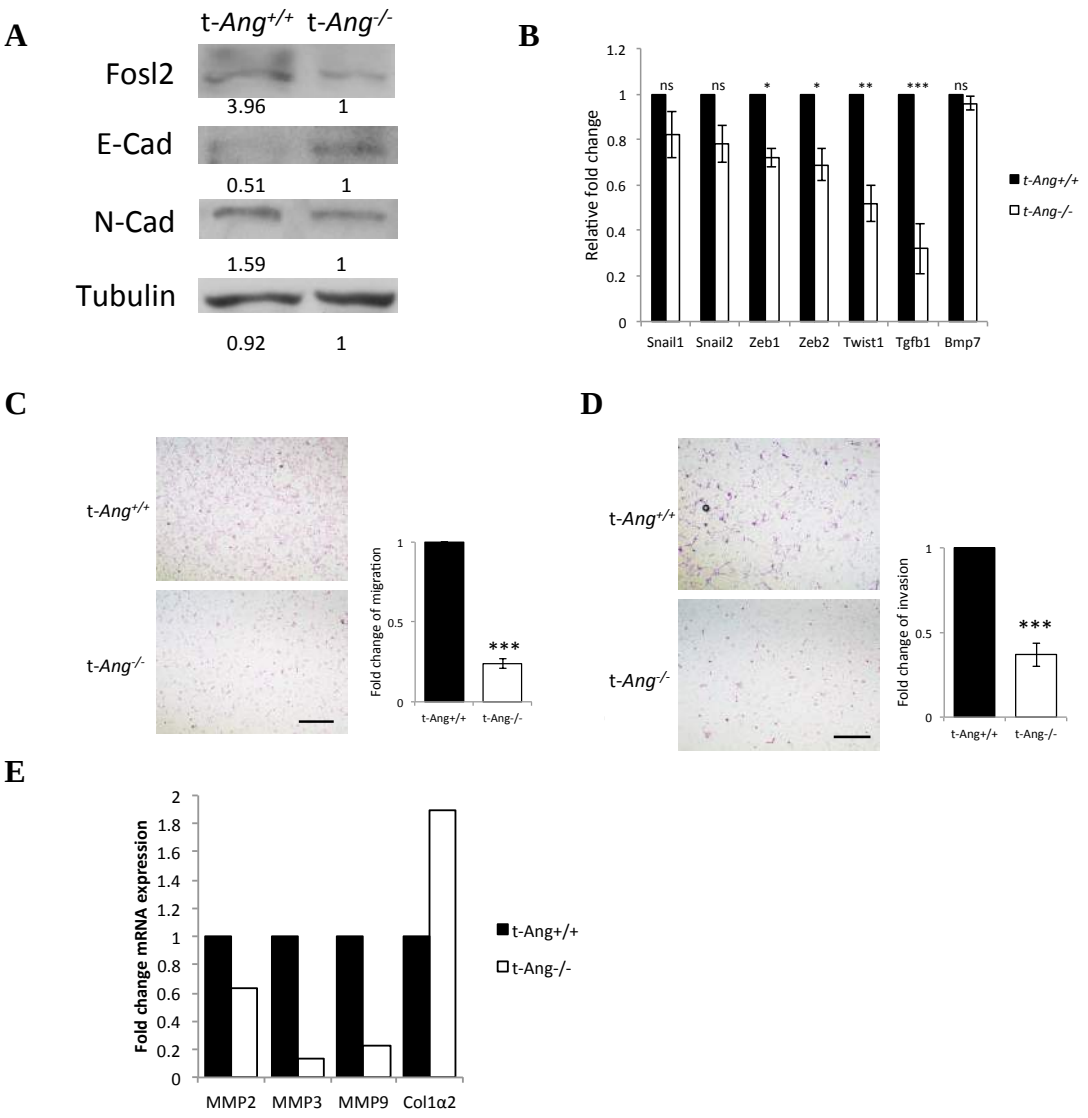

Figure 4.2. Further characterization of *Ang* knockout transformed MEF.

(A) WB of Fosl2, E-cad, N-cad in t-MEFs.

(B) qRT-PCR of major EMT factors in t-MEFs.

(C) t-*Ang*$^{-/-}$ MEF shows reduced cell migration. Transwell migration assays were performed, and data recorded at 24 hrs. Bar = 500 μm.

(D) t-*Ang*$^{-/-}$ MEF shows reduced cell invasion in transwell invasion assay.

(E) *Mmp2*, *Mmp3* and *Mmp9* expression measured by qRT-PCR in t-MEFs.

ANG is essential for rRNA transcription and proliferation of GBM

Oncogenic K-Ras can induce astrocyte transformation and form mouse GBM (Dasgupta, Li, Perry, & Gutmann, 2005)(Uhrbom et al., 2002). Considering the finding that Ang contributed to K-Ras-mediated MEF transformation, we hypothesized that GBM may also need ANG activity for its aggressive growth. Therefore, we first examined whether ANG is required for U87 proliferation by means of *ANG* knockdown. To obtain stable *ANG* knockdown U87 cell lines, four different shRNA sequences (scramble control, A4, E4, and E7; pGPIZ system) were used to package lentiviruses and transduce U87 at a MOI level of 2, which resulted in a ~86% infection rate before drug selection. All three shRNA achieved more than 70% knockdown at the ANG protein level, with E4 and E7 being more effective at 90% effieiency (Figure 4.3.A). We therefore used the highest knockdown clone E7 in subsequent experiments. To examine changes in rRNA transcription level as a consequence of *ANG* knockdown, U87-E7 was treated with 1 μg/ml recombinant ANG for 1 h before RNA extraction. Q-PCR showed a 5-fold decrease of 47S rRNA level in U87-E7 clone compared to the PBS control, and 1 hr treatment with exogenous ANG was able to recover partially the 47S rRNA abundance in the E7 cells (Figure 4.3.B). In a 7 day proliferation assay, E7 *ANG* knockdown clone showed a significantly lower cell number compared to the control and this change was attenuated by exogenous ANG but not by RNase A, indicating that the phenotype of *ANG* knockdown in U87 proliferation was specific to the reduced activity of ANG (Figure 4.3.C). To examine the proliferative effect of ANG in another GBM line, we generated *ANG* knockdown E7 and control stable lines from a glioblastoma-derived neural stem (GNS) line GNS-6-22, which is a subpopulation of primary human GBM that was

propagated in the undifferentiated sphere format. In contrast to differentiated lines like U87 and U251, GNS-6-22 exhibited high tumor initiating potential in the serum-free culture condition (Sherry et al., 2009). The capability of the GNS cells to form sphere in the serum-free culture medium represents self-renewal of undifferentiated stem cells. In the serial seeding conditions, we observed a reduced number of spheres as well as a smaller size of the spheres in E7 cells (Figure 4.3.D). Therefore, the proliferative effect of ANG manifested in both differentiated and undifferentiated GBM cell lines. Previous study in our lab had demonstrated that initiation of U87 xenograft in nude mice were delayed up to 35 days by a neutralizing monoclonal antibody 26-2F, which supports the hypothesis that other effects of ANG, in addition to angiogenesis, regulates GBM progression (Figure 4.3.E).

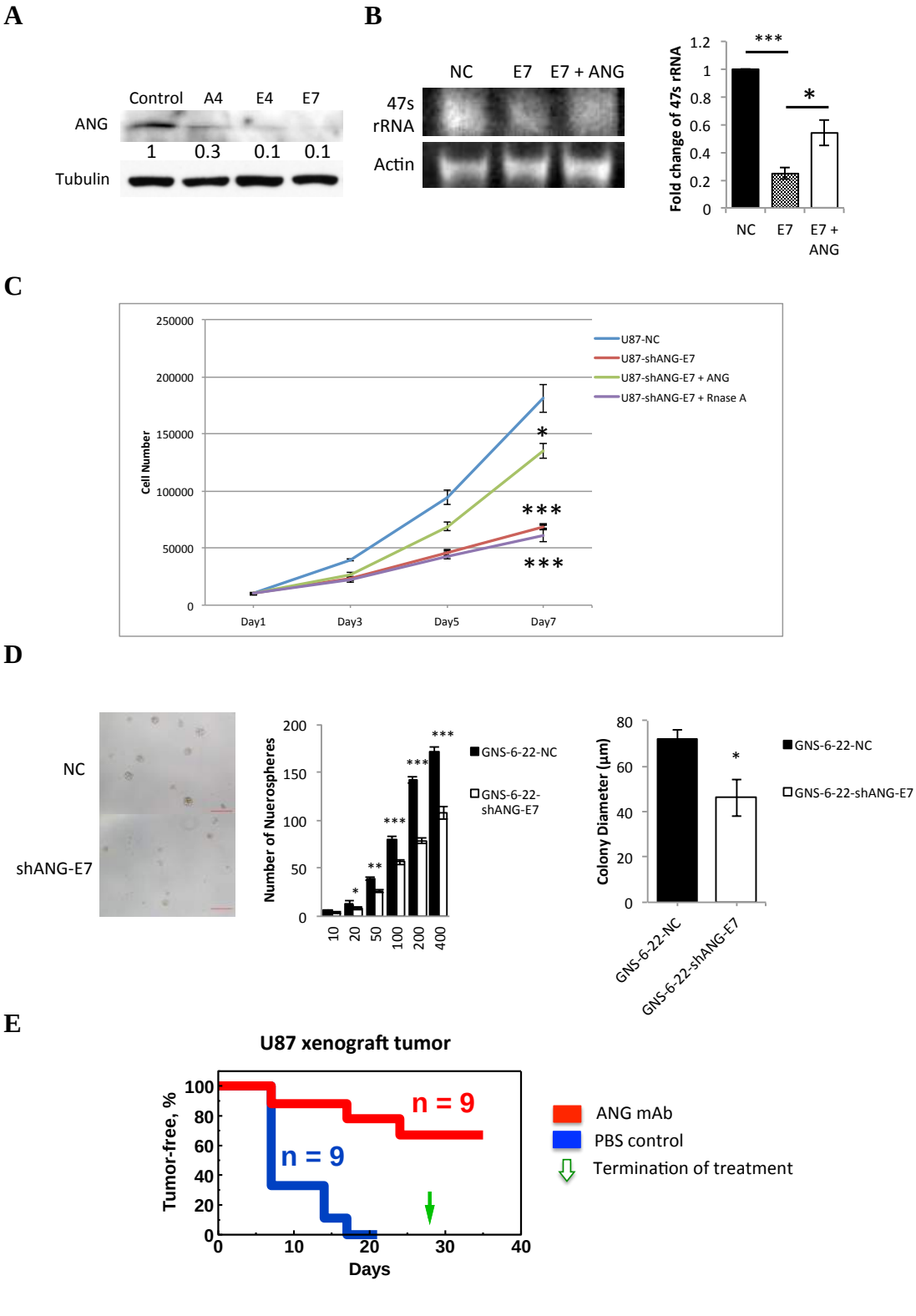
A
Control
A4
E4
E7
ANG
1
0.3
0.1
0.1
Tubulin
B
NC
E7
E7 + ANG
47s rRNA
Actin
Fold change of 47s rRNA
1.2
1
0.8
0.6
0.4
0.2
0
***
*
NC
E7
E7 + ANG
C
250000
200000
150000
100000
50000
0
Cell Number
Day1
Day3
Day5
Day7
U87-NC
U87-shANG-E7
U87-shANG-E7 + ANG
U87-shANG-E7 + Rnase A
*
***
***
D
NC
shANG-E7
Number of Nuerospheres
200
150
100
50
0
10
20
50
100
200
400
GNS-6-22-NC
GNS-6-22-shANG-E7
Colony Diameter (μm)
80
60
40
20
0
GNS-6-22-NC
GNS-6-22-shANG-E7
E
U87 xenograft tumor
Tumor-free, %
100
80
60
40
20
0
0
10
20
30
40
Days
n = 9
n = 9
ANG mAb
PBS control
Termination of treatment

Figure 4.3. ANG knockdown reduces 47S rRNA transcription and inhibits proliferation of glioblastoma tumor cells

(A) Lentiviral shRNA clones A4, E4, and E7 were used to knockdown *ANG* expression in U87 GBM cell line. Whole cell lysates were immunoblotted for ANG.

(B) Real-time PCR analysis of 47S rRNA transcription. Data were normalized to *GAPDH* control. The Q-PCR products were run in agarose gel.

(C) *ANG* knockdown reduces U87 proliferation, which was rescued by exogenous recombinant ANG (1μg/ml), but not by RNase A (1μg/ml).

(D) *ANG* knockdown in GNS-6-22 by shRNA clone E7 reduces sphere number and size in serial seeding assay. Control/NC, scramble shRNA. Bar = 200 μm. Error bar = SEM. *, $P < 0.05$; **, $P < 0.01$; ***, $P < 0.001$.

(E) ANG mAb 26-2F inhibits U87 tumor establishment in nude mice.

ANG regulates anchorage-independent growth and protects stressed-induced apoptosis of U87 cells

In the experiments to examine the function of ANG in anchorage-independent growth of U87, we found that either inhibition of ANG activity by a monoclonal antibody or knockdown of *ANG* expression by shRNA each was able to impair colony formation (Figure 4.4.A). Inhibition of ANG in U87 modestly reduced the number and the size of the colonies, accompanied by a modestly increased anoikis in the colonies. *ANG* knockdown E7 cells showed a more severely compromised colony formation capacity, with the majority of the colonies failed to reach a size of 50 μm in diameter, and showed a high apoptosis rate of 60%. Under the same conditions, the apoptosis rate of scramble control cells was less than 5% (Figure 4.4.B).

Increased apoptosis correlated with an impaired growth in agarose in both U87 and t-MEF. Pathway enrichment of genes that were correlated with ANG expression from a cohort of GBM patients revealed that ANG expression was highly associated ($P < 10^{-8}$) with the anti-apoptosis gene signature (Figure 4.4.C), in agreement with our data that inhibition of ANG increased apoptosis. Our lab has previously demonstrated an anti-apoptosis effect of ANG in neuronal cells (S. Li et al., 2010; 2012). We therefore examined whether ANG prevents apoptosis of U87 under stress conditions that are commonly found in fast proliferating cancers. We found that under oxidative, ER, and nutrient deprivation stresses, *ANG* knockdown increased apoptosis . Significantly, treatment of exogenous ANG reduced apoptosis in E7 cells, indicating the specificity of the knockdown (Figure 4.4.D). Among the three stress inducers, the ER stress condition induced the highest apoptosis increase, by nearly 30-fold. These data indicate that U87 is

sensitive to stresses, and that endogenous ANG is essential for preventing apoptosis under all three stress conditions.

A

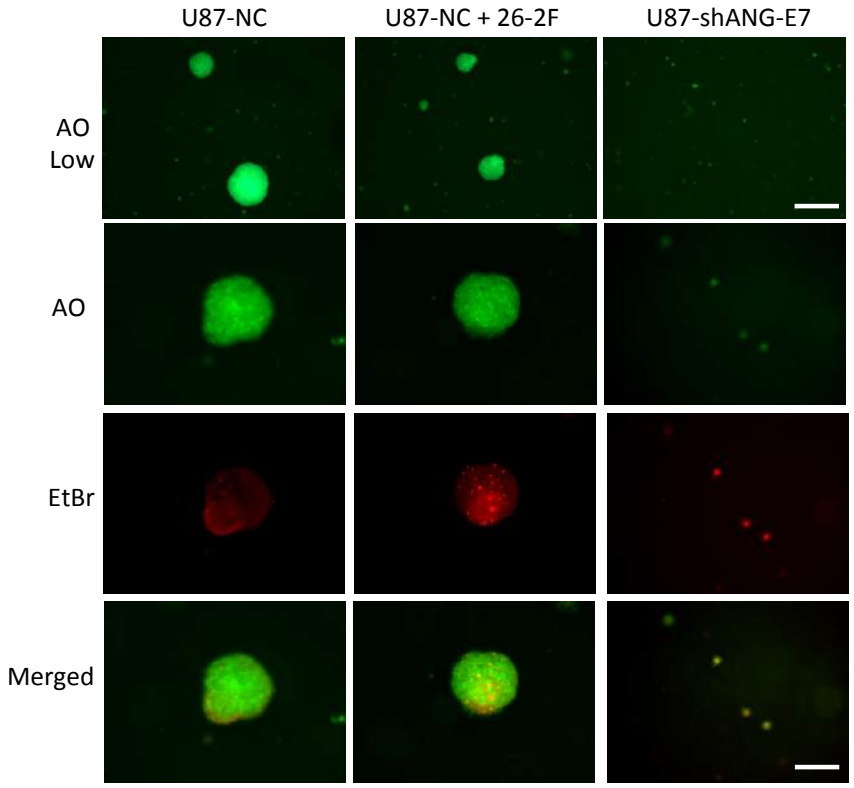

B

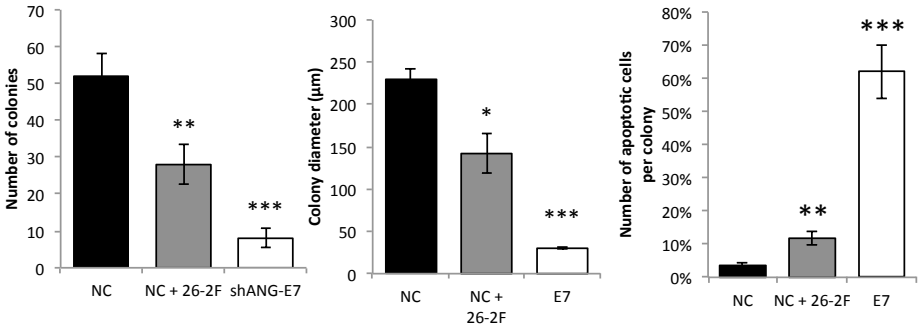

C

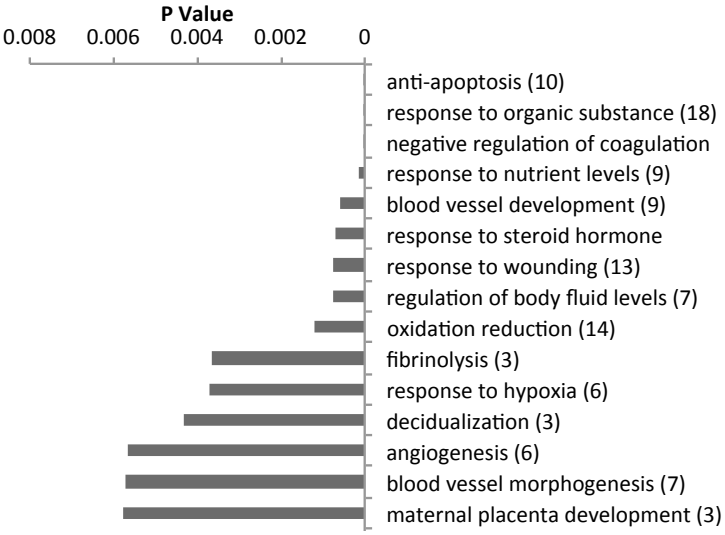
P Value
0.008
0.006
0.004
0.002
0
anti-apoptosis (10)
response to organic substance (18)
negative regulation of coagulation
response to nutrient levels (9)
blood vessel development (9)
response to steroid hormone
response to wounding (13)
regulation of body fluid levels (7)
oxidation reduction (14)
fibrinolysis (3)
response to hypoxia (6)
decidualization (3)
angiogenesis (6)
blood vessel morphogenesis (7)
maternal placenta development (3)

D

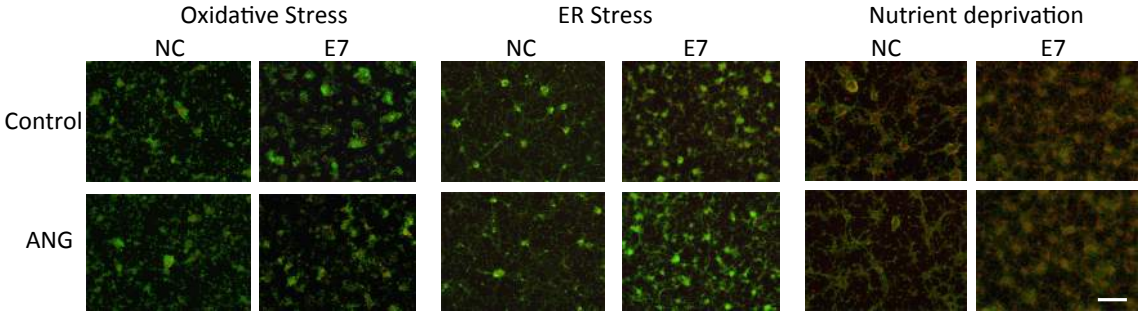
Oxidative Stress
ER Stress
Nutrient deprivation
NC
E7
NC
E7
NC
E7
Control
ANG

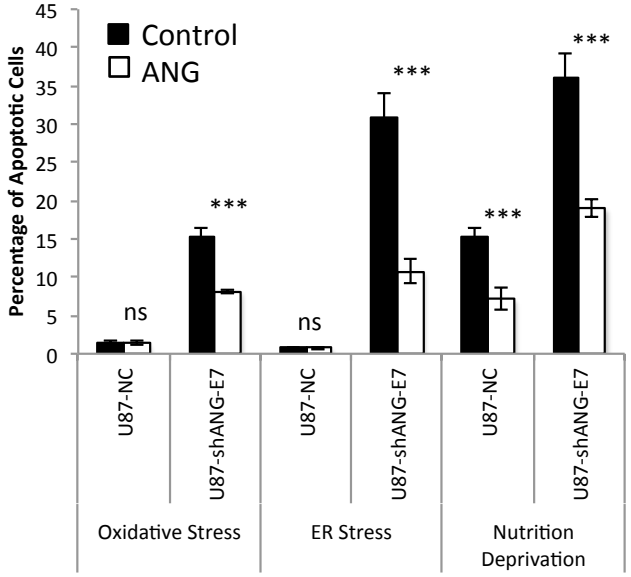
Percentage of Apoptotic Cells
45
40
35
30
25
20
15
10
5
0
Control
ANG
ns
***
ns
***
***
***
U87-NC
U87-shANG-E7
U87-NC
U87-shANG-E7
U87-NC
U87-shANG-E7
Oxidative Stress
ER Stress
Nutrition Deprivation

Figure 4.4. ANG inhibition reduces glioblastoma anchorage-independent growth and increases stress-induced apoptosis

(A) ANG monoclonal antibody 26-2F (50 μg/ml) or shRNA (E7) reduces anchorage-independent growth of U87 in agarose. High magnification of live cells, stained with acridine orange, and apoptotic cells stained positive with EtBr. Bar = 500 μm (low) and (high) 200 μm.

(B) Quantification of the number and size of the colonies and apoptosis rate in colonies.

(C) Pathways enrichment of genes correlated with ANG expression in a cohort of GBM patients. (TCGA, GBM Cell 2013)

(D) Apoptosis analysis of *ANG* knockdown U87 line E7 and the control by AO/EB staining. Cells were treated with or without ANG (1 μg/ml) under oxidative (SA, sodium arsenite), ER (Tunicamycin) stress or nutrient deprivation (starvation, plain DMEM) to examine stress-induced apoptosis. Bar = 500 μm.

ANG regulates GBM proliferation and apoptosis *in vivo*

In Chapter III, we showed that *Ang* knockout reduces mGBM invasion. Here, we aimed to determine additional changes in cell cycle and apoptosis in $Ang^{-/-}$ mGBM. In the control $Ang^{+/+}$ mGBM, the majority of actively cycling cells were found at the invasive edge and at the perivascular locations. The PCNA-positive cells were 84% and 70%, respectively, at these two locations, whereas only 5% of PCNA positive cells were found in the tumor core area (Figure 4.5.A). A similar high prevalence of proliferative cancer cells at the tumor peripheral was observed in other studies (Hambardzumyan, Amankulor, Helmy, Becher, & Holland, 2009; Keunen et al., 2011). *Ang* knockout decreased proliferation rate by 2-fold at the invasive edge and by nearly 10-fold at the perivascular location. Cell proliferation at the tumor core was not significantly different between the two groups. These data demonstrated that ANG played a more important role in invasion–related proliferation and that the signaling pathways mediating its pro-invasive and pro-survival functions during aggressive GBM progression maybe correlated. We have also found a striking difference in necrosis between wildtype and *Ang* deficient mGBM. There was a more than 2-fold increase in necrotic area and also a more intense eosin staining within the necrosis area in *Ang* knockout mGBM (Figure 4.5.B). Although we did not see an effect of *Ang* on cell cycle in the tumor core, there was a significant increase (>3-fold) in apoptosis. Increased apoptosis was also seen in the necrotic area in *Ang* deficient mGBM (2-fold) (Figure 4.5.C). In neomycin-treated $Ang^{+/+}$ mGBM tissues, increased apoptosis in the necrotic area was more profound (> 8 fold) (Figure 4.5.D). The stronger effect induced by neomycin may result from a compensatory mechanism in *Ang* knockout animals. Collectively, these results indicated that ANG

contributed to a faster cell cycling at the invasive edge and perivascular location while functioning as a pro-survival factor in in the rest area of GBM.

A

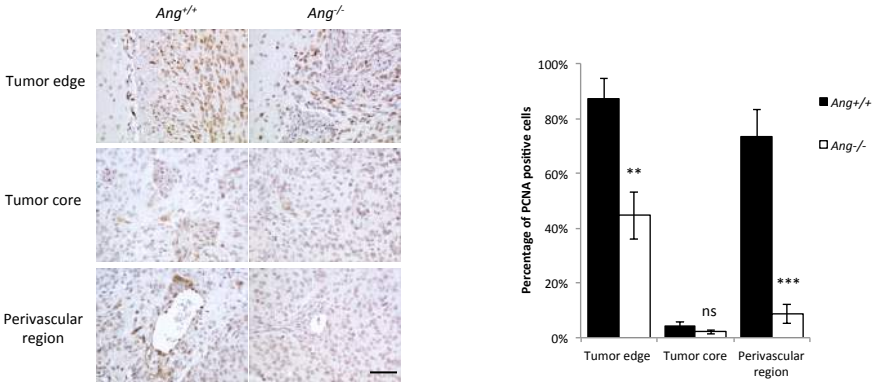

B

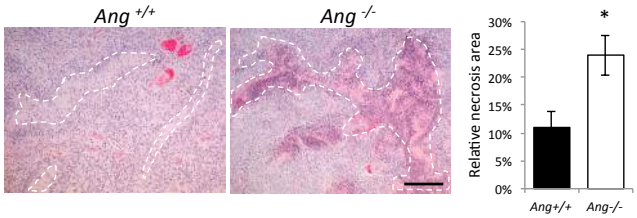

C

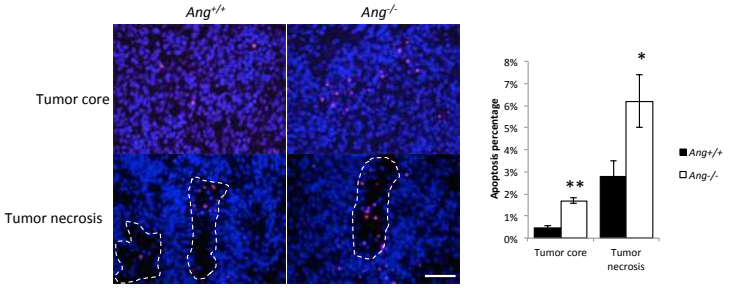

D

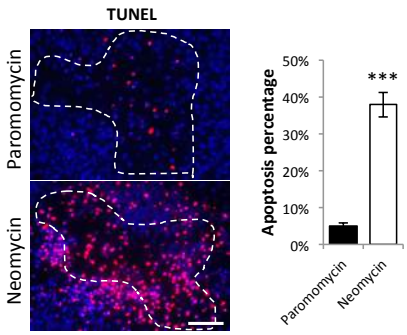

Figure 4.5. Ang regulates GBM proliferation and apoptosis *in vivo*

(A) PCNA immunohistochemistry staining for proliferative cells in $Ang^{+/+}$ and $Ang^{-/-}$ mouse glioblastoma at tumor invasive edge, tumor core and perivascular regions. Bar = 50 μm.

(B) Comparison of necrosis in $Ang^{+/+}$ and $Ang^{-/-}$ mGBM by H&E staining.

(C) Quantification of the percentage of apoptotic cells in $Ang^{+/+}$ and $Ang^{-/-}$ mGBM. Bar = 200 μm.

(D) Quantification of apoptosis in ANG inhibitor-treated $Ang^{+/+}$ mGBM.

ANG activates AKT and ERK in GBM

To understand how ANG mediates anti-apoptosis in GBM, we examined whether ANG activated AKT or ERK pathway as it has been reported in other cell lines (H.-M. Kim, Kang, Kim, Kang, & Chang, 2007; S Liu et al., 2001). We first examined the time course of 1 μg/ml ANG treatment in serum-starved U251 cells. AKT was gradually activated as ANG was uptaken by the cells. ERK activation appeared to be faster than AKT actiavtion, peaked at 30 min and subsided at 60 min (Figure 4.6.A). In the presence of 10% serum, ANG could still modestly stimulate ERK activation (1.3 fold) (Figure 4.6.B). These data indicate that ANG activates both PI3K/AKT and MEK/ERK pathways but it is not clear whether these two activations take place in parallel or one is dependent on the other. To reveal a potential interplay between the two pathways, we treated U87 with ANG in the presence of MEK inhibitor (PD98069) or PI3K inhibitor (LY29004) and examined ERK and AKT activation at 30 min and 120 min, the activation peak time for ERK and AKT activation, respectively . When MEK was inhibited, ANG-induced AKT activation was not affected, although the baseline level of p-AKT was lower. But in the presence of PI3K inhibitor, ANG-induced ERK activation was abolished (Figure 4.6.C). These data suggest that an active PI3K/AKT is required for ERK activation upon ANG induction.

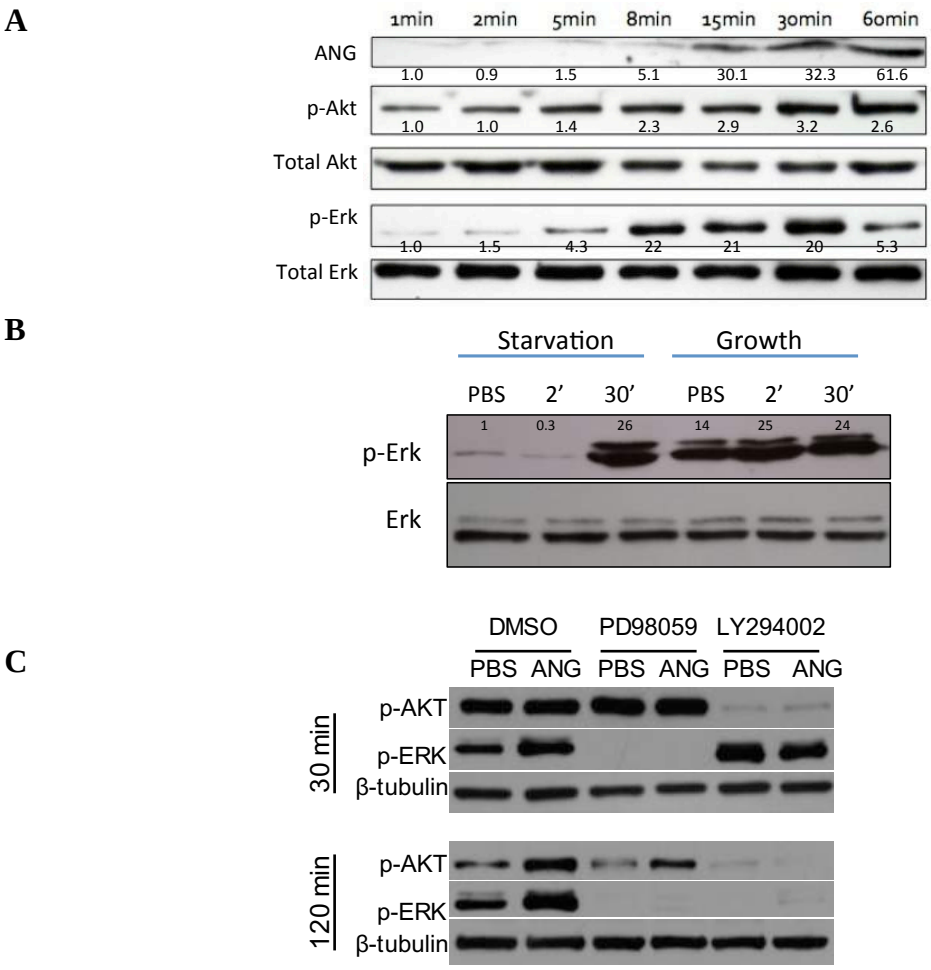

Figure 4.6. ANG activates AKT and ERK in GBM

(A) Serum-starved U251 was treated with ANG. Whole cell lysates were used for Western blotting. Band intensities were normalized to the total ERK or AKT of corresponding time points.

(B) Comparison of ANG-induced ERK activation in U251 between starvation and growth conditions.

(C) U251 was treated with ANG or PBS control in the presence of MEK or PI3K inhibitor. Square highlights the comparison mentioned in the result section. Band intensities were normalized to tubulin.

ANG induced cytoplasmic translocation and phosphorylation of FoxO1

We showed that ANG can activate AKT and ERK signaling in GBM cell lines but how they relate to anti-apoptosis was unknown. Previously, our lab has shown that ANG prevents serum-withdrawal induced apoptosis in P19 cells through inhibition of a series of Bcl-2-dependent processes including caspase-3 activation, poly ADP-ribose polymerase-1 cleavage, and nuclear translocation of apoptosis inducing factor (S. Li et al., 2010) (S. Li et al., 2012). However, how ANG enhances Bcl-2 activity was not addressed. BIM, a BH-3 pro-apoptotic protein whose expression is activated via AKT/FoxO1 and post-translationally modulated by ERK signaling, can inhibit the pro-survival activity of Bcl-2 (Gilley, 2003; O'Reilly et al., 2009). We therefore hypothesized that ANG regulates Bcl-2 activity through transcriptional (AKT/FoxO1) and post-translational (ERK) modulation of Bim (Figure 4.7.A). In order to test this hypothesis, we examined FoxO1 phosphorylation in response to ANG and found that p-FoxO1 was increased in ANG-treated U87 cells (Figure 4.7.B). Using immunofluorescence, we showed that p-FoxO1 was translocated to cytoplasm after ANG stimulation in U87 cells under both growth and starvation conditions (Figure 4.7.C). FoxO1 stability is regulated through direct phosphorylation by AKT. Upon phosphorylation, p-FoxO1 is subsequently relocated to cytoplasmic for degradation (Z. Fu & Tindall, 2008). The magnitude of increased cytoplasmic FoxO1 was 57% under starvation compared to 38% under growth condition, implying that ANG treatment could reduce FoxO1-mediated Bcl-2 activation.

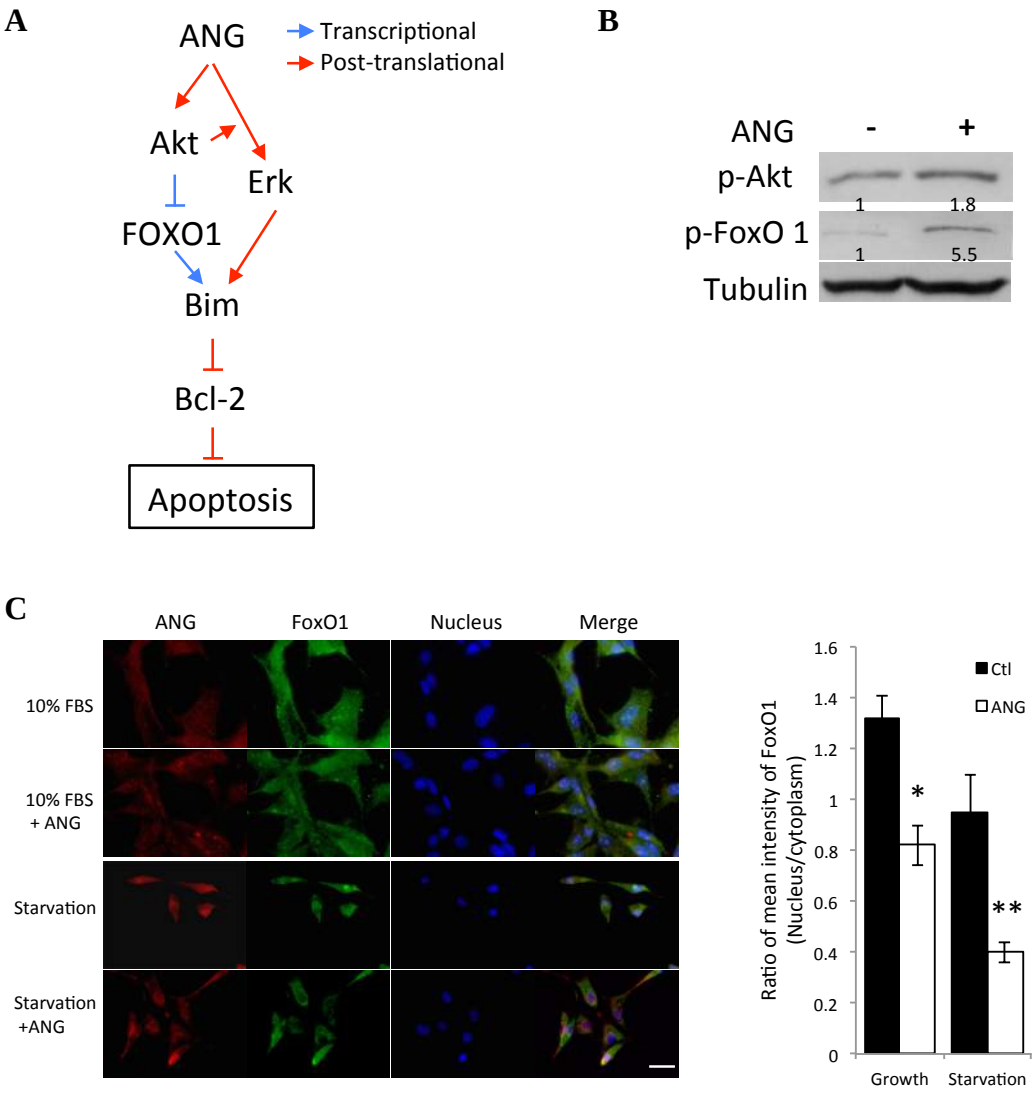

Figure 4.7. ANG induced cytoplasmic translocation and phosphorylation of FoxO1

(A) A proposed model of how ANG regulates Bcl-2.

(B) Exogenous ANG induces FoxO1 phosphorylation.

(C) Under growth and starvation conditions, exogenous ANG induces relocation of FoxO1 from nucleus to the cytoplasm. Bar = 50 µm.

Role of ANG GBM angiogenesis

GBM is a highly vascularized malignancy where vascular hyperplasia is a histological hallmark Anti-angiogenesis therapy with bevacizumab, a humanized anti-VEGF monoclonal antibody, results in vascular normalization and signs of improved neurological symptoms but no changes on overall survival (Friedman et al., 2009). The recurrent GBM tumors become VEGF-independent and show upregulation of other angiogenic factors, ANG and bFGF being the most significant (Lucio-Eterovic et al., 2009). ANG was required for bFGF, PDGF and VEGF to elicit endothelial cell proliferation (Kishimoto et al., 2005) and thus activation of ANG in bevacizumab-treated GBM could contribute to the resistance of tumors to anti-VEGF therapy. To better understand the role of ANG in GBM angiogenesis, we used the Matrigel plug assay to compare new blood vessel formation induced by *ANG* knockdown and control U87 cells (shANG-E4, shANG-E7, and scramble control NC). The three groups elicited varied levels of angiogenic reactions in B6 mice (Figure 4.9.A). The control group induced the strongest angiogenesis response, which was obvious even from the color of plugs. The main vessel that supplied the tumor plug was significantly larger in the control group. The tumor plugs were sectioned and stained for neovessel marker CD31. Quantitative analysis (Figure 4.9.B) showed that *ANG* knockdown resulted in a 4-fold reduction in vessel density as compared to the control group. The proliferation defect in *ANG* knockdown cells was not a confounding factor for the difference seen in the vessel density in this experiment, because we limited the experiment time to a short time frame and also because human U87 proliferation was largely suppressed by the mouse immune system. Involvement of ANG in GBM angiogenesis was also shown in an *in vitro*

angiogenesis assay, in which the conditioned medium of *ANG* knockdown U87 cells showed much reduced activity in inducing HUVEC tube formation (Figure 4.8.A-B).

To examine angiogenesis in the whole plug rather than in limited sections of the tumor, the relative expression of mouse endothelial cells markers, *mCD-31* and *mVE-cadherin*, were evaluated by qRT-PCR (Coltrini et al., 2013). Both markers were decreased in the E7 tumor plugs, indicating that there were less mouse endothelial cells recruited and/or proliferated in the entire Matrigel plug (Figure 4.9.C). Furthermore, we examined angiogenesis levels in PDGF-induced mGBM tumor sections and found a 2-fold decrease in the vessel density in Ang deficient mGBM tumors (Figure 4.9.D). Lastly, in neomycin-treated mGBM, we also observed a 2-fold decrease in vessel density (Figure 4.9.E). These data demonstrated that ANG is required for efficient angiogenesis of GBM *in vivo* and that daily s.c. injection of neomycin effectively inhibits mGBM angiogenesis.

A

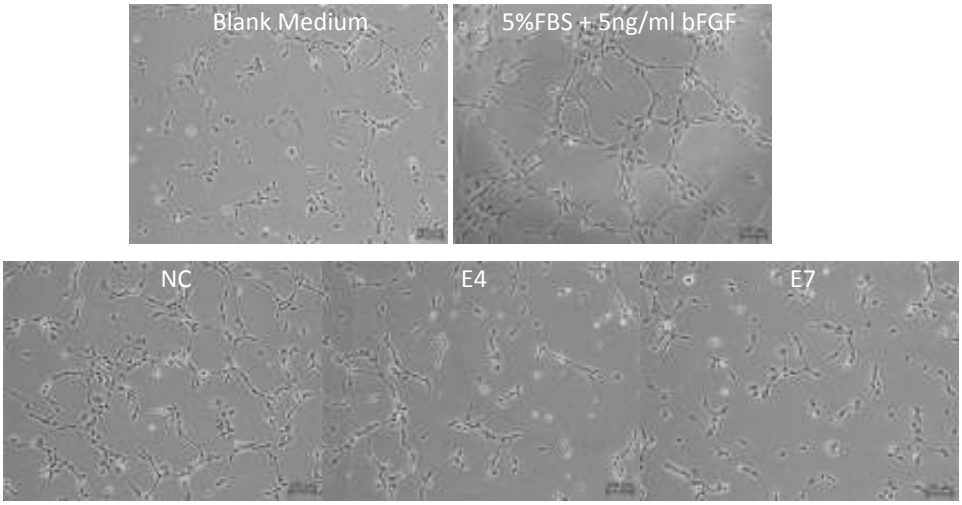

B

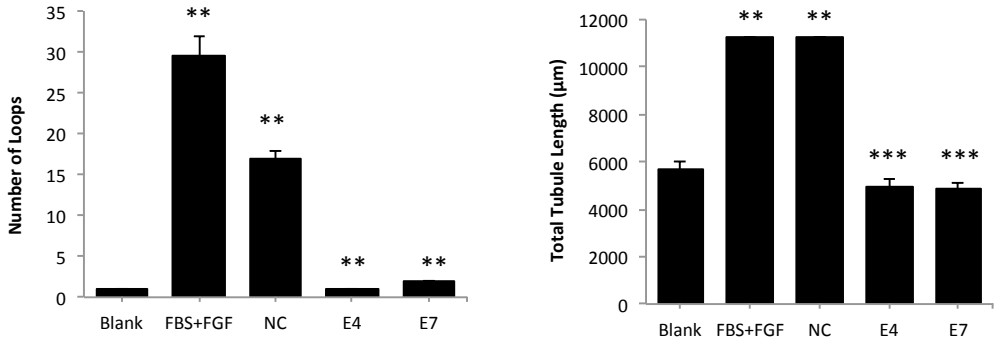

Figure 4.8. Reduced angiogenic activity in conditioned medium of ANG knockdown GBM cells

(A) The 3-day conditioned medium (without FBS) of U87 control and *ANG* knockdown clones (E4 and E7) were subjected to the HUVEC tube formation assay for angiogenic activity. Positive control, 5 % FBS + 5 ng/ml bFGF. The basal medium was used as the negative control.

(B) Quantification of tube formation from panel A.

A

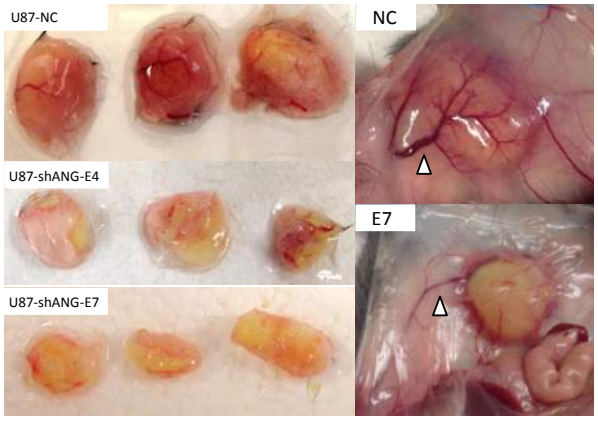
U87-NC
U87-shANG-E4
U87-shANG-E7
NC
E7

B

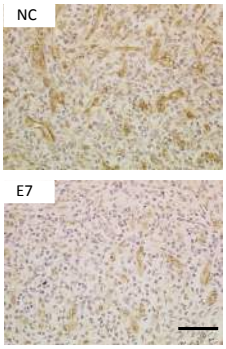
NC
E7

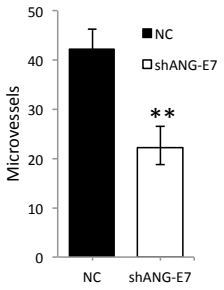
Microvessels
50
40
30
20
10
0
NC
shANG-E7
**
NC
shANG-E7

C

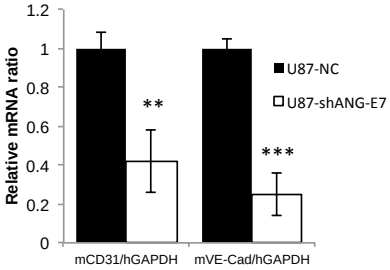
Relative mRNA ratio
1.2
1
0.8
0.6
0.4
0.2
0
**
***
U87-NC
U87-shANG-E7
mCD31/hGAPDH
mVE-Cad/hGAPDH

D

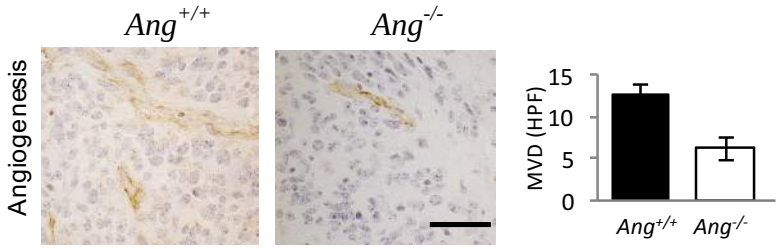
Ang+/+
Ang-/-
Angiogenesis
MVD (HPF)
15
10
5
0
Ang+/+
Ang-/-

E

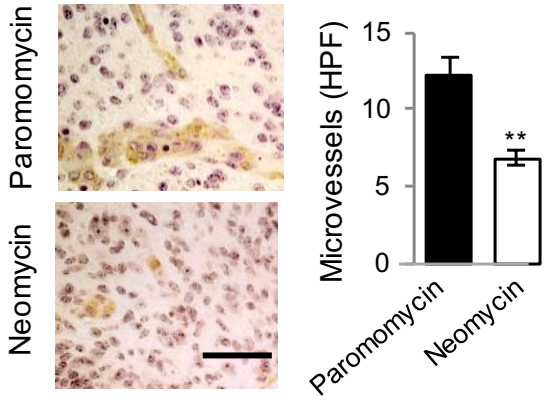
Paromomycin
Neomycin
Microvessels (HPF)
15
10
5
0
**
Paromomycin
Neomycin

Figure 4.9. ANG is required for *in vivo* angiogenesis of GBM

(A) Matrigel plugs containing U87-NC, U87-shANG-E4, and U87-shANG-E7 were dissected from mice skin 6 days after implantation. Arrowheads indicate the main vessel. N = 3.

(B) IHC staining of CD31 for neo-vessels in the Matrigel plug sections. Five random fields were examined from each sample. N = 2.

(C) Real-time PCR quantification of mouse endothelial cells in the tumor tissue. Total RNA was extracted by Trizol. The relative degree of angiogenesis was quantified by mouse *mCD31* and *mVE-Cad* markers, normalized to human tumor cells, *hGAPDH*. N = 2.

(D) $Ang^{+/+}$ and $Ang^{-/-}$ mouse glioblastoma sections were stained for CD31. Vessel density was quantified in three random fields for each sample. Bar = 200 μm. N = 3.

(E) Quantification of vessels stained with CD31 in drug-treated mGBM. Three random fields for each sample were used for quantification. N = 3.

Discussion

Role of ANG in GBM transformation

We hypothesized that constitutive ANG activity may elicit oncogenic effects as we showed in Chapter IV that lack of Ang activity inhibits anchorage-independent growth of tMEF and tumor establishment *in vivo.* This contention is supported by other reports that Ang promotes degradation of p53, a key tumor suppressor whose malfunction results in numerous cancers including GBM. Therefore, we chose an established transgenic proneural mouse GBM model to test this hypothesis. This *in vivo* animal model allowed us to examine the differences in the transformation of brain tumors from wildtype or *Ang* knockout and to study tumor microenvironment in a native environment without concerns of cross-species cell interactions. We chose the proneural GBM model because: 1) it is the most stubborn GBM subtype in response to aggressive treatment; 2) only in proneural and classical subtypes, higher ANG or PLXNB2 expression is correlated with worse survival, suggesting a more involving ANG function in the progression of these tumor subtypes.

As shown in Chapter III, reduced Ang activity shows gradually increased survivals in *Ang* heterozygous and homozygous knockout mGBM. However, this difference in survival is not likely to have resulted from reduced susceptibility to transformation in response to PDGFB, or from lower grade lesions in the *Ang* knockout mGBM, because all the *Ang* knockout mice showed brain lesions and all of the lesions examined possess histological hallmarks of GBM. It is not surprising because this tumor model relies on the deletion of tumor suppressor locus *Ink4a*/*Arf*, where loss of *Ink4a* leads to Rb inhibition

and absence of *Arf* leads to p53 degradation. The inhibitory effect of ANG on p53 might be redundant to *Arf* deletion, so it is possible that Rb inhibition alone is sufficient to drive mGBM transformation. In future studies, we can tease out these two possibilities by comparing p53 and its downstream effectors p21 and Bax between wildtype and *Ang* knockout GBM tissues. If p53 is higher in *Ang* knockout group compared to the control, it suggests the inhibitory effect of ANG on p53 is not redundant to *Arf* deletion. At the same time, we could expect hyper-activation of E2F1 as a compensatory mechanism for the residual p53 activity in *Ang* knockout mGBM.

ANG is not required for GBM transformation but contributes to GBM aggressiveness, which is consistent with the fibroblast transformation results, where SV40LT-mediated transformation overcomes slow proliferation due to lack of *Ang* expression in *Ang* knockout t-MEF in 2D culture. Ang activity is required for aggressive growth induced by oncogenic K-Ras in tMEF. Lack of Ang activity shows robust apoptosis in soft agarose, a phenotype linked to epithelial status. Indeed, there is higher E-cad and lower N-cad and downregulation of EMT-associated transcription factor and reduced TGF-β in *Ang* knockout tMEF. Given the dominant role of TGF-β in EMT, it is likely that *Ang* is required for maintaining K-Ras-induced, TGF-β-dependent mesenchymal status. Alternatively, lack of ANG can inhibit oncogenic K-Ras-induced malignant transformation by promoting apoptosome formation to raise the apoptosis threshold (Saikia et al., 2014). It was shown that ANG-mediated tiRNA production binds to Cyto c and inhibits Apaf-1 activation in apoptosome formation. Furthermore, lack of Ang

activity would fail to induce anti-apoptotic Bcl-2 translation facilitating apoptosis initiation.

ANG and GBM apoptosis

In human GBM, ANG expression is highly associated with genes that are involved in anti-apoptosis processes. We showed that *ANG* knockdown increased the sensitivity of U87 cells to various types of stresses. This indicates that ANG regulates the common apoptosis pathway induced by stresses of ROS, ER, and starvation.

We also showed that neomycin, an ANG inhibitor, induces a strong apoptosis response *in vivo* in the necrosis area of wildtype mGBM where a 5-fold higher apoptosis was observed in *Ang* knockout mGBM. In *Ang* knockout tumors, given the high embryonic lethality of *Ang* knockout embryos, there could be a compensatory mechanism for the loss of Ang activity. Therefore, it is conceivable that *Ang* wildtype tumor cells are more sensitive to pharmacological inhibition of Ang than *Ang* knockout cells.

Bcl-2 is an important mediator of the anti-apoptosis effect of ANG. Under stress condition, Bcl-2 expression is subjected to both transcriptional and translational control. One study showed that the NF-κB pathway is responsible partially for the Bcl-2 transcription activation by ANG (S. Li et al., 2010). Another study found that ANG can regulate p53 to increase Bcl-2 transcription (Sadagopan et al., 2012). Bcl-2 transcript contains an IRES element that would allow translation initiation in an ANG-dependent, IRES-mediated manner under the stress conditions. We proposed that ANG, other than

regulating Bcl-2 expression, also induces Bcl-2 activity by reducing BIM, the inhibitor of Bcl-2, through transcriptional suppression and post-translational inhibition via AKT/FoxO and ERK pathways, respectively. Our data showed that ANG/AKT activation led to increased p-FoxO1a and nuclear export of FoxO1a. Future studies should delineate how BIM (p-BIM) responds to ANG stimulation and verify that it can be regulated through the ANG/AKT/FoxO and the ANG/ERK pathways. Understanding of ANG-regulated BIM is important because apoptosis is a delicate balance between the levels of pro-apoptotic protein such as BIM and anti-apoptotic protein such as Bcl-2. In *TP53*-mutated tumor cells, where ANG cannot further upregulate Bcl-2 through the p53-dependent pathway, downregulation of BIM could be the dominant pathway underlying anti-apoptosis effects of ANG.

Chapter V

PLXNB2 mediates the effects of Angiogenin in glioblastoma

PLXNB2 was originally identified for its high expression in high-grade glioma (Shinoura et al., 1995). The recent unpublished data from our lab has demonstrated that PLXNB2 is the cell surface receptor for ANG. In the previous chapters, we have shown tumor-promoting effects of ANG in GBM. In this chapter, our goal is to demonstrate that PLXNB2 mediates the effects of ANG in GBM.

PLXNB2 expression predicts overall survival of proneural GBM patients

We analyzed publically available microarray data and found that *PLXNB2* expression is significantly upregulated in the higher grade of gliomas (Figure 5.1.A) (Sun et al., 2006). In a cohort of low-grade glioma patients, high PLXNB2 expression ($Z > 2$) significantly ($P < 0.000003$) correlated with a poor overall survival (Figure 5.1.B). PLXNB2 was originally identified in GBM by differential expression between malignant and benign brain tumors, and was implicated to play a role in brain tumor progression (Shinoura et al., 1995). We found that *PLXNB2* was upregulated by 2.2-fold in a cohort of GBM patients (TCGA, Cell 2013) as compared to normal brain tissues (Figure 5.1.C). However, there was no significant difference ($P = 0.07$) in overall survival between patients with high and low PLXNB2 expression in this high-grade glioma cohort (GBM, TCGA provisional) (Figure 5.1.D). Considering the various etiologies of different GBM subtypes, we thought that *PLXNB2* expression and its impact on disease progression might vary among different GBM subtypes. Relative to the average *PLXNB2* expression level in the whole GBM cohort, lower *PLXNB2* expression was found in the proneural and neural subtypes, while higher *PLXNB2* expression was found in the classical and mesenchymal subtypes (Figure 5.1.E). In mesenchymal and neural GBM subtypes,

PLXNB2 expression did not correlate with patients' overall survival (Figure 5.1.F). But in the proneural subtype, patients with lower *PLXNB2* expression survived longer with the median survival being 24 months, which is significantly longer that the median survival of 10.4 months observed in the *PLXNB2* normal group. Although high *PLXNB2* patients had significant worse survivals in the classical group, there were only three patients expressing high *PLXNB2* in this group, which renders the result unreliable.

A

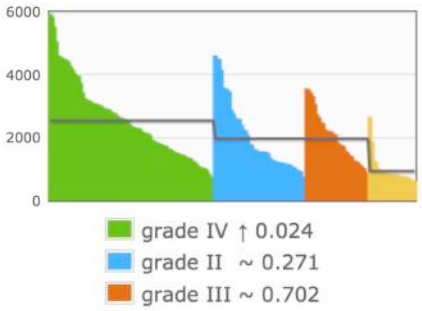
6000
4000
2000
0
grade IV ↑ 0.024
grade II ~ 0.271
grade III ~ 0.702

B

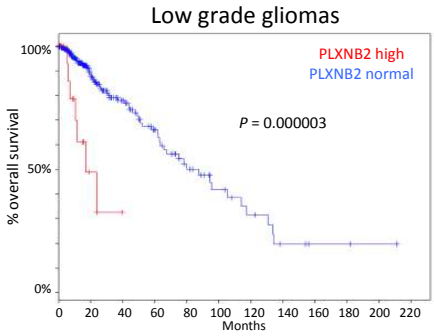
Low grade gliomas
PLXNB2 high
PLXNB2 normal
P = 0.000003
% overall survival
100%
50%
0%
0 20 40 60 80 100 120 140 160 180 200 220
Months

C

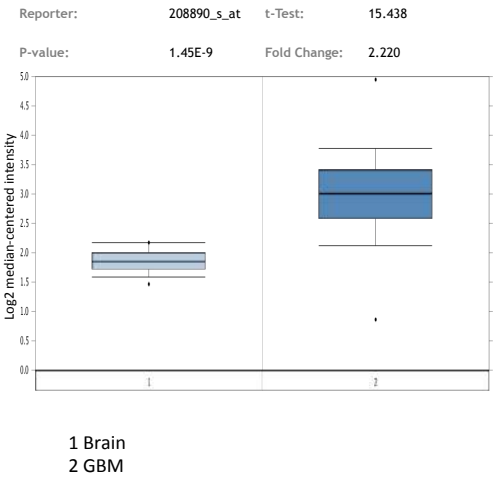
Reporter: 208890_s_at t-Test: 15.438
P-value: 1.45E-9 Fold Change: 2.220
Log2 median-centered intensity
1 Brain
2 GBM

D

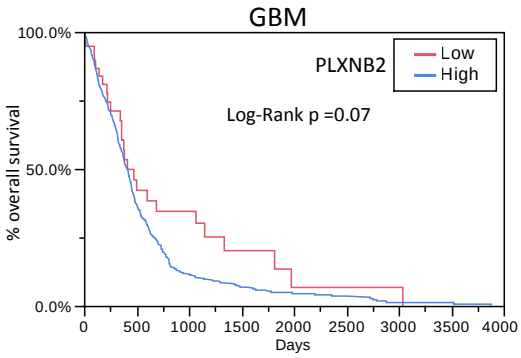
GBM
PLXNB2
Low
High
Log-Rank p =0.07
% overall survival
100.0%
50.0%
0.0%
0 500 1000 1500 2000 2500 3000 3500 4000
Days

E

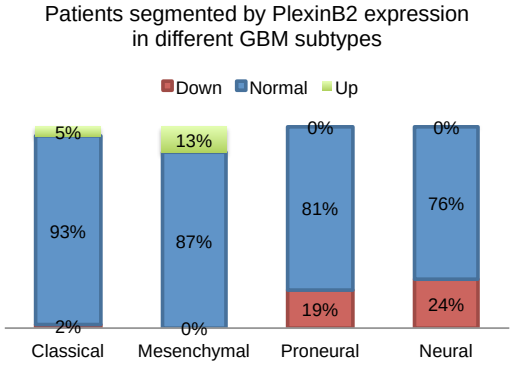
Patients segmented by PlexinB2 expression in different GBM subtypes
Down
Normal
Up
5%
93%
2%
13%
87%
0%
0%
81%
19%
0%
76%
24%
Classical
Mesenchymal
Proneural
Neural

F

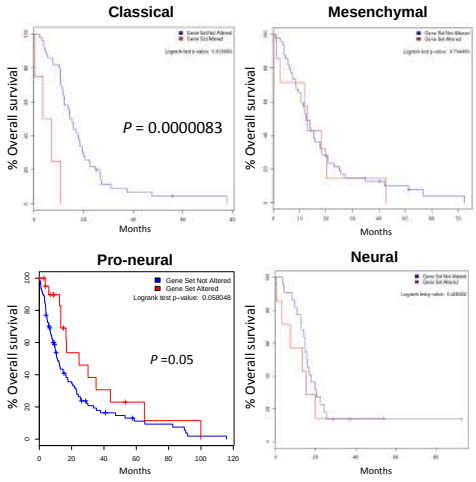
Classical
Mesenchymal
Pro-neural
Neural
P = 0.0000083
P =0.05
% Overall survival
Months

Figure 5.1. PLXNB2 expression is correlated with overall survival of proneural GBM patients

(A) PLXNB2 expression in gliomas of different grades (Sun et al., 2006).

(B) The survival plot of patients of low-grade glioma segmented by *PLXNB2* expression (Z > 2) (TCGA cohort, low grade, provisional).

(C) PLXNB2 expression in GBM patients is 2.2-fold higher than that in the control patients with non-neoplasm. (Control group, N = 10; TCGA GBM, N = 542). *P* = 1.45E-9. The Oncomine™ Platform (Life Technologies, Ann Arbor, MI) was used for analysis and visualization.

(D) The overall survival plots of GBM patients with high and low *PLXNB2* expression. Low (N = 38), High (N= 504) (TCGA, Cell 2013).

(E) *PLXNB2* expression variation (Z = 1.5) stratified by GBM subtypes (TCGA, Nature 2008. Classical N = 54, proneural N = 56, mesenchymal N = 56, neural N = 29).

(F) The overall survival plot of GBM patients of the four subtypes segmented by *PLXNB2* expression. Blue represents patients with PLXNB2 expression within Z score ± 1.5, and red represents the rest of the patients.

***PLXNB2* is constitutively expressed in GBM cell lines, and its knockdown inhibits proliferation and neurosphere formation.**

We examined PLXNB2 protein level in a panel of GBM cell lines including A172, U87, and U251 that were cultured in serum-containing medium, and GNS-6-22, GNS-11-1, and GBM-8 that were cultured in defined neural stem cell medium for neurospheres formation. In general, we found that PLXNB2 was lower in serum-cultured GBM lines than in neural stem cell medium cultured GNS lines. It was particularly low in U87 (Figure 5.2.A). Previously, our lab has shown that PLXNB2 expression is downregulated as cells grow denser in HUVEC but this density-dependent regulation was not seen in prostate cancer cell lines. Here, we showed that increased cellular density actually modestly increased PLXNB2 expression, suggesting that PLXNB2 may constitutively signal in GBM (Figure 5.2.B). To examine PLXNB2 function in GBM, we used two clones of lentiviral-mediated shRNA (shPb2-C1 and shPb2-D2) to knockdown *PLXNB2* expression in U87, U251, and GNS-6-22 lines. Between the two clones, the shPb2-D2 line is more effective in knocking down *PLXNB2* expression with a 90% knockdown efficiency in both U87 and U251 (Figure 5.2.C). We noticed significant morphology changes including reduced lamellipodium as a result of *PLXNB2* knockdown in U87 and U251 cells (Figure 5.2.C). Knockdown of *PLXNB2* inhibited proliferation of both U87 and U251 cells (Figure 5.2.D). Blocking the binding of ANG to PLXNB2 by an in-house generated PLXNB2 mAb #17 (40 μg/ml) resulted in a 37% reduction in U251 proliferation in a 5-day proliferation assay (Figure 5.2.E). Lower concentrations of mAb were not effective in inhibiting U251 proliferation. Similar results were obtained in A172 and U87 cells (Figure 5.2.F).

The inhibitory effect of PLXNB2 mAb toward proliferation is more significant in U87 cells that have a lower PLXNB2 level than that of U251 cells that have a higher PLXNB2 level. *PLXNB2* knockdown in GNS-6-22 GNS cells resulted in a reduction in both number and size of the neurospheres in serial seeding assays, suggesting that PLXNB2 is necessary for self-renewal of undifferentiated GBM stem cells (Figure 5.2.G-H). Overall, ANG-PLXNB2 signaling is active in differentiated and undifferentiated GBM cells.

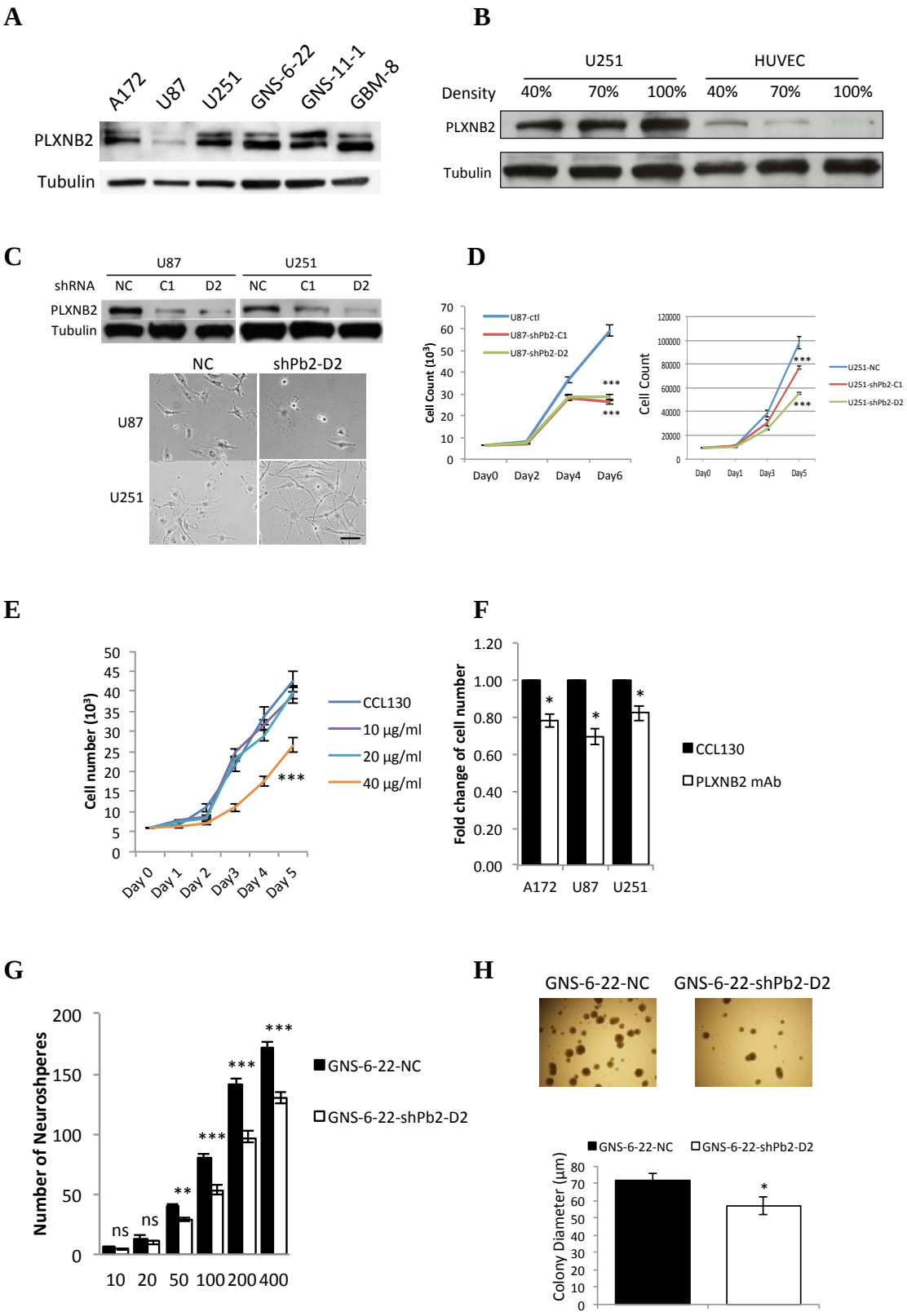
A
A172
U87
U251
GNS-6-22
GNS-11-1
GBM-8
PLXNB2
Tubulin
B
U251
HUVEC
Density
40%
70%
100%
40%
70%
100%
PLXNB2
Tubulin
C
U87
U251
shRNA
NC
C1
D2
NC
C1
D2
PLXNB2
Tubulin
NC
shPb2-D2
U87
U251
D
U87-ctl
U87-shPb2-C1
U87-shPb2-D2
Cell Count (10³)
Day0
Day2
Day4
Day6
***
***
Cell Count
Day0
Day1
Day3
Day5
***
***
U251-NC
U251-shPb2-C1
U251-shPb2-D2
E
Cell number (10³)
Day 0
Day 1
Day 2
Day3
Day 4
Day 5
***
CCL130
10 μg/ml
20 μg/ml
40 μg/ml
F
Fold change of cell number
A172
U87
U251
*
*
*
CCL130
PLXNB2 mAb
G
Number of Neuroshperes
ns
ns
**
***
***
***
10
20
50
100
200
400
GNS-6-22-NC
GNS-6-22-shPb2-D2
H
GNS-6-22-NC
GNS-6-22-shPb2-D2
GNS-6-22-NC
GNS-6-22-shPb2-D2
Colony Diameter (μm)
*

Figure 5.2. *PLXNB2* knockdown inhibits GBM proliferation and glioma neural stem cell sphere formation.

(A) PLXNB2 level in GBM cell line A172, U87, U251, GNS-6-22, GNS-11-1, and GBM-8.

(B) Density-independent expression of PLXNB2 in GBM line U251.

(C) *PLXNB2* knockdown induces morphologic changes of U87 and U251 cells. Bar = 50 μm.

(D) *PLXNB2* knockdown inhibits proliferation of U87 and U251 cells.

(E) PLXNB2 mAb inhibits U251 proliferation at 40 μg/ml in a 5-day proliferation assay.

(F) Relative sensitivity of PLXNB2 mAb (40 μg/ml) against of different GBM lines proliferation in a 2-day proliferation assay. CCL130 (40 μg/ml).

(G) *PLXNB2* knockdown decreases the number of GNS-6-22 neurospheres.

(H) GNS-6-22-shPb2-D2 showed reduced diameter of neurospheres.

PLXNB2 regulates anchorage-independent growth of U87 cells

Next, we examined whether PLXNB2 regulates anchorage independent growth of GBM. We generated a *PLXNB2* overexpression U87 cell line that has more than 8-fold increase of *PLXNB2* (U87-Pb2-O/E). This line was used together with the two knockdown lines (U87-shPb2-C1 and U87-shPb2-D2) in soft agarose assay to determine the effect of PLXNB2 on anchorage-independent growth of GBM (Figure 5.3.A). Colonies derived from U87-Pb2-O/E exhibited a more homogeneous size as compared to that from the control cells. U87-Pb2-O/E also had an increased proliferation as shown by the increased number of colonies and bigger diameters. However, this increased proliferation was accompanied by an increased apoptosis (Figure 5.3.B-C). In *PLXNB2* knockdown group, both the C1 and the D2 lines displayed compromised colony formation in terms of both numbers and diameters (Figure 5.3.C). The majority of *PLXNB2* knockdown colonies were just aggregates of a few highly apoptotic cells and very few large colonies were formed, indicating that the high apoptosis rate induced by *PLXNB2* knockdown is attributable to the defect in anchorage-independent growth. This resembled the high apoptosis of anchorage-independent growth we have seen in *ANG* knockdown GBM cells shown in Chapter IV. These data indicate that anchorage-independent growth of GBM can be regulated by PLXNB2, and that de-regulated PLXNB2 activity leads to increased apoptosis.

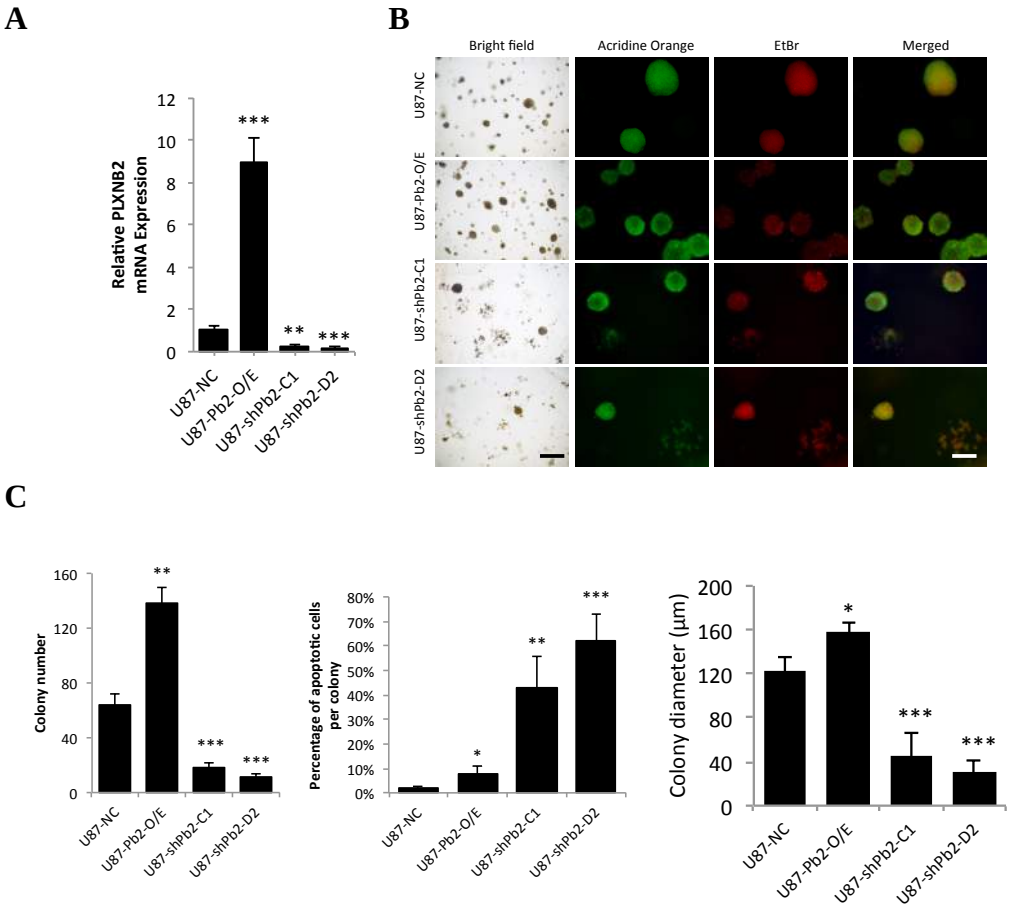

Figure 5.3. PLXNB2 regulates U87 anchorage independent growth.

(A) PLXNB2 overexpression cell line (U87-Pb2-O/E) was generated by transfecting a plasmid encoding PLXNB2 cDNA in pCL-neo backbone and selected by G418.

(B) PLXNB2 overexpression and knockdown cell lines were examined for anchorage-independent growth in agarose. AO/EB staining for apoptosis was conducted as mentioned above. Bar = 500 μm (phase contrast) and 200 μm (fluorescence).

(C) The number and the diameter of colonies, and the apoptotic rate per colony shown in (B) were quantified.

PLXNB2 regulates ANG uptake and mediates ERK activation and cell proliferation.

PLXNB2 cDNA plasmid was transfected into U251 cells at a low concentration. Without G418 selection, only a portion of cells overexpressed PLXNB2 as detected by red IF signal in PFA fixed cells (Figure 5.4.A). Exogenous ANG added before the fixation displayed nearly 30-fold increased binding to *PLXNB2*-transfected cell over the non-transfected cells (Figure 5.4.A). When U251 were fixed with methanol, which permeabilizes both plasma membrane and nuclear membrane, we also observed increased nuclear ANG in PLXNB2 overexpressed cell (Figure 5.4.B). After ANG is endocytosed, it is quickly translocated into the nucleus under growth condition (G. F. Hu et al., 2000). We showed that nuclear translocation of exogenous ANG was inhibited by PLXNB2 mAb as shown by decreased uptake rate and intensity (Figure 5.4.C). Thus, PLXNB2 is both necessary and sufficient to mediate ANG uptake.

In chapter IV, we have characterized the proliferative effect of ANG in GBM. To determine if this proliferative effect of ANG depends on PLXNB2, we treated U251-shPb2-D2 or scramble control line with ANG mAb 26-2F in a 3-day proliferation assay, and found that 26-2F treatment no longer inhibited proliferation of *PLXNB2* knockdown cell line (Figure 5.4.D), indicating that the effect of ANG in proliferation was dependent on PLXNB2. Using an inducible lentiviral shRNA system, we confirmed that ANG uptake was dependent on PLXNB2 and so was the subsequent ERK activation (Figure 5.4.E-F).

Semaphorin 4C (Sema4C) is the cognate ligand for PLXNB2 and their interaction has been shown to regulate axon guidance and processes during neural development (Maier

et al., 2011; Saha et al., 2012). Thus, we evaluated if ANG and Sema4C activate PLXNB2 in distinct manners. Upon either Sema4C (10 μg/ml) or ANG (1 μg/ml) stimulation, there was increased surface PLXNB2 puncta staining in U251, suggestive of PLXNB2 oligomerization and activation (Figure 5.4.G). We also detected ERK activation with either ligand (Figure 5.4.H). The higher ERK activation seemed to correlate with a stronger receptor activation in ANG-treated U251 cells than the Sema4C-treated cells. Interestingly, when both ligands were added to starved cells, ERK activation was abolished (Figure 5.4.H). The significance of this finding is unknown at present.

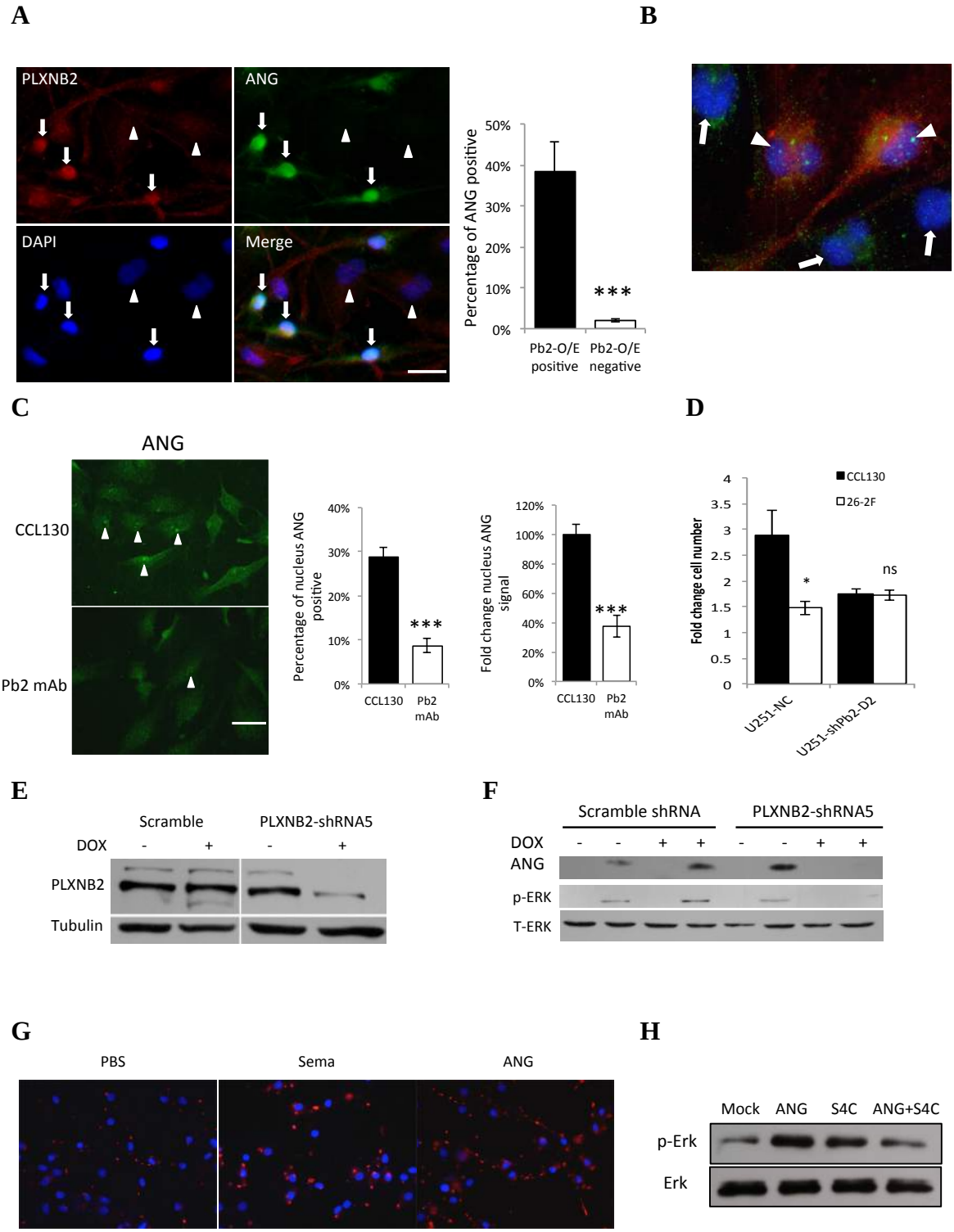
A
PLXNB2
ANG
DAPI
Merge
Percentage of ANG positive
50%
40%
30%
20%
10%
0%
***
Pb2-O/E positive
Pb2-O/E negative
B
C
ANG
CCL130
Pb2 mAb
Percentage of nucleus ANG positive
40%
30%
20%
10%
0%
***
CCL130
Pb2 mAb
Fold change nucleus ANG signal
120%
100%
80%
60%
40%
20%
0%
***
CCL130
Pb2 mAb
D
CCL130
26-2F
Fold change cell number
4
3.5
3
2.5
2
1.5
1
0.5
0
*
ns
U251-NC
U251-shPb2-D2
E
Scramble
PLXNB2-shRNA5
DOX
- + - +
PLXNB2
Tubulin
F
Scramble shRNA
PLXNB2-shRNA5
DOX
- - + + - - + +
ANG
p-ERK
T-ERK
G
PBS
Sema
ANG
H
Mock
ANG
S4C
ANG+S4C
p-Erk
Erk

Figure 5.4. PLXNB2 regulates ANG uptake and mediates ERK activation and proliferation.

(A) ANG preferentially binds to PLXNB2 overexpressing cells. The percentages of cells that are positive for ANG binding between the two populations are compared. Cells were fixed with 4% PFA without membrane permeabilization. Arrow: Pb2-O/E positive U251, arrowhead: Pb2-O/E negative U251.

(B) PLXNB2 overexpression increases nucleus localization of endogenous ANG. Cells were fixed with methanol for nuclear permeabilization.

(C) PLXNB2 mAb inhibits nuclear localization of exogenous ANG in U251 cells. Percentage of cells positive for nuclear ANG and the intensity of nuclear ANG signals were determined.

(D) PLXNB2 knockdown desensitizes ANG mAb. Bar = 200 μm.

(E) Knockdown of *PLXNB2* expression by a DOX inducible shRNA system in U251 cells.

(F) DOX-induced PLXNB2 knockdown inhibits ANG uptake and subsequent Erk activation in U251 cells.

(G) PLXNB2 immunofluorescence in U251 cells treated with PBS, Sema4c, or ANG for 30 min after overnight starvation. Cells were fixed with 4% PFA without membrane permeabilization. PLXNB2, red; DAPI, blue.

(H) ERK activation in U251 cells treated with Sema4C, ANG, or a combination of two for 30 min after overnight starvation.

Screen of receptor tyrosine kinase for potential ANG/PLXNB2 co-receptors in U251

How ERK and AKT are activated by ANG is unclear because PLXNB2 does not have a tyrosine kinase domain. ErbB-2 and c-Met have been reported to relay PLXNB1 signaling as a co-receptor for Sema4D (Giordano et al., 2002; Soong & Scott, 2013; Worzfeld et al., 2012). We, therefore, used a screening method to identify potential RTK co-receptors for ANG (Figure 5.5.A-B). We knew that ANG-induced ERK activation reached a peak at 30 min (Figure 4.6.A). At that time, ErbB4, Fgr, and PDGFR-alpha were activated but were then de-activated at 120 min (Figure 5.5.C-D). Notably, M-CSFR was consistently de-activated by ANG treatment at both time points. We did not observe c-Met activation in response to ANG stimulation though it has been reported as a co-receptor for Sema4C (Le et al., 2015). It was in agreement with our early findings that PLXNB2 activation by ANG differed from that by Sema4C.

Downregulation of ErbB3/pY1289 was found to be correlated with both ANG and PLXNB2 in gliomas (Figure 5.5.E-F). In our screening experiment, we also found that p-ErbB3 were downregulated at 120 min (Figure 5.5.D). ErbB3 was shown to be involved in regulation of GBM stem cells (P. A. Clark et al., 2012b). How de-phosphorylation of ErbB3 affects GBM is unknown. In summary, we found that ANG and Sema4C induce different signaling upon binding to PLXNB2. ANG-elicited signals include minor and temporal inhibition of numerous receptor tyrosine kinases. Further exploration of the effects of ANG on ErbB3 and M-CSFR is warranted.

A

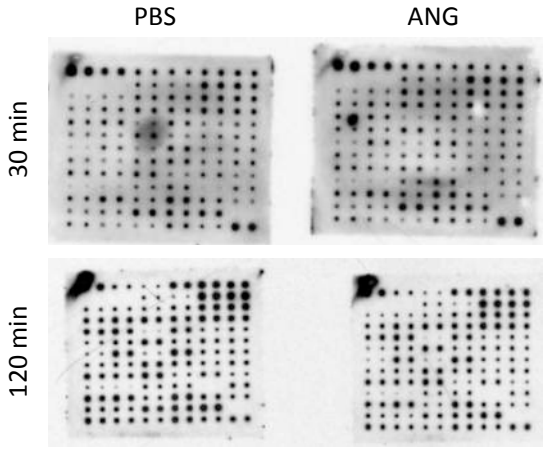

B

pos	pos	pos	ABL1	ACK	ALK
neg	neg	Axl	Blk	BMX	Btk
Csk	Dtk	EGFR	EphA1	EphA2	EphA3
EphA4	EphA5	EphA6	EphA7	EphA8	EphB1
EphB2	EphB3	EphB4	EphB6	ErbB2	ErbB3
ErbB4	FAK	FER	FGFR1	FGFR2	FGFR2
Fgr	FRK	Fyn	Hck	HGFR	IGF-I R
Insulin R	ItK	JAK1	JAK2	JAK3	LCK
LTK	Lyn	MATK	M-CSFR	MUSK	NGFR
PDGFR-a	PDGFR-b	PYK2	RET	ROR1	ROR2
ROS	RYK	SCFR	SRMS	SYK	Tec
Tie-1	Tie-2	TNK1	TRKB	TXK	NEG
Tyk2	TYRO10	VEGFR2	VEGFR3	zAP70	POS

C

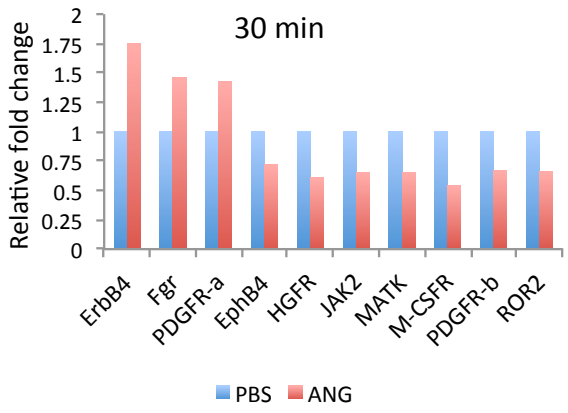

D

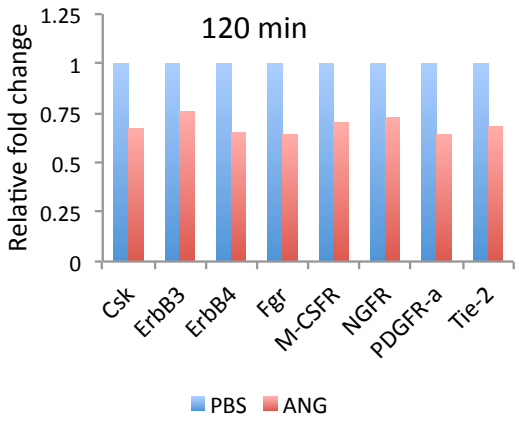

E

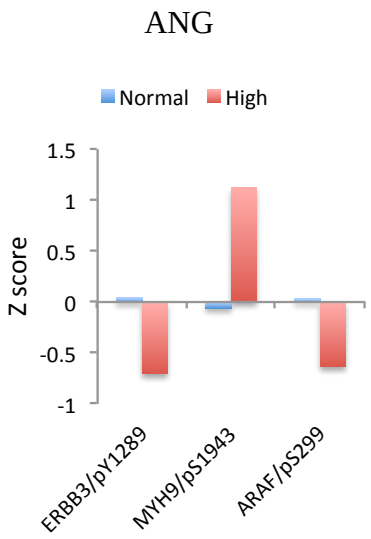

F

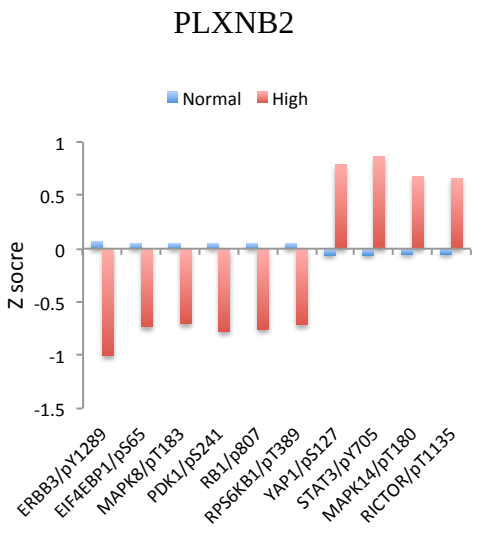

Figure 5.5. Receptor tyrosine kinase screen for ANG/PLXNB2 co-receptor in U251

(A) Dot blots of ANG or PBS treated (30 min and 120 min) U251 lysates.

(B) Pattern scheme of the receptor tyrosine kinase screen dot blot.

(C-D) Quantifications of top regulated RTK in U251 in response to ANG stimulation at 30 and 120 min.

(E) Changes in phosphorylation in GBM patients with high ANG expression compared to the rest of the cohort (TCGA, Cell 2013) ($P < 0.01$).

(F) Changes in phosphorylation in low-grade glioma patients with high PLXNB2 expression compared to the rest of the cohort (Low grade, TCGA provisional) ($P < 0.01$).

p120 is a novel PLXNB2 fragment that is involved in nuclear translocation of ANG

The full size PLXNB2 protein is a ~240 kDa (p240) type-I transmembrane glycoprotein (Figure 5.6.A) and its extracellular portion can be cleaved into a 170 kDa fragment (p170) and the rest including the remaining extracellular domain, transmembrane domain, and the small cytosolic tail can be detected as another fragment (p80) (Artigiani et al., 2003). The cleavage takes place at the plasma membrane and was required for effective PLXNB2 signaling. A similar cleavage action can be found in PLXNB1 but not PLXNB3 (Artigiani et al., 2003). Although p170 was still attached to the cell surface after cleavage, it is highly likely that it can also be freely released from the cells and induces paracrine signaling. To characterize the potentially released form of PLXNB2, we overexpressed PLXNB2 in 293T cells and examined PLXNB2 in concentrated conditioned medium of 293T-PLXNB2-overexpressing cells (293T-O/E). We found that

p170, a trace amount of p240, but surprisingly high level of p120, were released into the medium as shown by WB analysis with PLXNB2 #17 mAb (Figure 5.6.B). To validate our finding in the non-concentrated conditioned medium of non-PLXNB2-overexpressing cells, we conducted WB on conditioned medium from U87 and 293T together with the naïve culture medium as a control. Under this condition, we detected only p120 and confirmed that it was not from the naïve culture medium (containing 10% FBS) (Figure 5.6.C). To exclude the possibility that p120 or p170 was from cell debris or microvesicles, the conditioned medium was left untreated and centrifuged at 400g or 18,000g. We detected both p120 and p170 in U87 and LNCaP cells, but only p170 in 293T, irrespective of centrifugation methods (Figure 5.6.D). This suggested PLXNB2 overexpression gave rise to p120 in the conditioned medium. In summary, our results suggest that p170 can be released from plasma membrane and may be further processed into p120. Both p170 and p120 are highly likely to be in free soluble forms in the conditioned medium.

This p120 PLXNB2 fragment has not been reported before, and it may be produced by additional processing of p170 or p240 at cell surface, in the culture medium, or inside the cells. So we next examined if p120 is detectable in the whole cell lysates and tested if our mAb cross-reacts with mouse p120 (Figure 5.6.E). Both in-house mAb and a commercial PLXNB2 mAb can detect p120 in human and mouse whole cell lysates. The mouse motor neuron line NSC34 expressed p120 at an exceedingly high level and the mouse fibroblast cell line NIH3T3 had minimal p120. Interestingly, both cell lines expressed similar levels of p170, implying a potential lineage-dependent differential production of

p120. The in-house mAb can detect both full-length and p120 PLXNB2 in human and mouse cells whereas the commercial mAb can only detect p120 PLXBN2 in the two species.

Using immunofluorescence, we noticed the existence of nuclear PLXNB2. Nuclear PLXNB2 was also detected in U251 cells upon ANG stimulation, suggesting PLXNB2 may undergo nuclear translocation together with ANG (Figure 5.6.G). To confirm the existence of nuclear PLXNB2 biochemically, we treated U251 cells with ANG and then isolated nuclear and cytoplasmic fractions by subcellular fractionation. Western blotting showed that p120 was detected in cell nucleus, and that ANG stimulation increased nuclear p120 by more than 2-fold and affected the total cytoplasmic p170/p240 to a less extent (Figure 5.6.H). In time course experiments, we found that ANG stimulation led to a positive feedback to ANG/PLXNB2 expression through 60 min (Figure 5.6.I) and subsequently increased both p240 and p120 in U251 cells (Figure 5.6.J). These data supported our previous findings that p120 is the species of PLXN2 that mediates nuclear translocation of ANG. Overall, these data demonstrated that p120 PLXNB2 is highly expressed in neuronal cells and can be found in both conditioned medium and nuclear compartment. Furthermore, p120 PLXNB2 accumulates in the nucleus in response to ANG stimulation and may be involved in nuclear translocation of ANG.

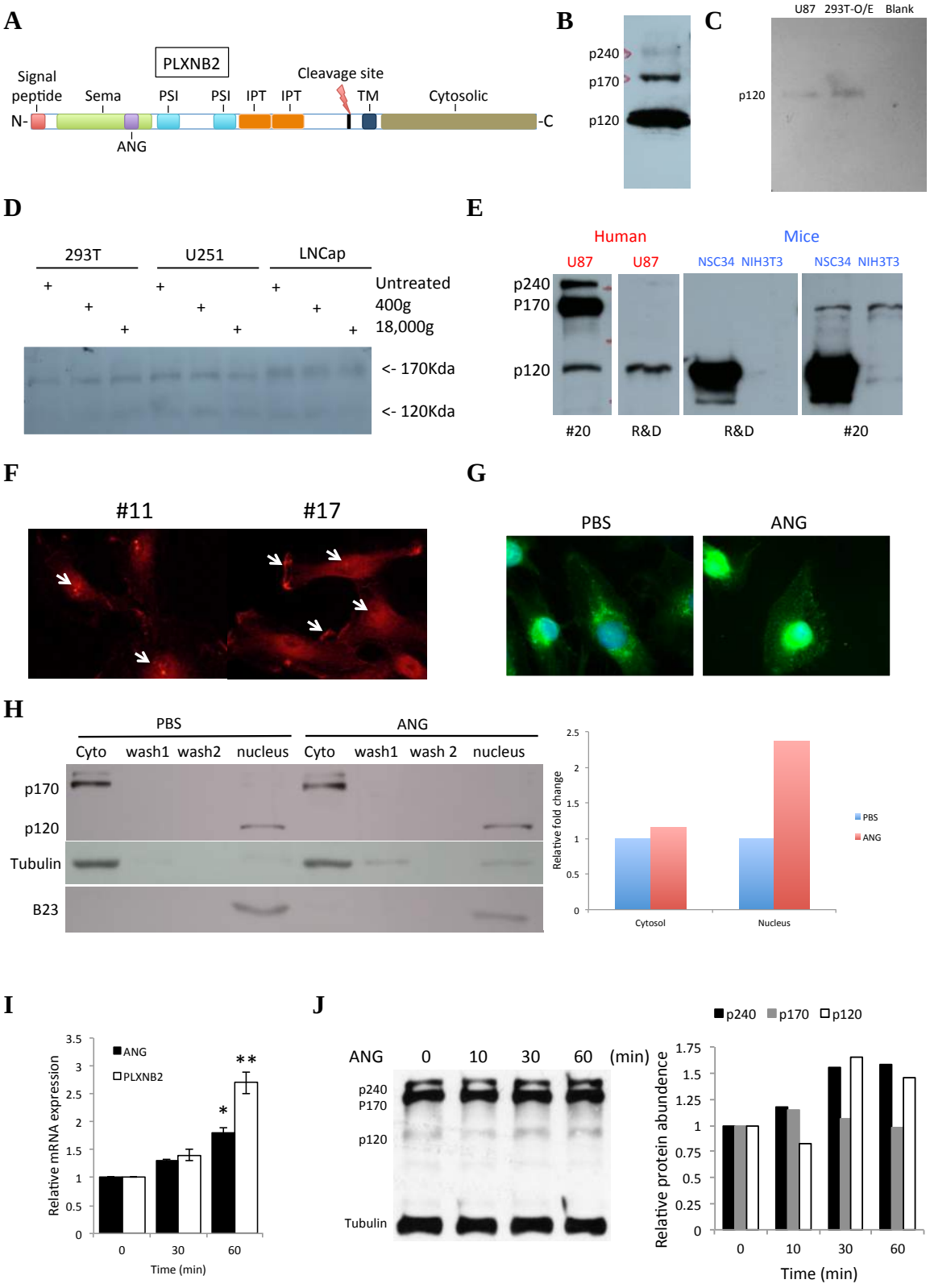
A
PLXNB2
Signal peptide
Sema
PSI
PSI
IPT
IPT
Cleavage site
TM
Cytosolic
N-
-C
ANG
B
p240
p170
p120
C
U87 293T-O/E Blank
p120
D
293T
U251
LNCap
Untreated
400g
18,000g
<- 170Kda
<- 120Kda
E
Human
Mice
U87
U87
NSC34 NIH3T3
NSC34 NIH3T3
p240
P170
p120
#20
R&D
R&D
#20
F
#11
#17
G
PBS
ANG
H
PBS
ANG
Cyto wash1 wash2 nucleus Cyto wash1 wash 2 nucleus
p170
p120
Tubulin
B23
Relative fold change
Cytosol
Nucleus
PBS
ANG
I
ANG
PLXNB2
Relative mRNA expression
Time (min)
J
ANG 0 10 30 60 (min)
p240
P170
p120
Tubulin
p240 p170 p120
Relative protein abundence
Time (min)

Figure 5.6. p120 is a novel PLXNB2 fragment that is involved in ANG nuclear translocation

(A) The scheme of PLXNB2 domains and the cleavage site.

(B) Western blot of analysis of PLXNB2 in concentrated (7-fold) conditioned medium of 293T-Pb2-O/E.

(C) Western blot analysis of PLXNB2 in of conditioned medium of U87, 293T-Pb2-O/E, and blank medium.

(D) Western blot analysis of PLXNB2 in untreated conditioned medium of 293T, U251, and LNCap, or that devoid of debris (400g centrifugation), exosomes (18,000g centrifugation).

(E) Western blot of human U87 and mouse NSC34 and NIH3T3 whole cell lysates blotted with in-house #20 PLXNB2 mAb or a commercial PLXNB2 mAb from R&D.

(F) Two PLXNB2 antibodies showed differential sensitivity to nuclear and cytosol PLXNB2. Arrows indicate PLXNB2 signals. Cells were fixed with methanol.

(G) U251 cells treated with ANG (500 ng/ml) or PBS for 30 min reveals accumulation of nuclear PLXNB2 in response to ANG. Cells were fixed with methanol.

(H) U251 cells treated with ANG or PBS were subcellular fractionated into cytosolic and nuclear fractions, and blotted for PLXNB2. Tubulin and B23 were used as normalization for cytosol and nucleus input, respectively.

(I) ANG and PLXNB2 mRNA expression in U251 cells treated with ANG for 0, 30 and 60 min.

(J) Western blot analysis of PLXNB2 fragments in whole cell lysates of U251 cells treated with ANG for 0, 10, 30 and 60 min. Protein normalized to tubulin.

PLXNB2 regulates GBM invasion

To examine the function of PLXNB2 in GBM invasion, U251-GFP-scramble and U251-RFP-PLXNB2-shRNA5 (knockdown efficiency ~80%, referred to Figure 5.4.E) were mixed and used to generate GBM chimeric spheroids. The spheroids usually formed around 2-3 days and then implanted into collagen to determine *in vitro* invasiveness. On day 0, fluorescence image showed that control cells and *PLXNB2* knockdown cells were equally mixed (Figure 5.7.A). From day 1 through day 3, there were more GFP cells invading into the matrix and the average distance cells had migrated was significantly greater in control U251 cells (green) than in *PLXNB2* knockdown U251 cells (red) (Figure 5.7.E-H). These results suggested that GBM tumors with lowPLXNB2 were less invasive than those with high PLXNB2.

In Chapter III, we have demonstrated that ANG promotes MMP-9-dependent GBM invasion. To confirm the reduced invasive phenotype observed in *PLXNB2* knockdown cells was due to the lack of ANG signaling, in the future experiment, we will treat the chimeric spheroid with ANG mAb 26-2F, and expect to see no difference in invasiveness between the control and *PLXNB2* knockdown cells.

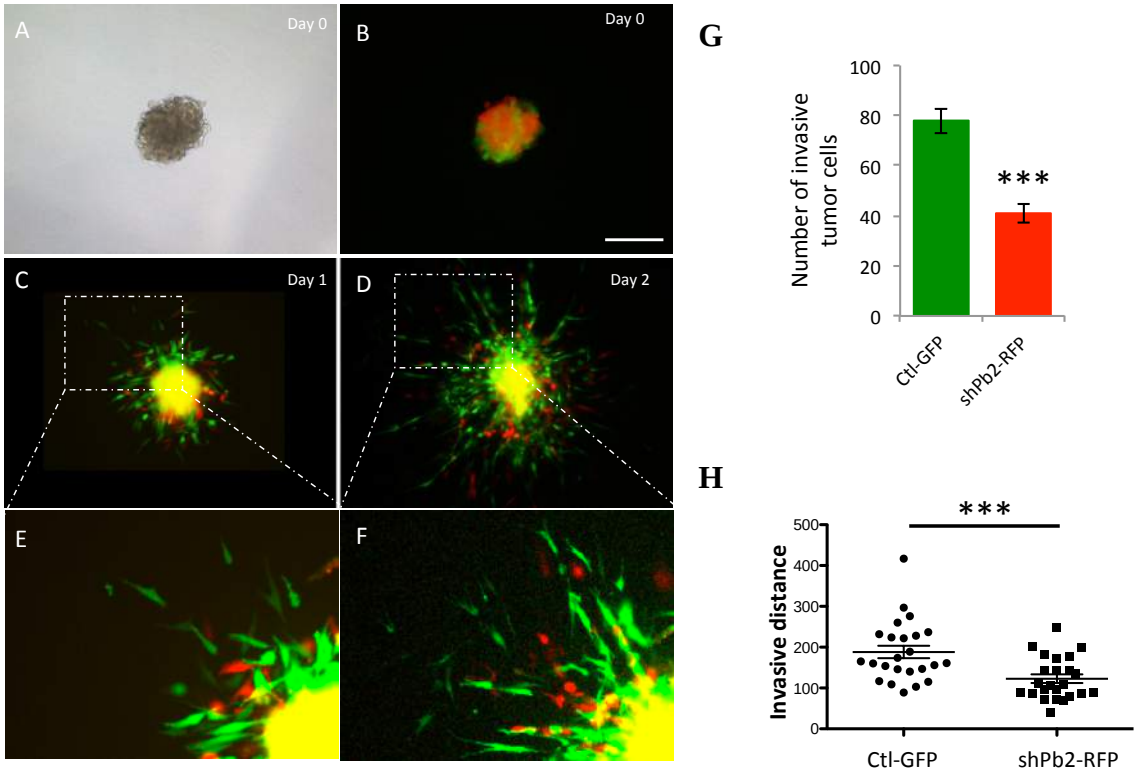

Figure 5.7. PLXNB2 regulates GBM migration and invasion.

(A) Phase contrast image of a spheroid consisting of control-GFP and shPb2-RFP U251 cells implanted in 3D collagen matrix.

(B) Fluorescence picture of the spheroid shown in A. Bar = 200 µm

(C-D) Fluorescence images of the spheroid invasion at day 1 and day 2.

(E-F) Enlarged regions of C-D.

(G) Number of active invading cells at day 2.

(H) Quantification of the invading distance of each tumor cells at day 2.

PLXNB2* knockdown inhibits GBM growth *in vivo

To assess PLXNB2 function *in vivo*, U87-NC and U87-shPb2-D2 lines were s.c. injected into nude mice to grow xenograft tumors. After 3 weeks, they were dissected and examined (Figure 5.9.A).We found that *PLXNB2* knockdown cells produced smaller xenograft tumor size, which had a 3-fold decrease in tumor mass compared to that of control cells. These results validated our *in vitro* findings that PLXNB2 regulated GBM proliferation (Figure 5.2.D).

We have also examined tumor-growing potential of *PLXNB2* knockdown cells in an orthotopic model. Control and *PLXNB2* knockdown U87 cells were stably transfected with lentiviral luciferase gene and i.c. injected into the SVZ region of the brain of nude mice. The *PLXNB2* knockdown group had a median survival of 27 days, which was significantly longer that the median survival of21 days in the control group (Figure 5.8.C). Weekly monitor of brain tumors via bioluminescence revealed a remarkably slower growth and smaller lesions in the knockdown group (Figure 5.8.D-E). The more drastic difference seen in the orthotopic xenografts than that in the ectopic model suggested that PLXNB2 is essential to mediate some important microenvironment signaling in the brain. Autopsy of the brain tissues showed apparent lesions in the injected hemisphere in both control and knockdown groups (Figure 5.8.F). The lesions form control cells appeared to be more aggressive because there were marked midline shift while those from *PLXNB2* knockdown cells only affected limited regional brain structure as seen in the sagittal section (Figure 5.8.F-G). Notably, the olfactory bulb of the control mouse brain was irretrievable in the sagittal section because of the loose tissue

textures, possibly as a result of invasion of highly proliferative and destructive tumor cells.

In the *PLXNB2* knockdown orthotopic tumors, PLXNB2 expression was absent and consequently ANG uptake was diminished (Figure 5.9.A). We used PCNA staining to examine tumor cell cycling and found a modest reduction in cycling cells in *PLXNB2* knockdown tumors at the core and a more significant decrease at the invasive edge (Figure 5.9.B-C). This reduced proliferation in *PLXNB2* knockdown tumors was accompanied by a lower level of activated ERK and AKT and a modest reduction of apoptosis (Figure 5.9.D-E). Interestingly, in *Ang* knockout mGBM apoptosis were significantly higher than that in the wildtype mGBM. These data suggested that ANG-independent function of PLXNB2 promotes apoptosis in GBM. Although no angiogenic activity of PLXNB2 has been reported, we observed a two-fold reduction of angiogenesis in PLXNB2 knockdown tumors (Figure 5.9.F). Yet, less angiogenesis may be due to an indirect effect of smaller tumor size of the *PLXNB2* knockdown xenografts.

ANG and MMP-9 were highly co-expressed at the invading tumor edge, as shown in Chapter II. In *PLXNB2* knockdown xenografts, expressions of both ANG and MMP-9 at the invading edge were diminished, suggesting that the majority of MMP-9 induction at the invasive edge was regulated by ANG/PLXNB2 (Figure 5.9.G). MMP-2 was also present at the invading edge but to a much less extent than MMP-9 (Figure 5.9.G). MMP-2 expression was inhibited by *PLXNB2* knockdown as well. It demonstrated that ANG/PLXNB2 signaling could activate multiple pro-invasive pathways during GBM

progression. These data encouraged us to examine further the therapeutic benefit of inhibiting PLXNB2 in a preclinical GBM mouse model.

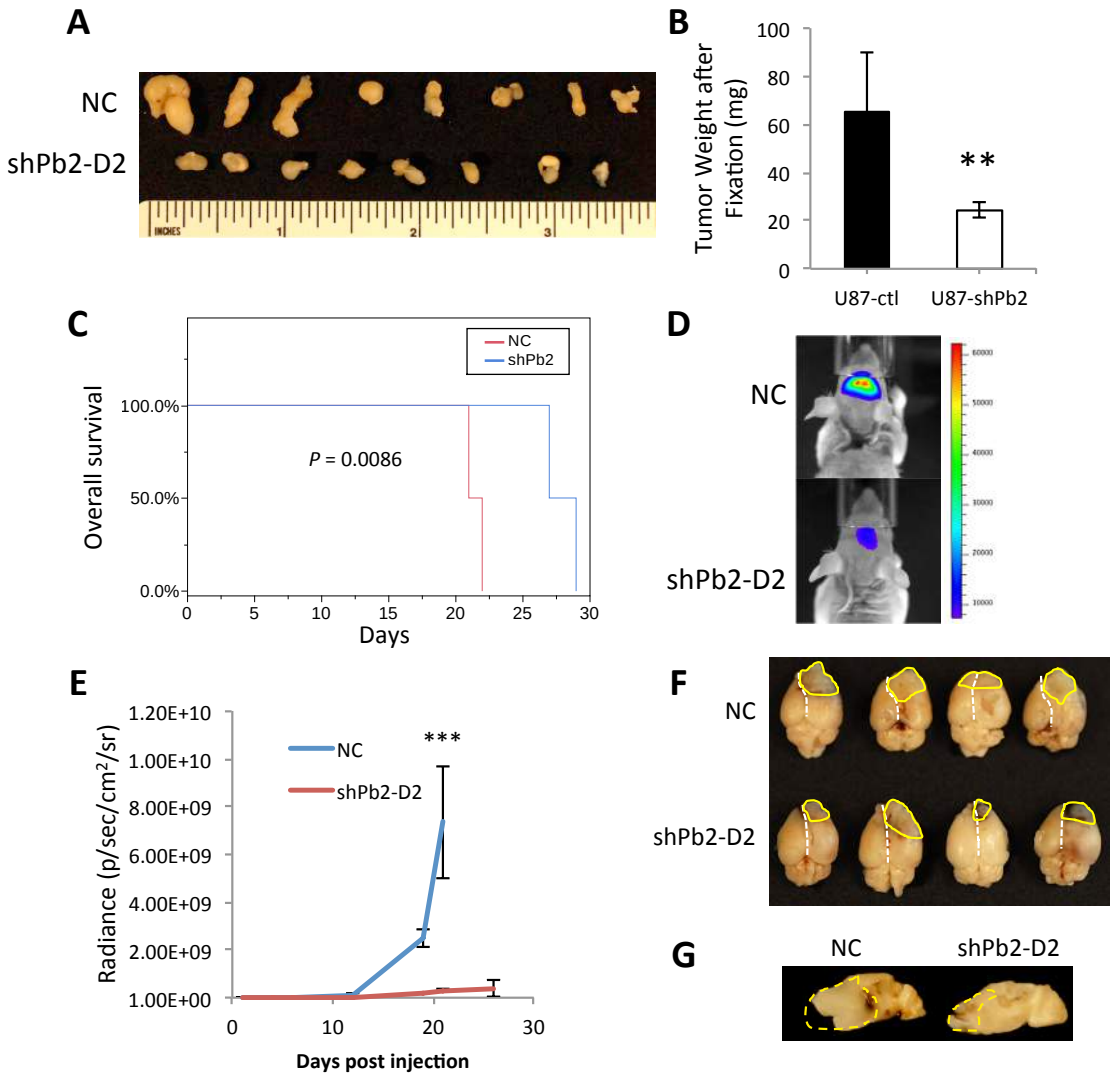

Figure 5.8. *PLXNB2* knockdown inhibits GBM *in vivo* growth.

(A) Ectopic U87-NC and U87-shPb2-D2 xenografts were harvested from the subcutaneous sites. *PLXNB2* knockdown groups had significantly smaller tumor size (N = 8 in each group).

(B) Weight of xenografts tumors shown in panel A.

(C) Survival analysis of U87-NC and U87-shPb2-D2 in the orthotopic tumor model (N= 4, in each group).

(D) Representative bioluminescence signal of mouse brain bearing luciferase-expressing U87 tumors.

(E) *In vivo* tumor growth rate of *PLXNB2* knockdown and scramble control cells measured by bioluminescence.

(F) Brain tissues autopsy exhibiting lesions that were circled by the yellow line. White dotted lines mark the midline of the brain.

(G) Dotted area in the sagittal brain sections marked the lesion size in the control and PLXNB2 knockdown groups.

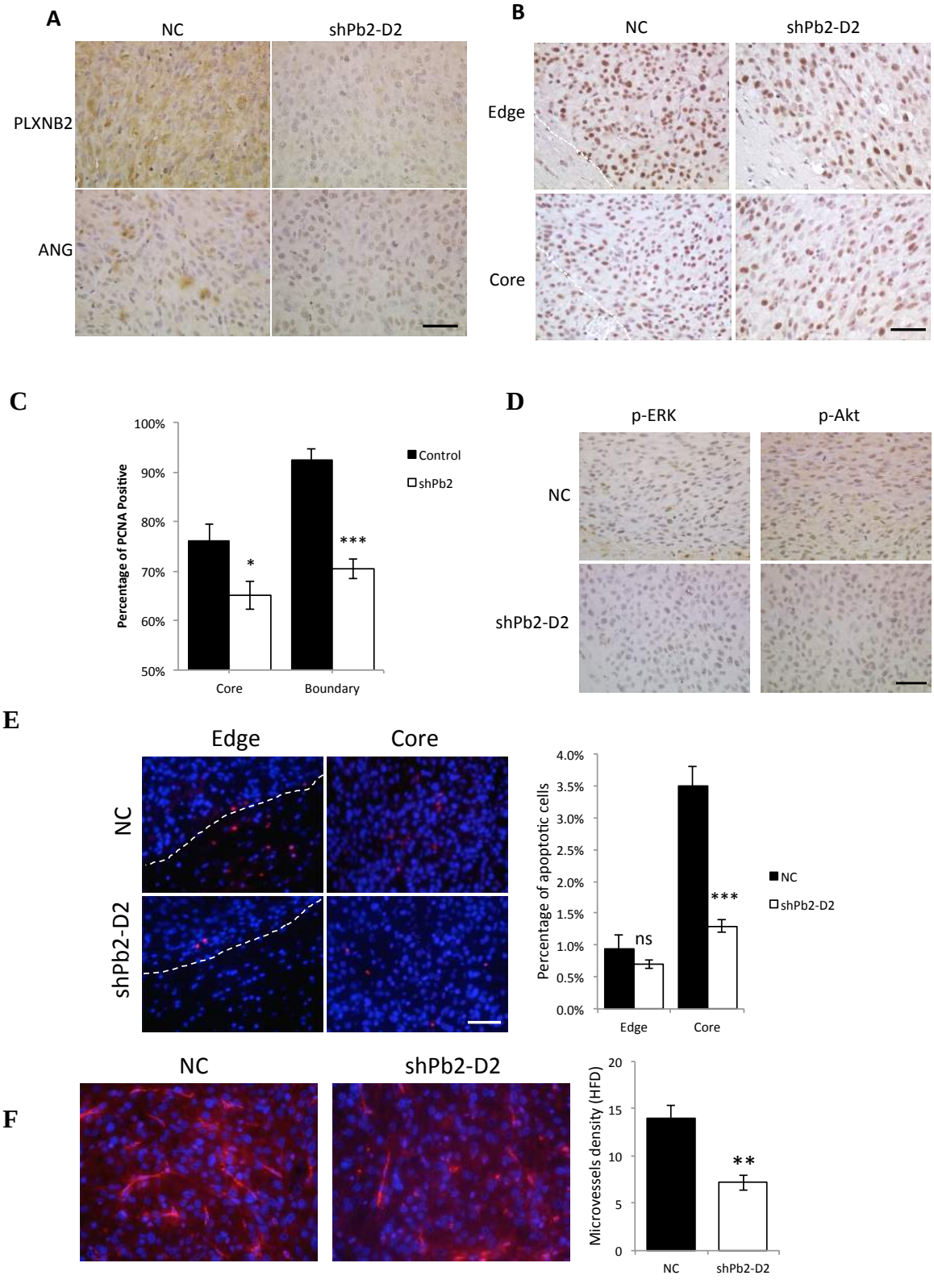
A
NC
shPb2-D2
PLXNB2
ANG
B
NC
shPb2-D2
Edge
Core
C
Percentage of PCNA Positive
100%
90%
80%
70%
60%
50%
Control
shPb2
*
***
Core
Boundary
D
p-ERK
p-Akt
NC
shPb2-D2
E
Edge
Core
NC
shPb2-D2
Percentage of apoptotic cells
4.0%
3.5%
3.0%
2.5%
2.0%
1.5%
1.0%
0.5%
0.0%
ns
***
NC
shPb2-D2
Edge
Core
F
NC
shPb2-D2
Microvessels density (HFD)
20
15
10
5
0
**
NC
shPb2-D2

G

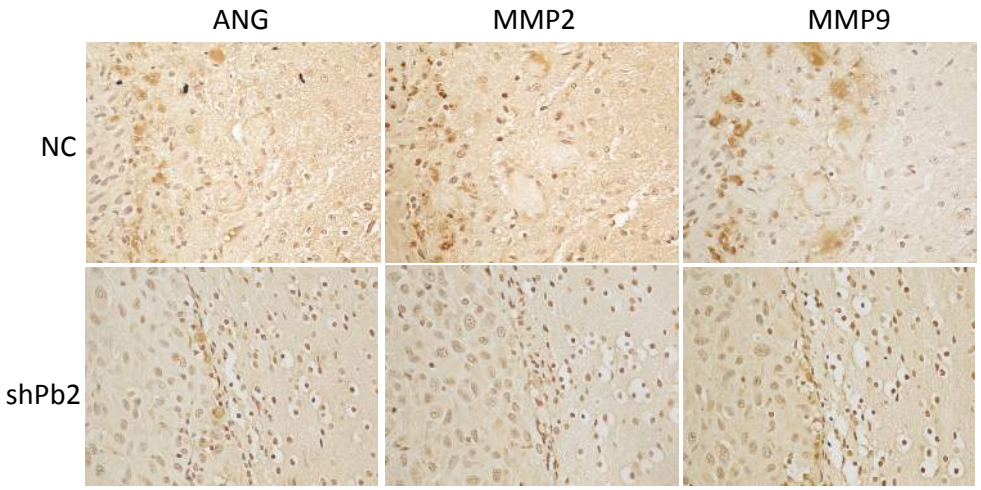

Figure 5.9. Characterization of *PLXNB2* knockdown orthotopic xenografts.

(A) IHC of ANG and PLXNB2 in the orthotopic xenografts.

(B) IHC of PCNA in the orthotopic xenografts at tumor edge and core.

(C) Quantification of PCNA positive cells shown in B.

(D) IHC of p-ERK and p-AKT in the orthotopic xenografts. Bar = 200 μm

(E) TUNEL staining and quantification of apoptotic cells in the orthotopic tumors.

Dotted line marks tumor edge. Bar = 50 μm.

(F) IF of CD31 and quantification of vessel density in the orthotopic xenografts.

(G) IHC of ANG, MMP-2, and MMP-9 in serial sections of the orthotopic xenografts

PLXNB2 mAb effects on a mouse proneural GBM model

PLXNB2 mAb #11 was purified from the culture medium of the hybridoma cells. The mAb and the mouse control IgG CCL130 showed high purity without other protein contamination on SDS-PAGE (Figure 5.10.A) and they were also spectrophotometrically pure as shown in the full-range absorption spectrum (Figure 5.10.B). Anti-tumor activity of this mAb was tested in the proneural mGBM by weekly i.p. injection of 10 mg/kg, starting one week after tumor induction. However, animals treated with this PLXNB2 mAb or with isotype-matched control antibody CCL130 had no significant difference in overall survival (Figure 5.10.C). Immunofluorescence staining of mouse antibody in the mouse brain tissues showed minimal binding of CCL130 to normal brain tissues and tumor cells, whereas PLXNB2 mAb was also not interacting with the tumor cells but surprisingly accumulated at a layer of unidentified structure close to the tumor invading edge (Figure 5.10.D). Therefore, one possible reason of PLXNB2 mAb #11 to fail to inhibit mGBM is that it did not reach the tumor target.

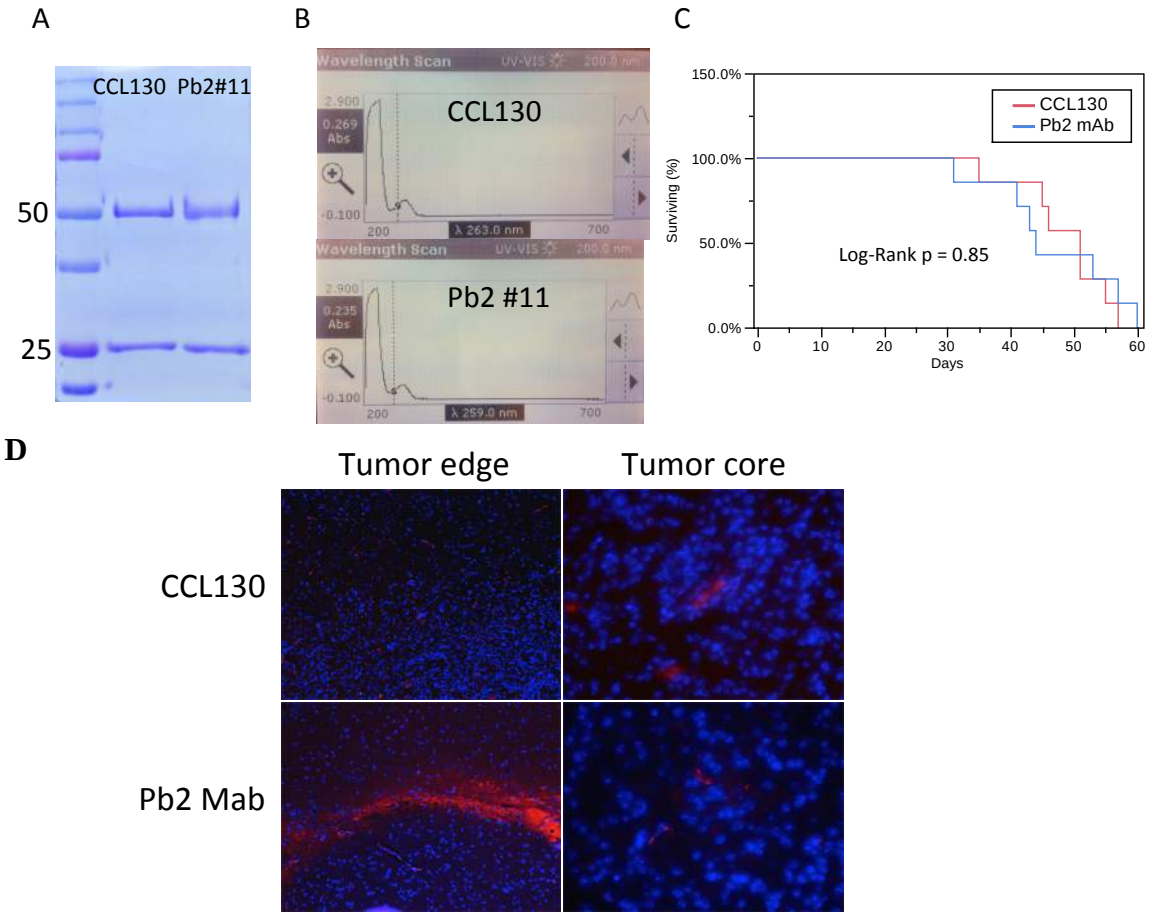

Figure 5.10. Lack of inhibitory effect of PLXNB2 mAb in mouse GBM.

(A) SDS-PAGE analysis of purified PLXNB2 mAb #11 from hybridoma cell culture medium and a mouse isotype control IgG, CCL130.

(B) Full-range absorption spectrum (200 – 700 nm) of purified #11 mAb and CCL130.

(C) Survival plot of two groups of mice received weekly i.p. injection of either #11 mAb or CCL130 at 10 mg/ml (N = 7).

(D) Immunofluorescence staining reveals binding of injected mAbs to a non-tumor region in mouse brain.

Discussion

Role of PLXNB2 in GBM

We showed that PLXNB2 has a prognostic significance in a cohort of human GBM patients. We used *in vitro* assays to demonstrate that *PLXNB2* knockdown led to a deficiency in anchorage-independent growth, tempered GBM proliferation, and impeded invasion. Consistently, orthotopic xenografts derived from *PLXNB2* knockdown cells had reduced proliferation, decreased angiogenesis, and lack of ANG signaling at the invasive edge. Contrary to the higher apoptosis seen in anchorage-independent culture of *PLXNB2* knockdown cells and *Ang* knockout mGBM tissues, the *PLXNB2* knockdown orthotopic xenografts showed only a modest reduction of apoptosis. It is possible that ANG-independent microenvironment signaling through PLXNB2 promotes apoptosis. Additionally, the difference in tumor growth due to *PLXBN2* knockdown is more significant in the orthotopic brain xenografts than in the s.c. ectopic xenografts, suggesting that brain specific factors contribute to GBM growth in a PLXNB2-dependent manner. In summary, these data suggest that there are distinct microenvironmental factors in the brain that regulate GBM apoptosis and progression through PLXNB2.

Notably, the luciferase signals differed by nearly 25-fold between the control and *PLXNB2* knockdown groups at the endpoint of the experiment, whereas histology analysis showed a difference of only ~10-fold. We thought that this discrepancy may result from two factors: 1) although we ensured the same MOI virus integration into the two groups, the actual luciferase protein may differ, as reduced ANG signaling in *PLXNB2* knockdown may reduce ribosome biogenesis and then protein translation; 2) the

control brain tissues have a better perfusion due to increased vessel density, so the luciferin could access more tumor cells in the control xenografts than the *PLXNB2* knockdown ones.

Recently, a study on PLXNB2 in GBM was published, showing similar findings on the prognostic significance of PLXNB2 in GBM and its pro-invasive effects (Le et al., 2015). In that study, PLXBN2 knockdown significantly impaired invasion in two different serum GBM lines and one GNS line. However, the impact of *PLXNB2* knockdown *in vivo* on apoptosis and cell cycling were not evident. The *PLXBN2* knockdown effects on U87 orthotopic xenografts growth was in agreement with our finding but not with another serum line LN229. Interestingly, it showed that *PLXNB2* knockdown significantly inhibited perivascular invasion in a GNS orthotopic xenograft. However, the study did not explain how PLXNB2 mediates perivascular invasion. Nonetheless, these findings provide excellent support to our hypothesis that ANG/PLXNB2 regulates perivascular invasion of GBM, because *PLXNB2* knockdown essentially blocks ANG/FOSL2/CD24 signaling pathway and exhibits a similar phenotype as seen in *Ang* knockout mGBM or neomycin treated mGBM. Another interesting aspect of this recently published study relates to reduced angiogenesis in PLXNB2 knockdown tumors, which is consistent with the findings with two serum lines (U87 and LN229) in that study and with the findings (U87) from our work. Reduced angiogenesis was initially anticipated as a secondary response to the slower tumor growth in *PLXNB2* knockdown tumor. However, in *PLXNB2* knockdown LN229 orthotopic xenografts, there were no significant differences in tumor growth but still a dramatic reduction in angiogenesis compared to the scramble

control, indicating that decreased angiogenesis was not due to less nutrient demands. The study did not address how *PLXNB2* knockdown led to reduced angiogenesis. Based on our finding that sPb2 facilitated ANG uptake in tumor cells, we proposed that tumor-secreted sPb2 could play an essential role in tumor angiogenesis by enhancing ANG uptake in endothelial cells. Once confirmed, this finding has significant implications as sPb2 may facilitate ANG uptake or intracellular signaling in non-PLXNB2 expressed cell by binding to its co-receptor or heparin sulfate. Its significance may extend beyond cancer angiogenesis as well because PLXNB2 is highly expressed during embryo development and in adult blood and immune system. The regulation of PLXNB2 surface cleavage adds another layer of regulation on ANG uptake in shaping the key processes mentioned above.

Lastly, we showed that our in-house mAb failed to extend survival in the proneural mouse model. There are a few factors that may lead to the failure of this experiment: 1) BBB limits antibody access to the brain lesions; 2) PLXNB2 #11 mAb may not recognize mouse Plxnb2. It showed high affinity binding to p120 but not to the cell surface p170/p240 in mouse cell lines shown in WB data (Figure 4.7.E); 3) the amount of antibody injection is not enough. In this study, we injected mAb at 10 mg/kg only once per week, while other studies used nearly 8 times more mAb injection, 40 mg/kg twice per week (Baker et al., 2014; Bekhite et al., 2011; Jiang et al., 2008; Martens et al., 2008; Moelling et al., 2002; Pasterkamp, 2012).

Chapter VI

Investigation of Angiogenin-induced tiRNA production in GBM

Under stress conditions, a small portion of tRNAs are cleaved by ANG and the product (tiRNA) conserves ATP consumption by inhibiting the translation initiation machinery and decreases apoptosis sensitivity by inhibiting Cyt c. The cyto-protective effect of tiRNA is a novel stress response that is utilized under both physiology and pathological conditions (Emara et al., 2010; Ivanov et al., 2011; Saikia et al., 2014; Skorupa et al., 2012; Yamasaki et al., 2009). However, the regulatory mechanisms that allow ANG to cleave tRNA are not fully understood. Early findings show that *RNH1* knockdown and eIF2α mutation both increased ANG-mediated tiRNA production (Yamasaki et al., 2009), and that tiRNA production was positively correlated with protein synthesis rate (Saikia et al., 2012) .

Stress-induced tiRNA is independent of autocrine ANG.

Numerous stresses conditions including hypertonic solution, high and low temperatures, hypoxia, ROS, and radiation induce ANG-mediated tiRNA production (H. Fu et al., 2009; Yamasaki et al., 2009). ANG is upregulated in hypoxia and inflammation conditions (Nakamura et al., 2006; Verselis et al., 1999) and was hypothesized to be upregulated under other stress conditions (S. Li & Hu, 2012). We investigated whether other stress conditions upregulate *ANG* expression and if tiRNA production is mediated through re-entry of secreted ANG in stressed cells. We found that *ANG* was induced in U251 by all three stress conditions tested, showing the highest upregulation of an 8-fold increase under nutrient deprivation, and a 2.2-fold and 1.7-fold inductions under oxidative and ER stress, respectively (Figure 6.1.A). However, tiRNA production was the highest under oxidative condition and followed by nutrient deprivation, while ER stress

could not induce discernable tiRNA in U251 (Figure 6.1.B). Apparently, upregulation of *ANG* was not correlated with the extents of tiRNA production under different stress conditions, suggesting that newly synthesized ANG cannot be fully accounted for tiRNA production. It is in agreement with early finding that the total cellular ANG were not significantly changed during the stress conditions (H. Fu et al., 2009). To demonstrate that secreted ANG does not significantly contribute to stress-induced tiRNA production, we applied ANG mAb 26-2F in an attempt to inhibit oxidative stress-induced autocrine ANG in U251 cells. We found that while 26-2F effectively inhibited exogenous ANG-induced tiRNA production, it did not affect oxidative stress-induced tiRNA (Figure 6.1.C), indicating that despite *ANG* upregulation under stress conditions, it is possible that ANG-mediated tiRNA production is induced by activation of the existing pool of ANG in the cells. It is also possible that ANG mAb did not fully neutralize the newly synthesized ANG under this condition.

RNH1 has been shown to negatively regulate ANG-mediated tiRNA, because RNH1 is a natural inhibitor for ANG, and *RNH1* knockdown gave rise to tiRNA even without oxidative stress, and could further potentiate stress-mediated tiRNA production (Yamasaki et al., 2009). These data suggested that *RNH1* inhibits ANG-mediated tiRNA production. It is possible that other factors, in addition to RNH1, may also control stress-induced tiRNA production. We used an *RNH1* knockdown HeLa cell line (~80% knockdown efficiency at protein level) (Pizzo et al., 2013) to test exogenous ANG-mediated tiRNA production without the presence of RNH1. We found a moderate increase of tiRNA at the baseline levels in the *RNH1* knockdown cells as compared to

control cells, but no significant difference in exogenous ANG-induced tiRNA between the control and *RNH1* knockdown HeLa lines. Based on these data, we tempt to think that tiRNA generated through exogenous ANG or stresses are mediated by two different mechanisms. Therefore, stress-induced tiRNA production is independent of secreted ANG and it is possible that other potential regulatory mechanisms govern tiRNA production.

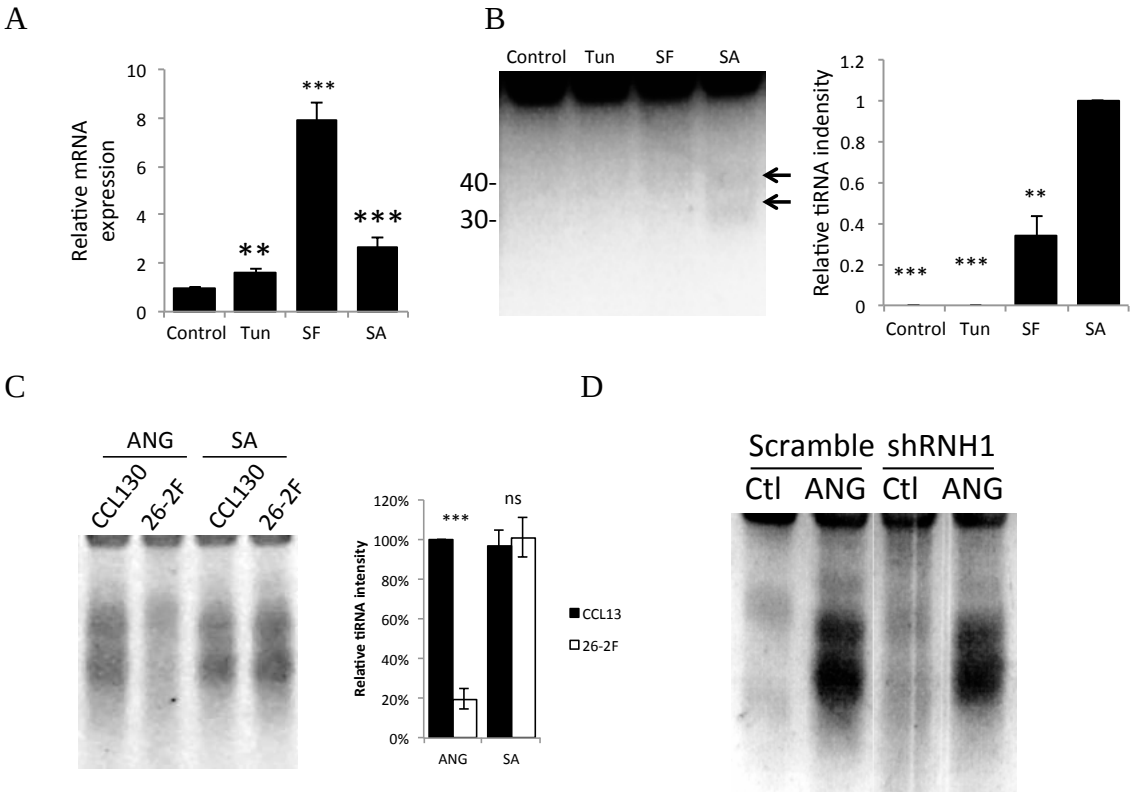

Figure 6.1. Stress-induced tiRNA is independent of secreted ANG.

(A) qRT-PCR of *ANG* mRNA levels in U251 cells treated with Tun (Tunicamycin, 12.5 µg/ml, 1h), starvation (serum free DMEM (SF), 24h), or SA (Sodium arsenite, 250 µM, 1h). Data were normalized to GAPDH internal control.

(B) Evaluation of tiRNA produced under the stress condition in A. Total RNA was separated on a 15% TBE-urea gel and detected with SYBR gold for tiRNA (30 - 50bp). Quantification of tiRNA abundance was normalized to SA treated sample (ImageJ, NIH).

(C) ANG mAb 26-2F (80 µg/ml) or matched isotype control (CCL130,80 µg/ml) were pre-incubated (15 min) with U251 cells before ANG (1 µg/ml) or SA treatment.

(D) tiRNA production in RNH1 knockdown or scramble control HeLa cells treated with ANG or PBS control.

Intracellular regulators of ANG-induced tiRNA production

To explore other intracellular regulators of tiRNA production, we measured exogenous ANG-induced tiRNA production in U251 cells in the presence of MEK, AKT, and PI3K inhibitors (Figure 6.2.A-B). MEK inhibition showed a non-significant 11% decrease of tiRNA whereas both AKT and PI3K inhibitors significantly decreased tiRNA production by 25% and 60%, respectively. Thus, PI3K/AKT signaling but not MEK/ERK seems to be involved in ANG-mediated tiRNA production. A combination of PI3K and AKT inhibitors almost completely prevented ANG-induced tiRNA production, showing a surprisingly additive effect of 82% reduction. We excluded the possibility that those reductions were due to impaired ANG uptake by the inhibitors (Figure 6.2.C). It suggests that other effector of PI3K signaling, for example, the PDK-SGK axis may also contribute to tiRNA production. Because exogenous ANG activates both PI3K/AKT and MEK/ERK pathways, these results suggest that tiRNA production by ANG is ERK independent but is closely regulated by the PI3K/AKT signaling axis.

The mTOR pathway controls anabolic cell growth and proliferation (J. Li, Kim, & Blenis, 2014), which is suppressed under stress conditions (Laplante & Sabatini, 2009). Inhibition of mTOR signaling potentiates exogenous ANG-mediated tiRNA production by a 1.7-fold increase, which was only modestly inhibited by PI3K inhibition (1.5-fold higher than the control). It is puzzling, because mTOR is downstream of PI3K/AKT axis that can also be activated by ANG. A plausible explanation could be that mTOR is responsible for an inhibitory mechanism that is independent of stimulation via PI3K/AKT in regulating ANG-mediated tiRNA production.

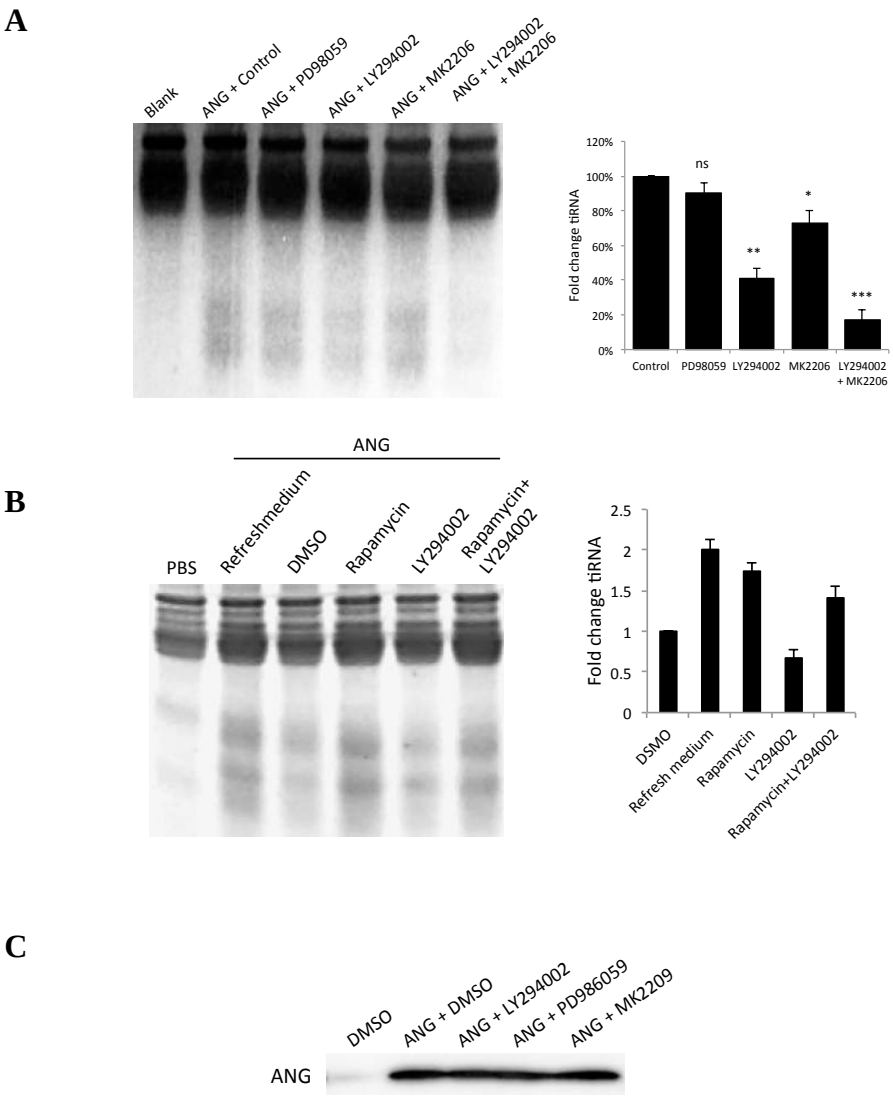

Figure 6.2. PI3K/AKT and mTOR pathways regulate ANG-induced tiRNA production independent of ANG uptake.

(A) The PI3K/AKT but not MEK inhibitor reduces ANG-induced tiRNA production in U251 cells.

(B) The mTOR inhibitor and refresh medium increases ANG-induced tiRNA production in U251 cells.

(C) The PI3K, AKT, or MEK inhibitor doesn't affect ANG uptake in U251 cells.

Extracellular regulators of ANG-induced tiRNA production

Exogenous ANG induced tiRNA production in a time- and concentration-dependent manner in U251. At this time period, we have shown in Chapter III that ANG uptake was gradually increased, suggesting that ANG uptake was the major contributor to tiRNA production (Figure 6.3.A). ANG uptake relies on its receptor, PLXNB2. The ability of exogenous ANG to produce tiRNA is correlated with PLXNB2 expression. For example, U87 cells express lower ANG receptor than do U251 cells, and it takes a higher ANG concentration (5 μg/ml) to generate an equivalent amount of tiRNA in U87 (Figure 6.3.H). Similarly, LNCaP cells have a higher PLXNB2 expression level than the other two prostate cancer cell lines (DU145 and PC-3) (data not shown) and were the most sensitive line to ANG-induced tiRNA production. The involvement of PLXNB2 in ANG-mediated tiRNA is also supported by the finding that an ANG variant (R70A), which does not bind to the receptor, was unable to induce tiRNA (Figure 6.3.B). Furthermore, knockdown of *PLXNB2* in U251 cells abolished ANG-induced tiRNA (Figure 6.3.C).

ANG-mediated tiRNA doesn't seem to require nuclear activity of ANG, because the nuclear localization sequence (NLS) variant of ANG (R33A), which can bind to the receptor but doesn't undergo nuclear translocation, showed no defect in producing tiRNA (Figure 6.3.B). These data suggest that tiRNA production likely takes place in the cytoplasm. This is consistent with the findings that stress inducers relocalize ANG to cytoplasm from nucleus (Emara et al., 2010; Pizzo et al., 2013).

Interestingly, when we changed the conditioned medium to fresh DMEM + 10% FBS before ANG was added, we noticed a robust 2-fold increase in exogenous ANG-mediated tiRNA (Figure 6.2.B), suggesting that the conditioned medium contained cell-secreted ANG inhibitor or that fresh FBS contains binding factors that can facilitate ANG uptake.

Given that Sema4C, the cognate ligand of PLXNB2, and the soluble PLXNB2/p170 (sPb2) can be secreted by tumor cells into the conditioned medium, their effects on tiRNA production was investigated. We found that ANG-induced tiRNA was enhanced in the presence of Sema4C, and surprisingly in the presence of sPb2 as well (Figure 6.3.E-F). These inductions corresponded to increased ANG uptake in U251 (Figure 6.3.G). It looked like that Sema4C and sPb2 facilitate ANG uptake by increasing the early uptake rate at 30 min, by 1.9- and 2.5-fold, respectively. At 60 min, ANG uptake was close to saturation and showed smaller differences in tiRNA production among the groups. In conclusion, we have found that ANG uptake rate is a major regulatory control for ANG-mediated tiRNA production, which can be modulated by PLXNB2, Sema4C, and sPb2.

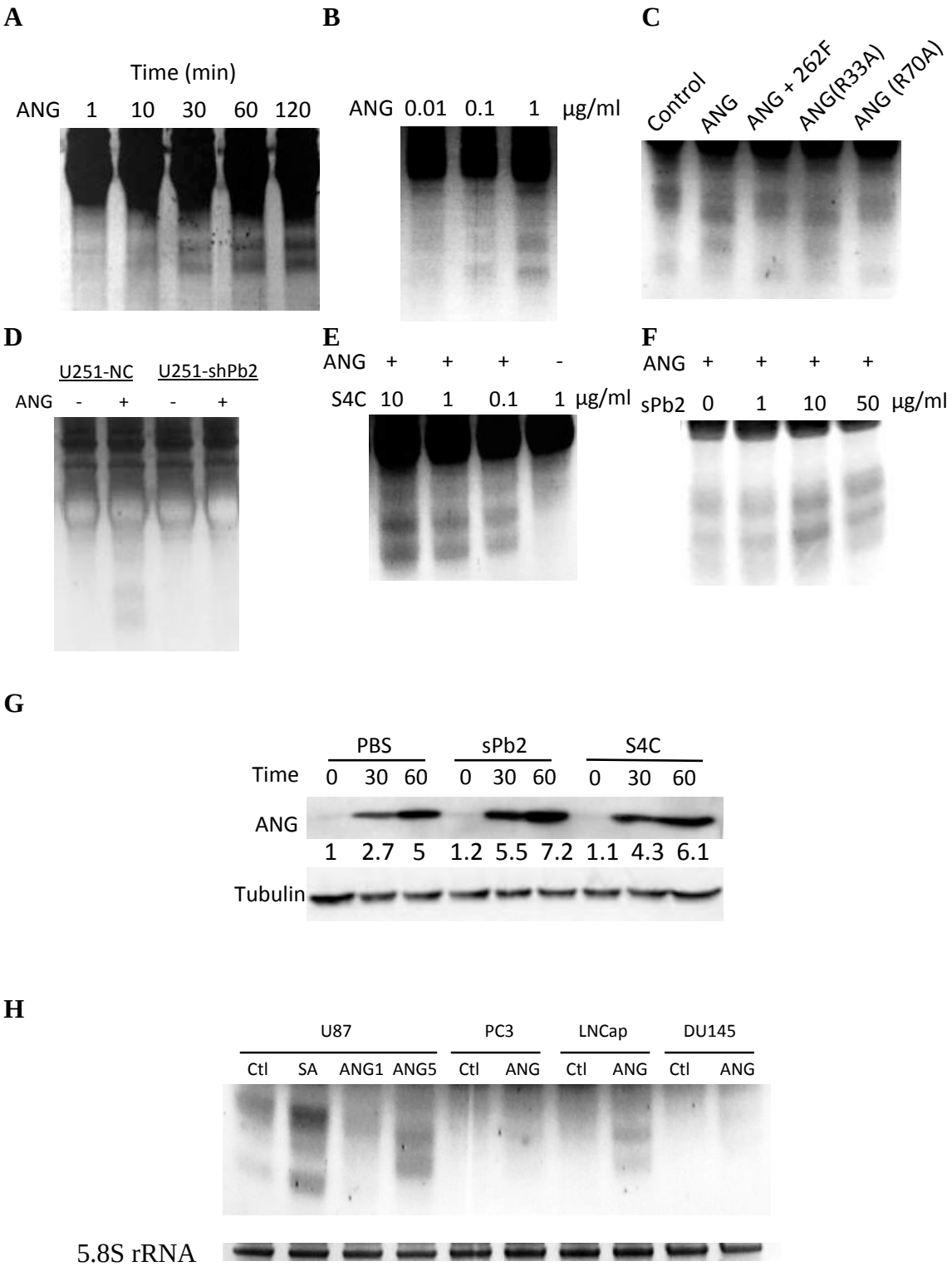
A
Time (min)
ANG 1 10 30 60 120
B
ANG 0.01 0.1 1 µg/ml
C
Control
ANG
ANG + 262F
ANG(R33A)
ANG (R70A)
D
U251-NC
U251-shPb2
ANG - + - +
E
ANG + + + -
S4C 10 1 0.1 1 µg/ml
F
ANG + + + +
sPb2 0 1 10 50 µg/ml
G
PBS
sPb2
S4C
Time 0 30 60 0 30 60 0 30 60
ANG
1 2.7 5 1.2 5.5 7.2 1.1 4.3 6.1
Tubulin
H
U87
PC3
LNCap
DU145
Ctl SA ANG1 ANG5 Ctl ANG Ctl ANG Ctl ANG
5.8S rRNA

Figure 6.3. Potential mechanism of exogenous ANG induced tiRNA.

(A-B) Exogenous ANG induces tiRNA in a time and concentration dependent manner.

(C) ANG receptor binding mutant (R70A) fails to induced tiRNA but nucleus translocation mutant (R33A) does.

(D) *PLXNB2* knockdown inhibits ANG-induced tiRNA.

(E-F) S4C and sPb2 increases ANG-induced tiRNA in a concentration-dependent manner.

(G) S4C and sPb2 facilitate ANG uptake in U251 cell line.

(H) ANG-induced tiRNA in different cell lines including U87, PC3, LNCap and DU145 cell line. SA, sodium arsenite; ANG/ANG1 (ANG 1 μg/ml), ANG5 (ANG 5 μg/ml). 5.8S rRNA shown as loading control.

Discussion

Regulation of tiRNA production

While the exact location of tiRNA production is still unknown, some evidence suggests that it may not take place in the nucleus because oxidative stress relocates the majority of nuclear ANG to the stress granules in the cytosol while generating tiRNA. Treating cells with ANG can also give rise to tiRNA, but given the majority of ANG immediately enters nucleus via receptor-mediated endocytosis (G. F. Hu et al., 2000), it would be interesting that tiRNA production is a direct effect the enzymatic action of ANG , although other argued that exogenous ANG can also be accumulated in cytosol (Hatzi et al., 2000).

We applied various signaling inhibitors together with exogenous ANG to examine the regulation of tiRNA production. We found that refresh FBS-containing culture medium, mTOR inhibition (rapamycin), Sema4C, sPb2, and knockdown of *RNH1* increased ANG-mediated tiRNA production, while MEK inhibitor had no effect, and PI3K inhibitor or AKT inhibitor significantly reduced tiRNA. Notably, a combination of PI3K and AKT inhibitors had a synergistic effect in inhibiting tiRNA production. We can conclude that the ERK pathway is not involved in regulation of tiRNA production.

The addition of PI3K inhibitor did not abolish the effect of rapamycin on ANG-dependent tiRNA induction. Since we exclude the role of MEK/ERK in tiRNA production, it remains possible that rapamycin treatment activates AKT-independent PI3K and promotes tiRNA production. In rapamycin-treated cells, there are feedback

mechanisms regulating AKT and ERK in the context of rapamycin concentration, duration, or cell type. For example, it has been reported that a low concentration of rapamycin activates both AKT and ERK whereas a high level of rapamycin inhibits AKT and ERK signaling (X.-G. Chen et al., 2010). Long-term treatment of rapamycin suppresses the pro-survival effect of AKT (Sarbassov et al., 2006). Therefore, we need to verify rapamycin-treated cells by examining AKT activation status and also apply a combination of rapamycin and AKT inhibitor in ANG-tiRNA assay.

RNH1 is a physiological inhibitor of ANG. During ROS stress, RNH1 undergo rapid degradation due to intramolecular disulfide bridges generated by random oxidation. Thus, ANG activity is de-repressed and is able to produce tiRNA. While, under other stress conditions, there is no noticeable degradation of RNH1, yet it remained possible that phosphorylation of RNH1 and spatial separation of RNH1 from ANG would allow for execution of the enzymatic activity of ANG. Given that PI3K/AKT pathway is required for tiRNA production, we hypothesize that ANG-dependent PI3K/AKT activation releases the inhibitory effect of RNH1 on ANG and allows tiRNA productions under stress conditions. Future study will focus on RNH1 and PI3K/AKT and begin to delineate the regulatory mechanism of ANG-mediated tiRNA production under stress or disease conditions.

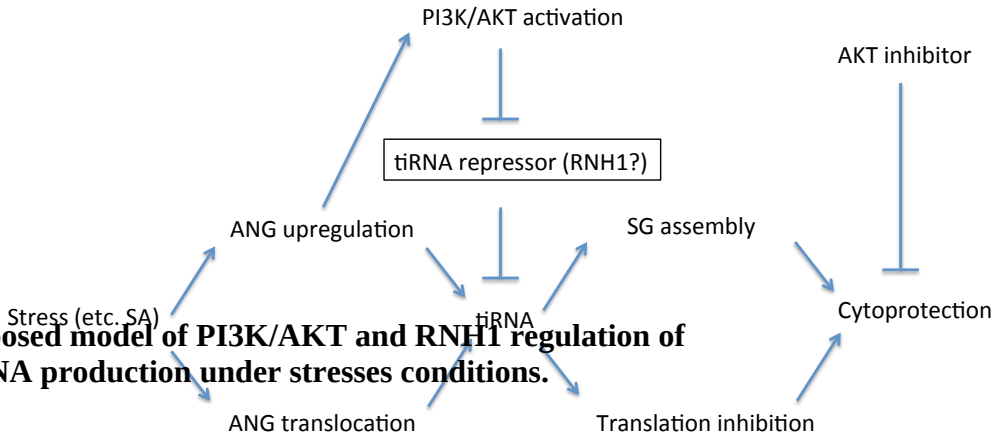

Figure 6.4 The proposed model of PI3K/AKT and RNH1 regulation of ANG-mediated tiRNA production under stresses conditions.

Chapter VII

Discussion and future directions

Upon identification of PLXNB2 as the cell surface receptor for ANG, we set out to find out the most relevant tumor type in which ANG is likely to play a significant role. We took advantage of the existing public microarray data to examine the expression of *PLXNB2* and its ligand *ANG* in various tumor types. GBM is one of the cancer types showing the highest expression of both *ANG* and *PLXNB2*. In fact, PLXNB2 was initially discovered in GBM by its differential expression as compared to the lower grade gliomas and normal brain tissue (Shinoura et al., 1995). The objective of this thesis research was to characterize the function of ANG in disease progression GBM and to examine if ANG inhibition can improve GBM survival.

ANG uptake in GBM

We demonstrated that exogenous ANG selectively binds to PLXNB2-overexpressing GBM cells and that PLXNB2 monoclonal antibody inhibited nuclear translocation of ANG. In *PLXNB2* knockdown cells, both ANG uptake and ERK activation were inhibited. Furthermore, an orthotopic xenograft derived from *PLXNB2* knockdown cells had diminished expression of ANG, MMP-2, and MMP-9 at the invasive front compared to the control. Thus, PLXNB2 is both sufficient and necessary for mediating ANG uptake and downstream signaling.

In U251 GBM cells, we observed significant ANG uptake from 15 min to 60 min. Although the methodology used for measuring ANG uptake could not distinguish intracellular verse surface ANG, the increasing signal was not likely due to the non-specific surface binding, because it is known that ANG receptor is highly expressed on

the cell surface and that ANG/Actin interaction is minimal when the receptor is present (G. F. Hu et al., 1997). It is also known that non-specific binding of ANG to cell surface is fast and is expected to be saturated at an early time point without incremental changes over time (Baker et al., 2014; Bicknell & Vallee, 1988).

Sema4C and the extracellular domain of PLXNB2 were able to enhance ANG uptake (Chapter V). Heparan sulfate on Syndecan-4 has been shown as an essential component of clathrin-mediated endocytosis of ANG (Liang et al., 2006; Skorupa et al., 2012). Differential expressions of those factors are thus likely to modulate the dynamic feature of ANG uptake. Thus, it seems that ANG uptake and nuclear translocation is cellular context-dependent.

ANG-PLXNB2 signaling axis and uptake and nuclear translocation of ANG

ANG activates numerous pathways including PI3K/AKT, SAPK/JNK, MEK/ERK, PLC, and PLA2 under different cellular contexts (Bicknell & Vallee, 1988; G. F. Hu et al., 1997; 2000; Shinoura et al., 1995). The signaling pathway linked to receptor activation, ANG uptake, and nuclear translocation and the resultant effect on anti-apoptosis, invasion, and proliferation have only been studied in isolated settings. Therefore, a coherent ANG signaling model is needed to pave the ground for informative ANG research in the future. According to the results of this thesis research, we are able to add one more biological process, perivascular invasion, to the known activities and pathways where ANG is involved (Figure 7.1).

Figure 7.1 Illustration of ANG downstream signaling and functions. Green arrow: activation. Red arrow: inhibition. Green box, protein or molecules. Blue box, biological process or effects.

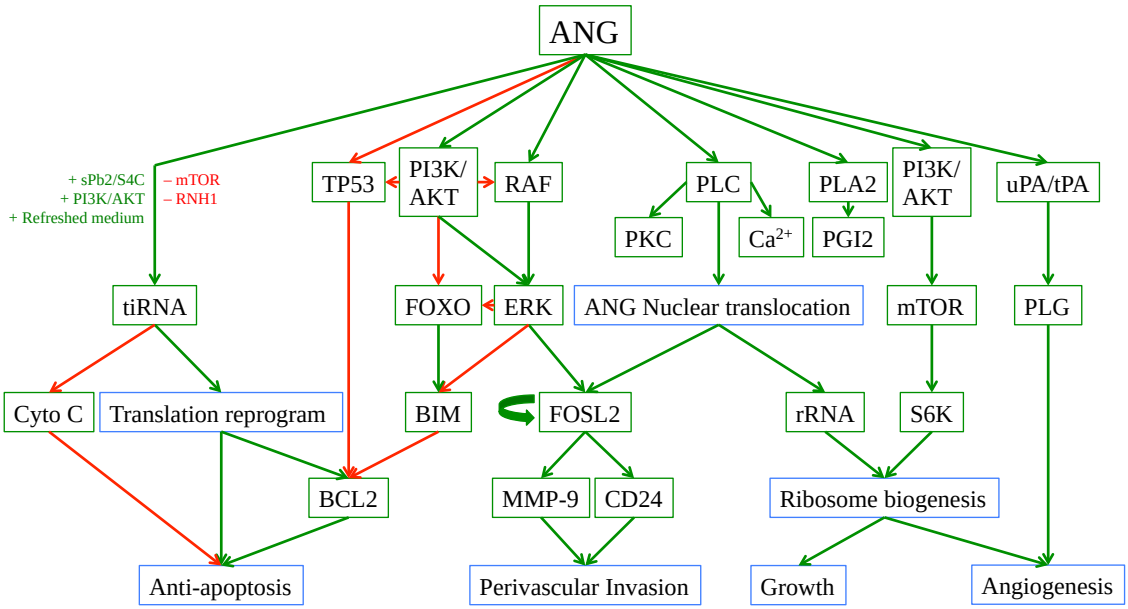

The PLC pathway is involved in nuclear translocation of ANG, as the latter is inhibited only by PLC inhibitors but not inhibitors of PKC, phosphotase, and tyrosine kinase (Baker et al., 2014; G. F. Hu, 1998). PLC activation is commonly linked to activation of G-protein-coupled receptor or receptor tyrosine kinase. A pertussis sensitive G protein is involved in ANG-induced PLA2 activation in endothelial cells (Bicknell & Vallee, 1989; Hayashida, Bartlett, Chen, & Park, 2010), suggesting the possibility that ANG can also be recognized by GPCR or ANG can modulate G protein activity without interacting with GPCR.

Identifying the RTK co-receptor or G protein mediator of PLXNB2 is important for elucidating ANG signaling, because how PLXNB2 activation leads to downstream AKT

and ERK activation is not well understood. In GBM cell line, ANG-induced ERK activation precedes AKT. ERK peaked at 8 min and diminished at 60 min, while AKT activation showed a slower response but sustaining from 30 min to 120 min. The early ERK activation is not likely to be mediated by GPCR because GPCR-dependent acute ERK response usually takes place around 8 min post-stimulation and peaks between 30-60 min (Gesty-Palmer et al., 2006; Le et al., 2015). However, the possibility that it involves a different mode of G-protein action could not be excluded. If so, would this G protein activation be the differentiator between ANG-induced and Sema4C-induced PLXNB2 activation? The decreased ERK activation at 60 min in U251 could be mediated by elevated AKT activation that leads to inhibition of RAF (Moelling, Schad, Bosse, Zimmermann, & Schweneker, 2002). ANG uptake persists during 30-60 min in spite of decreased ERK activation in this period. It is in agreement with previous findings that ANG-dependent SAPK/JNK, MEK/ERK, and PI3K/AKT activation are not involved in nuclear translocation of ANG. Interestingly, ANG-induced ERK activation requires minimal PI3K/AKT activity, as pre-incubation of PI3K inhibitor abolishes the activation of ANG towards both AKT and ERK activation, while MEK inhibitor fails to temper AKT activation. One possible explanation could be that the early ERK activation is mediated through PI3K/PKC/MEK/ERK pathway, which is the case for VEGF downstream signaling in vasculogenesis (Bekhite et al., 2011).

ANG activates PLXNB2 in a Sema4C-independent manner

One possible differentiator between ANG- and Sema4C-induced PLXNB2 activation may be the receptor dynamics upon stimulations by different ligands. Binding of Sema4C

to PLXNB2 likely involves receptor oligomerization as seen in other Plexin-Sema pairs (Pasterkamp, 2012). Receptor dimerization and oligomerization builds a network of reaction complex and facilitates downstream effectors recruitment or cross-talking with co-receptors, which have been reported to include GPCR, TGF receptor, Neuropilin and Plexin (Barton, Palacio, Iovine, & Berger, 2015; Bicknell & Vallee, 1988; George, O'Dowd, & Lee, 2002; Heinecke et al., 2009; Skorupa et al., 2012). Using immunofluorescence, we showed that both recombinant Sema4C and ANG increased puncta staining of PLXNB2 on cell surface, an indication of receptor oligomerization. It appears that Sema4C markedly intensifies each punctum while ANG stimulation increases the number of PLXNB2 puncta without affecting its intensity in each cell as compared to the PBS control. These data suggest that PLXNB2 reacts differently upon stimulations by ANG and Sema4C.

The second possible differentiator could be the co-receptor involved in PLXNB2 activation by ANG or Sem4C. Among the Plexin-B family protein, PLXNB1 has the most characterized signaling pathway. Its ligand Sema4D, besides activating Rac and Rho, also induces AKT and ERK activation. ErbB2 and c-Met are involved in Sema4D/PLXNB1 signaling as co-receptor and contribute to AKT and ERK activation. Alternatively, AKT and ERK can be indirectly activated through RhoA-induced contraction-mediated integrin activation (Basile, Gavard, & Gutkind, 2007). It has also been shown that c-Met serves as a co-receptor for Sema4C/PLXNB2 upon Sema4C stimulation (Le et al., 2015). Both GPCR and RTK initiate downstream AKT and ERK activation through the RAS pathway. The GPCR-PLC-PKC cascade has been shown to

activate IL-1β-induced AKT and ERK activation through RAS (Amin et al., 2003), However, GPCR-PLC-PKC does not seem to initiate the upstream cascade at least for the early ANG-dependent ERK signaling (30 min) in HUVE cells, because neomycin, an inhibitor of PLC, fails to suppress ANG-induced ERK activation (S Liu et al., 2001).

By examining the downstream signaling, for example, ERK activity, we can understand better how activated PLXNB2 interacts with its potential co-receptor or mediators. We showed that ANG induced 30% more ERK activation than Sema4C, but additional Sema4C in the presence of exogenous ANG abolished any ERK activation. Given the overlapping binding sites on PLXNB2, there could be two distinct modes of receptor activation by Sema4C and by ANG. In any given time, PLXNB2 only allows one dominant ligand binding. If this were true, additional Sema4C would inhibit ANG uptake by interfering with ANG-mediated PLXNB2 activation. However, we showed the opposite was true, that is, Sema4C facilitated ANG uptake and ANG-mediated tiRNA production in U251 in a dosage-dependent manner. An alternative hypothesis is that ERK activation is not directly related to PLXNB2 but to its co-receptor RTK, and then Sema4C would inhibit ANG-induced co-receptor activation without affecting PLXNB2 activation. If this was true, receptor activation-mediated ERK activation would be independent of ANG uptake. ERK and other downstream pathways would be activated by either ANG or Sema4C but through different co-receptors. In Sema4C-mediated PLXNB2 activation, c-Met has been shown to be co-activated (Le et al., 2015) while we showed that phosphorylation of c-Met was unchanged in response to ANG stimulation.

Thus, so far all the data is in agreement with our findings and the missing part would be to identify the co-receptor for ANG.

ANG in serum-culture cells and in GNS cells

In our *in vitro* studies, we primarily used U87 and U251 cells to interrogate intracellular signaling and function of ANG mainly because they are easy to culture. Genomic variations and altered gene expression that take place in GBM serum lines are concerns of the study, but we believe that based on the heterogeneous nature of GBM, there is hardly one model that can perfectly represent the original tumor. Therefore, the GBM serum line system provides a convenient platform for demonstrating the proof-of-concept in differentiated GBM cells. In my thesis study, I used a transgenic mouse model to corroborate the *in vitro* findings with cell lines. The relevance of those findings with human GBM needs to be confirmed with primary tissue culture and IHC in human biopsies.

Throughout the study, we have not examined the roles of ANG/PLXNB2 in GNS in details besides neurosphere formation, but it is a promising area considering our findings in the perivascular regions where GNS cells are tightly regulated by the microenvironment. ANG signaling seems more profound in GNS lines given their higher PLXNB2 expressions than those in serum lines. Knockdown of *ANG* or *PLXNB2* decreases the tumorigenic capability of GNS. However, this needs to be verified by xenograft experiments *in vivo*. ANG is very likely to regulate GNS stemness upstream of MMP-9/CD44/HIF2-α signaling if we can also demonstrate that ANG upregulates MMP-9 in GNS (Pietras et al., 2014). TGF-β signaling could be another hub through which

ANG modulate GNS stemness. First of all, ANG-dependent MMP-9 expression facilitates post-translation activation of TGF-β. Additionally, reduced *TGF-β* expression is found in *Ang* knockout tMEF. Thirdly, FOSL2, the mediator of the pro-invasive function of ANG, is involved in TGF-β signaling (Junfeng Wang et al., 2014), which is an important pathway maintaining GBM stemness (Peñuelas et al., 2009).

ANG and bevacizumab-resistant GBM

Bevacizumab inhibits excess VEGF activity in GBM and normalizes the rampant, dysfunctional brain vasculature of GBM patients. By normalizing the brain vasculature, bevacizumab reduces surgery- and tumor-related edema and thus improve patients' neurological conditions. However, because brain tumors tend to co-opt with vessel to invade and proliferate, it is possible that the normalized vessels, as a result of bevacizumab treatment, promotes tumor spread and invasion instead of local proliferation that usually end up with necrosis. My thesis study has found that ANG promotes CD24-mediated perivascular invasion of GBM. By inhibiting ANG activity in bevacizumab-treated GBM, we expect that tumor recurrence would be delayed and that patients survival extended.

In order to test whether targeting ANG could achieve a synergistic effect with anti-VEGF treatment, we could start i.p. injection of a combination of ANG inhibitor neomycin and a cross-species VEGF blocking antibody (Liang et al., 2006) shortly after tumor induction in the wild type mGBM. This experimental setup will allow us to compare ANG inhibitor head-to-head with VEGF inhibitor in treating GBM in the preclinical mGBM

model. The group receiving neomycin will show less perivascular invasion compared to the placebo, as we have shown in Figure 2.14.C. VEGF inhibition is expected to increase perivascular invasion (Baker et al., 2014). The combinational treatment will likely show a similar blockage of perivascular invasion as been shown in neomycin treatment, because neomycin will inhibit upregulated ANG upon VEGF inhibition. We expect that simultaneous inhibition of ANG and VEGF will result in a better overall survival than the two single-agent treatments. The rationale is that perivascularly invading GBM cells requires autocrine ANG signaling to: 1) maintain surface CD24 expression for interaction with P-selectin on endothelial cells, and 2) promote MMP-9 secretion that not only remodel perivascular ECM but also contribute to stemness of GNS cells at the niche through activating TGF-β and CD44 signaling. Thus, by inhibiting the alternative invasion pathway in anti-VEGF-resistant GBM, we would be able to achieve a significant survival extension.

PLXNB2 fragments and p120

The full-length PLXNB2 can be cleaved at a specific extracellular position to generate soluble fragment of p170, which can be detected in the conditioned medium. At the same time, a novel p120 was identified by our PLXNB2 monoclonal antibody in the conditioned medium. This fragment was also identified in another lab and was found to be the dominant PLXNB2 degradation product (Dr. Luca Tamagnone, personal communication). However, the exact identity and the amino acid sequence of p120 are unknown at present. The function of this fragment is interesting since it is present both extracellularly and intracellularly but exclusively in the nucleus. ANG stimulation

preferentially led to nuclear accumulation of p120. These data suggest that the intracellular p120 is likely to be the extracellular fragment of PLXNB2 that is responsible specifically for nuclear translocation of ANG. However, we do not know whether the production of p120 PLXNB2 happens intracellularly after ANG is endocytosed or extracellularly where it forms complex with free ANG in solution and then enter nucleus with ANG. Although we showed that p170 enhanced ANG uptake in U251 cells, how p120 might regulate this process is unknown. Other open questions are: 1) how the production of p120 is regulated. Both p120 and p170 could be the products of ectodomain shedding from PLXNB2, which is a conserved mechanism found in many surface proteins (Hayashida et al., 2010), and 2) what is the biological implication of p120 under physiological and pathological conditions. It seems that the extracellular function of p120 could be redundant to that of p170, but the existence of nuclear p120 suggests that it is p120, not p170, that could re-enter the cell.

One unsettled question about p120 is whether it is really derived from PLXNB2. Both our in-house PLXNB2 monoclonal antibody (recognizing extracellular ANG binding domain) and a commercial PLXNB2 monoclonal antibody can detect human p120 in WB. But only the in-house antibody recognized p170/p240 PLXNB2. If p120 is a degradation product of p170, the commercial antibody should have no problem detecting p170 given its ability to detect p120. Future studies with the help of mass spectrometry will identify what p120 is and how it is generated.

Conclusion

Overall, this thesis study presents:

1) Confirmation of known function of ANG in promoting angiogenesis, rRNA transcription, anti-apoptosis, and invasion with a GBM mouse model.
2) ANG is required for perivascular invasion of GBM through activation of FOSL2, a novel mediator of ANG and its downstream effectors CD24 and MMP-9.
3) Treating mGBM with ANG inhibitor effectively reduces perivascular invasion and extends survival.
4) Sema4C and sPb2 can facilitate cellular uptake of ANG.
5) New regulatory mechanism of ANG-mediated tiRNA production.
6) A novel relationship between ANG-induced AKT and ERK signaling.
7) A proposed model: p53-independent regulation of Bcl-2 by ANG.

References

Agarwal, S., Manchanda, P., Vogelbaum, M. A., Ohlfest, J. R., & Elmquist, W. F. (2013). Function of the blood-brain barrier and restriction of drug delivery to invasive glioma cells: findings in an orthotopic rat xenograft model of glioma. *Drug Metabolism and Disposition: the Biological Fate of Chemicals*, *41*(1), 33–39. http://doi.org/10.1124/dmd.112.048322

Aigner, S., Ramos, C. L., Hafezi-Moghadam, A., Lawrence, M. B., Friederichs, J., Altevogt, P., & Ley, K. (1998). CD24 mediates rolling of breast carcinoma cells on P-selectin. *The FASEB Journal : Official Publication of the Federation of American Societies for Experimental Biology*, *12*(12), 1241–1251.

Aigner, S., Sthoeger, Z. M., Fogel, M., Weber, E., Zarn, J., Ruppert, M., et al. (1997). CD24, a mucin-type glycoprotein, is a ligand for P-selectin on human tumor cells. *Blood*, *89*(9), 3385–3395.

Alcantara Llaguno, S., Chen, J., Kwon, C.-H., Jackson, E. L., Li, Y., Burns, D. K., et al. (2009). Malignant astrocytomas originate from neural stem/progenitor cells in a somatic tumor suppressor mouse model. *Cancer Cell*, *15*(1), 45–56. http://doi.org/10.1016/j.ccr.2008.12.006

Alimonti, A., Satta, F., Pavese, I., Burattini, E., Zoffoli, V., & Vecchione, A. (2003). Prevention of irinotecan plus 5-fluorouracil/leucovorin-induced diarrhoea by oral administration of neomycin plus bacitracin in first-line treatment of advanced colorectal cancer. *Annals of Oncology : Official Journal of the European Society for Medical Oncology / ESMO*, *14*(5), 805–806.

Amin, A. R. M. R., Ichigotani, Y., Oo, M. L., Biswas, M. H. U., Yuan, H., Huang, P., et al. (2003). The PLC-PKC cascade is required for IL-1beta-dependent Erk and Akt activation: their role in proliferation. *International Journal of Oncology*, *23*(6), 1727–1731.

Anand, M., Meter, T. E., & Fillmore, H. L. (2011). Epidermal growth factor induces matrix metalloproteinase-1 (MMP-1) expression and invasion in glioma cell lines via the MAPK pathway. *Journal of Neuro-Oncology*, *104*(3), 679–687. http://doi.org/10.1007/s11060-011-0549-x

Anderson, P., & Kedersha, N. (2009). Stress granules. *Current Biology : CB*, *19*(10), R397–8. http://doi.org/10.1016/j.cub.2009.03.013

Ang, J., Sheng, J., Lai, K., Wei, S., & Gao, X. (2013). Identification of estrogen receptor-related receptor gamma as a direct transcriptional target of angiogenin. *PLoS ONE*, *8*(8), e71487. http://doi.org/10.1371/journal.pone.0071487

Araki, K., Shimura, T., Suzuki, H., Tsutsumi, S., Wada, W., Yajima, T., et al. (2011). E/N-cadherin switch mediates cancer progression via TGF-β-induced epithelial-to-mesenchymal transition in extrahepatic cholangiocarcinoma. *British Journal of Cancer*, *105*(12), 1885–1893. http://doi.org/10.1038/bjc.2011.452

Artigiani, S., Barberis, D., Fazzari, P., Longati, P., Angelini, P., van de Loo, J.-W., et al. (2003). Functional regulation of semaphorin receptors by proprotein convertases. *The Journal of Biological Chemistry*, *278*(12), 10094–10101. http://doi.org/10.1074/jbc.M210156200

Asuthkar, S., Velpula, K. K., Chetty, C., Gorantla, B., & Rao, J. S. (2012). Epigenetic regulation of miRNA-211 by MMP-9 governs glioma cell apoptosis,

chemosensitivity and radiosensitivity. *Oncotarget*, *3*(11), 1439–1454.
Attwell, S., Roskelley, C., & Dedhar, S. (2000). The integrin-linked kinase (ILK) suppresses anoikis. *Oncogene*, *19*(33), 3811–3815. http://doi.org/10.1038/sj.onc.1203711
Awasthi, R., Pandey, C. M., Sahoo, P., Behari, S., Kumar, V., Kumar, S., et al. (2012). Dynamic contrast-enhanced magnetic resonance imaging-derived kep as a potential biomarker of matrix metalloproteinase 9 expression in patients with glioblastoma multiforme: a pilot study. *Journal of Computer Assisted Tomography*, *36*(1), 125–130. http://doi.org/10.1097/RCT.0b013e31823f6c59
Azzarelli, R., Pacary, E., Garg, R., Garcez, P., van den Berg, D., Riou, P., et al. (2014). An antagonistic interaction between PlexinB2 and Rnd3 controls RhoA activity and cortical neuron migration. *Nature Communications*, *5*, 3405. http://doi.org/10.1038/ncomms4405
Badet, J., Soncin, F., Guitton, J. D., Lamare, O., Cartwright, T., & Barritault, D. (1989). Specific binding of angiogenin to calf pulmonary artery endothelial cells. *Proceedings of the National Academy of Sciences of the United States of America*, *86*(21), 8427–8431.
Bady, P., Sciuscio, D., Diserens, A.-C., Bloch, J., van den Bent, M. J., Marosi, C., et al. (2012). MGMT methylation analysis of glioblastoma on the Infinium methylation BeadChip identifies two distinct CpG regions associated with gene silencing and outcome, yielding a prediction model for comparisons across datasets, tumor grades, and CIMP-status. *Acta Neuropathologica*, *124*(4), 547–560. http://doi.org/10.1007/s00401-012-1016-2
Bagci, T., Wu, J. K., Pfannl, R., Ilag, L. L., & Jay, D. G. (2009). Autocrine semaphorin 3A signaling promotes glioblastoma dispersal. *Oncogene*, *28*(40), 3537–3550. http://doi.org/10.1038/onc.2009.204
Baker, G. J., Yadav, V. N., Motsch, S., Koschmann, C., Calinescu, A.-A., Mineharu, Y., et al. (2014). Mechanisms of glioma formation: iterative perivascular glioma growth and invasion leads to tumor progression, VEGF-independent vascularization, and resistance to antiangiogenic therapy. *Neoplasia (New York, N.Y.)*, *16*(7), 543–561. http://doi.org/10.1016/j.neo.2014.06.003
Bao, S., Wu, Q., Li, Z., Sathornsumetee, S., Wang, H., Mclendon, R. E., et al. (2008). Targeting cancer stem cells through L1CAM suppresses glioma growth. *Cancer Research*, *68*(15), 6043–6048. http://doi.org/10.1158/0008-5472.CAN-08-1079
Bao, S., Wu, Q., Mclendon, R. E., Hao, Y., Shi, Q., Hjelmeland, A. B., et al. (2006). Glioma stem cells promote radioresistance by preferential activation of the DNA damage response. *Nature*, *444*(7120), 756–760. http://doi.org/10.1038/nature05236
Barker, F. G., Davis, R. L., Chang, S. M., & Prados, M. D. (1996). Necrosis as a prognostic factor in glioblastoma multiforme. *Cancer*, *77*(6), 1161–1166.
Barton, R., Palacio, D., Iovine, M. K., & Berger, B. W. (2015). A cytosolic juxtamembrane interface modulates plexin A3 oligomerization and signal transduction. *PLoS ONE*, *10*(1), e0116368. http://doi.org/10.1371/journal.pone.0116368
Basile, J. R., Gavard, J., & Gutkind, J. S. (2007). Plexin-B1 utilizes RhoA and Rho kinase to promote the integrin-dependent activation of Akt and ERK and endothelial cell motility. *The Journal of Biological Chemistry*, *282*(48), 34888–34895.

http://doi.org/10.1074/jbc.M705467200
Bárcena, C., Stefanovic, M., Tutusaus, A., Martinez-Nieto, G. A., Martinez, L., García-Ruiz, C., et al. (2015). Angiogenin secretion from hepatoma cells activates hepatic stellate cells to amplify a self-sustained cycle promoting liver cancer. *Scientific Reports*, *5*, 7916. http://doi.org/10.1038/srep07916
Beadle, C., Assanah, M. C., Monzo, P., Vallee, R., Rosenfeld, S. S., & Canoll, P. (2008). The role of myosin II in glioma invasion of the brain. *Molecular Biology of the Cell*, *19*(8), 3357–3368. http://doi.org/10.1091/mbc.E08-03-0319
Bekhite, M. M., Finkensieper, A., Binas, S., Müller, J., Wetzker, R., Figulla, H.-R., et al. (2011). VEGF-mediated PI3K class IA and PKC signaling in cardiomyogenesis and vasculogenesis of mouse embryonic stem cells. *Journal of Cell Science*, *124*(Pt 11), 1819–1830. http://doi.org/10.1242/jcs.077594
Bergers, G., & Benjamin, L. E. (2003). Tumorigenesis and the angiogenic switch. *Nature Reviews Cancer*, *3*(6), 401–410. http://doi.org/10.1038/nrc1093
Bhat, K. P. L., Balasubramaniyan, V., Vaillant, B., Ezhilarasan, R., Hummelink, K., Hollingsworth, F., et al. (2013). Mesenchymal differentiation mediated by NF-κB promotes radiation resistance in glioblastoma. *Cancer Cell*, *24*(3), 331–346. http://doi.org/10.1016/j.ccr.2013.08.001
Bhat, K. P. L., Salazar, K. L., Balasubramaniyan, V., Wani, K., Heathcock, L., Hollingsworth, F., et al. (2011). The transcriptional coactivator TAZ regulates mesenchymal differentiation in malignant glioma. *Genes & Development*, *25*(24), 2594–2609. http://doi.org/10.1101/gad.176800.111
Bicknell, R., & Vallee, B. L. (1988). Angiogenin activates endothelial cell phospholipase C. *Proceedings of the National Academy of Sciences of the United States of America*, *85*(16), 5961–5965.
Bicknell, R., & Vallee, B. L. (1989). Angiogenin stimulates endothelial cell prostacyclin secretion by activation of phospholipase A2. *Proceedings of the National Academy of Sciences of the United States of America*, *86*(5), 1573–1577.
Birlik, B., Canda, S., & Ozer, E. (2006). Tumour vascularity is of prognostic significance in adult, but not paediatric astrocytomas. *Neuropathology and Applied Neurobiology*, *32*(5), 532–538. http://doi.org/10.1111/j.1365-2990.2006.00763.x
Bjerke, L., Mackay, A., Nandhabalan, M., Burford, A., Jury, A., Popov, S., et al. (2013). Histone H3.3. mutations drive pediatric glioblastoma through upregulation of MYCN. *Cancer Discovery*, *3*(5), 512–519. http://doi.org/10.1158/2159-8290.CD-12-0426
Bleau, A.-M., Hambardzumyan, D., Ozawa, T., Fomchenko, E. I., Huse, J. T., Brennan, C. W., & Holland, E. C. (2009). PTEN/PI3K/Akt Pathway Regulates the Side Population Phenotype and ABCG2 Activity in Glioma Tumor Stem-like Cells. *Cell Stem Cell*, *4*(3), 226–235. http://doi.org/10.1016/j.stem.2009.01.007
Bonfoco, E., Chen, W., Paul, R., Cheresh, D. A., & Cooper, N. R. (2000). beta1 integrin antagonism on adherent, differentiated human neuroblastoma cells triggers an apoptotic signaling pathway. *Neuroscience*, *101*(4), 1145–1152.
Bonnal, S., Schaeffer, C., Créancier, L., Clamens, S., Moine, H., Prats, A.-C., & Vagner, S. (2003). A single internal ribosome entry site containing a G quartet RNA structure drives fibroblast growth factor 2 gene expression at four alternative translation initiation codons. *The Journal of Biological Chemistry*, *278*(41), 39330–39336.

http://doi.org/10.1074/jbc.M305580200
Brennan, C. W., Verhaak, R. G. W., McKenna, A., Campos, B., Noushmehr, H., Salama, S. R., et al. (2013). The somatic genomic landscape of glioblastoma. *Cell*, *155*(2), 462–477. http://doi.org/10.1016/j.cell.2013.09.034
Bunz, F., Hwang, P. M., Torrance, C., Waldman, T., Zhang, Y., Dillehay, L., et al. (1999). Disruption of p53 in human cancer cells alters the responses to therapeutic agents. *The Journal of Clinical Investigation*, *104*(3), 263–269. http://doi.org/10.1172/JCI6863
Calabrese, C., Poppleton, H., Kocak, M., Hogg, T. L., Fuller, C., Hamner, B., et al. (2007). A perivascular niche for brain tumor stem cells. *Cancer Cell*, *11*(1), 69–82. http://doi.org/10.1016/j.ccr.2006.11.020
Calaora, V., Chazal, G., Nielsen, P. J., Rougon, G., & Moreau, H. (1996). mCD24 expression in the developing mouse brain and in zones of secondary neurogenesis in the adult. *Neuroscience*, *73*(2), 581–594.
Cancer Genome Atlas Research Network. (2008). Comprehensive genomic characterization defines human glioblastoma genes and core pathways. *Nature*, *455*(7216), 1061–1068. http://doi.org/10.1038/nature07385
Cancer Genome Atlas Research Network, Genome Characterization Center, Chang, K., Creighton, C. J., Davis, C., Donehower, L., et al. (2013). The Cancer Genome Atlas Pan-Cancer analysis project. *Nature Genetics*, *45*(10), 1113–1120. http://doi.org/10.1038/ng.2764
Carlson, B. L., Pokorny, J. L., Schroeder, M. A., & Sarkaria, J. N. (2011). Establishment, maintenance and in vitro and in vivo applications of primary human glioblastoma multiforme (GBM) xenograft models for translational biology studies and drug discovery. *Current Protocols in Pharmacology / Editorial Board, S.J. Enna (Editor-in-Chief) ... [Et Al.]*, *Chapter 14*, Unit 14.16. http://doi.org/10.1002/0471141755.ph1416s52
Carro, M. S., Lim, W. K., Alvarez, M. J., Bollo, R. J., Zhao, X., Snyder, E. Y., et al. (2010). The transcriptional network for mesenchymal transformation of brain tumours. *Nature*, *463*(7279), 318–325. http://doi.org/10.1038/nature08712
Chen, X.-G., Liu, F., Song, X.-F., Wang, Z.-H., Dong, Z.-Q., Hu, Z.-Q., et al. (2010). Rapamycin regulates Akt and ERK phosphorylation through mTORC1 and mTORC2 signaling pathways. *Molecular Carcinogenesis*, *49*(6), 603–610. http://doi.org/10.1002/mc.20628
Cheng, E. H., Wei, M. C., Weiler, S., Flavell, R. A., Mak, T. W., Lindsten, T., & Korsmeyer, S. J. (2001). BCL-2, BCL-X(L) sequester BH3 domain-only molecules preventing BAX- and BAK-mediated mitochondrial apoptosis. *Molecular Cell*, *8*(3), 705–711.
Cheng, L., Huang, Z., Zhou, W., Wu, Q., Donnola, S., Liu, J. K., et al. (2013). Glioblastoma Stem Cells Generate Vascular Pericytes to Support Vessel Function and Tumor Growth. *Cell*, *153*(1), 139–152. http://doi.org/10.1016/j.cell.2013.02.021
Chetty, C., Vanamala, S. K., Gondi, C. S., Dinh, D. H., Gujrati, M., & Rao, J. S. (2012). MMP-9 induces CD44 cleavage and CD44 mediated cell migration in glioblastoma xenograft cells. *Cellular Signalling*, *24*(2), 549–559. http://doi.org/10.1016/j.cellsig.2011.10.008
Chida, K., Nagamori, S., & Kuroki, T. (1999). Nuclear translocation of Fos is stimulated

by interaction with Jun through the leucine zipper. *Cellular and Molecular Life Sciences : CMLS*, *55*(2), 297–302.

Chinot, O. L., Wick, W., Mason, W., Henriksson, R., Saran, F., Nishikawa, R., et al. (2014). Bevacizumab plus radiotherapy-temozolomide for newly diagnosed glioblastoma. *The New England Journal of Medicine*, *370*(8), 709–722. http://doi.org/10.1056/NEJMoa1308345

Clark, A. J., Lamborn, K. R., Butowski, N. A., Chang, S. M., Prados, M. D., Clarke, J. L., et al. (2012a). Neurosurgical management and prognosis of patients with glioblastoma that progresses during bevacizumab treatment. *Neurosurgery*, *70*(2), 361–370. http://doi.org/10.1227/NEU.0b013e3182314f9d

Clark, P. A., Iida, M., Treisman, D. M., Kalluri, H., Ezhilan, S., Zorniak, M., et al. (2012b). Activation of multiple ERBB family receptors mediates glioblastoma cancer stem-like cell resistance to EGFR-targeted inhibition. *Neoplasia (New York, N.Y.)*, *14*(5), 420–428.

Cloughesy, T. F., Cavenee, W. K., & Mischel, P. S. (2014). Glioblastoma: from molecular pathology to targeted treatment. *Annual Review of Pathology*, *9*, 1–25. http://doi.org/10.1146/annurev-pathol-011110-130324

Coldwell, M. J., deSchoolmeester, M. L., Fraser, G. A., Pickering, B. M., Packham, G., & Willis, A. E. (2001). The p36 isoform of BAG-1 is translated by internal ribosome entry following heat shock. *Oncogene*, *20*(30), 4095–4100. http://doi.org/10.1038/sj.onc.1204547

Coltrini, D., Di Salle, E., Ronca, R., Belleri, M., Testini, C., & Presta, M. (2013). Matrigel plug assay: evaluation of the angiogenic response by reverse transcription-quantitative PCR. *Angiogenesis*, *16*(2), 469–477. http://doi.org/10.1007/s10456-012-9324-7

Cooper, L. A. D., Gutman, D. A., Chisolm, C., Appin, C., Kong, J., Rong, Y., et al. (2012). The tumor microenvironment strongly impacts master transcriptional regulators and gene expression class of glioblastoma. *The American Journal of Pathology*, *180*(5), 2108–2119. http://doi.org/10.1016/j.ajpath.2012.01.040

Cuddapah, V. A., Robel, S., Watkins, S., & Sontheimer, H. (2014a). A neurocentric perspective on glioma invasion. *Nature Reviews Neuroscience*, *15*(7), 455–465. http://doi.org/doi:10.1038/nrn3765

Cuddapah, V. A., Robel, S., Watkins, S., & Sontheimer, H. (2014b). A neurocentric perspective on glioma invasion. *Nature Reviews Neuroscience*, *15*(7), 455–465. http://doi.org/10.1038/nrn3765

Cuddapah, V. A., Turner, K. L., Seifert, S., & Sontheimer, H. (2013). Bradykinin-induced chemotaxis of human gliomas requires the activation of KCa3.1 and ClC-3. *The Journal of Neuroscience : the Official Journal of the Society for Neuroscience*, *33*(4), 1427–1440. http://doi.org/10.1523/JNEUROSCI.3980-12.2013

Cuevas, P., Diaz-González, D., & Dujovny, M. (2003). Antiproliferative action of neomycin is associated with inhibition of cyclin D1 activation in glioma cells. *Neurological Research*, *25*(7), 691–693. http://doi.org/10.1179/016164103101202165

Cuevas, P., Diaz-González, D., & Dujovny, M. (2004a). Differentiation-inducing activity of neomycin in cultured rat glioma cells. *Neurological Research*, *26*(4), 401–403. http://doi.org/10.1179/016164104225016317

Cuevas, P., Diaz-González, D., & Dujovny, M. (2004b). Neomycin inhibits glioma cell migration. *Neurological Research*, *26*(3), 273–275. http://doi.org/10.1179/016164104225013941

Das, G., Shiras, A., Shanmuganandam, K., & Shastry, P. (2011). Rictor regulates MMP-9 activity and invasion through Raf-1-MEK-ERK signaling pathway in glioma cells. *Molecular Carcinogenesis*, *50*(6), 412–423. http://doi.org/10.1002/mc.20723

David, J. P., Rincon, M., Neff, L., Horne, W. C., & Baron, R. (2001). Carbonic anhydrase II is an AP-1 target gene in osteoclasts. *Journal of Cellular Physiology*, *188*(1), 89–97. http://doi.org/10.1002/jcp.1099

de Groot, J. F., Fuller, G., Kumar, A. J., Piao, Y., Eterovic, K., Ji, Y., & Conrad, C. A. (2010). Tumor invasion after treatment of glioblastoma with bevacizumab: radiographic and pathologic correlation in humans and mice. *Neuro-Oncology*, *12*(3), 233–242. http://doi.org/10.1093/neuonc/nop027

de Vries, H. E., Kuiper, J., de Boer, A. G., Van Berkel, T. J., & Breimer, D. D. (1997). The blood-brain barrier in neuroinflammatory diseases. *Pharmacological Reviews*, *49*(2), 143–155.

Del Duca, D., Werbowetski, T., & Del Maestro, R. F. (2004). Spheroid preparation from hanging drops: characterization of a model of brain tumor invasion. *Journal of Neuro-Oncology*, *67*(3), 295–303.

Deng, J., Gao, G., Wang, L., Wang, T., Yu, J., & Zhao, Z. (2012). CD24 expression as a marker for predicting clinical outcome in human gliomas. *Journal of Biomedicine & Biotechnology*, *2012*, 517172. http://doi.org/10.1155/2012/517172

Deng, S., Hirschberg, A., Worzfeld, T., Penachioni, J. Y., Korostylev, A., Swiercz, J. M., et al. (2007). Plexin-B2, but not Plexin-B1, critically modulates neuronal migration and patterning of the developing nervous system in vivo. *The Journal of Neuroscience : the Official Journal of the Society for Neuroscience*, *27*(23), 6333–6347. http://doi.org/10.1523/JNEUROSCI.5381-06.2007

Ding, L., Wang, Z., Yan, J., Yang, X., Liu, A., Qiu, W., et al. (2009). Human four-and-a-half LIM family members suppress tumor cell growth through a TGF-beta-like signaling pathway. *The Journal of Clinical Investigation*, *119*(2), 349–361. http://doi.org/10.1172/JCI35930

Du, R., Petritsch, C., Lu, K., Liu, P., Haller, A., Ganss, R., et al. (2008). Matrix metalloproteinase-2 regulates vascular patterning and growth affecting tumor cell survival and invasion in GBM. *Neuro-Oncology*, *10*(3), 254–264. http://doi.org/10.1215/15228517-2008-001

Dudani, A. K., & Ganz, P. R. (1996). Endothelial cell surface actin serves as a binding site for plasminogen, tissue plasminogen activator and lipoprotein(a). *British Journal of Haematology*, *95*(1), 168–178.

Dunn, G. P., Rinne, M. L., Wykosky, J., Genovese, G., Quayle, S. N., Dunn, I. F., et al. (2012). Emerging insights into the molecular and cellular basis of glioblastoma. *Genes & Development*, *26*(8), 756–784. http://doi.org/10.1101/gad.187922.112

Dutta, S., Bandyopadhyay, C., Bottero, V., Veettil, M. V., Wilson, L., Pins, M. R., et al. (2014). Angiogenin interacts with the plasminogen activation system at the cell surface of breast cancer cells to regulate plasmin formation and cell migration. *Molecular Oncology*, *8*(3), 483–507. http://doi.org/10.1016/j.molonc.2013.12.017

Eberle, K., Oberpichler, A., Trantakis, C., Krupp, W., Knüpfer, M., Tschesche, H., &

Seifert, V. (2000). The expression of angiogenin in tissue samples of different brain tumours and cultured glioma cells. *Anticancer Research*, *20*(3A), 1679–1684.
Eden, A., Gaudet, F., Waghmare, A., & Jaenisch, R. (2003). Chromosomal instability and tumors promoted by DNA hypomethylation. *Science (New York, NY)*, *300*(5618), 455. http://doi.org/10.1126/science.1083557
Emara, M. M., Ivanov, P., Hickman, T., Dawra, N., Tisdale, S., Kedersha, N., et al. (2010). Angiogenin-induced tRNA-derived stress-induced RNAs promote stress-induced stress granule assembly. *The Journal of Biological Chemistry*, *285*(14), 10959–10968. http://doi.org/10.1074/jbc.M109.077560
Evans, S. M., Judy, K. D., Dunphy, I., Jenkins, W. T., Hwang, W.-T., Nelson, P. T., et al. (2004). Hypoxia is important in the biology and aggression of human glial brain tumors. *Clinical Cancer Research : an Official Journal of the American Association for Cancer Research*, *10*(24), 8177–8184. http://doi.org/10.1158/1078-0432.CCR-04-1081
Fang, F., Orend, G., Watanabe, N., Hunter, T., & Ruoslahti, E. (1996). Dependence of cyclin E-CDK2 kinase activity on cell anchorage. *Science (New York, NY)*, *271*(5248), 499–502.
Fang, X., Zheng, P., Tang, J., & Liu, Y. (2010). CD24: from A to Z. *Cellular & Molecular Immunology*, *7*(2), 100–103. http://doi.org/10.1038/cmi.2009.119
Farin, A., Suzuki, S. O., Weiker, M., Goldman, J. E., Bruce, J. N., & Canoll, P. (2006). Transplanted glioma cells migrate and proliferate on host brain vasculature: a dynamic analysis. *Glia*, *53*(8), 799–808. http://doi.org/10.1002/glia.20334
Fears, C. Y., & Woods, A. (2006). The role of syndecans in disease and wound healing. *Matrix Biology : Journal of the International Society for Matrix Biology*, *25*(7), 443–456. http://doi.org/10.1016/j.matbio.2006.07.003
Fett, J. W., Olson, K. A., & Rybak, S. M. (1994). A monoclonal antibody to human angiogenin. Inhibition of ribonucleolytic and angiogenic activities and localization of the antigenic epitope. *Biochemistry*, *33*(18), 5421–5427.
Fett, J. W., Strydom, D. J., Lobb, R. R., Alderman, E. M., Bethune, J. L., Riordan, J. F., & Vallee, B. L. (1985). Isolation and characterization of angiogenin, an angiogenic protein from human carcinoma cells. *Biochemistry*, *24*(20), 5480–5486.
Folkman, J. (1971). Tumor angiogenesis: therapeutic implications. *The New England Journal of Medicine*, *285*(21), 1182–1186. http://doi.org/10.1056/NEJM197111182852108
Folkman, J., & Hochberg, M. (1973). Self-regulation of growth in three dimensions. *The Journal of Experimental Medicine*, *138*(4), 745–753.
Fontemaggi, G., Gurtner, A., Strano, S., Higashi, Y., Sacchi, A., Piaggio, G., & Blandino, G. (2001). The transcriptional repressor ZEB regulates p73 expression at the crossroad between proliferation and differentiation. *Molecular and Cellular Biology*, *21*(24), 8461–8470. http://doi.org/10.1128/MCB.21.24.8461-8470.2001
Forsyth, P. A., Wong, H., Laing, T. D., Rewcastle, N. B., Morris, D. G., Muzik, H., et al. (1999). Gelatinase-A (MMP-2), gelatinase-B (MMP-9) and membrane type matrix metalloproteinase-1 (MT1-MMP) are involved in different aspects of the pathophysiology of malignant gliomas. *British Journal of Cancer*, *79*(11-12), 1828–1835. http://doi.org/10.1038/sj.bjc.6690291
Freije, W. A., Castro-Vargas, F. E., Fang, Z., Horvath, S., Cloughesy, T., Liau, L. M., et

al. (2004). Gene expression profiling of gliomas strongly predicts survival. *Cancer Research*, *64*(18), 6503–6510. http://doi.org/10.1158/0008-5472.CAN-04-0452

Friedman, H. S., Prados, M. D., Wen, P. Y., Mikkelsen, T., Schiff, D., Abrey, L. E., et al. (2009). Bevacizumab alone and in combination with irinotecan in recurrent glioblastoma. *Journal of Clinical Oncology : Official Journal of the American Society of Clinical Oncology*, *27*(28), 4733–4740. http://doi.org/10.1200/JCO.2008.19.8721

Friedmann-Morvinski, D., Bushong, E. A., Ke, E., Soda, Y., Marumoto, T., Singer, O., et al. (2012). Dedifferentiation of neurons and astrocytes by oncogenes can induce gliomas in mice. *Science (New York, NY)*, *338*(6110), 1080–1084. http://doi.org/10.1126/science.1226929

Frisch, S. M., & Ruoslahti, E. (1997). Integrins and anoikis. *Current Opinion in Cell Biology*, *9*(5), 701–706.

Frisch, S. M., Schaller, M., & Cieply, B. (2013). Mechanisms that link the oncogenic epithelial-mesenchymal transition to suppression of anoikis. *Journal of Cell Science*, *126*(Pt 1), 21–29. http://doi.org/10.1242/jcs.120907

Frisch, S. M., Vuori, K., Kelaita, D., & Sicks, S. (1996a). A role for Jun-N-terminal kinase in anoikis; suppression by bcl-2 and crmA. *The Journal of Cell Biology*, *135*(5), 1377–1382.

Frisch, S. M., Vuori, K., Ruoslahti, E., & Chan-Hui, P. Y. (1996b). Control of adhesion-dependent cell survival by focal adhesion kinase. *The Journal of Cell Biology*, *134*(3), 793–799.

Fu, H., Feng, J., Liu, Q., Sun, F., Tie, Y., Zhu, J., et al. (2009). Stress induces tRNA cleavage by angiogenin in mammalian cells. *FEBS Letters*, *583*(2), 437–442. http://doi.org/10.1016/j.febslet.2008.12.043

Fu, Z., & Tindall, D. J. (2008). FOXOs, cancer and regulation of apoptosis. *Oncogene*, *27*(16), 2312–2319. http://doi.org/10.1038/onc.2008.24

Galli, R., Binda, E., Orfanelli, U., Cipelletti, B., Gritti, A., De Vitis, S., et al. (2004). Isolation and characterization of tumorigenic, stem-like neural precursors from human glioblastoma. *Cancer Research*, *64*(19), 7011–7021. http://doi.org/10.1158/0008-5472.CAN-04-1364

Gan, H. K., Cvrljevic, A. N., & Johns, T. G. (2013). The epidermal growth factor receptor variant III (EGFRvIII): where wild things are altered. *The FEBS Journal*, *280*(21), 5350–5370. http://doi.org/10.1111/febs.12393

Gan, H. K., Kaye, A. H., & Luwor, R. B. (2009). The EGFRvIII variant in glioblastoma multiforme. *Journal of Clinical Neuroscience : Official Journal of the Neurosurgical Society of Australasia*, *16*(6), 748–754. http://doi.org/10.1016/j.jocn.2008.12.005

Gao, J.-Q., Lv, Q., Li, L.-M., Tang, X.-J., Li, F.-Z., Hu, Y.-L., & Han, M. (2013). Glioma targeting and blood-brain barrier penetration by dual-targeting doxorubincin liposomes. *Biomaterials*, *34*(22), 5628–5639. http://doi.org/10.1016/j.biomaterials.2013.03.097

Gartel, A. L., & Tyner, A. L. (2002). The role of the cyclin-dependent kinase inhibitor p21 in apoptosis. *Molecular Cancer Therapeutics*, *1*(8), 639–649.

Gauger, K. J., Chenausky, K. L., Murray, M. E., & Schneider, S. S. (2011). SFRP1 reduction results in an increased sensitivity to TGF-β signaling. *BMC Cancer*, *11*, 59. http://doi.org/10.1186/1471-2407-11-59

George, S. R., O'Dowd, B. F., & Lee, S. P. (2002). G-protein-coupled receptor oligomerization and its potential for drug discovery. *Nature Reviews. Drug Discovery*, *1*(10), 808–820. http://doi.org/10.1038/nrd913

Gesty-Palmer, D., Chen, M., Reiter, E., Ahn, S., Nelson, C. D., Wang, S., et al. (2006). Distinct beta-arrestin- and G protein-dependent pathways for parathyroid hormone receptor-stimulated ERK1/2 activation. *The Journal of Biological Chemistry*, *281*(16), 10856–10864. http://doi.org/10.1074/jbc.M513380200

Gilley, J. (2003). FOXO transcription factors directly activate bim gene expression and promote apoptosis in sympathetic neurons. *The Journal of Cell Biology*, *162*(4), 613–622. http://doi.org/10.1083/jcb.200303026

Giordano, S., Corso, S., Conrotto, P., Artigiani, S., Gilestro, G., Barberis, D., et al. (2002). The semaphorin 4D receptor controls invasive growth by coupling with Met. *Nature Cell Biology*, *4*(9), 720–724. http://doi.org/10.1038/ncb843

Giraud, S., Greco, A., Brink, M., Diaz, J. J., & Delafontaine, P. (2001). Translation initiation of the insulin-like growth factor I receptor mRNA is mediated by an internal ribosome entry site. *The Journal of Biological Chemistry*, *276*(8), 5668–5675. http://doi.org/10.1074/jbc.M005928200

Goldman, S. A., & Chen, Z. (2011). Perivascular instruction of cell genesis and fate in the adult brain. *Nature Neuroscience*, *14*(11), 1382–1389. http://doi.org/10.1038/nn.2963

Graber, T. E., Baird, S. D., Kao, P. N., Mathews, M. B., & Holcik, M. (2010). NF45 functions as an IRES trans-acting factor that is required for translation of cIAP1 during the unfolded protein response. *Cell Death and Differentiation*, *17*(4), 719–729. http://doi.org/10.1038/cdd.2009.164

Grandal, M. V., Zandi, R., Pedersen, M. W., Willumsen, B. M., van Deurs, B., & Poulsen, H. S. (2007). EGFRvIII escapes down-regulation due to impaired internalization and sorting to lysosomes. *Carcinogenesis*, *28*(7), 1408–1417. http://doi.org/10.1093/carcin/bgm058

Greenway, M. J., Andersen, P. M., Russ, C., Ennis, S., Cashman, S., Donaghy, C., et al. (2006). ANG mutations segregate with familial and “sporadic” amyotrophic lateral sclerosis. *Nature Genetics*, *38*(4), 411–413. http://doi.org/10.1038/ng1742

Gritsenko, P. G., Ilina, O., & Friedl, P. (2012). Interstitial guidance of cancer invasion. *The Journal of Pathology*, *226*(2), 185–199. http://doi.org/10.1002/path.3031

Gruda, M. C., Kovary, K., Metz, R., & Bravo, R. (1994). Regulation of Fra-1 and Fra-2 phosphorylation differs during the cell cycle of fibroblasts and phosphorylation in vitro by MAP kinase affects DNA binding activity. *Oncogene*, *9*(9), 2537–2547.

Guadamillas, M. C., Cerezo, A., & Del Pozo, M. A. (2011). Overcoming anoikis--pathways to anchorage-independent growth in cancer. *Journal of Cell Science*, *124*(Pt 19), 3189–3197. http://doi.org/10.1242/jcs.072165

Hallahan, T. W., Shapiro, R., & Vallee, B. L. (1991). Dual site model for the organogenic activity of angiogenin. *Proceedings of the National Academy of Sciences of the United States of America*, *88*(6), 2222–2226.

Hambardzumyan, D., Amankulor, N. M., Helmy, K. Y., Becher, O. J., & Holland, E. C. (2009). Modeling Adult Gliomas Using RCAS/t-va Technology. *Translational Oncology*, *2*(2), 89–95.

Hamerlik, P., Lathia, J. D., Rasmussen, R., Wu, Q., Bartkova, J., Lee, M., et al. (2012).

Autocrine VEGF-VEGFR2-Neuropilin-1 signaling promotes glioma stem-like cell viability and tumor growth. *The Journal of Experimental Medicine*, *209*(3), 507–520. http://doi.org/10.1084/jem.20111424

Hartmann, A., Kunz, M., Köstlin, S., Gillitzer, R., Toksoy, A., Bröcker, E. B., & Klein, C. E. (1999). Hypoxia-induced up-regulation of angiogenin in human malignant melanoma. *Cancer Research*, *59*(7), 1578–1583.

Hatzi, E., Bassaglia, Y., & Badet, J. (2000). Internalization and processing of human angiogenin by cultured aortic smooth muscle cells. *Biochemical and Biophysical Research Communications*, *267*(3), 719–725. http://doi.org/10.1006/bbrc.1999.2015

Hayashida, K., Bartlett, A. H., Chen, Y., & Park, P. W. (2010). Molecular and cellular mechanisms of ectodomain shedding. *Anatomical Record (Hoboken, N.J. : 2007)*, *293*(6), 925–937. http://doi.org/10.1002/ar.20757

Heinecke, K., Seher, A., Schmitz, W., Mueller, T. D., Sebald, W., & Nickel, J. (2009). Receptor oligomerization and beyond: a case study in bone morphogenetic proteins. *BMC Biology*, *7*, 59. http://doi.org/10.1186/1741-7007-7-59

Henriksson, R., Asklund, T., & Poulsen, H. S. (2011). Impact of therapy on quality of life, neurocognitive function and their correlates in glioblastoma multiforme: a review. *Journal of Neuro-Oncology*, *104*(3), 639–646. http://doi.org/10.1007/s11060-011-0565-x

Hirschberg, A., Deng, S., Korostylev, A., Paldy, E., Costa, M. R., Worzfeld, T., et al. (2010). Gene deletion mutants reveal a role for semaphorin receptors of the plexin-B family in mechanisms underlying corticogenesis. *Molecular and Cellular Biology*, *30*(3), 764–780. http://doi.org/10.1128/MCB.01458-09

Hirukawa, S., Olson, K. A., Tsuji, T., & Hu, G.-F. (2005). Neamine inhibits xenografic human tumor growth and angiogenesis in athymic mice. *Clinical Cancer Research : an Official Journal of the American Association for Cancer Research*, *11*(24 Pt 1), 8745–8752. http://doi.org/10.1158/1078-0432.CCR-05-1495

Hjelmeland, A. B., Wu, Q., Heddleston, J. M., Choudhary, G. S., MacSwords, J., Lathia, J. D., et al. (2011). Acidic stress promotes a glioma stem cell phenotype. *Cell Death and Differentiation*, *18*(5), 829–840. http://doi.org/10.1038/cdd.2010.150

Holash, J. (1999). Vessel Cooption, Regression, and Growth in Tumors Mediated by Angiopoietins and VEGF. *Science (New York, NY)*, *284*(5422), 1994–1998. http://doi.org/10.1126/science.284.5422.1994

Holcik, M., Lefebvre, C., Yeh, C., Chow, T., & Korneluk, R. G. (1999). A new internal-ribosome-entry-site motif potentiates XIAP-mediated cytoprotection. *Nature Cell Biology*, *1*(3), 190–192. http://doi.org/10.1038/11109

Holland, E. C., Hively, W. P., DePinho, R. A., & Varmus, H. E. (1998). A constitutively active epidermal growth factor receptor cooperates with disruption of G1 cell-cycle arrest pathways to induce glioma-like lesions in mice. *Genes & Development*, *12*(23), 3675–3685.

Holliday, R. (1996). Neoplastic transformation: the contrasting stability of human and mouse cells. *Cancer Surveys*, *28*, 103–115.

Hooper, L. V., Stappenbeck, T. S., Hong, C. V., & Gordon, J. I. (2003). Angiogenins: a new class of microbicidal proteins involved in innate immunity. *Nature Immunology*, *4*(3), 269–273. http://doi.org/10.1038/ni888

Hormigo, A., Gu, B., Karimi, S., Riedel, E., Panageas, K. S., Edgar, M. A., et al. (2006).

YKL-40 and matrix metalloproteinase-9 as potential serum biomarkers for patients with high-grade gliomas. *Clinical Cancer Research : an Official Journal of the American Association for Cancer Research*, *12*(19), 5698–5704. http://doi.org/10.1158/1078-0432.CCR-06-0181

Horvath, S., Zhang, B., Carlson, M., Lu, K. V., Zhu, S., Felciano, R. M., et al. (2006). Analysis of oncogenic signaling networks in glioblastoma identifies ASPM as a molecular target. *Proceedings of the National Academy of Sciences of the United States of America*, *103*(46), 17402–17407. http://doi.org/10.1073/pnas.0608396103

Hovinga, K. E., Shimizu, F., Wang, R., Panagiotakos, G., Van Der Heijden, M., Moayedpardazi, H., et al. (2010). Inhibition of notch signaling in glioblastoma targets cancer stem cells via an endothelial cell intermediate. *Stem Cells (Dayton, Ohio)*, *28*(6), 1019–1029. http://doi.org/10.1002/stem.429

Howlett, A. R., Bailey, N., Damsky, C., Petersen, O. W., & Bissell, M. J. (1995). Cellular growth and survival are mediated by beta 1 integrins in normal human breast epithelium but not in breast carcinoma. *Journal of Cell Science*, *108 (Pt 5)*, 1945–1957.

Hu, B., Guo, P., Bar-Joseph, I., Imanishi, Y., Jarzynka, M. J., Bögler, O., et al. (2007). Neuropilin-1 promotes human glioma progression through potentiating the activity of the HGF/SF autocrine pathway. *Oncogene*, *26*(38), 5577–5586. http://doi.org/10.1038/sj.onc.1210348

Hu, G. F. (1997). Limited proteolysis of angiogenin by elastase is regulated by plasminogen. *Journal of Protein Chemistry*, *16*(7), 669–679.

Hu, G. F. (1998). Neomycin inhibits angiogenin-induced angiogenesis. *Proceedings of the National Academy of Sciences of the United States of America*, *95*(17), 9791–9795.

Hu, G. F., & Riordan, J. F. (1993). Angiogenin enhances actin acceleration of plasminogen activation. *Biochemical and Biophysical Research Communications*, *197*(2), 682–687. http://doi.org/10.1006/bbrc.1993.2533

Hu, G. F., Chang, S. I., Riordan, J. F., & Vallee, B. L. (1991). An angiogenin-binding protein from endothelial cells. *Proceedings of the National Academy of Sciences of the United States of America*, *88*(6), 2227–2231.

Hu, G. F., Riordan, J. F., & Vallee, B. L. (1997). A putative angiogenin receptor in angiogenin-responsive human endothelial cells. *Proceedings of the National Academy of Sciences of the United States of America*, *94*(6), 2204–2209.

Hu, G. F., Strydom, D. J., Fett, J. W., Riordan, J. F., & Vallee, B. L. (1993). Actin is a binding protein for angiogenin. *Proceedings of the National Academy of Sciences of the United States of America*, *90*(4), 1217–1221.

Hu, G. F., Xu, C. J., & Riordan, J. F. (2000). Human angiogenin is rapidly translocated to the nucleus of human umbilical vein endothelial cells and binds to DNA. *Journal of Cellular Biochemistry*, *76*(3), 452–462.

Hu, G., Riordan, J. F., & Vallee, B. L. (1994). Angiogenin promotes invasiveness of cultured endothelial cells by stimulation of cell-associated proteolytic activities. *Proceedings of the National Academy of Sciences of the United States of America*, *91*(25), 12096–12100.

Huang, R. Y.-J., Guilford, P., & Thiery, J. P. (2012). Early events in cell adhesion and polarity during epithelial-mesenchymal transition. *Journal of Cell Science*, *125*(Pt

19), 4417–4422. http://doi.org/10.1242/jcs.099697
Ibaragi, S., Yoshioka, N., Kishikawa, H., Hu, J. K., Sadow, P. M., Li, M., & Hu, G.-F. (2009a). Angiogenin-stimulated rRNA transcription is essential for initiation and survival of AKT-induced prostate intraepithelial neoplasia. *Molecular Cancer Research : MCR*, *7*(3), 415–424. http://doi.org/10.1158/1541-7786.MCR-08-0137
Ibaragi, S., Yoshioka, N., Li, S., Hu, M. G., Hirukawa, S., Sadow, P. M., & Hu, G. F. (2009b). Neamine Inhibits Prostate Cancer Growth by Suppressing Angiogenin-Mediated rRNA Transcription. *Clinical Cancer Research*, *15*(6), 1981–1988. http://doi.org/10.1158/1078-0432.CCR-08-2593
Infanger, D. W., Cho, Y., Lopez, B. S., Mohanan, S., Liu, S. C., Gursel, D., et al. (2013). Glioblastoma stem cells are regulated by interleukin-8 signaling in a tumoral perivascular niche. *Cancer Research*, *73*(23), 7079–7089. http://doi.org/10.1158/0008-5472.CAN-13-1355
Ishiuchi, S., Tsuzuki, K., Yoshida, Y., Yamada, N., Hagimura, N., Okado, H., et al. (2002). Blockage of Ca(2+)-permeable AMPA receptors suppresses migration and induces apoptosis in human glioblastoma cells. *Nature Medicine*, *8*(9), 971–978. http://doi.org/10.1038/nm746
Ivanov, P., Emara, M. M., Villen, J., Gygi, S. P., & Anderson, P. (2011). Angiogenin-induced tRNA fragments inhibit translation initiation. *Molecular Cell*, *43*(4), 613–623. http://doi.org/10.1016/j.molcel.2011.06.022
Ivanov, P., O'Day, E., Emara, M. M., Wagner, G., Lieberman, J., & Anderson, P. (2014). G-quadruplex structures contribute to the neuroprotective effects of angiogenin-induced tRNA fragments. *Proceedings of the National Academy of Sciences of the United States of America*, *111*(51), 18201–18206. http://doi.org/10.1073/pnas.1407361111
Jadhav, U., Chigurupati, S., Lakka, S. S., & Mohanam, S. (2004). Inhibition of matrix metalloproteinase-9 reduces in vitro invasion and angiogenesis in human microvascular endothelial cells. *International Journal of Oncology*, *25*(5), 1407–1414.
Jain, K. K. (2007). Use of nanoparticles for drug delivery in glioblastoma multiforme. *Expert Review of Neurotherapeutics*, *7*(4), 363–372. http://doi.org/10.1586/14737175.7.4.363
Jefferies, H. B., Fumagalli, S., Dennis, P. B., Reinhard, C., Pearson, R. B., & Thomas, G. (1997). Rapamycin suppresses 5'TOP mRNA translation through inhibition of p70s6k. *The EMBO Journal*, *16*(12), 3693–3704. http://doi.org/10.1093/emboj/16.12.3693
Jiang, F., Zhang, X., Kalkanis, S. N., Zhang, Z., Yang, H., Katakowski, M., et al. (2008). Combination therapy with antiangiogenic treatment and photodynamic therapy for the nude mouse bearing U87 glioblastoma. *Photochemistry and Photobiology*, *84*(1), 128–137. http://doi.org/10.1111/j.1751-1097.2007.00208.x
Jones, M. L., Ewing, C. M., Isaacsa, W. B., & Getzenberg, R. H. (2012). Prostate cancer-derived angiogenin stimulates the invasion of prostate fibroblasts. *Journal of Cellular and Molecular Medicine*, *16*(1), 193–201. http://doi.org/10.1111/j.1582-4934.2011.01283.x
Jun, H. J., Bronson, R. T., & Charest, A. (2014). Inhibition of EGFR induces a c-MET-driven stem cell population in glioblastoma. *Stem Cells (Dayton, Ohio)*, *32*(2), 338–

348. http://doi.org/10.1002/stem.1554
Kalluri, R., & Weinberg, R. A. (2009). The basics of epithelial-mesenchymal transition. *The Journal of Clinical Investigation*, *119*(6), 1420–1428. http://doi.org/10.1172/JCI39104
Katona, T. M., Neubauer, B. L., Iversen, P. W., Zhang, S., Baldridge, L. A., & Cheng, L. (2005). Elevated expression of angiogenin in prostate cancer and its precursors. *Clinical Cancer Research : an Official Journal of the American Association for Cancer Research*, *11*(23), 8358–8363. http://doi.org/10.1158/1078-0432.CCR-05-0962
Kehrer, D. F., Sparreboom, A., Verweij, J., de Bruijn, P., Nierop, C. A., van de Schraaf, J., et al. (2001). Modulation of irinotecan-induced diarrhea by cotreatment with neomycin in cancer patients. *Clinical Cancer Research : an Official Journal of the American Association for Cancer Research*, *7*(5), 1136–1141.
Kesari, S. (2011). Understanding glioblastoma tumor biology: the potential to improve current diagnosis and treatments. *Seminars in Oncology*, *38 Suppl 4*, S2–10. http://doi.org/10.1053/j.seminoncol.2011.09.005
Keunen, O., Johansson, M., Oudin, A., Sanzey, M., Rahim, S. A. A., Fack, F., et al. (2011). Anti-VEGF treatment reduces blood supply and increases tumor cell invasion in glioblastoma. *Proceedings of the National Academy of Sciences of the United States of America*, *108*(9), 3749–3754. http://doi.org/10.1073/pnas.1014480108
Kieran, D., Sebastia, J., Greenway, M. J., King, M. A., Connaughton, D., Concannon, C. G., et al. (2008). Control of motoneuron survival by angiogenin. *The Journal of Neuroscience : the Official Journal of the Society for Neuroscience*, *28*(52), 14056–14061. http://doi.org/10.1523/JNEUROSCI.3399-08.2008
Kim, E.-S., Kim, M.-S., & Moon, A. (2004). TGF-beta-induced upregulation of MMP-2 and MMP-9 depends on p38 MAPK, but not ERK signaling in MCF10A human breast epithelial cells. *International Journal of Oncology*, *25*(5), 1375–1382.
Kim, H.-M., Kang, D.-K., Kim, H. Y., Kang, S. S., & Chang, S.-I. (2007). Angiogenin-induced protein kinase B/Akt activation is necessary for angiogenesis but is independent of nuclear translocation of angiogenin in HUVE cells. *Biochemical and Biophysical Research Communications*, *352*(2), 509–513. http://doi.org/10.1016/j.bbrc.2006.11.047
Kishimoto, K., Liu, S., Tsuji, T., Olson, K. A., & Hu, G.-F. (2005). Endogenous angiogenin in endothelial cells is a general requirement for cell proliferation and angiogenesis. *Oncogene*, *24*(3), 445–456. http://doi.org/10.1038/sj.onc.1208223
Kishimoto, K., Yoshida, S., Ibaragi, S., Yoshioka, N., Hu, G.-F., & Sasaki, A. (2014). Neamine inhibits oral cancer progression by suppressing angiogenin-mediated angiogenesis and cancer cell proliferation. *Anticancer Research*, *34*(5), 2113–2121.
Kleene, R., Yang, H., Kutsche, M., & Schachner, M. (2001). The neural recognition molecule L1 is a sialic acid-binding lectin for CD24, which induces promotion and inhibition of neurite outgrowth. *The Journal of Biological Chemistry*, *276*(24), 21656–21663. http://doi.org/10.1074/jbc.M101790200
Kondo, S., Barna, B. P., Kondo, Y., Tanaka, Y., Casey, G., Liu, J., et al. (1996). WAF1/CIP1 increases the susceptibility of p53 non-functional malignant glioma cells to cisplatin-induced apoptosis. *Oncogene*, *13*(6), 1279–1285.
Kondo, T., & Raff, M. (2000). Oligodendrocyte precursor cells reprogrammed to become

multipotential CNS stem cells. *Science (New York, NY)*, *289*(5485), 1754–1757.
Kondoh, K., Terasawa, K., Morimoto, H., & Nishida, E. (2006). Regulation of nuclear translocation of extracellular signal-regulated kinase 5 by active nuclear import and export mechanisms. *Molecular and Cellular Biology*, *26*(5), 1679–1690. http://doi.org/10.1128/MCB.26.5.1679-1690.2006
Konofagou, E. E., Tung, Y.-S., Choi, J., Deffieux, T., Baseri, B., & Vlachos, F. (2012). Ultrasound-induced blood-brain barrier opening. *Current Pharmaceutical Biotechnology*, *13*(7), 1332–1345.
Koso, H., Takeda, H., Yew, C. C. K., Ward, J. M., Nariai, N., Ueno, K., et al. (2012). Transposon mutagenesis identifies genes that transform neural stem cells into glioma-initiating cells. *Proceedings of the National Academy of Sciences of the United States of America*, *109*(44), E2998–3007. http://doi.org/10.1073/pnas.1215899109
Koutroubakis, I. E., Xidakis, C., Karmiris, K., Sfiridaki, A., Kandidaki, E., & Kouroumalis, E. A. (2004). Serum angiogenin in inflammatory bowel disease. *Digestive Diseases and Sciences*, *49*(11-12), 1758–1762.
Kristiansen, G., Sammar, M., & Altevogt, P. (2004). Tumour biological aspects of CD24, a mucin-like adhesion molecule. *Journal of Molecular Histology*, *35*(3), 255–262.
Kroonen, J., Nassen, J., Boulanger, Y.-G., Provenzano, F., Capraro, V., Bours, V., et al. (2011). Human glioblastoma-initiating cells invade specifically the subventricular zones and olfactory bulbs of mice after striatal injection. *International Journal of Cancer Journal International Du Cancer*, *129*(3), 574–585. http://doi.org/10.1002/ijc.25709
Kumar, S., Park, S. H., Cieply, B., Schupp, J., Killiam, E., Zhang, F., et al. (2011). A pathway for the control of anoikis sensitivity by E-cadherin and epithelial-to-mesenchymal transition. *Molecular and Cellular Biology*, *31*(19), 4036–4051. http://doi.org/10.1128/MCB.01342-10
Kurachi, K., Davie, E. W., Strydom, D. J., Riordan, J. F., & Vallee, B. L. (1985). Sequence of the cDNA and gene for angiogenin, a human angiogenesis factor. *Biochemistry*, *24*(20), 5494–5499.
Kwiatkowska, A., & Symons, M. (2013). Signaling determinants of glioma cell invasion. *Advances in Experimental Medicine and Biology*, *986*, 121–141. http://doi.org/10.1007/978-94-007-4719-7_7
Lakka, S. S., Gondi, C. S., Yanamandra, N., Olivero, W. C., Dinh, D. H., Gujrati, M., & Rao, J. S. (2004). Inhibition of cathepsin B and MMP-9 gene expression in glioblastoma cell line via RNA interference reduces tumor cell invasion, tumor growth and angiogenesis. *Oncogene*, *23*(27), 4681–4689. http://doi.org/10.1038/sj.onc.1207616
Lal, A., Glazer, C. A., Martinson, H. M., Friedman, H. S., Archer, G. E., Sampson, J. H., & Riggins, G. J. (2002). Mutant epidermal growth factor receptor up-regulates molecular effectors of tumor invasion. *Cancer Research*, *62*(12), 3335–3339.
Lamouille, S., Xu, J., & Derynck, R. (2014). Molecular mechanisms of epithelial–mesenchymal transition. *Nature Publishing Group*, *15*(3), 178–196. http://doi.org/10.1038/nrm3758
Lang, K. J. D., Kappel, A., & Goodall, G. J. (2002). Hypoxia-inducible factor-1alpha mRNA contains an internal ribosome entry site that allows efficient translation

during normoxia and hypoxia. *Molecular Biology of the Cell*, *13*(5), 1792–1801. http://doi.org/10.1091/mbc.02-02-0017

Laplante, M., & Sabatini, D. M. (2009). mTOR signaling at a glance. *Journal of Cell Science*, *122*(Pt 20), 3589–3594. http://doi.org/10.1242/jcs.051011

Lathia, J. D., Gallagher, J., Heddleston, J. M., Wang, J., Eyler, C. E., Macswords, J., et al. (2010). Integrin alpha 6 regulates glioblastoma stem cells. *Cell Stem Cell*, *6*(5), 421–432. http://doi.org/10.1016/j.stem.2010.02.018

Le, A. P., Huang, Y., Pingle, S. C., Kesari, S., Wang, H., Yong, R. L., et al. (2015). Plexin-B2 promotes invasive growth of malignant glioma. *Oncotarget*, *6*(9), 7293–7304.

Lee, H. S., Lee, I. S., Kang, T. C., Jeong, G. B., & Chang, S. I. (1999). Angiogenin is involved in morphological changes and angiogenesis in the ovary. *Biochemical and Biophysical Research Communications*, *257*(1), 182–186. http://doi.org/10.1006/bbrc.1999.0359

Lee, J., Kotliarova, S., Kotliarov, Y., Li, A., Su, Q., Donin, N. M., et al. (2006). Tumor stem cells derived from glioblastomas cultured in bFGF and EGF more closely mirror the phenotype and genotype of primary tumors than do serum-cultured cell lines. *Cancer Cell*, *9*(5), 391–403. http://doi.org/10.1016/j.ccr.2006.03.030

Lee, S. R., & Collins, K. (2005). Starvation-induced cleavage of the tRNA anticodon loop in Tetrahymena thermophila. *The Journal of Biological Chemistry*, *280*(52), 42744–42749. http://doi.org/10.1074/jbc.M510356200

Leon, S. P., Folkerth, R. D., & Black, P. M. (1996). Microvessel density is a prognostic indicator for patients with astroglial brain tumors. *Cancer*, *77*(2), 362–372. http://doi.org/10.1002/(SICI)1097-0142(19960115)77:2<362::AID-CNCR20>3.0.CO;2-Z

Lewis, P. W., Müller, M. M., Koletsky, M. S., Cordero, F., Lin, S., Banaszynski, L. A., et al. (2013). Inhibition of PRC2 activity by a gain-of-function H3 mutation found in pediatric glioblastoma. *Science (New York, NY)*, *340*(6134), 857–861. http://doi.org/10.1126/science.1232245

Ley, R., Balmanno, K., Hadfield, K., Weston, C., & Cook, S. J. (2003). Activation of the ERK1/2 signaling pathway promotes phosphorylation and proteasome-dependent degradation of the BH3-only protein, Bim. *The Journal of Biological Chemistry*, *278*(21), 18811–18816. http://doi.org/10.1074/jbc.M301010200

Li, J., Kim, S. G., & Blenis, J. (2014). Rapamycin: one drug, many effects. *Cell Metabolism*, *19*(3), 373–379. http://doi.org/10.1016/j.cmet.2014.01.001

Li, L., Puliyappadamba, V. T., Chakraborty, S., Rehman, A., Vemireddy, V., Saha, D., et al. (2015). EGFR wild type antagonizes EGFRvIII-mediated activation of Met in glioblastoma. *Oncogene*, *34*(1), 129–134. http://doi.org/10.1038/onc.2013.534

Li, R., Riordan, J. F., & Hu, G. (1997). Nuclear translocation of human angiogenin in cultured human umbilical artery endothelial cells is microtubule and lysosome independent. *Biochemical and Biophysical Research Communications*, *238*(2), 305–312.

Li, S., & Hu, G.-F. (2012). Emerging role of angiogenin in stress response and cell survival under adverse conditions. *Journal of Cellular Physiology*, *227*(7), 2822–2826. http://doi.org/10.1002/jcp.23051

Li, S., Hu, M. G., Sun, Y., Yoshioka, N., Ibaragi, S., Sheng, J., et al. (2013). Angiogenin

mediates androgen-stimulated prostate cancer growth and enables castration resistance. *Molecular Cancer Research*, *11*(10), 1203–1214. http://doi.org/10.1158/1541-7786.MCR-13-0072

Li, S., Yu, W., & Hu, G.-F. (2012). Angiogenin inhibits nuclear translocation of apoptosis inducing factor in a Bcl-2-dependent manner. *Journal of Cellular Physiology*, *227*(4), 1639–1644. http://doi.org/10.1002/jcp.22881

Li, S., Yu, W., Kishikawa, H., & Hu, G.-F. (2010). Angiogenin prevents serum withdrawal-induced apoptosis of P19 embryonal carcinoma cells. *The FEBS Journal*, *277*(17), 3575–3587. http://doi.org/10.1111/j.1742-4658.2010.07766.x

Li, Z., Bao, S., Wu, Q., Wang, H., Eyler, C., Sathornsumetee, S., et al. (2009). Hypoxia-inducible factors regulate tumorigenic capacity of glioma stem cells. *Cancer Cell*, *15*(6), 501–513. http://doi.org/10.1016/j.ccr.2009.03.018

Liang, W.-C., Wu, X., Peale, F. V., Lee, C. V., Meng, Y. G., Gutierrez, J., et al. (2006). Cross-species vascular endothelial growth factor (VEGF)-blocking antibodies completely inhibit the growth of human tumor xenografts and measure the contribution of stromal VEGF. *The Journal of Biological Chemistry*, *281*(2), 951–961. http://doi.org/10.1074/jbc.M508199200

Liebner, S., Fischmann, A., Rascher, G., Duffner, F., Grote, E. H., Kalbacher, H., & Wolburg, H. (2000). Claudin-1 and claudin-5 expression and tight junction morphology are altered in blood vessels of human glioblastoma multiforme. *Acta Neuropathologica*, *100*(3), 323–331.

Liu, C., Sage, J. C., Miller, M. R., Verhaak, R. G. W., Hippenmeyer, S., Vogel, H., et al. (2011). Mosaic analysis with double markers reveals tumor cell of origin in glioma. *Cell*, *146*(2), 209–221. http://doi.org/10.1016/j.cell.2011.06.014

Liu, S, Yu, D., Xu, Z. P., Riordan, J. F., & Hu, G. F. (2001). Angiogenin activates Erk1/2 in human umbilical vein endothelial cells. *Biochemical and Biophysical Research Communications*, *287*(1), 305–310. http://doi.org/10.1006/bbrc.2001.5568

Liu, Y., Zhang, X., An, S., Wu, Y., Hu, G., & Wu, Y. (2015). Pharmacokinetics of neamine in rats and anti-cervical cancer activity in vitro and in vivo. *Cancer Chemotherapy and Pharmacology*, *75*(3), 465–474. http://doi.org/10.1007/s00280-014-2658-7

Lixin, R., Efthymiadis, A., Henderson, B., & Jans, D. A. (2001). Novel properties of the nucleolar targeting signal of human angiogenin. *Biochemical and Biophysical Research Communications*, *284*(1), 185–193. http://doi.org/10.1006/bbrc.2001.4953

Louis, D. N., Ohgaki, H., Wiestler, O. D., Cavenee, W. K., Burger, P. C., Jouvet, A., et al. (2007). The 2007 WHO classification of tumours of the central nervous system. *Acta Neuropathologica*, *114*(2), 97–109. http://doi.org/10.1007/s00401-007-0243-4

Lu, P., Takai, K., Weaver, V. M., & Werb, Z. (2011). Extracellular matrix degradation and remodeling in development and disease. *Cold Spring Harbor Perspectives in Biology*, *3*(12). http://doi.org/10.1101/cshperspect.a005058

Lucio-Eterovic, A. K., Piao, Y., & de Groot, J. F. (2009). Mediators of glioblastoma resistance and invasion during antivascular endothelial growth factor therapy. *Clinical Cancer Research : an Official Journal of the American Association for Cancer Research*, *15*(14), 4589–4599. http://doi.org/10.1158/1078-0432.CCR-09-0575

Lyons, S. A., Chung, W. J., Weaver, A. K., Ogunrinu, T., & Sontheimer, H. (2007).

Autocrine glutamate signaling promotes glioma cell invasion. *Cancer Research*, *67*(19), 9463–9471. http://doi.org/10.1158/0008-5472.CAN-07-2034

Maier, V., Jolicoeur, C., Rayburn, H., Takegahara, N., Kumanogoh, A., Kikutani, H., et al. (2011). Semaphorin 4C and 4G are ligands of Plexin-B2 required in cerebellar development. *Molecular and Cellular Neurosciences*, *46*(2), 419–431. http://doi.org/10.1016/j.mcn.2010.11.005

Mani, S. A., Guo, W., Liao, M.-J., Eaton, E. N., Ayyanan, A., Zhou, A. Y., et al. (2008). The epithelial-mesenchymal transition generates cells with properties of stem cells. *Cell*, *133*(4), 704–715. http://doi.org/10.1016/j.cell.2008.03.027

Martens, T., Laabs, Y., Günther, H. S., Kemming, D., Zhu, Z., Witte, L., et al. (2008). Inhibition of glioblastoma growth in a highly invasive nude mouse model can be achieved by targeting epidermal growth factor receptor but not vascular endothelial growth factor receptor-2. *Clinical Cancer Research : an Official Journal of the American Association for Cancer Research*, *14*(17), 5447–5458. http://doi.org/10.1158/1078-0432.CCR-08-0147

Martineau, Y., Le Bec, C., Monbrun, L., Allo, V., Chiu, I.-M., Danos, O., et al. (2004). Internal ribosome entry site structural motifs conserved among mammalian fibroblast growth factor 1 alternatively spliced mRNAs. *Molecular and Cellular Biology*, *24*(17), 7622–7635. http://doi.org/10.1128/MCB.24.17.7622-7635.2004

Martinez, L. A., Yang, J., Vazquez, E. S., Rodriguez-Vargas, M. D. C., Olive, M., Hsieh, J.-T., et al. (2002). p21 modulates threshold of apoptosis induced by DNA-damage and growth factor withdrawal in prostate cancer cells. *Carcinogenesis*, *23*(8), 1289–1296.

Mitchell, S. A., Spriggs, K. A., Bushell, M., Evans, J. R., Stoneley, M., Le Quesne, J. P. C., et al. (2005). Identification of a motif that mediates polypyrimidine tract-binding protein-dependent internal ribosome entry. *Genes & Development*, *19*(13), 1556–1571. http://doi.org/10.1101/gad.339105

Miyake, M., Goodison, S., Lawton, A., Gomes-Giacoia, E., & Rosser, C. J. (2014). Angiogenin promotes tumoral growth and angiogenesis by regulating matrix metallopeptidase-2 expression via the ERK1/2 pathway. *Oncogene*, –. http://doi.org/10.1038/onc.2014.2

Mizoguchi, M., Betensky, R. A., Batchelor, T. T., Bernay, D. C., Louis, D. N., & Nutt, C. L. (2006). Activation of STAT3, MAPK, and AKT in malignant astrocytic gliomas: correlation with EGFR status, tumor grade, and survival. *Journal of Neuropathology and Experimental Neurology*, *65*(12), 1181–1188. http://doi.org/10.1097/01.jnen.0000248549.14962.b2

Moelling, K., Schad, K., Bosse, M., Zimmermann, S., & Schweneker, M. (2002). Regulation of Raf-Akt Cross-talk. *The Journal of Biological Chemistry*, *277*(34), 31099–31106. http://doi.org/10.1074/jbc.M111974200

Monea, S., Lehti, K., Keski-Oja, J., & Mignatti, P. (2002). Plasmin activates pro-matrix metalloproteinase-2 with a membrane-type 1 matrix metalloproteinase-dependent mechanism. *Journal of Cellular Physiology*, *192*(2), 160–170. http://doi.org/10.1002/jcp.10126

Montana, V., & Sontheimer, H. (2011). Bradykinin Promotes the Chemotactic Invasion of Primary Brain Tumors. *The Journal of Neuroscience : the Official Journal of the Society for Neuroscience*, *31*(13), 4858–4867.

http://doi.org/10.1523/JNEUROSCI.3825-10.2011
Montanaro, L., Treré, D., & Derenzini, M. (2008). Nucleolus, ribosomes, and cancer. *The American Journal of Pathology*, *173*(2), 301–310. http://doi.org/10.2353/ajpath.2008.070752
Mori, S., Chang, J. T., Andrechek, E. R., Matsumura, N., Baba, T., Yao, G., et al. (2009). Anchorage-independent cell growth signature identifies tumors with metastatic potential. *Oncogene*, *28*(31), 2796–2805. http://doi.org/10.1038/onc.2009.139
Moroianu, J., & Riordan, J. F. (1994). Nuclear translocation of angiogenin in proliferating endothelial cells is essential to its angiogenic activity. *Proceedings of the National Academy of Sciences of the United States of America*, *91*(5), 1677–1681.
Moss, T. (2004). At the crossroads of growth control; making ribosomal RNA. *Current Opinion in Genetics & Development*, *14*(2), 210–217. http://doi.org/10.1016/j.gde.2004.02.005
Murakami, M., Sonobe, M. H., Ui, M., Kabuyama, Y., Watanabe, H., Wada, T., et al. (1997). Phosphorylation and high level expression of Fra-2 in v-src transformed cells: a pathway of activation of endogenous AP-1. *Oncogene*, *14*(20), 2435–2444. http://doi.org/10.1038/sj.onc.1201077
Murakami, M., Ui, M., & Iba, H. (1999). Fra-2-positive autoregulatory loop triggered by mitogen-activated protein kinase (MAPK) and Fra-2 phosphorylation sites by MAPK. *Cell Growth & Differentiation : the Molecular Biology Journal of the American Association for Cancer Research*, *10*(5), 333–342.
Musumeci, G., Magro, G., Cardile, V., Coco, M., Marzagalli, R., Castrogiovanni, P., et al. (2015). Characterization of matrix metalloproteinase-2 and -9, ADAM-10 and N-cadherin expression in human glioblastoma multiforme. *Cell and Tissue Research*. http://doi.org/10.1007/s00441-015-2197-5
Muzio, M., Stockwell, B. R., Stennicke, H. R., Salvesen, G. S., & Dixit, V. M. (1998). An induced proximity model for caspase-8 activation. *The Journal of Biological Chemistry*, *273*(5), 2926–2930.
Nagane, M., Coufal, F., Lin, H., Bögler, O., Cavenee, W. K., & Huang, H. J. (1996). A common mutant epidermal growth factor receptor confers enhanced tumorigenicity on human glioblastoma cells by increasing proliferation and reducing apoptosis. *Cancer Research*, *56*(21), 5079–5086.
Nagane, M., Levitzki, A., Gazit, A., Cavenee, W. K., & Huang, H. J. (1998). Drug resistance of human glioblastoma cells conferred by a tumor-specific mutant epidermal growth factor receptor through modulation of Bcl-XL and caspase-3-like proteases. *Proceedings of the National Academy of Sciences of the United States of America*, *95*(10), 5724–5729.
Nakamura, M., Yamabe, H., Osawa, H., Nakamura, N., Shimada, M., Kumasaka, R., et al. (2006). Hypoxic conditions stimulate the production of angiogenin and vascular endothelial growth factor by human renal proximal tubular epithelial cells in culture. *Nephrology, Dialysis, Transplantation : Official Publication of the European Dialysis and Transplant Association - European Renal Association*, *21*(6), 1489–1495. http://doi.org/10.1093/ndt/gfl041
Nieoullon, V., Belvindrah, R., Rougon, G., & Chazal, G. (2005). mCD24 regulates proliferation of neuronal committed precursors in the subventricular zone. *Molecular and Cellular Neuroscience*, *28*(3), 462–474.

http://doi.org/10.1016/j.mcn.2004.10.007
Nishina, H., Sato, H., Suzuki, T., Sato, M., & Iba, H. (1990). Isolation and characterization of fra-2, an additional member of the fos gene family. *Proceedings of the National Academy of Sciences of the United States of America*, *87*(9), 3619–3623.
Nisticò, P., Bissell, M. J., & Radisky, D. C. (2012). Epithelial-mesenchymal transition: general principles and pathological relevance with special emphasis on the role of matrix metalloproteinases. *Cold Spring Harbor Perspectives in Biology*, *4*(2). http://doi.org/10.1101/cshperspect.a011908
Norden, A. D., Drappatz, J., Muzikansky, A., David, K., Gerard, M., McNamara, M. B., et al. (2009). An exploratory survival analysis of anti-angiogenic therapy for recurrent malignant glioma. *Journal of Neuro-Oncology*, *92*(2), 149–155. http://doi.org/10.1007/s11060-008-9745-8
O'Reilly, L. A., Kruse, E. A., Puthalakath, H., Kelly, P. N., Kaufmann, T., Huang, D. C. S., & Strasser, A. (2009). MEK/ERK-Mediated Phosphorylation of Bim Is Required to Ensure Survival of T and B Lymphocytes during Mitogenic Stimulation. *Journal of Immunology (Baltimore, Md : 1950)*, *183*(1), 261–269. http://doi.org/10.4049/jimmunol.0803853
Ocaña, O. H., Córcoles, R., Fabra, A., Moreno-Bueno, G., Acloque, H., Vega, S., et al. (2012). Metastatic colonization requires the repression of the epithelial-mesenchymal transition inducer Prrx1. *Cancer Cell*, *22*(6), 709–724. http://doi.org/10.1016/j.ccr.2012.10.012
Ogden, A. T., Waziri, A. E., Lochhead, R. A., Fusco, D., Lopez, K., Ellis, J. A., et al. (2008). Identification of A2B5+CD133- tumor-initiating cells in adult human gliomas. *Neurosurgery*, *62*(2), 505–14– discussion 514–5. http://doi.org/10.1227/01.neu.0000316019.28421.95
Olson, K. A., Fett, J. W., French, T. C., Key, M. E., & Vallee, B. L. (1995). Angiogenin antagonists prevent tumor growth in vivo. *Proceedings of the National Academy of Sciences of the United States of America*, *92*(2), 442–446.
Olson, K. A., French, T. C., Vallee, B. L., & Fett, J. W. (1994). A monoclonal antibody to human angiogenin suppresses tumor growth in athymic mice. *Cancer Research*, *54*(17), 4576–4579.
Olson, K. A., Verselis, S. J., & Fett, J. W. (1998). Angiogenin is regulated in vivo as an acute phase protein. *Biochemical and Biophysical Research Communications*, *242*(3), 480–483. http://doi.org/10.1006/bbrc.1997.7990
Othman, Z., Sulaiman, M. K., Willcocks, M. M., Ulryck, N., Blackbourn, D. J., Sargueil, B., et al. (2014). Functional analysis of Kaposi's sarcoma-associated herpesvirus vFLIP expression reveals a new mode of IRES-mediated translation. *RNA (New York, NY)*, *20*(11), 1803–1814. http://doi.org/10.1261/rna.045328.114
Overdevest, J. B., Knubel, K. H., Duex, J. E., Thomas, S., Nitz, M. D., Harding, M. A., et al. (2012). CD24 expression is important in male urothelial tumorigenesis and metastasis in mice and is androgen regulated. *Proceedings of the National Academy of Sciences of the United States of America*, *109*(51), E3588–96. http://doi.org/10.1073/pnas.1113960109
Ozawa, T., Riester, M., Cheng, Y.-K., Huse, J. T., Squatrito, M., Helmy, K., et al. (2014). Most human non-GCIMP glioblastoma subtypes evolve from a common proneural-

like precursor glioma. *Cancer Cell*, *26*(2), 288–300. http://doi.org/10.1016/j.ccr.2014.06.005

Pan, S.-C., Wu, L.-W., Chen, C.-L., Shieh, S.-J., & Chiu, H.-Y. (2012a). Angiogenin expression in burn blister fluid: implications for its role in burn wound neovascularization. *Wound Repair and Regeneration : Official Publication of the Wound Healing Society [and] the European Tissue Repair Society*, *20*(5), 731–739. http://doi.org/10.1111/j.1524-475X.2012.00819.x

Pan, X., Xiong, D., Yao, X., Xin, Y., Zhang, L., & Chen, J. (2012b). Up-regulating ribonuclease inhibitor inhibited epithelial-to-mesenchymal transition and metastasis in murine melanoma cells. *The International Journal of Biochemistry & Cell Biology*, *44*(6), 998–1008. http://doi.org/10.1016/j.biocel.2012.03.008

Pardridge, W. M. (2005). The blood-brain barrier: bottleneck in brain drug development. *NeuroRx : the Journal of the American Society for Experimental NeuroTherapeutics*, *2*(1), 3–14. http://doi.org/10.1602/neurorx.2.1.3

Pardridge, W. M. (2012). Drug transport across the blood-brain barrier. *Journal of Cerebral Blood Flow and Metabolism : Official Journal of the International Society of Cerebral Blood Flow and Metabolism*, *32*(11), 1959–1972. http://doi.org/10.1038/jcbfm.2012.126

Park, E.-H., Lee, J. M., Blais, J. D., Bell, J. C., & Pelletier, J. (2005). Internal translation initiation mediated by the angiogenic factor Tie2. *The Journal of Biological Chemistry*, *280*(22), 20945–20953. http://doi.org/10.1074/jbc.M412744200

Pasterkamp, R. J. (2012). Getting neural circuits into shape with semaphorins. *Nature Reviews Neuroscience*, *13*(9), 605–618. http://doi.org/10.1038/nrn3302

Pavlov, N., Hatzi, E., Bassaglia, Y., Frendo, J.-L., Evain Brion, D., & Badet, J. (2003). Angiogenin distribution in human term placenta, and expression by cultured trophoblastic cells. *Angiogenesis*, *6*(4), 317–330. http://doi.org/10.1023/B:AGEN.0000029412.95244.81

Peñuelas, S., Anido, J., Prieto-Sánchez, R. M., Folch, G., Barba, I., Cuartas, I., et al. (2009). TGF-beta increases glioma-initiating cell self-renewal through the induction of LIF in human glioblastoma. *Cancer Cell*, *15*(4), 315–327. http://doi.org/10.1016/j.ccr.2009.02.011

Perälä, N., Jakobson, M., Ola, R., Fazzari, P., Penachioni, J. Y., Nymark, M., et al. (2011). Sema4C-Plexin B2 signalling modulates ureteric branching in developing kidney. *Differentiation; Research in Biological Diversity*, *81*(2), 81–91. http://doi.org/10.1016/j.diff.2010.10.001

Perrot, V. (2002). Plexin B Regulates Rho through the Guanine Nucleotide Exchange Factors Leukemia-associated Rho GEF (LARG) and PDZ-RhoGEF. *Journal of Biological Chemistry*, *277*(45), 43115–43120. http://doi.org/10.1074/jbc.M206005200

Petz, M., Them, N., Huber, H., Beug, H., & Mikulits, W. (2012). La enhances IRES-mediated translation of laminin B1 during malignant epithelial to mesenchymal transition. *Nucleic Acids Research*, *40*(1), 290–302. http://doi.org/10.1093/nar/gkr717

Piccoli, R., Olson, K. A., Vallee, B. L., & Fett, J. W. (1998). Chimeric anti-angiogenin antibody cAb 26-2F inhibits the formation of human breast cancer xenografts in athymic mice. *Proceedings of the National Academy of Sciences of the United States*

of America, *95*(8), 4579–4583.
Pichlmeier, U., Bink, A., Schackert, G., Stummer, W., ALA Glioma Study Group. (2008). Resection and survival in glioblastoma multiforme: an RTOG recursive partitioning analysis of ALA study patients. *Neuro-Oncology*, *10*(6), 1025–1034. http://doi.org/10.1215/15228517-2008-052
Pietras, A., Katz, A. M., Ekström, E. J., Wee, B., Halliday, J. J., Pitter, K. L., et al. (2014). Osteopontin-CD44 Signaling in the Glioma Perivascular Niche Enhances Cancer Stem Cell Phenotypes and Promotes Aggressive Tumor Growth. *Stem Cell*, *14*(3), 357–369. http://doi.org/10.1016/j.stem.2014.01.005
Pizzo, E., Sarcinelli, C., Sheng, J., Fusco, S., Formiggini, F., Netti, P., et al. (2013). Ribonuclease/angiogenin inhibitor 1 regulates stress-induced subcellular localization of angiogenin to control growth and survival. *Journal of Cell Science*, *126*(Pt 18), 4308–4319. http://doi.org/10.1242/jcs.134551
Pollard, S. M., Yoshikawa, K., Clarke, I. D., Danovi, D., Stricker, S., Russell, R., et al. (2009). Glioma stem cell lines expanded in adherent culture have tumor-specific phenotypes and are suitable for chemical and genetic screens. *Cell Stem Cell*, *4*(6), 568–580. http://doi.org/10.1016/j.stem.2009.03.014
Poncet, C., Frances, V., Gristina, R., Scheiner, C., Pellissier, J. F., & Figarella-Branger, D. (1996). CD24, a glycosylphosphatidylinositol-anchored molecules is transiently expressed during the development of human central nervous system and is a marker of human neural cell lineage tumors. *Acta Neuropathologica*, *91*(4), 400–408.
Pozner, A., Goldenberg, D., Negreanu, V., Le, S. Y., Elroy-Stein, O., Levanon, D., & Groner, Y. (2000). Transcription-coupled translation control of AML1/RUNX1 is mediated by cap- and internal ribosome entry site-dependent mechanisms. *Molecular and Cellular Biology*, *20*(7), 2297–2307.
Pyatibratov, M. G., Tolkatchev, D., Plamondon, J., Xu, P., Ni, F., & Kostyukova, A. S. (2010). Binding of human angiogenin inhibits actin polymerization. *Archives of Biochemistry and Biophysics*, *495*(1), 74–81. http://doi.org/10.1016/j.abb.2009.12.024
Rahme, G. J., & Israel, M. A. (2015). Id4 suppresses MMP2-mediated invasion of glioblastoma-derived cells by direct inactivation of Twist1 function. *Oncogene*, *34*(1), 53–62. http://doi.org/10.1038/onc.2013.531
Rajashekhar, G., Loganath, A., Roy, A. C., & Wong, Y. C. (2002). Expression and localization of angiogenin in placenta: enhanced levels at term over first trimester villi. *Molecular Reproduction and Development*, *62*(2), 159–166. http://doi.org/10.1002/mrd.10116
Rajashekhar, G., Loganath, A., Roy, A. C., & Wong, Y. C. (2003). Over-expression and secretion of angiogenin in intrauterine growth retardation placenta. *Molecular Reproduction and Development*, *64*(4), 397–404. http://doi.org/10.1002/mrd.10229
Ramaswamy, P., Aditi Devi, N., Hurmath Fathima, K., & Dalavaikodihalli Nanjaiah, N. (2014). Activation of NMDA receptor of glutamate influences MMP-2 activity and proliferation of glioma cells. *Neurological Sciences : Official Journal of the Italian Neurological Society and of the Italian Society of Clinical Neurophysiology*, *35*(6), 823–829. http://doi.org/10.1007/s10072-013-1604-5
Ramos-DeSimone, N., Hahn-Dantona, E., Sipley, J., Nagase, H., French, D. L., & Quigley, J. P. (1999). Activation of matrix metalloproteinase-9 (MMP-9) via a

converging plasmin/stromelysin-1 cascade enhances tumor cell invasion. *The Journal of Biological Chemistry*, *274*(19), 13066–13076.
Rangarajan, A., Hong, S. J., Gifford, A., & Weinberg, R. A. (2004). Species- and cell type-specific requirements for cellular transformation. *Cancer Cell*, *6*(2), 171–183. http://doi.org/10.1016/j.ccr.2004.07.009
Rao, J. S., Steck, P. A., Mohanam, S., Stetler-Stevenson, W. G., Liotta, L. A., & Sawaya, R. (1993). Elevated levels of M(r) 92,000 type IV collagenase in human brain tumors. *Cancer Research*, *53*(10 Suppl), 2208–2211.
Re, F., Zanetti, A., Sironi, M., Polentarutti, N., Lanfrancone, L., Dejana, E., & Colotta, F. (1994). Inhibition of anchorage-dependent cell spreading triggers apoptosis in cultured human endothelial cells. *The Journal of Cell Biology*, *127*(2), 537–546.
Reilly, K. M., Loisel, D. A., Bronson, R. T., McLaughlin, M. E., & Jacks, T. (2000). Nf1;Trp53 mutant mice develop glioblastoma with evidence of strain-specific effects. *Nature Genetics*, *26*(1), 109–113. http://doi.org/10.1038/79075
Reinhold, H. S., Calvo, W., Hopewell, J. W., & van der Berg, A. P. (1990). Development of blood vessel-related radiation damage in the fimbria of the central nervous system. *International Journal of Radiation Oncology, Biology, Physics*, *18*(1), 37–42.
Rheinbay, E., Suvà, M. L., Gillespie, S. M., Wakimoto, H., Patel, A. P., Shahid, M., et al. (2013). An aberrant transcription factor network essential for Wnt signaling and stem cell maintenance in glioblastoma. *Cell Reports*, *3*(5), 1567–1579. http://doi.org/10.1016/j.celrep.2013.04.021
Ricci-Vitiani, L., Pallini, R., Biffoni, M., Todaro, M., Invernici, G., Cenci, T., et al. (2010). Tumour vascularization via endothelial differentiation of glioblastoma stem-like cells. *Nature*, *468*(7325), 824–828. http://doi.org/10.1038/nature09557
Rieger, J., Wick, W., & Weller, M. (2003). Human malignant glioma cells express semaphorins and their receptors, neuropilins and plexins. *Glia*, *42*(4), 379–389. http://doi.org/10.1002/glia.10210
Riemenschneider, M. J., Jeuken, J. W. M., Wesseling, P., & Reifenberger, G. (2010). Molecular diagnostics of gliomas: state of the art. *Acta Neuropathologica*, *120*(5), 567–584. http://doi.org/10.1007/s00401-010-0736-4
Rizzolio, S., Rabinowicz, N., Rainero, E., Lanzetti, L., Serini, G., Norman, J., et al. (2012). Neuropilin-1-dependent regulation of EGF-receptor signaling. *Cancer Research*, *72*(22), 5801–5811. http://doi.org/10.1158/0008-5472.CAN-12-0995
Roney, K. E., O'Connor, B. P., Wen, H., Holl, E. K., Guthrie, E. H., Davis, B. K., et al. (2011). Plexin-B2 negatively regulates macrophage motility, Rac, and Cdc42 activation. *PLoS ONE*, *6*(9), e24795. http://doi.org/10.1371/journal.pone.0024795
Russo, M. A., Paolillo, M., Sanchez-Hernandez, Y., Curti, D., Ciusani, E., Serra, M., et al. (2013). A small-molecule RGD-integrin antagonist inhibits cell adhesion, cell migration and induces anoikis in glioblastoma cells. *International Journal of Oncology*, *42*(1), 83–92. http://doi.org/10.3892/ijo.2012.1708
Sadagopan, S., Veettil, M. V., Chakraborty, S., Sharma-Walia, N., Paudel, N., Bottero, V., & Chandran, B. (2012). Angiogenin functionally interacts with p53 and regulates p53-mediated apoptosis and cell survival. *Oncogene*. http://doi.org/10.1038/onc.2011.648
Saha, B., Ypsilanti, A. R., Boutin, C., Cremer, H., & Chédotal, A. (2012). Plexin-B2 regulates the proliferation and migration of neuroblasts in the postnatal and adult

subventricular zone. *The Journal of Neuroscience : the Official Journal of the Society for Neuroscience*, *32*(47), 16892–16905. http://doi.org/10.1523/JNEUROSCI.0344-12.2012

Saikia, M., Jobava, R., Parisien, M., Putnam, A., Krokowski, D., Gao, X. H., et al. (2014). Angiogenin-Cleaved tRNA Halves Interact with Cytochrome c, Protecting Cells from Apoptosis during Osmotic Stress. *Molecular and Cellular Biology*, *34*(13), 2450–2463. http://doi.org/10.1128/MCB.00136-14

Saikia, M., Krokowski, D., Guan, B.-J., Ivanov, P., Parisien, M., Hu, G.-F., et al. (2012). Genome-wide identification and quantitative analysis of cleaved tRNA fragments induced by cellular stress. *The Journal of Biological Chemistry*. http://doi.org/10.1074/jbc.M112.371799

Sarbassov, D. D., Ali, S. M., Sengupta, S., Sheen, J.-H., Hsu, P. P., Bagley, A. F., et al. (2006). Prolonged rapamycin treatment inhibits mTORC2 assembly and Akt/PKB. *Molecular Cell*, *22*(2), 159–168. http://doi.org/10.1016/j.molcel.2006.03.029

Sato, H., Kita, M., & Seiki, M. (1993). v-Src activates the expression of 92-kDa type IV collagenase gene through the AP-1 site and the GT box homologous to retinoblastoma control elements. A mechanism regulating gene expression independent of that by inflammatory cytokines. *The Journal of Biological Chemistry*, *268*(31), 23460–23468.

Schaefer, M., Pollex, T., Hanna, K., Tuorto, F., Meusburger, M., Helm, M., & Lyko, F. (2010). RNA methylation by Dnmt2 protects transfer RNAs against stress-induced cleavage. *Genes & Development*, *24*(15), 1590–1595. http://doi.org/10.1101/gad.586710

Scheel, C., & Weinberg, R. A. (2011). Phenotypic plasticity and epithelial-mesenchymal transitions in cancer and normal stem cells? *International Journal of Cancer Journal International Du Cancer*, *129*(10), 2310–2314. http://doi.org/10.1002/ijc.26311

Scherer, H. J. (1938) Structural development in gliomas. *The American Journal of Cancer*, (34), 333–351.

Schinkel, A. (1999). P-Glycoprotein, a gatekeeper in the blood-brain barrier. *Advanced Drug Delivery Reviews*, *36*(2-3), 179–194.

Schlaepfer, D. D., Hanks, S. K., Hunter, T., & van der Geer, P. (1994). Integrin-mediated signal transduction linked to Ras pathway by GRB2 binding to focal adhesion kinase. *Nature*, *372*(6508), 786–791.

Schröder, C., Schumacher, U., Müller, V., Wirtz, R. M., Streichert, T., Richter, U., et al. (2010). The transcription factor Fra-2 promotes mammary tumour progression by changing the adhesive properties of breast cancer cells. *European Journal of Cancer*, *46*(9), 1650–1660. http://doi.org/10.1016/j.ejca.2010.02.008

Schuler, P. J., Bendszus, M., Kuehnel, S., Wagner, S., Hoffmann, T. K., Goldbrunner, R., & Vince, G. H. (2012). Urokinase plasminogen activator, uPAR, MMP-2, and MMP-9 in the C6-glioblastoma rat model. *In Vivo (Athens, Greece)*, *26*(4), 571–576.

Sebastià, J., Kieran, D., Breen, B., King, M. A., Netteland, D. F., Joyce, D., et al. (2009). Angiogenin protects motoneurons against hypoxic injury. *Cell Death and Differentiation*, *16*(9), 1238–1247. http://doi.org/10.1038/cdd.2009.52

Senner, V., Sturm, A., Baur, I., Schrell, U. H., Distel, L., & Paulus, W. (1999a). CD24 promotes invasion of glioma cells in vivo. *Journal of Neuropathology and Experimental Neurology*, *58*(8), 795–802.

Senner, V., Sturm, A., Baur, I., Schrell, U. H., Distel, L., & Paulus, W. (1999b). CD24 promotes invasion of glioma cells in vivo. *Journal of Neuropathology and Experimental Neurology*, *58*(8), 795–802.

Serrano, I., McDonald, P. C., Lock, F. E., & Dedhar, S. (2013). Role of the integrin-linked kinase (ILK)/Rictor complex in TGFβ-1-induced epithelial-mesenchymal transition (EMT). *Oncogene*, *32*(1), 50–60. http://doi.org/10.1038/onc.2012.30

Shapiro, R., Riordan, J. F., & Vallee, B. L. (1986). Characteristic ribonucleolytic activity of human angiogenin. *Biochemistry*, *25*(12), 3527–3532.

Shcheglovitova, O. N., Maksyanina, E. V., Ionova, I. I., Rustam'yan, Y. L., & Komolova, G. S. (2003). Cow milk angiogenin induces cytokine production in human blood leukocytes. *Bulletin of Experimental Biology and Medicine*, *135*(2), 158–160.

Sheng, J., Yu, W., Gao, X., Xu, Z., & Hu, G.-F. (2013). Angiogenin Stimulates Ribosomal RNA Transcription by Epigenetic Activation of the Ribosomal DNA Promoter. *Journal of Cellular Physiology*, *229*(4), 521–529. http://doi.org/10.1002/jcp.24477

Sherrill, K. W., Byrd, M. P., Van Eden, M. E., & Lloyd, R. E. (2004). BCL-2 translation is mediated via internal ribosome entry during cell stress. *The Journal of Biological Chemistry*, *279*(28), 29066–29074. http://doi.org/10.1074/jbc.M402727200

Sherry, M. M., Reeves, A., Wu, J. K., & Cochran, B. H. (2009). STAT3 Is Required for Proliferation and Maintenance of Multipotency in Glioblastoma Stem Cells. *Stem Cells (Dayton, Ohio)*, *27*(10), 2383–2392. http://doi.org/10.1002/stem.185

Shi, J., Kahle, A., Hershey, J. W. B., Honchak, B. M., Warneke, J. A., Leong, S. P. L., & Nelson, M. A. (2006). Decreased expression of eukaryotic initiation factor 3f deregulates translation and apoptosis in tumor cells. *Oncogene*, *25*(35), 4923–4936. http://doi.org/10.1038/sj.onc.1209495

Shin, S. I., Freedman, V. H., Risser, R., & Pollack, R. (1975). Tumorigenicity of virus-transformed cells in nude mice is correlated specifically with anchorage independent growth in vitro. *Proceedings of the National Academy of Sciences of the United States of America*, *72*(11), 4435–4439.

Shinoura, N., Shamraj, O. I., Hugenholz, H., Zhu, J. G., McBlack, P., Warnick, R., et al. (1995). Identification and partial sequence of a cDNA that is differentially expressed in human brain tumors. *Cancer Letters*, *89*(2), 215–221.

Singh, S. K., Clarke, I. D., Terasaki, M., Bonn, V. E., Hawkins, C., Squire, J., & Dirks, P. B. (2003). Identification of a cancer stem cell in human brain tumors. *Cancer Research*, *63*(18), 5821–5828.

Singh, S. K., Hawkins, C., Clarke, I. D., Squire, J. A., Bayani, J., Hide, T., et al. (2004). Identification of human brain tumour initiating cells. *Nature*, *432*(7015), 396–401. http://doi.org/10.1038/nature03128

Skorupa, A., King, M. A., Aparicio, I. M., Dussmann, H., Coughlan, K., Breen, B., et al. (2012). Motoneurons secrete angiogenin to induce RNA cleavage in astroglia. *The Journal of Neuroscience : the Official Journal of the Society for Neuroscience*, *32*(15), 5024–5038. http://doi.org/10.1523/JNEUROSCI.6366-11.2012

Skorupa, A., Urbach, S., Vigy, O., King, M. A., Chaumont-Dubel, S., Prehn, J. H. M., & Marin, P. (2013). Angiogenin induces modifications in the astrocyte secretome: relevance to amyotrophic lateral sclerosis. *Journal of Proteomics*, *91*, 274–285. http://doi.org/10.1016/j.jprot.2013.07.028

Slowik, F., & Balogh, I. (1980). Extracranial spreading of glioblastoma multiforme. *Zentralblatt Für Neurochirurgie*, *41*(1), 57–68.
Smith, M., Burke, Z., Humphries, A., Wells, T., Klein, D., Carter, D., & Baler, R. (2001). Tissue-specific transgenic knockdown of Fos-related antigen 2 (Fra-2) expression mediated by dominant negative Fra-2. *Molecular and Cellular Biology*, *21*(11), 3704–3713. http://doi.org/10.1128/MCB.21.11.3704-3713.2001
Smith, S. C., Oxford, G., Wu, Z., Nitz, M. D., Conaway, M., Frierson, H. F., et al. (2006). The metastasis-associated gene CD24 is regulated by Ral GTPase and is a mediator of cell proliferation and survival in human cancer. *Cancer Research*, *66*(4), 1917–1922. http://doi.org/10.1158/0008-5472.CAN-05-3855
Snuderl, M., Fazlollahi, L., Le, L. P., Nitta, M., Zhelyazkova, B. H., Davidson, C. J., et al. (2011). Mosaic amplification of multiple receptor tyrosine kinase genes in glioblastoma. *Cancer Cell*, *20*(6), 810–817. http://doi.org/10.1016/j.ccr.2011.11.005
Soeda, A., Hara, A., Kunisada, T., Yoshimura, S.-I., Iwama, T., & Park, D. M. (2015). The evidence of glioblastoma heterogeneity. *Scientific Reports*, *5*, 7979. http://doi.org/10.1038/srep07979
Son, M. J., Woolard, K., Nam, D.-H., Lee, J., & Fine, H. A. (2009). SSEA-1 is an enrichment marker for tumor-initiating cells in human glioblastoma. *Cell Stem Cell*, *4*(5), 440–452. http://doi.org/10.1016/j.stem.2009.03.003
Soncin, F., Strydom, D. J., & Shapiro, R. (1997). Interaction of heparin with human angiogenin. *The Journal of Biological Chemistry*, *272*(15), 9818–9824.
Soong, J., & Scott, G. (2013). Plexin B1 inhibits MET through direct association and regulates Shp2 expression in melanocytes. *Journal of Cell Science*, *126*(Pt 2), 688–695. http://doi.org/10.1242/jcs.119487
Stachowiak, E. K., Maher, P. A., Tucholski, J., Mordechai, E., Joy, A., Moffett, J., et al. (1997). Nuclear accumulation of fibroblast growth factor receptors in human glial cells--association with cell proliferation. *Oncogene*, *14*(18), 2201–2211. http://doi.org/10.1038/sj.onc.1201057
Steidinger, T. U., Slone, S. R., Ding, H., Standaert, D. G., & Yacoubian, T. A. (2013). Angiogenin in Parkinson disease models: role of Akt phosphorylation and evaluation of AAV-mediated angiogenin expression in MPTP treated mice. *PLoS ONE*, *8*(2), e56092. http://doi.org/10.1371/journal.pone.0056092
Steidinger, T. U., Standaert, D. G., & Yacoubian, T. A. (2011). A neuroprotective role for angiogenin in models of Parkinson's disease. *Journal of Neurochemistry*, *116*(3), 334–341. http://doi.org/10.1111/j.1471-4159.2010.07112.x
Stein, I., Itin, A., Einat, P., Skaliter, R., Grossman, Z., & Keshet, E. (1998). Translation of vascular endothelial growth factor mRNA by internal ribosome entry: implications for translation under hypoxia. *Molecular and Cellular Biology*, *18*(6), 3112–3119.
Stojic, J., Hagemann, C., Haas, S., Herbold, C., Kühnel, S., Gerngras, S., et al. (2008). Expression of matrix metalloproteinases MMP-1, MMP-11 and MMP-19 is correlated with the WHO-grading of human malignant gliomas. *Neuroscience Research*, *60*(1), 40–49. http://doi.org/10.1016/j.neures.2007.09.009
Stoneley, M., Paulin, F. E., Le Quesne, J. P., Chappell, S. A., & Willis, A. E. (1998). C-Myc 5' untranslated region contains an internal ribosome entry segment. *Oncogene*, *16*(3), 423–428. http://doi.org/10.1038/sj.onc.1201763
Strydom, D. J., Fett, J. W., Lobb, R. R., Alderman, E. M., Bethune, J. L., Riordan, J. F.,

& Vallee, B. L. (1985). Amino acid sequence of human tumor derived angiogenin. *Biochemistry*, *24*(20), 5486–5494.

Sturm, D., Witt, H., Hovestadt, V., Khuong-Quang, D.-A., Jones, D. T. W., Konermann, C., et al. (2012). Hotspot mutations in H3F3A and IDH1 define distinct epigenetic and biological subgroups of glioblastoma. *Cancer Cell*, *22*(4), 425–437. http://doi.org/10.1016/j.ccr.2012.08.024

Sun, L., Hui, A.-M., Su, Q., Vortmeyer, A., Kotliarov, Y., Pastorino, S., et al. (2006). Neuronal and glioma-derived stem cell factor induces angiogenesis within the brain. *Cancer Cell*, *9*(4), 287–300. http://doi.org/10.1016/j.ccr.2006.03.003

Suzuki, T., Murakami, M., Onai, N., Fukuda, E., Hashimoto, Y., Sonobe, M. H., et al. (1994). Analysis of AP-1 function in cellular transformation pathways. *Journal of Virology*, *68*(6), 3527–3535.

Tamagnone, L., & Comoglio, P. M. (2000). Signalling by semaphorin receptors: cell guidance and beyond. *Trends in Cell Biology*, *10*(9), 377–383.

Tamagnone, L., Artigiani, S., Chen, H., He, Z., Ming, G. I., Song, H., et al. (1999). Plexins are a large family of receptors for transmembrane, secreted, and GPI-anchored semaphorins in vertebrates. *Cell*, *99*(1), 71–80.

Tamaki, M., McDonald, W., Amberger, V. R., Moore, E., & Del Maestro, R. F. (1997). Implantation of C6 astrocytoma spheroid into collagen type I gels: invasive, proliferative, and enzymatic characterizations. *Journal of Neurosurgery*, *87*(4), 602–609. http://doi.org/10.3171/jns.1997.87.4.0602

Tanaka, S., Louis, D. N., Curry, W. T., Batchelor, T. T., & Dietrich, J. (2013). Diagnostic and therapeutic avenues for glioblastoma: no longer a dead end? *Nature Reviews. Clinical Oncology*, *10*(1), 14–26. http://doi.org/10.1038/nrclinonc.2012.204

Tanos, T., Marinissen, M. J., Leskow, F. C., Hochbaum, D., Martinetto, H., Gutkind, J. S., & Coso, O. A. (2005). Phosphorylation of c-Fos by members of the p38 MAPK family. Role in the AP-1 response to UV light. *The Journal of Biological Chemistry*, *280*(19), 18842–18852. http://doi.org/10.1074/jbc.M500620200

Taraboletti, G., D'Ascenzo, S., Borsotti, P., Giavazzi, R., Pavan, A., & Dolo, V. (2002). Shedding of the matrix metalloproteinases MMP-2, MMP-9, and MT1-MMP as membrane vesicle-associated components by endothelial cells. *The American Journal of Pathology*, *160*(2), 673–680. http://doi.org/10.1016/S0002-9440(10)64887-0

Thiele, C. J., Li, Z., & McKee, A. E. (2009). On Trk--the TrkB signal transduction pathway is an increasingly important target in cancer biology. *Clinical Cancer Research : an Official Journal of the American Association for Cancer Research*, *15*(19), 5962–5967. http://doi.org/10.1158/1078-0432.CCR-08-0651

Thiyagarajan, N., Ferguson, R., Subramanian, V., & Acharya, K. R. (2012). Structural and molecular insights into the mechanism of action of human angiogenin-ALS variants in neurons. *Nature Communications*, *3*, 1121. http://doi.org/10.1038/ncomms2126

Thomas, S., Harding, M. A., Smith, S. C., Overdevest, J. B., Nitz, M. D., Frierson, H. F., et al. (2012). CD24 is an effector of HIF-1-driven primary tumor growth and metastasis. *Cancer Research*, *72*(21), 5600–5612. http://doi.org/10.1158/0008-5472.CAN-11-3666

Thompson, D. M., Lu, C., Green, P. J., & Parker, R. (2008). tRNA cleavage is a conserved response to oxidative stress in eukaryotes. *RNA (New York, NY)*, *14*(10),

2095–2103. http://doi.org/10.1261/rna.1232808
Tkachenko, E., Lutgens, E., Stan, R.-V., & Simons, M. (2004). Fibroblast growth factor 2 endocytosis in endothelial cells proceed via syndecan-4-dependent activation of Rac1 and a Cdc42-dependent macropinocytic pathway. *Journal of Cell Science*, *117*(Pt 15), 3189–3199. http://doi.org/10.1242/jcs.01190
Torres-Vázquez, J., Gitler, A. D., Fraser, S. D., Berk, J. D., Van N Pham, Fishman, M. C., et al. (2004). Semaphorin-plexin signaling guides patterning of the developing vasculature. *Developmental Cell*, *7*(1), 117–123. http://doi.org/10.1016/j.devcel.2004.06.008
Tsai, B. P., Jimenez, J., Lim, S., Fitzgerald, K. D., Zhang, M., Chuah, C. T. H., et al. (2014). A novel Bcr-Abl-mTOR-eIF4A axis regulates IRES-mediated translation of LEF-1. *Open Biology*, *4*(11), 140180. http://doi.org/10.1098/rsob.140180
Tsai, J. H., Donaher, J. L., Murphy, D. A., Chau, S., & Yang, J. (2012). Spatiotemporal regulation of epithelial-mesenchymal transition is essential for squamous cell carcinoma metastasis. *Cancer Cell*, *22*(6), 725–736. http://doi.org/10.1016/j.ccr.2012.09.022
Tso, C.-L. (2011). Molecular Pathways of Glioblastoma and Glioblastoma Stem Cells, 1–32.
Tsuji, T., Sun, Y., Kishimoto, K., Olson, K. A., Liu, S., Hirukawa, S., & Hu, G.-F. (2005). Angiogenin is translocated to the nucleus of HeLa cells and is involved in ribosomal RNA transcription and cell proliferation. *Cancer Research*, *65*(4), 1352–1360. http://doi.org/10.1158/0008-5472.CAN-04-2058
Uhrbom, L., & Holland, E. C. (2001). Modeling gliomagenesis with somatic cell gene transfer using retroviral vectors. *Journal of Neuro-Oncology*, *53*(3), 297–305.
Uhrbom, L., Dai, C., Celestino, J. C., Rosenblum, M. K., Fuller, G. N., & Holland, E. C. (2002). Ink4a-Arf loss cooperates with KRas activation in astrocytes and neural progenitors to generate glioblastomas of various morphologies depending on activated Akt. *Cancer Research*, *62*(19), 5551–5558.
Valsesia-Wittmann, S., Magdeleine, M., Dupasquier, S., Garin, E., Jallas, A.-C., Combaret, V., et al. (2004). Oncogenic cooperation between H-Twist and N-Myc overrides failsafe programs in cancer cells. *Cancer Cell*, *6*(6), 625–630. http://doi.org/10.1016/j.ccr.2004.09.033
van Es, M. A., Schelhaas, H. J., van Vught, P. W. J., Ticozzi, N., Andersen, P. M., Groen, E. J. N., et al. (2011). Angiogenin variants in Parkinson disease and amyotrophic lateral sclerosis. *Annals of Neurology*, *70*(6), 964–973. http://doi.org/10.1002/ana.22611
Varelas, X., & Wrana, J. L. (2012). Coordinating developmental signaling: novel roles for the Hippo pathway. *Trends in Cell Biology*, *22*(2), 88–96. http://doi.org/10.1016/j.tcb.2011.10.002
Veeravalli, K. K., & Rao, J. S. (2012). MMP-9 and uPAR regulated glioma cell migration. *Cell Adhesion & Migration*, *6*(6), 509–512. http://doi.org/10.4161/cam.21673
Verhaak, R. G. W., Hoadley, K. A., Purdom, E., Wang, V., Qi, Y., Wilkerson, M. D., et al. (2010). Integrated genomic analysis identifies clinically relevant subtypes of glioblastoma characterized by abnormalities in PDGFRA, IDH1, EGFR, and NF1. *Cancer Cell*, *17*(1), 98–110. http://doi.org/10.1016/j.ccr.2009.12.020

Verselis, S. J., Olson, K. A., & Fett, J. W. (1999). Regulation of angiogenin expression in human HepG2 hepatoma cells by mediators of the acute-phase response. *Biochemical and Biophysical Research Communications*, *259*(1), 178–184. http://doi.org/10.1006/bbrc.1999.0744

Wakimoto, H., Mohapatra, G., Kanai, R., Curry, W. T., Yip, S., Nitta, M., et al. (2012). Maintenance of primary tumor phenotype and genotype in glioblastoma stem cells. *Neuro-Oncology*, *14*(2), 132–144. http://doi.org/10.1093/neuonc/nor195

Wang, Jialiang, Wang, H., Li, Z., Wu, Q., Lathia, J. D., Mclendon, R. E., et al. (2008a). c-Myc is required for maintenance of glioma cancer stem cells. *PLoS ONE*, *3*(11), e3769. http://doi.org/10.1371/journal.pone.0003769

Wang, Jian, Sakariassen, P. Ø., Tsinkalovsky, O., Immervoll, H., Bøe, S. O., Svendsen, A., et al. (2008b). CD133 negative glioma cells form tumors in nude rats and give rise to CD133 positive cells. *International Journal of Cancer Journal International Du Cancer*, *122*(4), 761–768. http://doi.org/10.1002/ijc.23130

Wang, Junfeng, Sun, D., Wang, Y., Ren, F., Pang, S., Wang, D., & Xu, S. (2014). FOSL2 positively regulates TGF-β1 signalling in non-small cell lung cancer. *PLoS ONE*, *9*(11), e112150. http://doi.org/10.1371/journal.pone.0112150

Wang, L., Zhang, Z. G., Zhang, R. L., Gregg, S. R., Hozeska-Solgot, A., LeTourneau, Y., et al. (2006). Matrix metalloproteinase 2 (MMP2) and MMP9 secreted by erythropoietin-activated endothelial cells promote neural progenitor cell migration. *The Journal of Neuroscience : the Official Journal of the Society for Neuroscience*, *26*(22), 5996–6003. http://doi.org/10.1523/JNEUROSCI.5380-05.2006

Wang, Maode, Wang, T., Liu, S., Yoshida, D., & Teramoto, A. (2003). The expression of matrix metalloproteinase-2 and -9 in human gliomas of different pathological grades. *Brain Tumor Pathology*, *20*(2), 65–72.

Wang, Rong, Chadalavada, K., Wilshire, J., Kowalik, U., Hovinga, K. E., Geber, A., et al. (2010). Glioblastoma stem-like cells give rise to tumour endothelium. *Nature*, *468*(7325), 829–833. http://doi.org/10.1038/nature09624

Warnakulasuriyarachchi, D., Cerquozzi, S., Cheung, H. H., & Holcik, M. (2004). Translational induction of the inhibitor of apoptosis protein HIAP2 during endoplasmic reticulum stress attenuates cell death and is mediated via an inducible internal ribosome entry site element. *The Journal of Biological Chemistry*, *279*(17), 17148–17157. http://doi.org/10.1074/jbc.M308737200

Wei, S., Gao, X., Du, J., Su, J., & Xu, Z. (2011). Angiogenin enhances cell migration by regulating stress fiber assembly and focal adhesion dynamics. *PLoS ONE*, *6*(12), e28797. http://doi.org/10.1371/journal.pone.0028797

Weiner, H. L., Weiner, L. H., & Swain, J. L. (1987). Tissue distribution and developmental expression of the messenger RNA encoding angiogenin. *Science (New York, NY)*, *237*(4812), 280–282.

Williams, P. D., Bennett, D. B., Gleason, C. R., & Hottendorf, G. H. (1987). Correlation between renal membrane binding and nephrotoxicity of aminoglycosides. *Antimicrobial Agents and Chemotherapy*, *31*(4), 570–574.

Winkler, F., Kienast, Y., Fuhrmann, M., Baumgarten, Von, L., Burgold, S., Mitteregger, G., et al. (2009). Imaging glioma cell invasion in vivoreveals mechanisms of dissemination and peritumoral angiogenesis. *Glia*, *57*(12), 1306–1315. http://doi.org/10.1002/glia.20850

Wolfenson, H., Lavelin, I., & Geiger, B. (2013). Dynamic regulation of the structure and functions of integrin adhesions. *Developmental Cell*, *24*(5), 447–458. http://doi.org/10.1016/j.devcel.2013.02.012

Worzfeld, T., Swiercz, J. M., Looso, M., Straub, B. K., Sivaraj, K. K., & Offermanns, S. (2012). ErbB-2 signals through Plexin-B1 to promote breast cancer metastasis. *The Journal of Clinical Investigation*, *122*(4), 1296–1305. http://doi.org/10.1172/JCI60568

Xia, W., Fu, W., Cai, L., Kong, H., Cai, X., Liu, J., et al. (2012). Identification and characterization of FHL3 as a novel angiogenin-binding partner. *Gene*, *504*(2), 233–237. http://doi.org/10.1016/j.gene.2012.05.019

Xu, J., Lamouille, S., & Derynck, R. (2009). TGF-beta-induced epithelial to mesenchymal transition. *Cell Research*, *19*(2), 156–172. http://doi.org/10.1038/cr.2009.5

Xu, T., Chen, J., Lu, Y., & Wolff, J. E. (2010). Effects of bevacizumab plus irinotecan on response and survival in patients with recurrent malignant glioma: a systematic review and survival-gain analysis. *BMC Cancer*, *10*, 252. http://doi.org/10.1186/1471-2407-10-252

Xu, Z.-P., Tsuji, T., Riordan, J. F., & Hu, G.-F. (2002). The nuclear function of angiogenin in endothelial cells is related to rRNA production. *Biochemical and Biophysical Research Communications*, *294*(2), 287–292. http://doi.org/10.1016/S0006-291X(02)00479-5

Xu, Z.-P., Tsuji, T., Riordan, J. F., & Hu, G.-F. (2003). Identification and Characterization of an Angiogenin-Binding DNA Sequence That Stimulates Luciferase Reporter Gene Expression †. *Biochemistry*, *42*(1), 121–128. http://doi.org/10.1021/bi020465x

Yamasaki, S., & Anderson, P. (2008). Reprogramming mRNA translation during stress. *Current Opinion in Cell Biology*, *20*(2), 222–226. http://doi.org/10.1016/j.ceb.2008.01.013

Yamasaki, S., Ivanov, P., Hu, G.-F., & Anderson, P. (2009). Angiogenin cleaves tRNA and promotes stress-induced translational repression. *The Journal of Cell Biology*, *185*(1), 35–42. http://doi.org/10.1083/jcb.200811106

Yao, X., Li, D., Xiong, D.-M., Li, L., Jiang, R., & Chen, J.-X. (2013). A novel role of ribonuclease inhibitor in regulation of epithelial-to-mesenchymal transition and ILK signaling pathway in bladder cancer cells. *Cell and Tissue Research*, *353*(3), 409–423. http://doi.org/10.1007/s00441-013-1638-2

Yilmaz, M., & Christofori, G. (2009). EMT, the cytoskeleton, and cancer cell invasion. *Cancer Metastasis Reviews*, *28*(1-2), 15–33. http://doi.org/10.1007/s10555-008-9169-0

Yoshioka, N., Wang, L., Kishimoto, K., Tsuji, T., & Hu, G. F. (2006). A therapeutic target for prostate cancer based on angiogenin-stimulated angiogenesis and cancer cell proliferation. *Proceedings of the National Academy of Sciences of the United States of America*, *103*(39), 14519–14524. http://doi.org/10.1073/pnas.0606708103

Zha, J., Harada, H., Yang, E., Jockel, J., & Korsmeyer, S. J. (1996). Serine phosphorylation of death agonist BAD in response to survival factor results in binding to 14-3-3 not BCL-X(L). *Cell*, *87*(4), 619–628.

Zhang, M., Song, T., Yang, L., Chen, R., Wu, L., Yang, Z., & Fang, J. (2008). Nestin and

CD133: valuable stem cell-specific markers for determining clinical outcome of glioma patients. *Journal of Experimental & Clinical Cancer Research : CR*, *27*, 85. http://doi.org/10.1186/1756-9966-27-85

Zhao, Y., Lyons, C. E., Xiao, A., Templeton, D. J., Sang, Q. A., Brew, K., & Hussaini, I. M. (2008). Urokinase directly activates matrix metalloproteinases-9: a potential role in glioblastoma invasion. *Biochemical and Biophysical Research Communications*, *369*(4), 1215–1220. http://doi.org/10.1016/j.bbrc.2008.03.038

Zhao, Y., Xiao, A., diPierro, C. G., Carpenter, J. E., Abdel-Fattah, R., Redpath, G. T., et al. (2010). An extensive invasive intracranial human glioblastoma xenograft model: role of high level matrix metalloproteinase 9. *The American Journal of Pathology*, *176*(6), 3032–3049. http://doi.org/10.2353/ajpath.2010.090571

Zhou, N., Fan, W., & Li, M. (2009). Angiogenin is expressed in human dermal papilla cells and stimulates hair growth. *Archives of Dermatological Research*, *301*(2), 139–149. http://doi.org/10.1007/s00403-008-0907-5

Zhu, H., Acquaviva, J., Ramachandran, P., Boskovitz, A., Woolfenden, S., Pfannl, R., et al. (2009). Oncogenic EGFR signaling cooperates with loss of tumor suppressor gene functions in gliomagenesis. *Proceedings of the National Academy of Sciences of the United States of America*, *106*(8), 2712–2716. http://doi.org/10.1073/pnas.0813314106

Zhu, Z., Khan, M. A., Weiler, M., Blaes, J., Jestaedt, L., Geibert, M., et al. (2014). Targeting self-renewal in high-grade brain tumors leads to loss of brain tumor stem cells and prolonged survival. *Cell Stem Cell*, *15*(2), 185–198. http://doi.org/10.1016/j.stem.2014.04.007

Zhu, Z., Sanchez-Sweatman, O., Huang, X., Wiltrout, R., Khokha, R., Zhao, Q., & Gorelik, E. (2001). Anoikis and metastatic potential of cloudman S91 melanoma cells. *Cancer Research*, *61*(4), 1707–1716.